The Epstein-Barr virus BCL-2 homologues: interactions with cellular BCL-2 proteins and their role in apoptosis

By

Rachael Charlotte Cartlidge

A thesis submitted to the University of Birmingham
for the degree of DOCTOR OF PHILOSOPHY

School of Cancer Sciences
College of Medical and Dental Sciences
The University of Birmingham
May 2015

UNIVERSITY OF
BIRMINGHAM

University of Birmingham Research Archive

e-theses repository

This unpublished thesis/dissertation is copyright of the author and/or third parties. The intellectual property rights of the author or third parties in respect of this work are as defined by The Copyright Designs and Patents Act 1988 or as modified by any successor legislation.

Any use made of information contained in this thesis/dissertation must be in accordance with that legislation and must be properly acknowledged. Further distribution or reproduction in any format is prohibited without the permission of the copyright holder.

ABSTRACT

Epstein-Barr virus (EBV) encodes two viral BCL-2 homologues, BHRF1 and BALF1. BHRF1 is expressed in a subset of EBV-positive Burkitt's lymphoma (BL) tumours; as BHRF1 is highly anti-apoptotic, expression could result in treatment-resistant BL. Little is known about BALF1, including whether BALF1 is pro- or anti-apoptotic.

Interactions between BHRF1 and cellular BCL-2 homologues have not been fully characterised, but previous studies have focused on BIM as a key binding partner. We stably expressed wild-type or mutant vBCL-2s in EBV-negative BL lines to investigate interactions between BHRF1 and cellular BCL-2 homologues. The ability to bind BIM, whilst well documented, had no impact on BHRF1-mediated protection. Our data suggests that BHRF1's protective ability may be mediated through binding to BID and BAK. This work also identified two amino acids, located in the binding groove of BHRF1, which are highly important for protein function.

We detected BALF1 expression, at potentially functionally relevant levels, in a wide variety of EBV-associated tumour lines. BALF1 mRNA was detectable in lines with highly varied patterns of viral gene expression, indicating that expression is not restricted to one part of the viral life-cycle. In BL, BALF1 was found to be anti-apoptotic, and co-operated with, rather than antagonized, BHRF1.

ACKNOWLEDGEMENTS

I would like to thank my supervisors, Professor Martin Rowe and Dr. Gemma Kelly, for their excellent supervision, time, support and endless patience. I would also like to thank the members of the B cell group, especially Dr. Claire Shannon-Lowe and Dr. Rose Tierney, for all their help and wisdom, and for making the group such a nice place to work. Many thanks to Dr. Mark Kvansakul, for kindly providing the BHRF1 mutants, which have formed the basis of this thesis. Thanks also to Dr. Marco Herold for the use of his lentivirus system and his help throughout this project. I would like to thank my friends and family for all their patience and support, and my loving boyfriend Richard, for always being there when I needed help and advice, and for putting up with me in my more stressful periods. Finally, I would like to sincerely thank my funding bodies, the University of Birmingham and the Kay Kendall leukaemia fund, without whom this project would not have taken place.

Table of Contents

List of Illustrations

List of Tables

Abbreviations

β2M:	**Beta-2-micoglobulin**
BAD:	**BCL-2 associated death promoter**
BAK:	**BCL-2 antagonist/killer protein**
BARTs:	**BamHI A rightward transcripts**
BAX:	**BCL-2 associated X protein**
BCL-2:	**B cell lymphoma 2**
BCR:	**B cell receptor**
BCLXL:	**B cell lymphoma extra large**
BID:	**BH3-intereacting-domain death agonist**
BIM:	**BCL-2 interacting mediator of cell death**
BL:	**Burkitt's lymphoma**
cDNA:	**Complementary DNA**
cFLIP:	**FLICE inhibitory protein**
Co-IP:	**Co-immunoprecipitation**
CMV:	**Cytomegalovirus**
DED:	**Death effector domain**
DISC:	**Death induced signalling complex**
DNA:	**Deoxyribonucleic acid**
Dox:	**Doxycycline**
EBV:	**Epstein-Barr virus**
FACS:	**Fluorescence-activated cell sorting**
FADD:	**Fas associated death domain**
FCS:	**Foetal calf serum**

GAPDH:	**Glyceraldehyde-3-phosphate dehydrogenase**
GC:	**Germinal centre**
GFP:	**Green fluorescent protein**
HL:	**Hodgkin lymphoma**
IFN	**Interferon**
Ig:	**Immunoglobulin**
IL:	**Interleukin**
IM:	**Infectious mononucleosis**
IRES:	**Internal ribosome entry site**
ITC:	**Isothermal titration calorimetry**
Kbp:	**Kilobase pair**
Lat:	**Latency**
LCL:	**Lymphoblastoid cell lines**
LMP:	**Latent membrane protein**
MHC:	**Major histocompatability complex**
miRNA:	**Micro-RNA**
MOM:	**Mitochondrial outer membrane**
NK cell:	**Natural killer cell**
NPC:	**Nasopharyngeal carcinoma**
ORF:	**Open reading frame**
PBS:	**Phosphate buffer saline**
PCR:	**Polymerase chain reaction**
PI:	**Propidium iodide**
PTLD:	**Post-transplant lymphoproliferative disorder**

PUMA:	**P53 upregulated mediator of apoptosis**
PTP:	**Permeability transition pore**
QPCR:	**Quantitative polymerase chain reaction**
RNA:	**Ribonucleic acid**
RPM:	**Revolutions per minute**
RT:	**Reverse transcription**
SDS:	**Sodium dodecyl sulphate**
Tet:	**Tetracycline**
TetR:	**Tetracycline repressor protein**
TNF:	**Tumour necrosis factor**
TNFR:	**Tumour necrosis factor receptor**
TRAF:	**TNFR associated factor**
UTR:	**Untranslated region**
WT:	**Wild-type**

1.0 Introduction

1.1 Importance of cell death

Cell death is important for many processes during development. It sculpts the developing embryo by removing whole fields of cells (for example, between the digits), it regulates the number of neurons in the nervous system and removes whole unwanted structures (e.g. the embryo tail) (1). Cell death is required for homeostasis and for removal of cells which present a risk, such as those which have undergone DNA damage, and is the most primitive and conserved cellular reaction to viral infection. To recognise the importance of cell death it is worth considering the implications of its deregulation. Unscheduled or excessive cell death can lead to chronic neurodegenerative diseases such as Alzheimer's and Parkinson's disease among others (2, 3), whereas repression of death is one of the steps essential for tumorigenesis (4). Without cell death the accumulation of cells with errors in DNA replication and genome alterations will quickly build up, increasing the likelihood that a cell will acquire all the mutations it needs to become cancerous (e.g. sustained proliferation, immune evasion and potential for metastasis, to name but a few). Cell death repression is also required for sustained growth of cancer cells, and alterations can confer resistance against cancer therapies such as cytotoxic agents and radiation (5).

Deregulation of cell death is also important for viruses and, in order to successfully infect host cells, viruses have been forced to develop strategies for avoiding cell death and for keeping the cell alive long enough for the viral life cycle to complete. As many viruses have the ability to inhibit the induction of cell death through various means, the well known association between certain viruses and cancer is not surprising (reviewed in (6)).

The understanding of how a virus can interact with, and manipulate, the host cell machinery to prevent cell death, will not only lead to improved knowledge of the virus but could ultimately

result in more treatments for cell death related diseases, and to better, more targeted, anti-cancer therapies.

1.2 Forms of Cell death

Cell death can be divided into two categories: necrosis and programmed cell death. In necrosis, cells are killed at random, following irreparable cell damage. They do not follow the normal apoptotic pathway but lose membrane integrity and undergo an uncontrolled release of cellular contents (7). Of programmed cell death, apoptosis and autophagy are the two main categories, although evidence is now emerging to show that in some cases necrosis can be regulated by certain death receptor pathways, a form of death known as programmed necrosis or 'necroptosis' (reviewed in (8)). During autophagy, cellular homeostasis is maintained through the recycling of intra-cellular proteins and organelles. This removes damaged or unwanted organelles and also provides an energy source when the cell is in nutrient depleted conditions, functioning as a survival mechanism (9). However, under certain conditions, autophagy can lead to cell death and may be activated or suppressed by components of pathways which also regulate apoptosis, such as BCL-2 and BH3 mimetics(9, 10).

Apoptosis is important during many normal processes including immunity and B cell development. During passage through the germinal centre, centroblasts that have acquired crippling mutations during somatic hyper-mutation, or lack high affinity antibodies, are removed through apoptosis (11).

Unlike autophagy, entry into apoptosis results in irreversible damage to the cell through the action of cysteine-aspartic acid proteases (caspases) and leads to cell death. Cells undergoing apoptosis show a series of morphological changes which are, in the most part, similar, regardless of cell type or apoptotic agent (12). In the early stages of apoptosis, cells shrink,

nuclear chromatin condenses and extracellular matrix attachments start to break down. Later, blebbing on the cell surface can be seen to occur and the condensed chromatin begins to disassemble. The entire cell, including organelles, condenses and splits into membrane bound vesicles known as 'apoptotic bodies'. These keep cellular contents contained and limit the release of potentially harmful enzymes into the cellular matrix. Finally these apoptotic bodies are taken up by cells and are broken down through the lysosomal pathway (12).

The vast majority of apoptotic signals act through two major pathways; the extrinsic, which receives extra-cellular signals, and the intrinsic, or mitochondrial, which acts in response to internal cell stress. Both of these pathways result in the activation of the caspase cascade and death of the cell through the activity of cysteine-aspartic acid proteases.

1.2.1 Extrinsic apoptosis

The extrinsic apoptosis pathway is initiated by the activation of a death receptor on the target cell by binding to a death ligand located on an opposing cell, or free and soluble in the extracellular matrix. These death receptors are members of the tumour necrosis factor receptor (TNFR) superfamily and bind to the family of tumour necrosis factor (TNF) ligands. These death ligands include TNF, FasL and TRAIL and are usually expressed by immune cells including macrophages, dendritic cells, T, NK and NKT cells (13). The death ligands interact with receptors which contain a conserved intracellular death domain of approximately 80 residues but which are otherwise diverse in structure. Six main death receptors are currently known: TNFR1 (CD120a), CD95 (Fas/APO-1), DR3 (APO-3, TRAMP, LARD, and WSL1), TRAIL-R1 (DR4), TRAIL-R2 (DR5) and DR6 (14). Ligand binding causes multimerization of the trimeric receptors and leads to recruitment of Fas-associated death domain protein (FADD) and formation of the death induced signalling complex (DISC) (see Figure 1.1).

Fas is probably the most studied of the death receptors. Binding of FasL results in the formation of Fas trimers and the recruitment of the DISC to the FasR death domain (Figure 1.1A). FADD is as universal accessory protein, facilitating interaction between receptors containing a death domain and cytoplasmic proteins. It is recruited to Fas through interactions between the Fas death domain and its own. The N-terminal death effector domain (DED) of FADD is unmasked by interaction with Fas allowing it to recruit pro-caspase 8, pro-caspase 10 and FLICE inhibitory protein (c-FLIP) to the DISC. Other proteins including Daxx, FAP-1, FLASH, RIP and FAF-1 are also recruited to the DISC but their function here is largely unknown. Once in the DISC pro-caspases 8 and 10 self cleave into caspases 8 and 10. These are released into the cytoplasm and caspase 8 goes on to cleave pro-caspases 3, 6 and 7 (reviewed in (14, 15)). Caspase 3 cleaves several substrates including structural proteins, DNA repair enzymes and endonuclease inhibitors. It can also induce other caspases, including 6 and 7, resulting in amplification of the apoptotic signal. In cases where there is insufficient Caspase 8 to cleave downstream caspases, the cleavage of BID into pro-apoptotic t-BID by Caspase 8 might become a major pathway (16). T-BID then goes on to activate apoptosis through the mitochondrial pathway and induces release of cytochrome C which leads to cleavage of pro-Caspase 9. Hence both the intrinsic and extrinsic apoptotic pathways are linked (15, 16).

With the exception of TNFR1, the other death receptors propagate the apoptotic signal in a similar manner to Fas, through the formation of the DISC. TNFR-1, when bound to its ligand, TNFα, mediates signalling involving the formation of two complexes (1 and 2) (Figure 1.1B). Complex 1 forms at the membrane and is composed of TNFR-1, TNF, TRADD (TNFR associated death domain), TRAF 1/2 (TNFR associated factor) and RIP. This then signals through the NFκB pathway which paradoxically exerts an anti-apoptotic effect by preventing the cleavage of pro-caspase 3 but also has a role in the regulation of the inflammatory response and immune

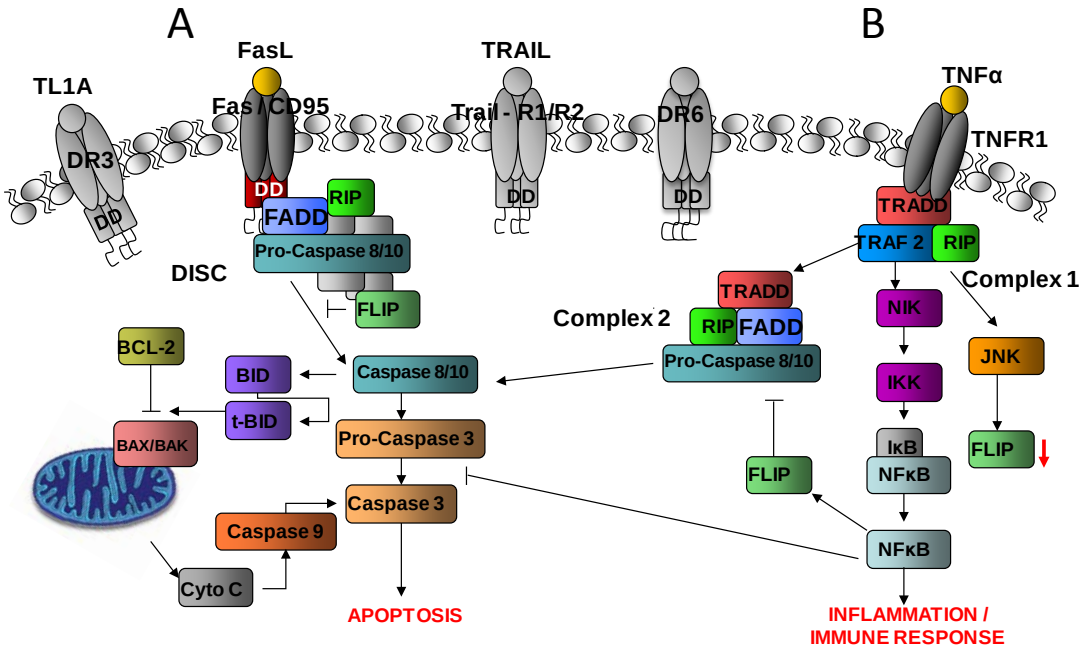

Figure 1.1: Extrinsic Apoptosis pathway**.** Only signalling through the Fas pathway and TNFR1 have been shown for simplicity although the other receptors function in a similar manner to Fas. (A) When activated by FasL the DISC complex forms at the Fas death domain (DD). In the case of Fas this contains FADD and RIP among other proteins. Interaction with Fas allows FADD to recruit pro-caspases 8 and 10 to the DISC. The pro-caspases then cleave and are released to propagate the apoptotic signal through cleavage of other pro-caspases or of BID which leads into the mitochondrial apoptosis pathway. (B) Activation of TNFR1 results in the formation of two complexes, 1 and 2. Complex 1 acts on the NFκB and JNK pathways which modulate inflammation and the immune response. Components of complex 1 translocate to the cytoplasm and bind FADD and Pro-Caspase 8/10 to become complex 2 which leads to caspase cleavage. The ratio between expression of complex 1 and 2 is regulated by levels of FLIP which are raised by NFκB activation and inhibit complex 2 formation and pro-caspase 8/10 cleavage. The levels of FLIP can also be lowered by activation of the JNK pathway which then promotes apoptosis. This figure is adapted from (14,15).

function through transcription factors NFκB and c-Jun. Complex 1 does not contain FADD or pro-caspase 8 but can translocate to the cytoplasm where it binds FADD and pro-caspase 8 to become complex 2 which goes on to activate pro-caspase 8 and initiate apoptosis (14). Levels of FLIP determine the ratio between anti-apoptotic complex 1 and pro-apoptotic complex 2. When complex 1 activates the NFκB pathway the levels of FLIP are elevated and act to inhibit the formation of complex 2 and apoptosis. If the receptor signalling does not reach the threshold required to activate the NFκB pathway then apoptosis is free to occur. TNFα ligation can also activate JNK signalling through a series of kinases. JNK acts to increase the degradation of FLIP through E3 ubiquitin ligase so promoting the formation of complex 2 and apoptosis (15, 17, 18).

1.2.2. Intrinsic apoptosis

The intrinsic or mitochondrial pathway to apoptosis (reviewed in (19)), is initiated in response to internal stress and implemented through permeabilisation of the mitochondria. This mitochondrial step is regulated by BCL-2 family members, which can act to either induce or repress apoptosis (20).

The intrinsic pathway can be induced in response to a number of cell stimuli including growth factor withdrawal, γ-irradiation and various cytotoxic drugs (21). The initiation of this pathway leads to loss of mitochondrial structural integrity and the release of pro-apoptotic factors such as cytochrome C through outer mitochondrial membrane permeabilisation. Cytochrome C promotes the activation of caspase proteases; specifically it interacts with a Caspase 9 complex, to promote a cascade of initiator and effector caspases. Eventually exposure of phosphatydylserine is seen on the outer leaflet of the plasma membrane and, finally there is loss of the barrier function of the plasma membrane (12).

The intrinsic pathway is regulated by a series of pro- and anti-apoptotic proteins, all of which show some homology to BCL-2. These interact to up- or down-regulate apoptosis depending on their levels of activation. The anti-apoptotic proteins are localised to the cytoplasmic face of the mitochondrial membrane. They include BCL-2 and its close relatives BCL_{XL} and BCL_W, and the less conserved MCL1, among others (21, 22).

The pro-apoptotic proteins are split into two groups which greatly differ in their relatedness to BCL-2. The BH3-only proteins have only one BH domain and relatively little homology to BCL-2; at least 11 have so far been identified including: BID (BH3-intereacting-domain death agonist), BIM (BCL-2 interacting mediator of cell death), BAD (BCL-2 associated death promoter), PUMA (P53 upregulated mediator of apoptosis), NOXA and BIK (19). The BH3-only proteins act as sensors of cellular stress and pass on signals to the pro-apoptotic multi-domain proteins BAX and BAK (BCL-2 associated X protein and BCL-2 antagonist/killer protein) (23). BAX and BAK have a much greater homology to BCL-2. In response to apoptotic signals, BAX and BAK form homodimers, which regulate the permeability of the mitochondrial membrane. These complexes cause large pores to form in the mitochondrial membrane leading to the permeabilisation of the mitochondria, the release of cytochrome C and the propagation of the caspase cascade (19, 23). The BCL-2 proteins and their interactions will be discussed in more detail in section 1.3.

1.2.3 The caspase cascade

This process of cellular breakdown and dismantling of cellular components is initiated by the step-wise activation of caspases. They act to cleave certain cellular polypeptides, including some that perform 'housekeeping' roles or cellular repair. The cumulative effect of cleavage of downstream polypeptides is to disable repair of cellular components, stop the cell cycle,

inactivate anti-apoptotic proteins, encourage breakdown and disassembly of cellular structures and to mark the cell for engulfment and disposal (24).

Caspases are initially found as inactive precursors: apoptotic signals cause them to become activated through cleavage at internal aspartic acid residues. This enables healthy cells to keep these potentially lethal proteins inactive but allows rapid activation of the caspase cascade upon the initiation of apoptosis (see Figure 1.2).

Caspases are all similar in amino acid sequence and structure. They are composed of three domains; an N-terminal pro-domain and a large and small sub-unit (24). There are around 12 human caspases identified which are split into two groups; initiators and effectors. Initiator caspases (caspases 2,8,9,10) initiate the caspase cascade after receiving a signal from the various apoptotic pathways. Initiator caspases have a long pro-domain which allows their recruitment to receptor complexes and scaffold proteins where they are activated. When active, they cleave and activate pro-forms of the effecter caspases (caspases 3,6,7) which are then able to cleave several hundred other proteins within the cell to trigger apoptosis (25, 26). These effecter caspases have short, or absent, pro-domains and, once activated, are thought to carry out the actual demolition of the cell with the help of other destructive enzymes which are themselves activated by the caspases. Over 400 proteins have been identified as substrates for caspases although only a few of these have been directly linked to markers of apoptosis (27). However, many appear to be involved in structural and housekeeping systems and hence their cleavage disrupts many vital cellular processes (26, 27).

During apoptosis, release of cytochrome C leads to the formation of the mitochondrial apoptosome, a caspase activating complex in the cytoplasm built around Apaf1. In the absence of cytochrome C, Apaf1 exists as a monomer in the cytoplasm. In the presence of cytochrome C and ATP, Apaf1 is recruited into the apoptosome scaffold where several Apaf1

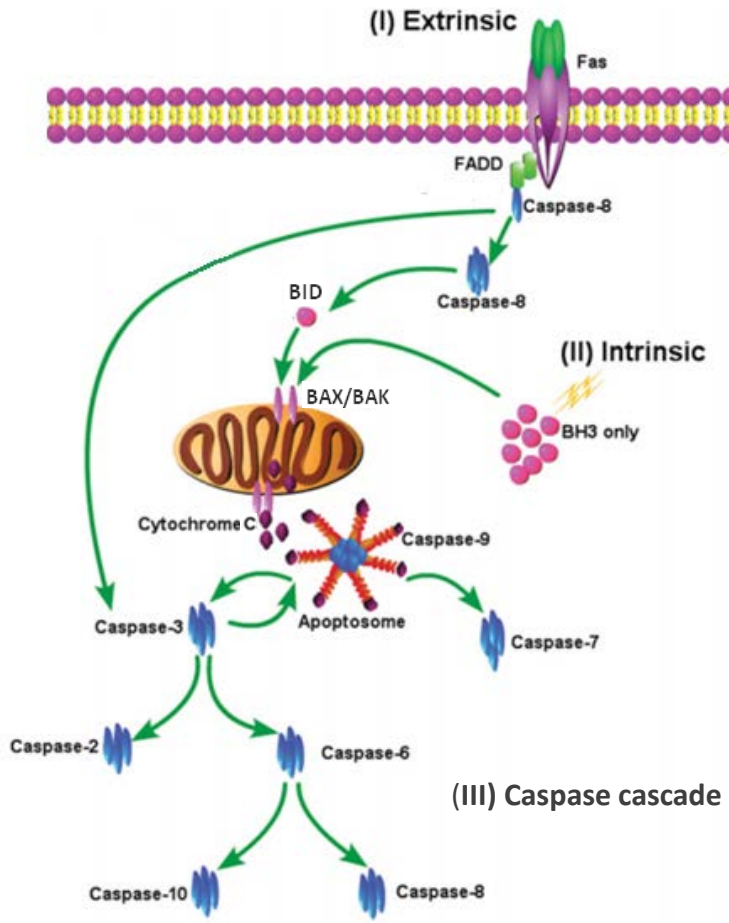

Figure 1.2: Activation of the caspase cascade through apoptotic pathways. The two main apoptotic pathways are shown (I) Extrinsic apoptosis pathway. Activation of Fas by Fas ligand causes pro-caspase 8 to be recruited to FADD and activated through close proximity with other caspases. Activated caspase 8 cleaves pro-caspase 3 or BID depending on whether death receptor stimulation has resulted in high or low levels of caspase 8 respectively. (II) Intrinsic apoptosis. Apoptotic stimuli activate and up-regulate BH3-only proteins which interact with BCL-2 homologues and BAX/BAK to cause mitochondrial membrane pore formation. BID can be cleaved by caspase 8 to t-Bid which also helps to activate BAX and BAK and provides a link with the extrinsic pathway. (III) Caspase cascade. Cytochrome C is released through pores in mitochondria and recruits Apaf1 and caspase 9 to the apoptosome. Caspase 9 is activated in the apoptosome and activates caspase 3 and 7. Caspase 3 activates downstream caspases to propagate the cascade which eventually leads to cleavage of housekeeping proteins and breakdown of the cell. Adapted from (26)

proteins are brought into proximity with a similar number of caspase 9 dimers (28). The configuration of the apoptosome holds caspase 9 dimers closely together resulting in auto-activation due to a low level of catalytic activity in the inactive caspases (29). Caspase 9 then activates caspases 3 and 7, caspase 3 goes on to activate caspases 2 and 6 and also activates more caspase 9 to continue the cascade (reviewed in (26)). Caspase 8, activated during the extrinsic apoptotic pathway (see section 1.2.1), can also directly activate caspase 3, or can work through BID to activate the caspase cascade through mitochondrial permeabilisation (16, 30).

1.3 BCL-2 and its role in apoptosis

1.3.1 Discovery of BCL-2

The mechanism of apoptosis is highly conserved between organisms. The first regulators of apoptosis were found in *Caenorhabditis elegans* (*C. elegans)*, known as CED-3 and CED-4*,* and were found to be essential for cell death. A third gene, CED-9*,* was found to prevent this function (31). Pro-apoptotic CED-4 is bound to CED-9 but is released by apoptotic signals and the binding of EGL-1. When the activator CED-4 is released it binds to CED-3 to initiate cell death. The first mammalian regulator, BCL-2, or B cell lymphoma 2, was later discovered, due to its activation through the (14;18) chromosomal translocation in follicular lymphoma (32-34). This translocation moved the BCL-2 encoding gene from its normal position of chromosome 18 to chromosome 14 and under the control of the immunoglobulin transcription enhancer, leading to the over-expression of BCL-2 (33). It was found to enable the survival of otherwise cytokine dependent hematopoietic cells in the absence of cytokine (35).

BCL-2 was discovered to be a structural and functional homologue of CED-9*,* and is able to replace CED-9 in the apoptotic pathway of *C. elegans* (36, 37). Unlike other oncogenes known at the time, BCL-2 inhibited cell death instead of promoting proliferation. It was found to co-operate with c-myc to immortalise B cells, with c-myc driving proliferation and BCL-2 preventing apoptosis (35).

Other proteins in the *C. elegans* cell death pathway were later found to be homologues of mammalian pro-apoptotic BCL-2 homologues. EGL-1 has mammalian counterparts, the BH3 only homologues: BIK, BID, BAD, BIM, NOXA and PUMA to name a few. CED-4 was also found to be a homologue of Apaf1 (mentioned above). In *C. elegans.* CED-4 and CED-9 interact directly, unlike the mammalian system in which Apaf1 is not sequestered by BCL-2. Once released CED-4 goes on to activate the caspase CED-3 (38).

1.3.2 BCL-2 and mammalian pro-survival homologues

BCL-2 is most highly expressed in foetal and rapidly dividing cells. It seems to be mainly involved in survival of immune cells and may act to prevent the death of antigen receptor selected B cells. It is important for the survival of mature B and T cells, with *BCL-2*$^{-/-}$ mice suffering from loss of B and T cells through apoptosis, and later complete breakdown of the immune system (39). *BCL-2*$^{-/-}$ mice die of polycystic kidney disease and are stunted and grey. This can be reversed by also knocking down *BIM,* illustrating how the pathway works through inhibitory interactions (40).

The whole BCL-2 pathway takes the form of three different groups, consisting of both pro- and anti-apoptotic proteins (see Figure 1.3). All members of the BCL-2 family share homology to at least one BCL-2 homology, or BH, domain (22).

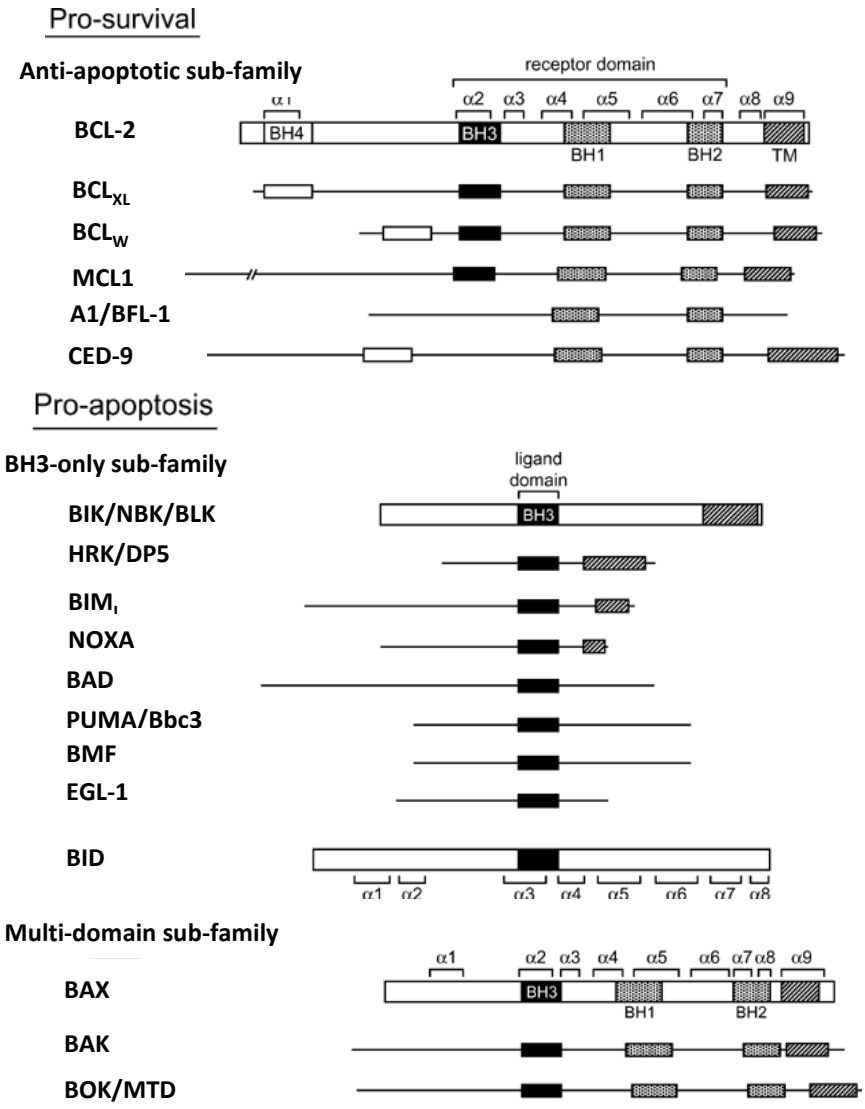

Figure 1.3: The three BCL-2 subfamilies. BH 1-4 domains determine the level of homology with BCL-2. The α helices (α1-9) which make up these domains are shown. BH 1-3 domains of anti-apoptotic BCL-2 proteins form a binding groove for the BH3 domains of the pro-apoptotic ligands. The carboxy terminal transmembrane domains (TM) that target many BCL-2 proteins to intracellular membranes are also shown. Anti-apoptotic BCL-2 homologues usually contain at least three BH domains. The pro-apoptotic homologues are split in two groups. BAX and BAK are members of the multi-domain (or BAX) sub-family which contain three BH domains. The BH3-only sub-family contain only the BH3 domain (ligand domain) which binds the binding groove of anti-apoptotic proteins. Adapted from (22)

Most pro-survival members of the BCL-2 family possess at least two BCL-2 α-helical homology domains (usually BH1 and BH2) out of the four possible conserved motifs (BH1, BH2, BH3 and BH4). They may possess more BH domains depending on their similarity to BCL-2 (36). They also possess a C-terminal hydrophobic domain (36, 41) that targets them to intracellular membranes. These proteins are localised on the cytoplasmic face of intracellular membranes, mostly on the outer mitochondrial membrane but have also been found on the nuclear envelope and endoplasmic reticulum. Although the function of nuclear envelope localised BCL-2 is not known it has been suggested that BCL-2 present on the endoplasmic reticulum may have a role in controlling intracellular calcium levels, which are known to influence apoptosis (42, 43).

The anti-apoptotic group members include 6 proteins but the most studied are BCL-2 and its close relatives BCL_{XL} (B-cell lymphoma-extra large), BCL_W (BCL-2L2; BCL-2-like protein 2), and MCL1, among others. BCL-2, BCL_{XL} and BCL_w have been shown to protect cells from a wide range of apoptotic stimuli including cytokine deprivation, chemotherapeutic drugs and irradiation with UV and γ radiation. Less conserved members of the anti-apoptotic BCL-2 subfamily, such as MCL1 and A1 (bfl-1), also have a protective effect (22). Although MCL1 is able to protect from apoptotic stimuli by binding to BIM it is also easily degraded through ubiquitylation, accounting for its short half life when compared to other anti-apoptotic BCL-2 homologues (44).

The levels of homology to BCL-2 vary, with the amino acid sequence identities of BCL_{XL}, BCL_W and MCL1 being 43.8%, 36.5% and 22.5% respectively, but all cause resistance to apoptosis *in vivo* and *in vitro* (45). Anti-apoptotic proteins form a hydrophobic groove, made up of the BH1, 2 and 3 domains, which can be bound by pro-apoptotic BCL-2 homologues. The pro-apoptotic

proteins expose their BH3 domains after activation and bind the anti-apoptotic proteins by inserting this BH3 domain into the hydrophobic groove (43, 46).

The hydrophobic C domain of anti-apoptotic BCL-2 homologues BCL_{XL} and BCL_{W} occludes the binding domain and so must undergo a conformational change to enable binding to intracellular membranes (BAX employs a similar mechanism which is discussed later). This change may involve displacement of the C terminal domain by binding of BH3-only homologues, and enables relocation to intra-cellular membranes. The C terminal domain of BCL-2 may be more exposed, explaining why it is more often located on membranes than within the cytoplasm (22).

The levels of anti-apoptotic proteins are heavily regulated both transcriptionally and by protein modification and turnover. The production and stability of MCL1 is regulated by cytokine levels (47). BCL-2 can be regulated by miRNAs miR-15a and miR-16-1 which directly interact with the 3' UTR of BCL-2 mRNA (48). MiR-15a and miR-16-1 have been found to be mutated or down-regulated in the majority of CLL cases (49), as well as some diffuse large B cell lymphomas (50). This down-regulation has been shown to lead to an increase in the level of BCL-2 and cellular resistance to apoptosis (48).

Cellular anti-apoptotic BCL-2 proteins may also be regulated post-translationally by apoptosis inducing caspases. Bellows and colleagues have found that caspase 3 cleaves BCL-2 proteins at Asp-34 and $BCL\text{-}_{XL}$ at Asp-61 and 76 to give an N terminally truncated protein that has lost its anti-apoptotic function. Mutation of this cleavage site between α helices 1 and 2 increases the anti-apoptotic effect of BCL-2. Furthermore cleavage often leads to the release of a pro-apoptotic C terminal domain which can contribute to cell death by acting upon mitochondria, in order to accelerate the caspase cascade. In this way a caspase feed-back loop may form, in which caspases activated through routes other than the intrinsic pathway, are able to cleave

BCL-2 into a pro-apoptotic product which can then go on to activate more caspases and promote apoptosis (51-53).

1.3.3. Pro-apoptotic BCL-2 homologues

The pro-apoptotic BCL-2 homologues fall into two sub-families, differentiated by their number of BH3 domains (see Figure 1.3). The BH3-only sub-family are sensors of cellular stress and apoptotic signals, and include BIM, PUMA, NOXA and BID. The second sub-family are the multi-domain pro-apoptotic homologues, which, when activated, form pores in the mitochondrial membrane to release cytochrome C and initiate the caspase cascade. Examples of these proteins include BAX and BAK.

1.3.3.1 BH3-only BCL-2 homologues

The BH3-only proteins have only the BH3 domain and relatively little homology to BCL-2. They include BIM, PUMA, BID, BIK, NOXA and BAD, as the most characterised, although at least 11 have so far been found in mammals (54). The BH3-only proteins are structurally similar but each have their own specific pattern of binding (see Figure 1.4). BIM, PUMA and BID bind to all the anti-apoptotic BCL-2 homologues and are also the only known BH3-only proteins to interact directly with BAX and BAK (20, 55). The other BH3-only proteins do not bind to BAX or BAK but have varying abilities to bind the anti-apoptotic homologues (56). BAD is only known to be able to bind BCL-2, BCL_W and BCL_{XL}, and NOXA binds only to MCL1 and A1 anti-apoptotic proteins (57).

BH3-only proteins respond to signals of cell stress. Different proteins are expressed in different cell types. They can be induced/activated by various signals. For example, PUMA and NOXA are

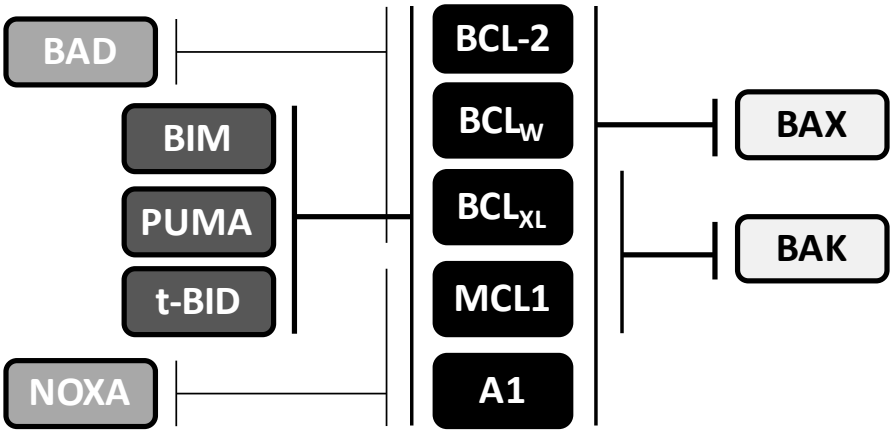

Figure 1.4: Binding specificities of the main BCL-2 homologues. The main BH3-only BCL-2 homologues have distinct binding specificities for the anti-apoptotic BCL2 homologues. BIM, PUMA and t-BID bind BCL-2, BCL$_W$, BCL$_{XL}$, MCL1 and A1. BAD binds BCL-2, BCL$_W$ and BCL$_{XL.}$ Noxa bind only MCL1 and A1. The anti-apoptotic BCL-2 homologues also have specificities for the multi-domain proteins although there is some contention surrounding this. BCL2, BCL$_W$, BCL$_{XL}$, MCL1 and A1 most likely bind to BAX whereas only BCL$_{XL}$ and A1 bind BAK (20, 74, 359)

induced by the tumour suppressor p53 in response to DNA damage (58) and BIM is up-regulated by transcription factors in response to endoplasmic reticulum stress and growth factor deprivation (57, 59). Along with BMF, BIM also appears to monitor the cytoskeleton and is sequestered to micro-tubules via dynein motor complexes (22, 60).

Many of the BH3-only proteins are detectable at reasonably high levels in healthy cells and are regulated by post-translational mechanisms. BIM is targeted for ubiquitylation in healthy cells by ERK-mediated phosphorylation but is released from this by growth factor withdrawal (57). BAD is phosphorylated in healthy cells and held inactive by 14-3-3 scaffold proteins. Its activation requires dephosphorylation, at which point it is released to interact with anti-apoptotic homologues (22). As discussed in 1.2.1 and 1.3.6, BID is cleaved to its active form t-BID by caspase 8 in response to signals from the extrinsic apoptotic pathway.

The tumour suppressor role of BH3-only BCL-2 homologues has been illustrated using mice with single or double knockouts of BH3-only homologues. These mice display resistance to cell death stimuli, including drugs used in chemotherapy, and accelerated tumour development (19, 61).

1.3.3.2 Multi-domain pro-apoptotic BCL-2 homologues

There are only three known pro-apoptotic multi-domain BCL-2 homologues; BAX, BAK and BOK. BOK is expressed everywhere but is found at the highest levels in reproductive and brain tissue (62), whereas BAX and BAK are more widely expressed. The presence of either BAX or BAK has been found to be essential for apoptosis in a range of cell types (43). The multi-domain homologues are similar to the anti-apoptotic homologues except for the absence of the BH4 domain (see Figure 1.3). Originally it was the lack of BH4 which was thought to differentiate between pro and anti-apoptotic homologues with otherwise similar structures. However, it is

now thought that it is the degree to which BH3 domain is packed within the hydrophobic core that makes this distinction. Proteins like BAX, in which the BH3 domain is free to insert within the groove of anti-apoptotic homologues, are pro-apoptotic, and it has been shown that substituting the BH3 domain of BCL-2 for the BAX BH3 domain causes BCL-2 to become pro-apoptotic (63).

BAX and BAK are the most studied of the multi-domain homologues and have interesting structural differences which affect their sub-cellular localisation. The c-terminus of BAX, the area which contains the trans-membrane localisation sequence, folds in upon itself and is hidden within the BAX hydrophobic binding groove. Because of this, BAX is cystolic within healthy cells and remains a monomer due to the blockage of the binding groove (57). Under apoptotic stimuli BH3-only proteins may interact with BAX in a 'hit and run mechanism' (see Figure 1.5) which induces a conformational change in BAX leading to the release of the c-terminus and BH3 domain, and translocation to the mitochondrial membrane (64). Alternatively, BAX and BAK may become active when relieved from the repression of anti-apoptotic BCL-2 homologues by the activation of BH3-only BCL-2 homologues (65).

BAK activation may be less complicated. BAK is permanently bound to the outer mitochondrial membrane and, in healthy cells, may be held inactive by interactions with anti-apoptotic homologues. During apoptosis, the anti-apoptotic proteins are displaced by pro-apoptotic BH3-only homologues, and BAK is activated (see section 1.3.4). Alternatively, BAK may be activated by transient interactions with BH3-only proteins which are then displaced (64). Upon activation, the BH3 domain of BAK is exposed and occupies the BH3 binding groove of another activated BAK molecule. This forms a symmetrical dimer which interacts with other dimers, through the BH3 domains and grooves, to form homo-oligomers (see Figure 1.5) (65, 66).

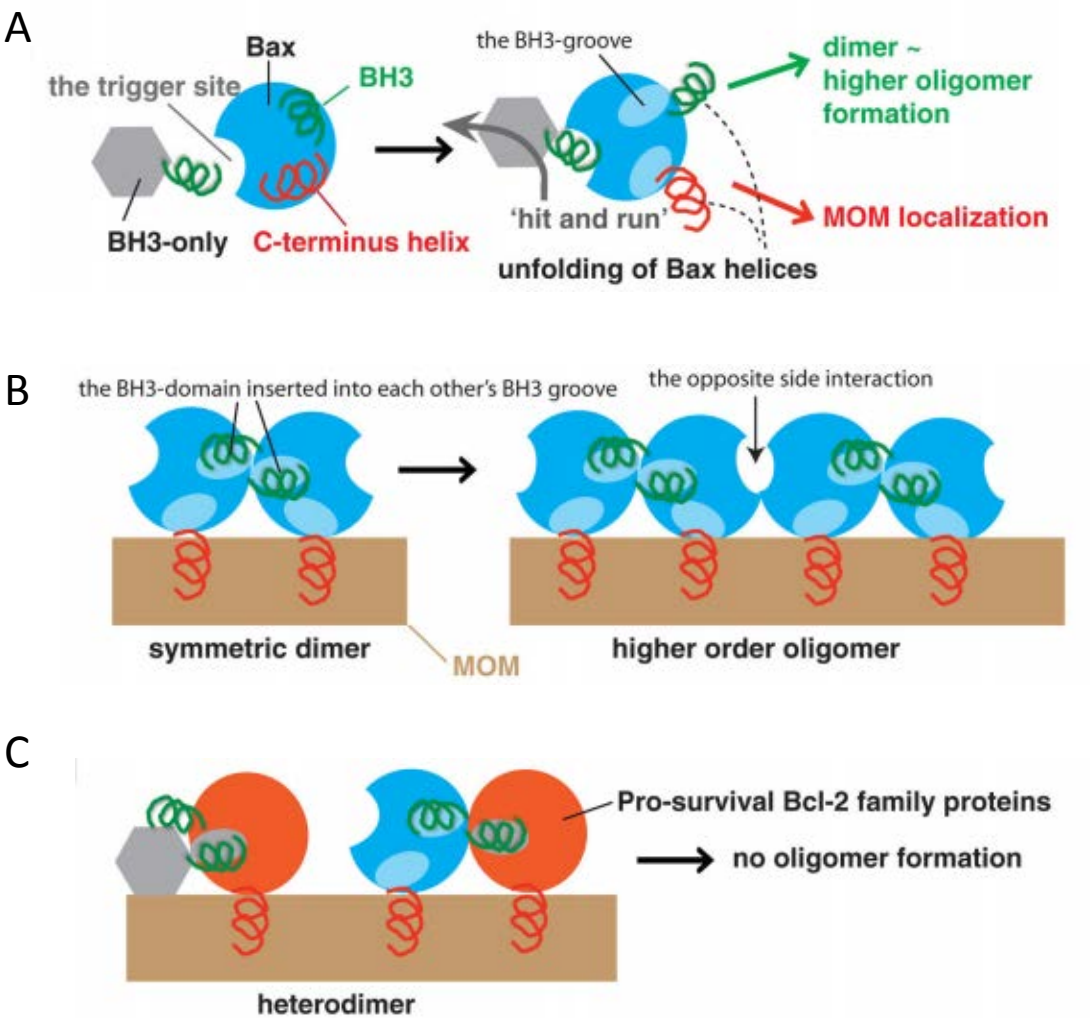

Figure 1.5: Hit and Run method of BAX activation. (A) BAX activation is initiated by binding of a BH3-only protein. This induces a conformational change which unfolds the C-terminus and BH3 domain. The BH3-only protein then dissociates from BAX which translocates to the mitochondrial membrane. (B) The C-terminal domain is inserted with the mitochondrial membrane and BAX or BAK dimerise with another BAX or BAK by inserting the BH3 domain into the adjacent binding groove on the other molecule. Homo-dimers then come together to form homo-oligomers. (C) Anti-apoptotic proteins inhibit mitochondrial membrane permealisation (MOM) by sequestering BH3-only proteins or holding activated BAX/BAK inactive and preventing homo-dimer formation. From (64)

Mitochondrial membrane permeabilisation represents the 'point of no return' in the cell death pathway. In healthy cells mitochondria are permeable to small molecules through specific channels. Once this permeability increases over a certain threshold, proteins such as cytochrome C are released into the cytoplasm. There are two main modes of mitochondrial membrane permeabilisation and BAX and BAK are thought to have a role in both. The first is permeabilisation through the permeability transition pore (PTP). The PTP regulates the exchange of metabolites between the mitochondria and cytosol in order to maintain the trans-membrane potential needed for oxidative phosphorylation. The PTP opens transiently which results in a rapid rise in inner mitochondrial membrane permeability. This, in turn, results in an influx of water, due to osmosis, and swelling of the mitochondria. If left unchecked the swelling will eventually burst the outer membrane (19). BAX and BAK are thought to bind to members of the PTP complex, presumably to prevent closure of the pore, (67). A second mechanism by which BAX and BAK permeabilise the outer mitochondrial membrane is through oligomerising to form pores. It is not known how many oligomers of BAX or BAK are required for formation but there is evidence that a minimum of four BAX molecules were required for cytochrome C to pass through artificial membranes whereas complexes of at least eight were seen in dying cells (68). BCL-2 homologues have been found to have similarity to the translocation domain of diphtheria toxin, which forms a pore through which the killing domain of the toxin is translocated from the endosome to the cytosol (69). The pore structure formed by BAX, known as lipid pores or α-pores, are also similar to those formed by diphtheria toxin (64). It is not known precisely how BAX and BAK pores form but it is thought that conformational changes resulting from oligomerisation force pores to open, either through only the c-terminal trans-membrane domains or through additional insertion of α-helices 5 and 9 across the membrane, with α-helix 6 lining the exposed surface (65, 70).

1.3.4 BCL-2 homologue interaction

Until 10 years ago it was believed that apoptosis was determined by the balance between levels of pro-apoptotic multi-domain proteins and anti-apoptotic BCL-2 homologues. Increase in the levels of pro-apoptotic proteins in response to cell stress would cause the cell to die, whereas an increase in anti-apoptotic protein levels would halt apoptosis. This was known as the rheostat model. However, apoptosis can occur without changes in the levels of pro and anti-apoptotic proteins, so the rheostat model is likely to be an oversimplification. These findings indicated the presence of a third family of BCL-2 homologues, which can regulate the pro and anti-apoptotic proteins (19).

This class of proteins was found to be the BH3-only homologues which respond to apoptotic stimuli.

There have been multiple mechanisms that have been put forward to explain precisely the complex series of interactions that result in activation of BAX and BAK or act to keep them inoperative and several mutually non-exclusive models have been proposed.

One model, the 'indirect activation model', suggests that BCL-2 anti-apoptotic proteins bind and sequester the multi-domain effecter proteins and prevent them from forming pores in the mitochondrial outer membrane. BH3-only proteins bind the anti-apoptotic proteins, occupying the BH3 binding groove and preventing binding of multi-domain proteins BAX and BAK. This theory states that the release of BAX and BAK from the binding of anti-apoptotic proteins is enough to enable them to initiate apoptosis (71). However, this does not take into account that inactive BAX is cytoplasmic, inert and exists as a monomer, away from the mitochondrial localisation of most of the anti-apoptotic homologues (72).

It has also been reported that some BH3-only proteins are also able to directly bind BAX and BAK (20) and so may have functions other than to sequester the BH3 binding pockets of the anti-apoptotic proteins. There is evidence that BAX and BAK are not held inactive by anti-apoptotic proteins and that their activation requires binding of BH3-only homologues instead of release from anti-apoptotic proteins (73). These finding have led to the postulation of a new 'two-class' model for regulation by BH3-only proteins.

In the 'two-class' model, the BH3-only proteins are divided into 'activators' (BIM, PUMA and BID) and 'sensitizers' (BAD, NOXA, BIK and Bmf) (20).

In unstressed cells, 'activator' BH3-only proteins may be bound and held inactive by the anti-apoptotic proteins. When apoptotic stimuli occur the 'activator' proteins are released from the anti-apoptotic proteins due to displacement by 'sensitizer' proteins. The 'activator' BH3-only proteins are then able to go on to bind and directly activate multi-domain proteins BAX and BAK through binding to their BH3 domain (19, 56).

This hierarchy of the binding ability BH3-only proteins is now broadly accepted although there is still some disagreement over whether BAX and BAK are activated directly (through binding by BH3-only proteins) or indirectly (through release of inhibition). Some studies have shown, in BIM/BID double knockout mice, that BH3-only activators are not essential for BAX and BAK mediated cell death (74). However, others have demonstrated that, not only is anti-apoptotic protein repression not enough to indirectly activate BAX and BAK, but that BH3-only homologues other than BIM, PUMA and BID may have a reduced ability to directly activate BAX/BAK (75).

Supporters of the indirect mechanism point to the lack of evidence of complexes of BAX/BAK and BH3-only proteins such as t-BID and BIM. This could be explained by a 'hit and run' mechanism, where the initial insertion of a BH3-only protein into the BAX groove displaces the

trans-membrane domain, BAX may then undergo a conformational change to turn the BH3 domain outwards. This could disrupt the binding to the BH3-only activator but leave the BH3 domain free to form homo-dimers (see above and Figure 1.5) (65). BAX and BAK are also able to undergo auto-activation and, in small quantities, become spontaneously active or may be activated by other molecules such as p53 (76).

As neither the direct nor indirect model completely explain the evidence surrounding the activation of BAX and BAK it is likely that elements of both models are correct (77). Dewson *et al.* have suggested a situation which goes some way to unifying the direct and indirect models (see Figure 1.6).

In healthy cells the pool of activator BH3-only proteins and the spontaneously activated BAK/BAX are both held inactive by the binding of anti-apoptotic proteins. Apoptotic stimuli cause a rise in levels of BH3-only pro-apoptotics. Anti-apoptotic proteins are sequestered by 'sensitiser' BH3-only proteins and the binding of 'activators' and activated BAX/BAK to anti-apoptotics is displaced by 'sensitisers'. BAX/BAK are activated by 'activators' through a hit and run mechanism and can auto-activate other BAX/BAK molecules. Activated BAX/BAK form homodimers at the mitochondrial membrane which come together to form homo-oligomers and eventually pores. Mitochondrial permeabilisation occurs and is followed by cell death (65).

1.3.5 BH3 mimetics

A number of BH3 mimetics are being trialled as potential inhibitors of anti-apoptotic BCL-2 homologues. Many cancers show increased expression of anti-apoptotic homologues. The BH3 domains of BH3-only homologues or small synthetic peptides are being screened for their affinity to anti-apoptotic homologues and their ability to abrogate BCL-2 function (78). The most promising of these is ABT-737, although it is ineffective against over-expression of MCL1

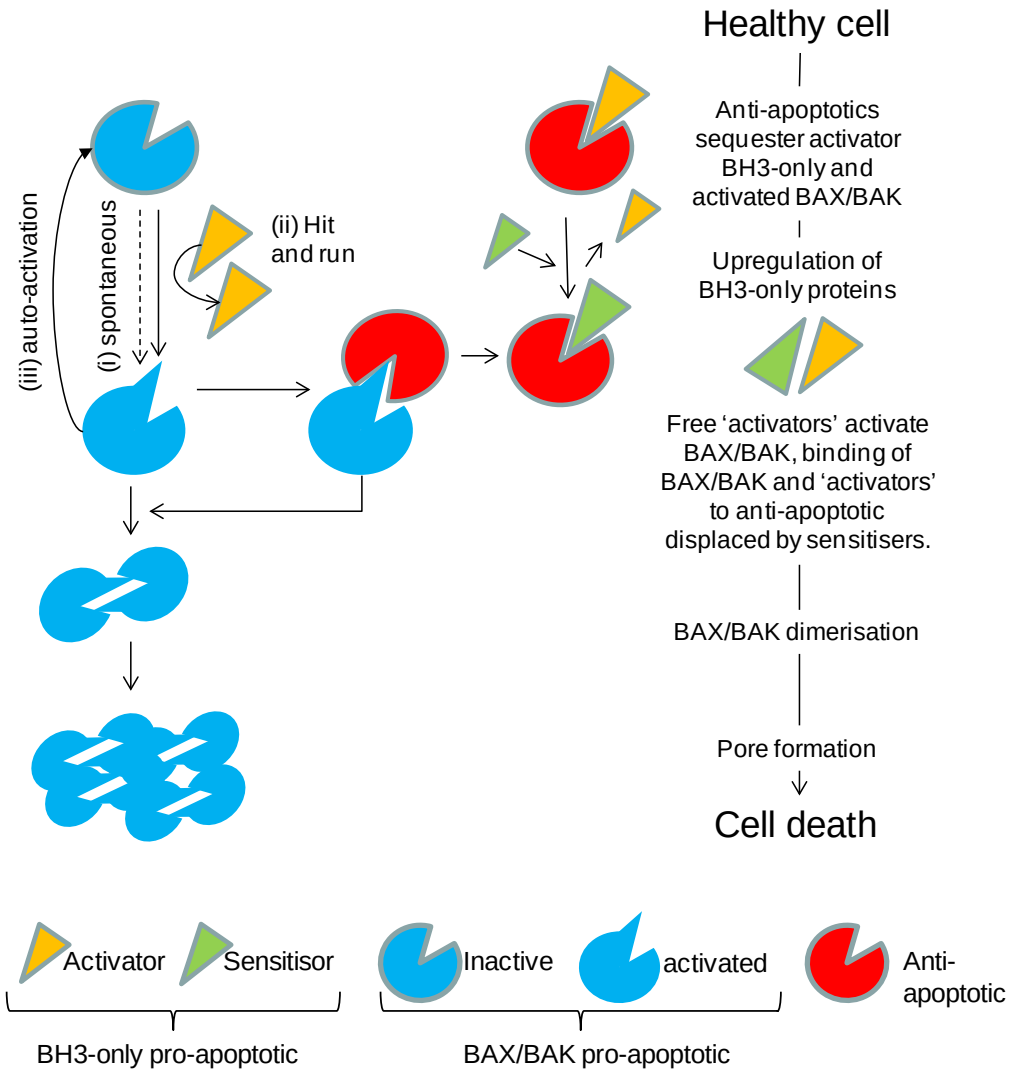

Figure 1.6: Combined model for BAX and BAK activation. In healthy cells anti-apoptotic proteins sequester the 'activator' BH3-only proteins. (i) Any spontaneously activated BAX or BAK is bound and kept inactive by anti-apoptotics. Apoptotic stimuli activate and up-regulate BH3-only homologues, both activators (BIM, PUMA and BID) and sensitisers (BAD, NOXA, BIK and BMF). 'Activators' bound to anti-apoptotic proteins are displaced by 'sensitisers' and become free to activate BAX/BAK by the hit and run mechanism (ii). (iii) Activated BAX/BAK can perform auto-activation to quickly increase the pool of active molecules. Upon activation BAX translocates to the mitochondrial membrane. At the mitochondrial membrane activated BAX/BAK bind to form homodimers. Foci of activated BAX/BAK form and dimers join to give homo-oligomers which eventually aggregate to form pores. Pore formation leads to mitochondrial membrane permeabilisation and cell death. Adapted from (65)

and does not affect the function of the viral BCL-2 homologues BHRF1 (see section 1.4.1). Many cancers can be said to be addicted to over-expression of anti-apoptotic BCL-2 homologues, as these are required to sequester the BH3-only homologues activated by apoptotic signals such as myc deregulation. Mimetics such as ABT-737 have the ability to displace pro-apoptotics, such as BIM, from BCL-2's binding pocket, leaving them free to activate BAX and BAK. In this way cancer cells could be said to be primed for death and become very sensitive to apoptotic stimuli once the protection of BCL-2 has been removed. For this reason BH3 mimetics are unlikely to have as dramatic an effect on normal cells and so may be a good addition to cancer therapies (79).

1.3.6 Overlap of extrinsic and intrinsic apoptosis pathways

Although intrinsic and extrinsic apoptosis appear to occur through separate pathways and are initiated by different stimuli, there is a degree of connection between the two. There is evidence that over-expression of BCL-2, BCL_{XL} or MCL1 can inhibit TRAIL induced apoptosis (80), as can the loss of BAX and BAK expression (81, 82). Activation of caspase 3 by caspase 8, and the propagation of the caspase cascade, depends on the levels of caspase 8 activated by extrinsic apoptotic signals. If activated caspase 8 levels are insufficient not enough caspase 3 will be activated to reach the threshold required for downstream caspase activation. In this case cleavage of the BH3-only protein, BID into t-BID may be favoured (16, 30). T-BID then goes on to interact with other BCL-2 homologues in the intrinsic apoptotic pathway to induce the caspase cascade through mitochondrial membrane permeabilisation and the release of cytochrome C. The intrinsic pathway is dependent on the levels of anti-apoptotic BCL-2, interaction through BID provides a way in which extrinsic cell death can be controlled by BCL-2 levels. In certain cell types, e.g. hepatocytes, the levels of caspase 8 are never high enough to

cleave sufficient caspase 3 and so activation of the cascade always occurs through the formation of the apoptosome. This means that in hepatocytes, all receptor mediated cell death is sensitive to BCL-2 levels (83).

1.3.7 Viral BCL-2 homologues

It is advantageous for viruses to be able to control the apoptotic machinery of the host cell. It is important for the virus life cycle to prevent apoptosis that may occur upon infection and during viral replication.

Virus may modulate the apoptotic response through encoding anti-apoptotic viral BCL-2 homologues. BCL-2 homologues encoded by α and γ herpes virus share a homology of around 20-30% with each other as well as with cellular BCL-2. They all contain a BH1 domain and most contain BH2, with both BH1 and BH2 being essential for the binding of the BH3 domain of BH3-only proteins and the repression of apoptosis by BCL-2 homologues. The BH3 domain, which has a role in the pro-apoptotic functions of BCL-2, is not conserved in the viral homologues and, similarly to the cellular BCL-2 homologues, there is no conservation in the BH4 domain which may not have a functional role in protein-protein interactions (84).

The adenovirus E1B 19k gene was the first gene identified that suggested that viruses were able to modulate apoptosis to control the outcome of viral infection. Comparison of E1B 19K and the BCL-2 gene found that, although the sequence homology to BCL-2 is weak, E1B 19K contains conserved BH domains similar to those of BCL-2 (85). Since then, E1B 19K has been shown to interact with members of the BCL-2 family (86). Through binding to BAX, E1B 19K can block BAX induced apoptosis, and can functionally substitute for BCL-2 during virus infection and oncogenic transformation (86, 87).

The Fowlpox virus (FVP), the only true poxvirus known to express a BCL-2 homologue, encodes a protein similar to cellular MCL1 (88). However, Poxviruses contain several non-BCL-2 anti-apoptotic proteins such as FLICE-inhibitory proteins (vFLIPs) and caspase inhibitory serpins, and so may not require an extensive array of viral BCL-2 homologues. Poxvirus-like African swine fever virus (ASFV) encodes A179L, a BCL-2 homologue which can protect from apoptosis in both mammalian and Sf9 insect cells through interactions with BAX, BAK, BID and NOXA (89).

There are also many members of the Herpesvirus family which contain structural or functional viral BCL-2 homologues. Herpesviruses contain many examples of host-acquired genes which drive cell cycle progression and proliferation, often activate the cellular apoptotic machinery and so viruses will tend to also encode anti-apoptotic genes to counteract this effect (88).

Human Cytomegalovirus, or CMV, encodes several proteins that can interfere with apoptosis in order to favour proliferation. Viral mitochondria-localised inhibitor of apoptosis, or vMIA, is probably the best characterised and has been shown to prevent apoptosis in response to death receptor stimulation and cytotoxic agents, although it has very little structural or sequence similarity to BCL-2 (90). It is located on the mitochondria and can physically bind solely with BAX through electrostatic interactions through the region between the BH2 and BH3 domains of BAX. vMIA is able to recruit BAX to the mitochondria where it is neutralised, however, it is not able to do the same with BAK (91).

Members of the Herpesvirus family are separated into alpha, beta and gamma sub-families dependant on location of lytic infection, host range and reproductive cycle and growth rate. Gamma herpesviruses are the only herpesviruses shown to be associated with cancers so it is very interesting that these may encode viral versions of BCL-2. Anti-apoptotic BCL-2 homologues encoded by the gamma herpesviruses include M11 which is encoded by murine γ-

HV68 and can protect against a variety of apoptotic stimuli including Tumour Necrosis Factor α (TNFα) treatment but, unlike cellular BCL-2, is mainly located in the cytoplasm (92). It has been shown to be active during the lytic and latent state of γ-HV68 but knockdown only shows a significant effect during the reactivation of the virus from the latent to lytic cycles (93-95).

Kaposi's sarcoma associated Herpesvirus (KSHV) is the causative agent of Kaposi's sarcoma, a cancer of the lymphatic endothelium. The KSHV BCL-2 homologue, KSBCL-2, is expressed early in lytic cycle and has homology to cellular BCL-2 in the BH1 and BH2 domains (84). It is not known if KSBCL-2 maintains the cells during the lytic replication of the virus or if, like M11 of murine γ-HV68, it is involved in viral reactivation from latent to lytic cycle (95).

Like many other herpesviruses, the Epstein Barr virus (EBV) has acquired the ability to avoid apoptosis by influencing the intrinsic apoptosis pathway using viral proteins that either interact with, or have homology to BCL-2. Unlike other γ herpes viruses, which only encode one BCL-2 homologue, EBV encodes two; BHRF1 and BALF1 (see sections 1.4.1 and 1.4.2). Both these proteins may be able to protect against apoptosis, although there is contention as to the role of BALF1 (41, 96).

1.4 EBV viral BCL-2 homologues and apoptosis

1.4.1 BHRF1

Of the two viral BCL-2 homologue encoded by EBV, BHRF1 is the best characterised and has been shown to be potently anti-apoptotic (97). In EBV infected lymphocytes, it is expressed as an immediate early lytic cycle gene from its own lytic promoter. Protein and mRNA can be detected in the first 24 hours after EBV infection (98).

One of the only lesions in which BHRF1 is highly expressed *in vivo* is oral hairy leukoplakia. This is a lesion of tongue mucosa mainly observed in immuno-suppressed patients, in which EBV is constantly in lytic cycle, with very few latent gene products detectable (99, 100).

Interestingly, it has recently been found that, in certain situations, BHRF1 can also be expressed in latency due to a deletion of EBNA2 and the restricted transcription from the Wp promoter. This leads to expression of EBNAs 1, 3A, 3B, 3C, and a truncated form of EBNA-LP. The deletion also places a copy of the Wp promoter immediately upstream of BHRF1 (see section 1.9.1). It has also been shown that BHRF1 is present at low levels in totally latent populations of LCLs (101, 102). Wp continues to constitutively express at low levels even in LCLs in which the Cp promoter has been activated. If BHRF1 can also be driven by the Wp promoter then it explains the low level of expression in LCLs, as well as the peak in expression shortly after infection, (when expression is mainly from Wp), and the tail off in BHRF1 expression, as Cp becomes active.

1.4.1.1 BHRF1 protein structure and folding

The BHRF1 protein contains two central hydrophobic helices, α5 and partially buried α6, surrounded by amphipathic α helices, α1, 2, 3, 4 and 7. BHRF1 also contains a C terminal hydrophobic domain which localises it to intra-cellular membranes, mainly the outer mitochondrial membrane, similarly to BCL-2 (Figure 1.7A) (103).

The first α helix corresponds to the BH4 region of BCL_{XL} and, like other anti-apoptotic BCL-2 homologues, is not well conserved, leading to the conclusion that the BH4 domain is not essential for BCL-2 homologue function (46).

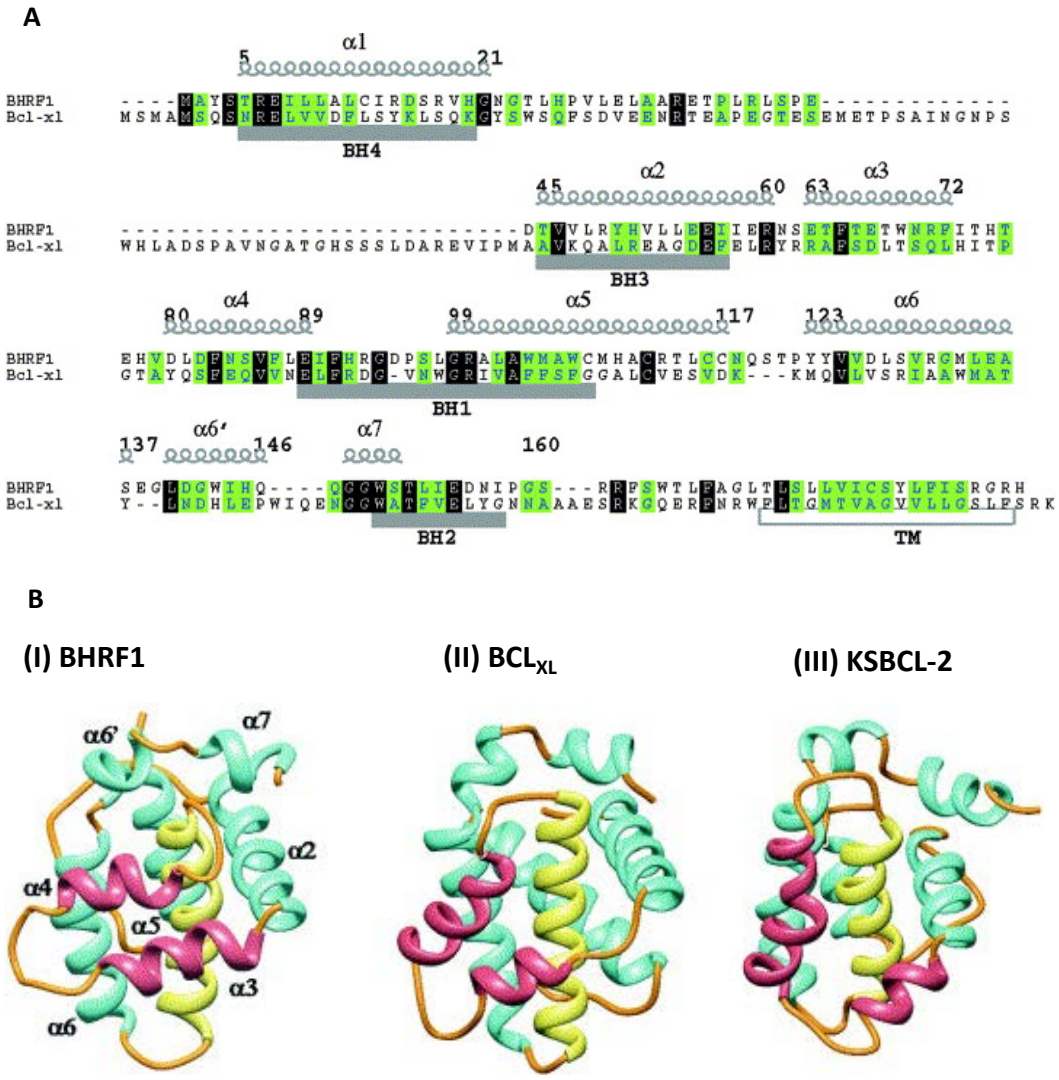

Figure 1.7: The various domains of BHRF1: (A) an alignment of BHRF1 against cellular BCL-2 with BH domains and α helices highlighted to show the regions of homology. (B) Structure of (I) BHRF1, (II) BCL_{XL} and (III) KSBCL-2. The hydrophobic BH3 binding groove formed by BH1 (α3 and α4) is highlighted in red. The binding groove is in a different position and binding is more restricted in BHRF1 than in BCL_{XL} and KSBCL-2. Taken from (46)

The helices α3 and α4 make up the BH1 domain, which forms the hydrophobic groove, essential for binding to the BH3 domains of pro-apoptotic BH3 only and multi-domain proteins (104).

BHRF1 has around 38% sequence homology to BCL-2; however, the extent of its structural homology to BCL-2 and BCL-2 homologues is much greater. Both viral and cellular anti-apoptotic BCL-2 homologues tend to share the same number of α helices, all of similar lengths and folded in the same overall structure (Figure 1.7B). However, there are some important differences between the viral and cellular BCL-2s (46).

The hydrophobic groove, essential for the binding of BH3 domains, is shorter and less exposed in BHRF1 compared to cellular BCL-2, due to the positions of α3 and α4 (46). In order to bind the BH3 domains of cellular proteins, the binding domain undergoes a significant structural change at α helices 3 and 4, to widen the groove and allow entry of the BH3 domain (104).

The loop connecting the α1 and α2 helices in BHRF1 is much shorter, and less conserved, than that of BCL-2. In cellular BCL-2 this loop may contains a caspase cleavage site which could enable BCL-2 to be cleaved by caspase 3 to release a pro-apoptotic C terminal fragment. In contrast, BHRF1, in common with most herpesvirus BCL-2 homologues have been shown to be constitutively anti-apoptotic (52) (Figure 1.7A). By this method EBV is able to avoid the cellular mechanisms of regulation and constitutively represses apoptosis (105).

1.4.1.2 BHRF1 and protection from apoptotic stimuli

BHRF1 can protect for a multitude of apoptotic stimuli including DNA damage, growth factor withdrawal and viral infection (106, 107). BHRF1 also functions downstream of BID to protect from extrinsic stimuli such as TRAIL and FAS induced apoptosis (107, 108). BHRF1 was first shown to protect against serum depletion and ionomycin (97). BHRF1 was later shown to

protect against apoptosis induced by gamma radiation and common chemotherapeutic drugs, including etoposide, doxorubicin, AraC and staurosporin, indicating it as a possible cause of chemotherapy resistance in EBV positive malignancy (104, 106). BHRF1 has also been shown to protect form apoptosis *in vivo.* Eμ-myc mice, representative of BL, become resistant to AraC, etoposide and cyclophosphamide treatment when inoculated with tumour cells overexpressing BHRF1 (104).

1.4.1.3 BHRF1's interaction with BCL-2 homologues

There is still much to be discovered about the hetero-dimerisation of viral BCL-2 homologues with cellular BCL-2 family proteins, as the hetero-dimerisation of cellular BCL-2 with its pro-apoptotic homologues is also not totally understood. It is thought that BHRF1 is able to directly interact with BAK, BIM, BID and PUMA (84) and may also bind BIK/Nbk and Nip3, members of the BH3 only sub-family (105).

It is not clear which of BHRF1's interactions are critical for the inhibition of cell death. One hypothesis, which has its limitations, is that BHRF1 may bind to a subset of BIM to repress activation of the multi-domain pro-death proteins (109). Previously it was thought that BHRF1 sequesters all free BIM to prevent it binding to BAK/BAX. However, even under cell stress there is still free BIM available in BHRF1 expressing cells. Apoptotic signals may induce a subset of BIM to undergo a conformational change in order to activate BAK/BAX, and it could be this subset that BHRF1 sequesters to prevent apoptosis. Alternatively, as postulated by Desbien *et al,* BHRF1 could bind a small amount of BIM and cause it to permanently undergo a conformational change before releasing it (109). These kind of catalytic interactions have been seen with other BCL-2 homologues, such as the hit and run activation of BAX and BAK (65). However, Desbien *et al.* only looked at the binding of BHRF1 to BIM, BAK and BAX, and did not

include any other BH3-only BCL-2 homologues (109), despite BHRF1 being shown to also bind the BH3 domains of BID and PUMA (84). BHRF1 can protect BIM negative cell lines (110), showing that Interaction with BIM cannot be the only mode of BHRF1 protection. These BH3-BHRF1 interactions need further investigation, understanding how BHRF1 interacts with cellular BCL-2 proteins could aid our understanding of the role of EBV in cancer.

1.4.2 BALF1

Marshall *et al*. 1999 predicted that the BALF ORF also encodes another viral BCL-2 homologue. BALF1 is unusual for the fact that EBV is the only known Herpes virus to contain a second BCL-2 homologue. It has been suggested that BALF1 may compensate for EBV's lack of v-FLICE inhibitory proteins found in other Herpes viruses (96). Marshall *et al.* originally showed that BALF1 was able to protect cells against apoptosis induced by treatment with anti-Fas, IFN-γ, cyclohexamide and tumour necrosis factor α (96). However, Bellows *et al.* 2002 were later unable to show an anti-apoptotic effect for BALF1 in response to sindibis virus induced apoptosis and over-expression of BAX (41). Contrary to the findings of Marshall *et al.* 1999 they actually found that BALF1 was able to inhibit the function of BHRF1. It was reported that BALF1 was able to restore the cell death induced by over-expression of BAX that was otherwise repressed by BHRF1, although it did not actually enhance the killing ability of BAX (41). BALF1 was also able to act on KSBCL-2 but was not able to inhibit the function of cellular BCL_{XL} (41).

BALF1 has 20% homology to BCL_{XL} and contains the BH1 to BH4 homology domains, although, like other vBCL-2s, the BH3 domain is less well conserved. BALF1 actually has a greater similarity to cellular BCL-2 and BCL_{XL} than does BHRF1 (96).

Unlike BHRF1, the BH4 domain of BALF1, a domain with little known function not well conserved in vBCL-2s, has a high degree of similarity to that of BCL-2 BH4. BALF1 also lacks a C

terminal fragment capable of insertion into membranes and so would be mainly cystolic and has been shown not to co-localise with BHRF1 (41). Finally, the BH1 domain glycine, essential for anti-apoptotic function in most BCL-2 homologues has been mutated to a serine (96).

BALF1 is translated from a conserved internal methionine within the BALF gene. The first in frame methionine at the beginning of the gene is less well conserved and, in EBV, encodes what is known as BALF0 (Figure 1.8) (41). BALF0 has many of the same properties as BALF1, it has lost the ability to become pro-apoptotic through caspase cleavage and is able to restore cell death repressed by BHRF1. When attempting to separate the roles of BALF1 and BALF0 in the abrogation of BHRF1 function in response to serum withdrawal and epotoside, M. Lee and S. Hope were unable to determine any difference in function (111). They theorised that an anti-apoptotic effect of BALF0 could explain the differing results seen by Marshall *et al.* 1999 and Bellows *et al.* 2002 but found that transfection of epithelial and B cells with plasmids expressing either BALF1 or BALF0 caused a loss of viability and increased the number of cells undergoing differentiation (111).

Similarly to BHRF1, the BALF1 gene is also located downstream of a latent promoter and BALF1 and BALF0 may be expressed during latency, as well as being expressed as an early antigen during lytic replication (112).

It has been suggested that BALF1 is able to interact with BHRF1 in the same manner as a cellular BH3 only protein. Bellows *et al.* showed that BHRF1 co-immunoprecipitated with BALF1 but not BALF0, although this result could have been a result of detergents used in the preparation of cell lysates and may not occur *in vivo.* To check this result they looked cellular co-localisation of BHRF1 and BALF1 but found that BHRF1 is localised on mitochondrial outer membranes whereas BALF1 and BALF0 are localised in the cytoplasm and do not change localisation in response to death stimuli (41). Therefore, BALF1 may inhibit the function of

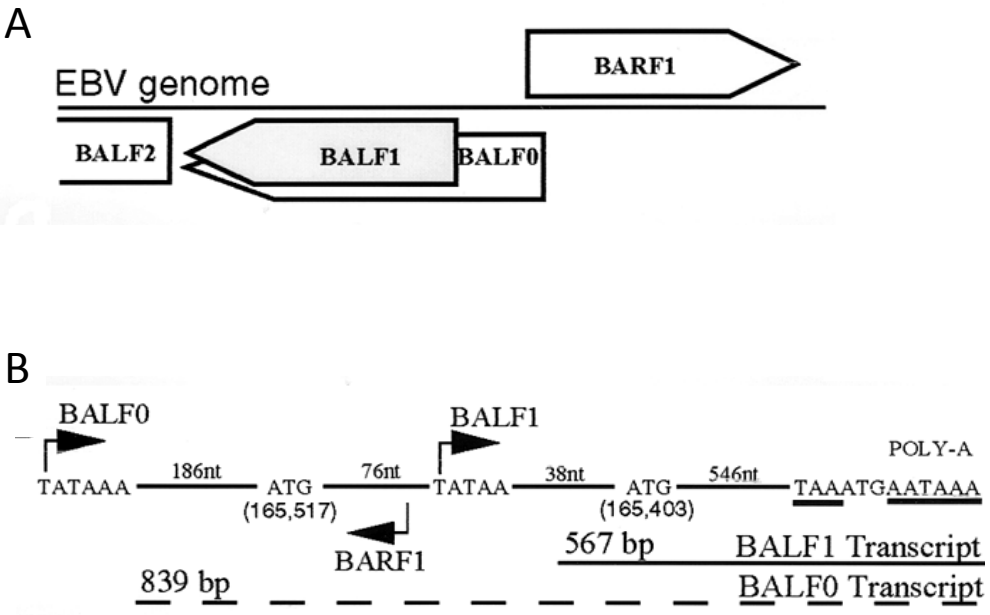

Figure 1.8: The open reading frames of BALF1 and BALF0: (A) diagram of genome region containing BALF1, boxes indicate the open reading frames. (B) diagram in reverse orientation showing BALF1 and BALF0 transcripts and sizes as well as. Taken from (41)

BHRF1 through an indirect mechanism as they have not been found to co-localise in cells and co-immunoprecipitation experiments do not show a direct interaction (105). Any regulation of BHRF1 function by BALF1 may occur by competition for the same downstream factors, or through transient interactions that could bring about alterations to the BHRF1 protein (41, 105).

1.5 Classification of Epstein-Barr virus

1.5.1 Scientific Classification

EBV, officially known as Human Herpes virus 4 (HHV4), belongs to the Herpesviridae family within the order Herpesvirales. Herpes viruses are distinct viruses with linear double stranded DNA genomes.

The Herpesviridae family is comprised of primate herpesviruses, eight of which are associated with Humans; Herpes simplex virus types 1 and 2, Varicella Zoster, EBV, Human cytomegalovirus, Human herpesviruses 6 and 7 and Kaposi's sarcoma associated herpesvirus. EBV is classified as a gamma-herpesvirus. It belongs to the lymphocryptovirus genera, which are predominately B cell lymphotrophic, and is the only Human herpesvirus of this genus (113).

1.5.2 The discovery of Epstein-Barr Virus (EBV)

The characterisation of Burkitt lymphoma (BL) in 1958, by the surgeon Denis Burkitt, was the initial step leading to the discovery of the Epstein Barr virus (EBV) (114). His observations led him to speculate that the cancer could be the result of an infectious agent, opening up the possibility of a viral role in BL development (115, 116). In 1964 Epstein, Anchong and Barr established cell lines from Burkitt lymphoma biopsies and used electron microscopy to show

the presence of herpesvirus-like particles (117). Through collaboration with Walter and Gertrude Henle in Philadelphia EBV was officially classified as a new herpesvirus in 1965 (118). As research into EBV progressed it was discovered that the virus asymptotically infects 90% of the world's adult population (119).

In otherwise healthy populations, Walter and Gertrude Henle identified EBV as the causative agent of infectious mononucleosis (IM), a clinical manifestation of primary EBV infection in adulthood (120). EBV was established as the first virus to cause human cancer after its oncogenic properties were demonstrated *in vitro* and *in vivo* through the transformation of peripheral blood B cells and the formation of tumours in immuno-suppressed primates infected with cell free virus (121, 122). Since this time EBV has been identified as a factor in many malignancies other than BL.

1.6 Patterns of EBV gene expression *in vitro* and *in vivo*

The EBV genome consists of ~175 kilobase pairs of double-stranded DNA (123), and includes ~100 open reading frames (124, 125). The vast majority of EBV genes are dedicated to lytic infection (124). The virus primarily infects B cells (126-130), though evidence from EBV associated malignancies also supports its ability to infect epithelial (131), natural killer (NK) (132) and T cells (133). The EBV viral life cycle involves both lytic and a latent stages, both of which are supported by B cells (134).

Lytic infection may occur in tonsillar B cells during viral reactivation or primary infection (135-138). Broadly speaking, lytic genes can be divided into immediate early, early and late genes (124, 125). Immediate early genes include viral transactivators responsible for activating lytic infection (BZLF1 and BRLF1) (139, 140), early genes are primarily involved in genome

replication e.g. the viral polymerase BALF5 (141-143), while late genes mainly encode structural proteins needed to assemble the virus particle (141-143).

EBV latent genes comprise 6 nuclear antigens (EBNA-LP, EBNA1, EBNA2, EBNA3A, EBNA3B and EBNA 3C) (144-147), 3 membrane proteins (LMP1, LMP2A, LMP2B), the BCL-2 homologue BHRF1 (101), and a collection of non-coding RNAs (EBERs and BARTs) (148) and viral miRNAs (149). EBV is capable of several different types of latent infection, which are classified according to the exact latent genes expressed (Figure 1.9) (reviewed in (150)). Following primary EBV infection *in vivo*, the virus establishes a persistent latent infection in memory B cells termed Latency 0; in this context, only non-coding RNAs (151, 152) and selected viral miRNAs are expressed (153).

By contrast, expression of all EBV latent genes is termed Latency III (154). Specifically, the six EBNA proteins and BHRF1 are transcribed from the C and W promoters (155), while the LMPs and non-coding RNAs are transcribed from their own respective promoters (154). This particular type of latency is interchangeably referred to as the growth transforming program (154), because infecting B cells *in vitro* results in uncontrolled proliferation and, potentially, the generation of immortal cell lines termed lymphoblastoid cell lines (LCLs) (121, 156). A Latency III pattern of gene expression has been observed in IM tonsils, supporting the involvement of EBV latent genes during primary infection *in vivo* (157); most of these genes are not expressed during long term viral persistence, however, as a result of pressure from the host immune system (158). Latency III transcripts are also observed in B cells during post-transplant lymphoproliferative disorder (159-161) and AIDS-lymphoma (162-166), consistent with EBV proliferation in the absence of the host immune system.

The Latency II pattern of gene expression is more restricted than Latency III, but more expansive than Latency 0. The C and W promoters are inactive though EBNA1 is expressed,

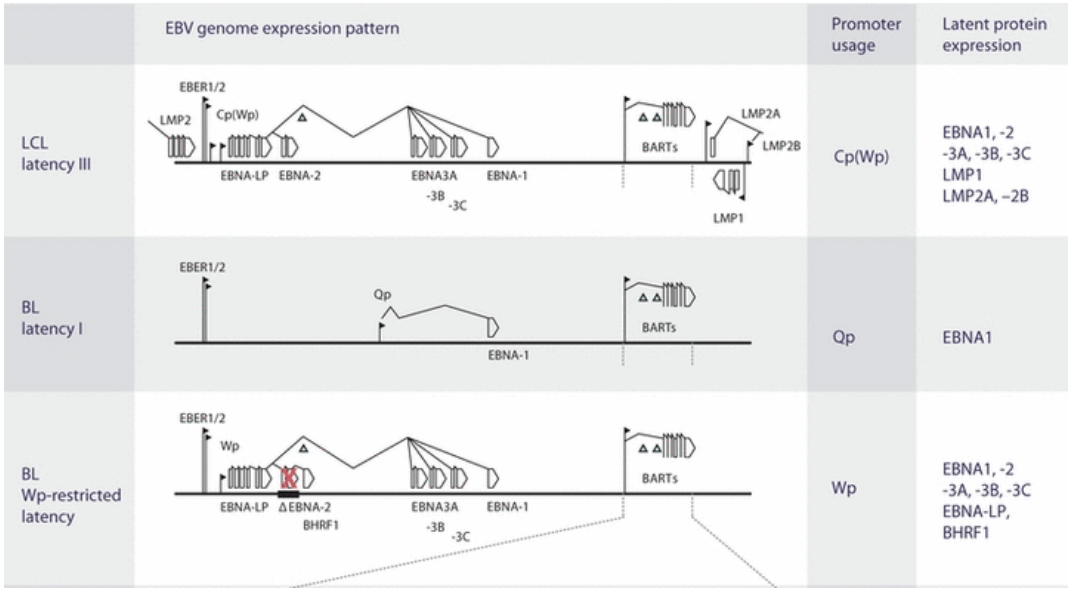

Figure 1.9: The three forms of EBV latent antigen expression in B cells: In latency I a single EBNA1 antigen is expressed from the Qp promoter, with the only other expression being of the BARTs and EBERs. B cells transformed into LCLs *in vitro* have a less restricted form of expression and express all EBNA antigens from the C promoters as well as the LMPs, BARTs and EBERs. A low level of expression from the W promoter is also present in LCLs. In Wp restricted latency the EBNA2 gene is deleted with the whole *Bam*H1 and Y1 and Y2 fragment of the c-terminus of EBNA-LP. EBNA2 is not able to activate the C promoter leading to constitutive expression from Wp. LMP promoter activation by EBNA2 also does not occur. This gives a less restricted form of expression than in latency I BL, with EBNA1, the EBNA3s, a truncated form of EBNA-LP (tr-EBNA-LP) and the BARTs and EBERs expressed. Adapted from (101 and 150)

albeit from downstream promoter Q (167), while the LMPs and non-coding RNAs are again expressed from their own promoters (167-171). This particular form of gene expression is characteristic of Reed Sternberg cells in Hodgkin lymphoma (HL) and epithelial cells of nasopharyngeal carcinoma (NPC) (172-174), and may play a role during primary infection *in vivo* as supported by the detection of Latency II gene expression in IM tonsil germinal centre B cells (175).

Finally, the Latency I program involves the expression of EBNA1 is from promoter Q and the non-coding RNAs from their respective promoters (167, 176). The detection of Latency I expression in replicating B cells in the blood of IM patients supports an involvement of this latency program in persistence *in vivo* (177). Latency I was first characterized in Burkitt lymphoma (BL); a subset of apoptosis resistant BL, termed W-promoter-restricted BL (Wp BL), expresses a truncated form of EBNA-LP (t-EBNALP), EBNA1, EBNA3A, -3B, -3C and BHRF1, all from Wp (101, 178, 179). The contribution of these additional gene products to apoptosis restriction are discussed elsewhere (see section 1.9.1).

1.7 EBV infection and persistence *in vivo*

In vivo primary infection with EBV usually occurs at an early age and is asymptotic (180). However, infection during adolescence or later can result in a self-limiting lymphoproliferative disease known as infectious mononucleosis or IM (181). EBV is spread through salivary contact and enters through the lymphoepithelium that lines the oropharynx (182). It is unclear as to whether it is oropharangeal epithelial cells or B lymphocytes which are initially infected. Evidence points towards an initial infection of B cells followed by virus amplification, infection of epithelial cells and shedding of infectious virus into the saliva (183-185). Evidence for B cells being the site of EBV persistence comes from X-linked agammaglobulinemia (XLA) patients who

lack mature B cells and who show no detectable EBV DNA in either blood or throat washings, which should be present with even a low level of epithelial infection (186). However, evidence of lytic replication has been observed in tongue epithelium of immune-compromised Aids patients (99) and occasionally in immune-competent carriers (187), indicating that infection of epithelial cells does have a role in primary infection.

EBV initially establishes a lytic infection within the oropharynx and a latent infection in circulating peripheral B cells. Virus replication within the oropharynx and the proliferation and expansion of the B cell pool results in a strong cytotoxic T lymphocyte (CTL) response, predominantly against lytic antigens, which is responsible for the symptoms of IM. The production of large numbers of $CD8^+$ CTLs leads to hyper-activation of the immune system (188, 189); however, this fails to completely clear the infection, and EBV remains detectable in throat washings and in a latent form within the B cell pool (122).

As well as virus replication within the oropharynx IM patients also show infection of the B cell pool circulating within the blood stream, typically one in 10^4 cells (190, 191). It has been shown that infection of the B cell system is underway long before any symptoms of IM become apparent (192). After amplification of cytotoxic EBV specific T cells has taken place there remain some EBV infected B cells which have evaded the immune response and a balance is reached with typically 1 in 10^5-10^6 peripheral B cells infected (193).

The targets of EBV are primarily resting naïve B cells, which it then drives to become proliferating lymphoblasts (194). The drive towards proliferation by EBV mirrors that which occurs through antigen activation (152). Infected tonsillar B cells differ in both morphology and antigen expression (195, 196). Most are proliferating LCL-like cells with a latency III pattern of expression. However, there are other subsets, which express EBNA2 without LMP1 or have a

latency II Hodgkin's Disease like morphology, known as the default programme, and express LMPs without detectable EBNA2 (197).

Long term, EBV persists in a very restricted form of latency, latency 0, within the memory B cell pool (151). Although the mechanism of entry into the memory B cell pool is controversial, the widely-accepted germinal centre (GC) model predicts that infection of naive B cells mirrors their activation by antigen and drives them towards proliferation (152). Naive B cells are activated by antigen stimulation, although, in the case of infection, this activation occurs as a result of the growth transforming programme and the Lat III pattern viral gene expression (198). Infected B cells are driven to the follicle where formation of the germinal centre occurs and viral gene expression is down-regulated to a Lat II Hodgkin-like programme, referred to as the default pattern. LMP1 and 2 mimic CD40 ligand binding and activation of the B cell receptor (BCR), respectively, to constitutively feed the B cell signals that encourage survival within the germinal centre and formation of memory B cells (199). In memory B cells latent gene expression is down modulated to latency 0, or 'the latency programme', where only EBERs and BARTs are expressed (152).

Another model to explain how EBV establishes itself in memory B cells is that of the direct infection of memory B cells without going through the GC (196, 197). X-linked lymphoproliferative (XLP) patients, who cannot form germinal centres, still harbour latent EBV, indicating that EBV can persist without going through a GC reaction (200). Latent EBV can be found in IM patients, within B cell subsets which arise independently of the GC. These include non-isotype switched memory B cells (201, 202) and tonsilar B cells, which localise to extra follicular sites as opposed to the GC (134, 197). IM derived tonsilar B cells do not express two of the GC markers (CD10 and CD77) but express a third (CD38) as a consequence of growth activation (201).

EBV can reactivate from latently infected memory B cells *in vivo* and produce plasma cells which localise to mucosal surfaces such as the oropharynx (203). A limited number of these then reactivate the lytic programme to release virus into the tonsils. Infected epithelial cells may play a role in amplifying the amount of virus in the saliva and infection of new B cells serves to replenish the reservoir of infected cells (183).

1.8 Apoptosis modulation by EBV

1.8.1 Apoptosis modulation by lytic cycle antigens

In latently infected cells, BZLF1, along with BRLF1, is a key regulator of the switch from latent to lytic cycle. BZLF1 recognises, and binds to, CpG methylated promoters (204). Upon infection EBV immediately establishes a latency in order to restrict antigen expression and avoid the host immune response. As the latent phase continues, promoters are slowly methylated and are eventually activated by BZLF1 which drives the entry into lytic cycle and productive infection (205). To escape the host response that comes with activation of the lytic phase BZLF1 has the ability to down-regulate CD74, the invariant chain involved in the translocation of MHC class II, which present antigen to $CD4^+$ T cells (206). CD74 also has a role in upregulating BCL-2 and BCL_{XL} (207), and so CD74 down-regulation is required for immune evasion but also results in increased propensity for apoptosis.

This increased susceptibility to apoptosis is mainly countered by the expression of the viral BCL-2 homologues BHRF1 and BALF1. Together, BHRF1 and BALF1 are essential for preventing apoptosis during primary infection (98) and are expressed as early genes to suppress apoptosis during lytic cycle (96, 97) (see section 1.4).

BARF1is also expressed as an early protein during the lytic cycle. The protein is secreted into the extra-cellular matrix and acts as a receptor of human colony stimulating factor 1 (hCSF-1). BARF1 modulates the host immune response by antagonising soluble hCSF-1 (208). HCSF-1 has a role in differentiation and proliferation and may also modulate the immune response and T-cell proliferation. (209). While there is evidence that BARF1 can modulate apoptosis and have a transforming effect it is also now known to also be expressed during latency(210) and so will be discussed in later sections.

There is some evidence that in a gastric cancer cell background ectopically expressed BARF1 can influence transcription of certain genes involved in apoptosis and cell growth. These may include pro-apoptotic genes such as caspases. BARF1 may induce cells to leave senescence and start to proliferate by up-regulation of proliferation promoting genes, FOS and C-JUN (210). BARF1 may also be able to activate anti-apoptotic BCL-2 expression in Akata cells and cause tumour formation in SCID mice (211).

It is not known whether it is the intracellular form of BARF1 that up-regulates BCL-2, or if the secreted form activates cellular pathways which eventually raise BCL-2 levels. It is also not known whether the apparent proliferation inducing abilities of BARF1 are real or whether BARF1 merely enables oncogenically transformed cells to proliferate without undergoing apoptosis ((212) see Figure 1.10 for detailed overview).

1.8.2 Apoptosis modulation during latency

When EBV transforms normal B cells into lymphoblastoid cell lines (LCLs) latent gene expression is established from the Cp and Wp promoters, with the Cp promoter being highly active with a low level of expression from the Wp promoter (101). A wide range of genes are expressed including six nuclear antigens, EBNA1, 2, 3a, 3b, 3c and –LP, three membrane

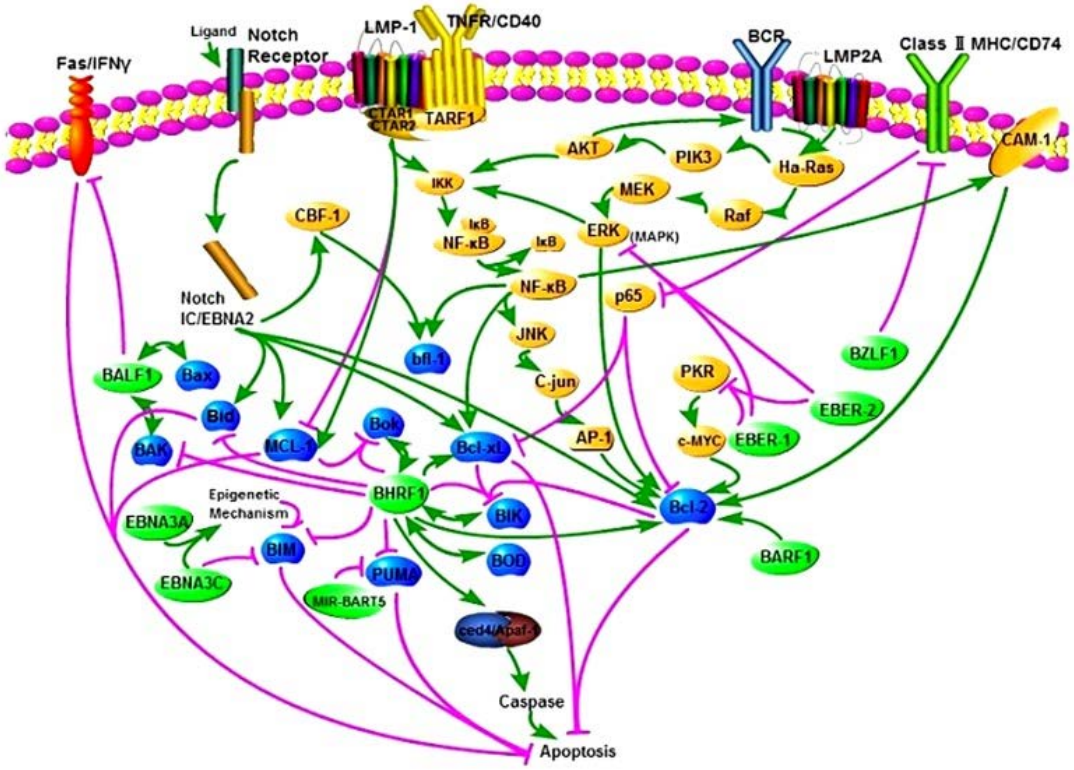

Figure 1.10: EBV interactions with the Bcl2 family: EBV interacts with BCL-2 homologues directly and interferes with cellular apoptotic pathways. BZLF1 down-regulates BCL-2 and BCL_{XL} by down-regulating CD74 which aids in avoiding the immune response. Pro-survival EBV interactions are shown in green. Expression of BHRF1 and BALF1 can counteract BCL-2 and BCL_{XL} down-regulation by interacting with cellular pro-apoptotic BCL-2 homologues including BAX and BAK and, in the case of BHRF1, also many BH3-only homologues. BARF1 up-regulates BCL-2 protein. LMP1 inserts into the cell membrane and mimics the signalling of activated CD40. LMP1 rapidly, but transiently, up-regulates MCL1 then activates the NFκB pathway to up-regulate BCL-2 and A1 (BFL-1). LMP2a also up-regulates BCL-2 and BCL_{XL} through Ras activation and the NFκB pathway. EBNA2 up-regulates the anti-apoptotic and some pro-apoptotic BCL-2 homologues. EBNA3a and 3c down-regulate pro-apoptotic BIM through epigentic mechanisms. EBER-1 and 2 inhibit PKR and up-regulate BCL-2 and miR-BART5 can down-regulate PUMA. Adapted from (212)

proteins, LMP1, 2a and 2b (213), non coding EBER RNAs and BARTs (*Bam*HIA rightward transcripts) which encode many miRNAs (101, 176). This unrestricted expression of latent antigens has the potential to induce an anti-viral response and to drive infected cells into apoptosis. To counteract this, along with having functions involved in proliferation etc. many of these proteins also interact, directly or indirectly, with cellular BCL-2 homologues (Figure 1.10). Understanding the role that EBV latent antigens play in apoptosis will help us better understand the many EBV related malignancy in which EBV maintains various patterns of latent gene expression.

1.8.2.1 EBNAs

EBNA mRNAs are transcribed as a long primary transcript from the Wp promoter immediately after infection, and then later from the Cp promoter (214, 215). The individual EBNA mRNAs are generated by differential splicing of the same 'rightward' transcript (reviewed by (216)). EBNA1 is a nuclear phospho-protein required for the replication and maintenance of the viral genome. It is essential for regulating transcription of the transforming genes and acts by maintaining origin recognition complexes which bind to plasmid origins of DNA synthesis, and also aids retention of plasmids in the host cell (217). EBNA1 binds to the origin of replication *oriP* to up-regulate transcription from both Wp and Cp promoters (218).

The switch from Wp to Cp promoters observed in early B cell infection is a result of the transactivation of the Cp promoter by the acidic phospho-protein EBNA2 (219). Mutation of the EBNA2 binding region upstream of Cp leads to increased transcription of Wp and a decrease in transcription from Cp (218). EBNA2 transcriptionally activates cellular and viral genes with a promoter core sequence of GTGGGAA and to the gene by sequence specific binding protein, RBP-Jκ, a Notch activated transcription factor (220). The ability to bind RBP-Jκ

makes EBNA2 functionally equivalent to Notch (221). Interaction with RBP-Jκ may also lead to up-regulation of the anti-apoptotic BCL-2 homologue A1 (222). EBNA2 trans-activates the LMP promoters and the cellular growth genes; CD21, CD23 and c-myc (223, 224).

The EBNA3 family of proteins (EBNA 3a, 3b and 3c) are encoded by a tandem arrangement of genes with a similar organisation (146). They act *in vitro* to activate transcription from the LMP1 promoter in the presence of EBNA2 and are also associated with RBP-Jκ indicating a role in transcriptional regulation (225-228). This competes with the binding of RBP-Jκ by EBNA2 enabling EBNA3a and EBNA3c to act as regulators of EBNA2 function (213). EBNA3 proteins also bind to chk2/cds1 checkpoint kinase and in doing so can disrupt the G_2/M cell cycle checkpoint (229).

EBNA3a and 3c have been found to co-operate to down-regulate the pro-apoptotic protein BIM and are essential for immortalisation of B cells (230). This most likely occurs at the transcriptional level through epigenetic regulation and CpG methylation. This probably provides another mechanism for EBV to overcome the apoptotic effect of Eμ-myc seen in BL lines as well as the activation of myc by EBNA2 (231). There is an unconfirmed report that EBNA3b also up-regulates the expression of cellular BCL-2, although the mechanism for this is not known (232).

1.8.2.2 LMP1 and LMP2a and 2b

The latent membrane protein LMP1 is essential for transformation, and is transcribed from an EBNA2 activated latency III promoter, a latency II STAT regulated promoter and a lytic promoter which expresses truncated LMP1 during late lytic cycle (233-235).

LMP1 has three domains 1) a short N-terminal tail which tethers the protein to the membrane and protrudes into the cytoplasm, 2) six trans-membrane loops which may have a role in

regulating autophagy (236,) 3) a long C-terminal cytoplasmic region with three domains (CTAR-1 to -3) (237). These CTAR domains provide docking sites for various adaptor proteins such as TRADD, RIP and JAK-3 proteins and signal through a plethora of pathways including NFκB, JAK/STAT and JNK (238, 239). In this way LMP1 functions as a viral mimic of the TNFR1 family member, CD40 (see Figure 1.1 for an overview of TNFR signalling).

LMP1 has been shown *in vitro* to up-regulate anti-apoptotic cellular BCL-2 homologues MCL-1 and BCL-2. The up-regulation of MCL1 occurs rapidly following LMP1 expression indicting that it functions as an immediate response to enable cells to survive until BCL-2 is maximally up-regulated after around 48-72 hours. MCL-1 up-regulation by LMP1 is transient and falls off once BCL-2 is expressed (240).

LMP1 and cellular BCL-2 are known to act synergistically to overcome growth inhibition induced by p53 in B cells (241). This appears to be specific to B cells and is a result of the ability of LMP1 to activate NFκB (242). The up-regulation of anti-apoptotic BCL-2 homologues may be involved in the selection of memory B cells from the germinal centre pool. These cells have been programmed to die unless selected by antigen recognition at which point BCL-2 is thought to be up-regulated. EBV may use LMP1 to mimic this process and allow infected cells to survive and become memory B cells (241).

Finally, LMP1 also acts to up-regulate A1. The importance of A1 upregulation may relate to the fact that LMP1 regulates itself through induction of the unfolded protein response and autophagy, induced by the N-terminal domain and six transmembrane domains(243). However, the unfolded protein response and autophagy also have the potential to lead to apoptosis. This effect is blocked by the C-terminal domain of LMP1 which up-regulates expression of anti-apoptotic A1 through its ability to mimic CD40 signalling. In this way reactions to the N-

terminal and transmembrane domains are prevented from driving the cell into apoptosis (244, 245).

The LMP2 family, LMP2a and LMP2b, have similar almost identical structures, with twelve trans-membrane domains and a cytoplasmic C-terminus 27 amino acids long. The LMP2s are not essential for transformation but LMP2a has been shown to mimic B cell receptor (BCR) activation (246). The N-terminal domain of LMP2a engages BCR associated signalling pathways and promotes survival (247). This survival effect may be through the NF-κB mediated upregulation of Survivin, BCL-2 and BCL_{XL} (248-251). Overall LMP2a appears to maintain EBV latency and prevents inappropriate activation of the lytic cycle by blocking B cell receptor signals which would lead to virus reactivation but mimicking B cell receptor activation in other pathways to maintain cell survival (216, 252). However, LMP2a may also be able to induce lytic cycle in the absence of BCR receptor signalling, providing a way to control lytic activation independently of the BCR (253).

(254)LMP2b lacks this N terminal domain needed for LMP2a function, but may have a role in down-regulating the level of LMP2a in order to promote activation into lytic cycle (252, 254).

1.8.2.3 EBERs and BARTs

The non-coding EBER-1 and EBER-2 transcripts are expressed in all forms of latency to the extent that they are sometimes used as indicators of latent infection (176). They are small RNAs expressed in very high numbers and bind to double stranded RNA. They may interact with, and inhibit the double stranded RNA dependent protein kinase (PKR). PKR is induced by interferon and activated by double stranded RNAs produced during viral replication, it acts to cause shutdown of protein translation in infected cells and may be a form of antiviral response (255). Studies of EBER expression in a variety of EBV loss and EBV negative cell lines have

shown that EBER expression protects cells from IFNα induced apoptosis various cell lines (256-258), although this protection may not be solely dependent on PKR (257, 259). EBERs also up-regulate the expression of BCL-2 through interaction with PKR but the mechanism for this is unknown (257).

BARTs are small, non-coding RNAs that are processed into miRNAs and expressed in both epithelial and B cells during all forms of latent and lytic cycles. There are at least 21 miRNAs, of 22–24 nucleotides in length, expressed from BART RNA derived introns (176). BART miRNAs have been found to negatively influence the expression of several EBV genes including BALF5 and LMP1 (260, 261), as well as cellular PUMA (262) by repressing translation or inducing mRNA degradation. The 3’ UTR of LMP1 has several complimentary matches to BART miRNAs. Binding of these miRNAs can suppress LMP1 expression and prevent over-expression which can lead to loss of proliferation and susceptibility to apoptosis (261, 263). Both clusters of BART miRNAs down-regulate the pro-apoptotic BCL-2 homologue BIM post-transcriptionally by binding to miRNA recognition sites within the 3' UTR (264).

1.8.2.4 BHRF1

Although traditionally thought to be a lytic cycle antigen, the vBCL-2 homologue, BHRF1, has now been shown to be expressed during latency(101). This was first discovered in Wp restricted BL lines, in which, latent expression is restricted to the Wp promoter due to deletion of a fragment spanning the EBNA2 gene(101). It is known that the Wp promoter remains active at low levels in LCLs (218, 265) and BHRF1 was also found to be expressed at low levels in LCLs(101).

BHRF1 is known to be highly anti-apoptotic(97)(for more detail see section 1.4.1) and to protect from a variety of anti-apoptotic stimuli including chemotherapeutic agents(106). This could have important implications for the treatment of EBV related malignancies, especially BL, in which 15% of endemic cases express the Wp-restricted form of EBV(101).

1.9 Burkitt lymphoma:

The discovery of endemic Burkitt lymphoma by Denis Burkitt led to the discovery of EBV (see section 1.5.3). However, EBV is not required for the development of Burkitt lymphoma. Two other forms of BL exist, sporadic and AIDS-associated, which occur worldwide but with a lower incidence than endemic BL (266). Whereas endemic BL is nearly always EBV associated, EBV is a contributing factor in only 15–80% of sporadic cases, depending on geographic location, and 40% of AIDS-associated cases (267). BL is a tumour derived from germinal centre B cells and presents slightly differently depending on the form. Endemic BL usually presents in children as a tumour on the jaw or within the abdomen, whereas sporadic BL is seen in older children and adults, and causes an abdominal mass to form (267).

All forms of BL share the chromosomal translocation of MYC on chromosome 8 with one of the immunoglobulin genes on chromosome 14, 2 or 22. It has been proposed that these translocations most likely arise during the germinal centre reaction through the action of AID, the enzyme involved in somatic hypermutation and class switch recombination (268). This translocation causes the MYC oncogene to become constitutively active and drives cell growth and proliferation but also increases sensitivity to apoptosis (269, 270). MYC induces a large number of pro-apoptotic genes and inhibits the expression of anti-apoptotics as a failsafe to prevent oncogenesis from the over-expression of MYC (271, 272) (reviewed in (273) (Figure 1.11).

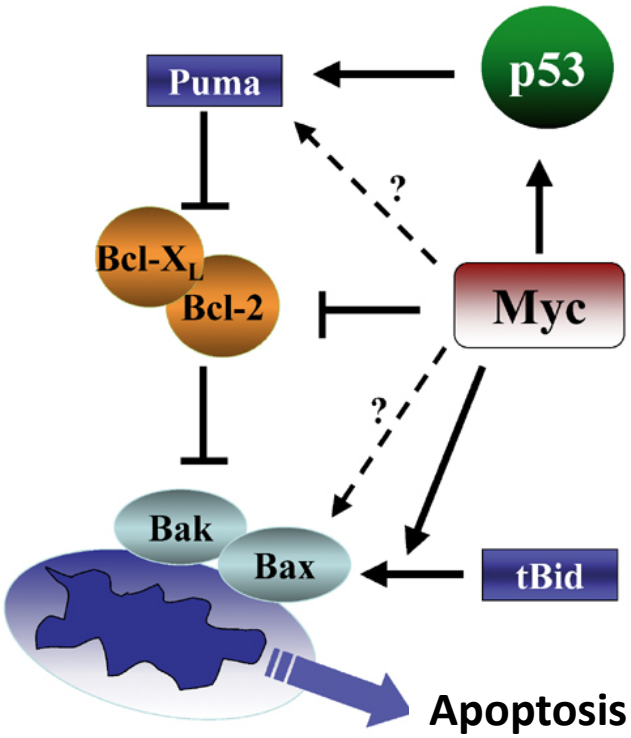

Figure 1.11: Myc interactions with the BCL-2 family. Myc can upregulte levels of PUMA through direct activation or through activation of p53. Myc can suppress the levels of BCL-2 and BCL_{XL} , either directly or through PUMA. Myc provokes the mitochondrial localisation of t-BID. Myc may activate BAX directly but also contributes to BAX and BAK activation through PUMA and BID. (Adapted from 272)

In order to undergo tumorgenesis cells need to aquire other mutations in addition to MYC translocation to counteract the apoptotic effect of MYC. These take the form of genetic mutations or epigenetic modifications that suppress the apoptotic pathway. In BL cells these alterations often occur in p53, with 30% of endemic BL tumours and 70% of BL cell lines having mutations in p53(274). Those cells that do have a wild type p53 often have changes at some other point in the p53 pathway such as over-expression of MDM2(275) (reviewed in (276)).

The observation that EBV positive BL is more resistant to apoptosis than BL lines that have spontaneously lost EBV indicates that EBV can also contribute to the suppression of MYC induced apoptosis (256). In endemic BL only EBNA1 protein is expressed and this has been shown to inhibit apoptosis in the absence of the viral genome (277). For example, EBNA1 may be able to destabilise p53 or MDM2 by binding the ubiquitin-specific protease USP7 which would normally stabilise P53 and MDM2 (278). EBNA1 provides protection for BL lines against low levels of apoptotic stimuli. However, the EBERs and BART non-coding RNAs are also expressed and have been shown to interact with cell death pathways and down-regulate pro-apoptotic BCL-2 homologues (see section 1.8.2).

1.9.1 Wp-restricted BL and BHRF1:

In EBV positive Burkitt lymphoma there are two forms of latency which are quite different from latency III seen in LCLs (Figure 1.10). The first, found in cells containing a wild-type EBV genome, is known as latency 1 and expresses EBERs and BARTs as well as just one protein, EBNA1, from the EBNA1 specific promoter, Qp (148, 279). The second form of latency in BL is known as Wp restricted latency where the W promoter is used to express all EBNA proteins, except EBNA2, including a truncated form of EBNA-LP and also the BARTs and EBERs (178). Wp restricted EBV has arisen by infection of the progenitor cell with a mutant EBV genome

containing a deletion of the EBNA2 gene and some upstream and downstream sequences. The EBNA2 deletion also removes the whole *Bam*H1 Y fragment as well the Y1 and Y2 exons of the C-terminus of EBNA-LP to give a truncated form (178). The deletion of the EBNA2 gene causes the W promoter to remain active, as the C promoter is not activated in the absence of EBNA2 (176). This results in an expression pattern more similar to LCLs than to Lat I BL, with expression of EBNA1, the EBNA3s, truncated EBNA-LP, BARTs and EBERs, but not of EBNA2 or the LMPs. Similar effects have been observed when the EBNA2 binding region upstream of Cp is mutated leading to transcription down-regulated from Cp but up-regulated from Wp (218).

The Wp restricted form of latency is expressed in 15% of endemic BL cases, which is high for a mutation which is so rare. Expression of the least restricted form of latency (Lat III) in which all latent antigens are expressed, increases immunogenicity *in vivo* and is not compatible with the BL phenotype or high c-myc expression *in vitro* (280, 281). As Wp restricted latency is selected for, not against, this indicates that EBNA2 and the LMPs are the source of incompatibility between the virus and c-myc driven growth programme (282).

Wp restricted latency offers much higher protection against cell death caused by factors such as environmental stress and apoptosis inducing drugs such as anti-IgM and ionomycin than latency 1 infection. When compared to EBV-loss lines latency 1 infection gives only partial protection at low doses. This could also explain why a rare mutant such as the EBNA2 deletion is found at such high numbers in BL patients (101, 282).

The heightened protection of Wp lines from apoptosis was initially thought to be the result of truncated EBNA-LP or the EBNA3s. Although truncated EBNA-LP may be protective (283), it is not detectable in all Wp restricted BLs even though they show a resistant phenotype (179). Kelly *et al.* found that transfection of EBNA3 expressing plasmids into latency I BL lines Sav and Akata gave no protection from apoptosis induced by ionomycin and anti-IgM, despite the

ability of EBNA3a and 3c to down-regulate BIM (see section 1.8.2)(101, 230). After the discovery of BHRF1 expression in Wp restricted BL, the BHRF1 protein became another possible mediator of the apoptotic resistance in Wp BL. The latent expression of BHRF1, is sufficient to protect latency I and EBV loss BL lines from apoptosis (101). BHRF1 has also been found to be expressed at lower levels in LCLs (101), and is promiscuously expressed immediately after infection when Wp is transiently active (98).

The expression of BHRF1 during latency coupled with its strong anti-apoptotic ability may have important implications for the treatment of EBV related malignancies. BL usually responds well to chemotherapy and yet approximately 10–25% of paediatric and 14–53% of adult patients with BL will relapse despite intensive chemotherapy, and face an extremely poor prognosis (284). This resistant subset of BL could be a result of latent BHRF1 expression. BHRF1 has been shown to render Eμ-myc mice resistant to treatment (104). Treatment of BL could greatly benefit from agents which sensitise BL cells to chemotherapy, either to overcome resistance to chemotherapy or to avoid using very aggressive treatment regimen on frail patients. More knowledge of how BHRF1 protects from apoptosis in BL lines, and how it interacts with cellular BCL-2 homologues, could further knowledge into BL pathogenesis and possible mechanisms for overcoming resistance to treatment.

1.10 Aims and objectives

In this work we focused on the ability of the EBV encoded viral BCL-2 homologues, BHRF1 and BALF1, to protect from apoptosis.

BHRF1 is known to have a strong anti-apoptotic effect(97) and previous studies have shown that it is expressed in latent BL lines and could potentially cause BL to be resistant to treatment *in vivo*(101, 285).

This protein has a 38% sequence homology to cellular anti-apoptotic BCL-2, but a much greater structural similarity(46). However, it is not known how similar BHRF1 is to BCL-2 in terms of its interactions with cellular pro-apoptotic BCL-2 homologues, and how these mechanisms translate into the ability of BHRF1 to protect from different apoptotic stimuli. We aimed to determine the ability of BHRF1 to bind cellular pro-apoptotic BCL-2 homologues in an EBV negative BL background and the importance of certain BCL-2 homologues for the function of BHRF1. To look at binding to cellular BCL-2 homologues we used mutants of BHRF1, kindly provided by Dr. Marc Kvansakul. These contain point mutations of several amino acids within the binding groove of BHRF1, the area which interacts with the BH3 domains of cellular anti-apoptotic BCL-2 homologues.

In chapter 3 we describe the construction of a lentivirus vector, TREX(gene)UTG, from two precursor lentivirus plasmids, donated by Dr. Marco Herold(286).

Cloning and HA tagging of the BHRF1 wild type protein was performed, and protein expression from the lentivirus, transduced into two EBV negative BL backgrounds, was characterised.

In chapter 4 we describe the BHRF1 binding groove mutants. They were expressed using lentiviruses in the same manner as the wild type. We tested their ability to protect from apoptosis induced by a variety of cytotoxic drugs, working through several different pathways. We aimed to determine the ability of BHRF1 to protect from apoptosis when binding to specific cellular BCL-2 homologues was prevented. This was achieved through the individual binding groove mutations which reduced binding to BCL-2 homologues, and through knockdown of pro-apoptotic BCL-2 homologues. In this manner we aimed to determine which

BCL-2 homologues were bound by BHRF1 and were important for its anti-apoptotic effect. Secondly, we aimed to discover if any of the amino acids mutated in the BHRF1 binding groove were essential for its function.

In chapter 5 we focused on the second viral BCL-2 homologue, BALF1. This protein is not well characterised and there is contention as to whether it is pro- or anti-apoptotic, when it is expressed, and whether it can inhibit BHRF1(41, 96, 98, 112).

Firstly, we aimed to determine if BALF1 is expressed during latency, and if so, if this expression is restricted to a latency or cell type. Secondly, we aimed to determine if BALF1 was pro- or anti-apoptotic, and, thirdly, if BALF1 was able to abrogate the function of BHRF1.

2. Materials and methods

2.1 Cell Culture

2.1.1 Cell Lines

The present study used a number of EBV-positive cell lines derived from BL tumours, including Latency I BL lines Chep-BL, MutuI-BL cl.59, Sav-BL, Ezema-BL, Akata-BL, Kem-BL and Dante-BL (287, 288), Latency III BL lines MutuIII-BL and GlorIII-BL, and Wp-restricted BL lines Avako-BL, Salina-BL and Oku-BL (178). EBV-negative cell lines derived from sporadic BL tumours included DG75 (289), BL2 (290) and BL41 (291).

In addition, a number of virus-transformed LCLs were used in this study: X50/7 LCL (292) and CD+OKU (178), IM51.1, IM81.1, IM83.1 and IM93.1 (293), and EH LCL1 and EH LCL2 (294). IM51.1, IM81.1, IM83.1 and IM93.1 are spontaneously transformed B cell lines derived from the peripheral blood of infectious mononucleosis patients. EH LCL1 and EH LCL2 were obtained by infecting EBV-negative B cells with recombinant 2089 EBV.

RNA from three lines of EBV positive T/natural killer (NK) cell origin and two lines with epithelial cell origin was used, one originating from chronic active EBV (SNK10) and two others from T/NK cell lymphomas (SNK1 (295) and SNK6 (296)) (297). SNT8 and SNT16 are T cell lymphoma lines which were established from a nasal T cell lymphoma (SNT8) (298) and peripheral blood from a case of chronic active EBV (SNT16) (297). C666.1 is an EBV positive nasopharyngeal carcinoma line with an epithelial origin and latency II phenotype (299), AGS + EBV is a gastric carcinoma cell line, with an epithelial cell line, infected *in vivo* with EBV (300). RNA from the Hodgkin lymphoma line, L591, was also analysed (301, 302).

The 293FT cell line (Invitrogen) was used to package lentivirus stocks.

2.1.2 Maintenance of Cell Lines

All cells were grown at 37^0C with 5% CO_2. Adherent cells and suspension cells were grown in 100mm plates and 25cm^2 flasks, respectively. BL lines were maintained in exponential growth in RPMI 1640 (Sigma) supplemented with 10% foetal calf serum (FCS) (Biosera), 20nM bathocupronine disulfonic acid (Sigma), 50mM α-thioglycerol (Sigma), 1mM pyruvic acid (GIBCO), 2mM L-glutamine (GIBCO) and penicillin/streptomycin (GIBCO). 293FT cells were grown in RPMI 1640 supplemented with 10% heat-inactivated FCS (56^0C for 1 hour) and 200µg/ml G418 (Life Technologies).

2.1.3 Cryopreservation and Recovery of Cell Lines

Approximately 10^7 cells were harvested at exponential growth (suspension cells) or 80% confluence (adherent cells), and collected by centrifugation at 450 x g. The cells were resuspended in ~1ml freezing media (RPMI/40% FCS, 10% dimethylsulphoxide (DMSO) and 2mM L-glutamine) and transferred to a sterile freezing vial. Cells were cooled gradually at a rate of 1°C per minute, by storage overnight at -80°C in a freezing container filled with isopropanol (Mr. Frosty^{TM}). For long-term storage, freezing vials were transferred to the gas phase of liquid nitrogen (-180°C).

When needed, cells were thawed at 37°C for 1–2 minutes, transferred to 15ml of pre-warmed media, centrifuged for 5 minutes at 450 x g, resuspended in 10ml media and transferred to a 25cm2 flask (suspension cells) or a 100mm plate (adherent cells).

2.2 Quantitative RT-PCR Analysis

2.2.1 RNA Extraction

Approximately 1-3 x 10^6 cells were collected by centrifugation. RNA isolation was then performed using the Nucleospin RNA (Machery-Nagel) mini kit as per manufacturer's instructions, including an optional DNAse I treatment using the DNA-free™ (Ambion) kit. RNA samples were eluted in 60µl of nuclease-free H_2O (Ambion), concentrations assesed using a Nanodrop spectrophotometer (Thermo Scientific), and finally diluted to 100ng/µl. All RNA preparations were stored at -80°C.

2.2.2 Reverse transcription

All cDNA synthesis was performed using the qScriptTM cDNA supermix (Quanta Biosciences) kit, as per manufacturer's instructions. Approximately 500ng input RNA was reverse transcribed in a 20µl reaction volume and incubated for 5 minutes at room temperature, to allow for optimal primer annealing, followed by 1 hour at 42°C and 5 minutes at 90°C. Following synthesis, cDNA was diluted to a total volume of 100 µl, using nuclease-free H_2O, and stored at -20°C.

2.2.3 QPCR

Levels of latent BHRF1 and BALF1 transcripts were determined by QPCR, using published primers and probes (101). A new assay was designed to detect lentivirus-expressed latent BHRF1 transcripts (unpublished). EBV plasmid standard (unpublished data) is a new plasmid used to calculate EBV gene copy number; it contains one copy of each EBV gene along with a single copy each of the cellular housekeeping genes

glyceraldehyde-3-phosphate dehydrogenase (GAPDH), phosphoglycerate kinase 1 (PGK1) and Beta-2 microglobulin (B2M). Real time quantitative PCR was performed on an Applied Biosystems 7500 machine. All samples were run in triplicate as follows: 10 minutes at 95°C, followed by 40 cycles of 15 seconds at 95°C and 60 seconds at 60°C. Serial dilutions of either Avako-BL (lentivirus assay) or EBV copy number plasmid (unpublished data) (latent BHRF1, BALF1) were run in duplicate on the same plate, in order to generate a standard curve for relative quantification. Data was normalized to either cellular GAPDH (Assay ID: NM_002046.3), PGK1 (Assay ID: NM_000291.2) or B2M (Assay ID: NM_004048.2) expression, using commercially available assays (Applied Biosystems). Normalized data were either expressed relative to Avako-BL (assigned a value of 1) or EBV copy number plasmid (expressed as copy number).

2.3 Western blotting

2.3.1 Protein Quantification

Approximately $7x10^6$ cells were collected by centrifugation, washed twice in ice-cold phosphate buffered saline (PBS) and placed on ice. Cells were lysed and proteins solubilised via the addition of 50µl Urea buffer (9M Urea, 5mM EGTA, 5mM EDTA, 2-4% CHAPS, 1% DTT); cells were further disrupted by sonication for 20 seconds.

Determination of protein concentration was determined using the Bio-Rad DDC Protein Assay. Briefly, aliquots of cell lysates were diluted 5-fold in Urea buffer. Duplicate 5µl samples were placed in a 96 well plate; additionally, duplicate 5µl protein standards containing 5, 2, 1, 0.5, 0.2 and 0.1mg/ml BSA were loaded in order to generate a standard

curve for protein quantification. Reagents A (25µl) and B (200µl) were added to each well, as per manufacturer's instructions, after which the microplate was left to incubate at RT for 15 minutes. Absorbance was measured at 630nm using a 96 well plate reader, and protein concentration determined against a line of best fit drawn on the BSA standard curve.

Protein samples were then diluted to a 2 mg/ml concentration using Gel Sample Buffer (0.4M sodium 2-mercaptoethanesulfonate (MESNA), 125mM Tris-HCL pH 6.8, 0.004% v/v bromophenol blue, 4% v/v SDS and 20% v/v glycerol), and denatured by boiling for 10 minutes. Samples were either used directly or stored at -20°C.

2.3.2 Protein Electrophoresis and Membrane Transfer

NuPAGE 4-12% Bis-Tris gels (Invitrogen) were assembled into the XCell SureLock Mini-Cell system, as per manufacturer's instructions, using 1x NuPage MES SDS running buffer (Invitrogen) diluted in distilled water. Protein samples were re-solubilised at -80°C for 5 minutes and 20µg protein added per well. Additionally, 10µl SeeBlue Plus2 Prestained Standard (Invitrogen) was added to one well. Protein electrophoresis was performed at 100V, 250mA for 90 minutes.

Upon completion, the gel casing was cracked open, and the gel assembled into an XCell II blot module (Invitrogen) together with a PVDF membrane, as per manufacturer's instructions. The PVDF membrane was pre-soaked up to 10 seconds in 100% methanol, and then in transfer buffer (2.5mM Tris-Base (Fisher Chemicals), 0.192M Glycine (Sigma), 20% Methanol) until needed. Protein transfer was performed at 30V for 100 minutes, using transfer buffer.

2.3.3 Membrane Blocking, Antibody Binding and Detection

Following transfer, the PVDF membrane was washed 3 times for 5 minutes in PBS with 0.1% Tween-20 (PBS-T) and blocked 1 hour in 5% milk diluted with PBS-T on a rocking platform. Primary antibodies were diluted in 5% milk PBS-T and incubated with the PVDF membrane, either at RT for 2 hours or at 4°C overnight. Following primary antibody binding, membranes were washed at least 6 times over 30 minutes. Secondary antibodies conjugated to Horseradish peroxidise (Sigma) were diluted n 5% milk PBS-T and incubated with the PVDF membrane at RT for 1 hour. Following secondary antibody binding, membranes were washed as before (see Table 2.1 for antibodies).

The PVDF membrane was treated with Amersham ECL western blotting detection reagents (GE healthcare), as per manufacturer's instructions, and loaded into a film cassette together with a CL Xposure X-ray film (Thermo Scientific). The film was exposed for an appropriate length of time and developed using a Kodak X OMAT 1000 film processor.

2.4 Construction of Plasmid Vectors

2.4.1 PCR of Cloning Inserts

Reaction volumes were made up as follows: 500ng of template DNA, 5µl 2mM dNTPs (Fermentas), 1U Expand High Fidelity Enzyme Mix and 1X buffer with $MgCl_2$ (Roche), and 1.5µl each of a 1µM forward and 1µM reverse primer in a final reaction volume of 25µl (see Table 2.2). The PCR reaction was run under the following conditions: 94°C for 5 minutes, 54^0C for 30 seconds, 35 cycles of 94°C for 60s, 56°C for 60s and 72°C for 1 minute, and a final extension of 72°C for 10 minutes. The PCR product was A-tailed using 5U of standard Taq

Table 2.1: Antibodies used in Western Blot

Target Protein	Primary Antibody	Animal	Final dilution	Primary Antibody	Working Dil.
BHRF1	5B11; In House	Mouse	1/500	HRP goat anti-mouse; Sigma	1/1000
HA	3F10; Roche	Mouse	1/1000	HRP goat anti-rat; Sigma	1/1000
HA	HA.11 clone 16B12; Covance	Mouse	1/500	HRP goat anti-mouse; Sigma	1/1000
BAD	C-7; Santa-Cruz	Mouse	1/1000	HRP goat anti-mouse; Sigma	1/1000
BAK	N-20; Santa-Cruz	Goat	1/200	HRP donkey anti-goat; Sigma	1/10000
BAX	N-20; Santa-Cruz	Rabbit	1/500	HRP goat anti-rabbit; Sigma	1/2000
BCL-2	C-2; Santa-Cruz	Mouse	1/200	HRP goat anti-mouse; Sigma	1/1000
BCL-XL	H-5; Santa-Cruz	Mouse	1/200	HRP goat anti-mouse; Sigma	1/1000
BID	Bid #2002; Cell Signalling	Rabbit	1/1000	HRP goat anti-rabbit; Sigma	1/2000
BIM	Bim #2819; Cell Signalling	Rabbit	1/1000	HRP goat anti-rabbit; Sigma	1/2000
PUMA	Puma #4976, Cell signalling	Rabbit	1/1000	HRP goat anti-rabbit; Sigma	1/2000
PUMA	D-20; Santa-Cruz	Goat	1/1000	HRP donkey anti-goat; Sigma	1/10000
MCL-1	22; Santa-Cruz	Mouse	1/200	HRP goat anti-mouse; Sigma	1/1000
NOXA	FL-54; Santa-Cruz	Rabbit	1/200	HRP goat anti-rabbit; Sigma	1/2000
β-Actin	β-Actin; Sigma	Mouse	1/10000	HRP goat anti-mouse; Sigma	1/1000
Calregulin	Calregulin; Santa-Cruz	Goat	1/1000	HRP donkey anti-goat; Sigma	1/10000

Table 2.2 PCR and sequencing primers	
PCR primers for replication of cloning insert	
HABHRF1 (forward primer) 5’ – 3’	
GCAGATCTACCATGTACCCATACGATGTTCCAGATTACGCTGCCTATTCAACAAGGGAGATACTGTTAG	
BHRF1 (forward primer) 5’ – 3’	
GCAGATCTACCATGGCCTATTCAACAAGGGAGATAC	
BHRF1 (reverse primer) 5’ – 3’	
AAGAATTCTTAATTAATTAGTGTCTTCCTCTGGAGATAAATAAATAACTAC	
HABALF1 (forward primer) 5’ – 3’	
GCAGATCTACCATGTACCCATACGATGTTCCAGATTACGCTAGGCCAGCCAAGTCTACAGATTCTGTG	
BALF1 (reverse primer) 5’ – 3’	
AAGAATTCTTAATTAATTACAAAGATTTCAGGAAGTCAGTCAGGCTG	
Lentivirus specific sequencing primers 5’ – 3’	
PAC1 FTGW F	CAGGGACAGCAGAGATCCAG
PAC1 R	TCTACGTGGCAGCGCTC
TREX F	GCTCGTTTAGTGAACCGTCAGA

DNA polymerase (Roche), supplemented with 1µl 25mM $MgCl_2$ and 2mM ATP (Fermentas), and incubated at 70°C for 30 minutes.

2.4.2 Restriction Digestion

PCR-amplified inserts and recipient plasmid vector DNA were cut in single or double digests reactions using standard restriction enzymes (Promega or Roche), or Fast Digest restriction enzymes (Fermentas). Typically, 1ug of DNA was digested in a 20ul volume comprising 1µl (1U) restriction enzyme and a 1x concentration of the corresponding restriction enzyme buffer. Reaction volumes were incubated for 30 to 60 minutes (Fast Digest enzymes) or 3 hours (Standard enzymes) at 37°C.

Following digestion, cut vector was capped with Alkaline Phosphatase (Roche), which selectively cleaves terminal phosphate groups to prevent re-ligation of vector DNA. Briefly, cut vector was subjected to two rounds of treatment with 1U of alkaline phosphatase incubation at 37^0C for 30 minutes. Capping was not performed on vectors intended to receive oligonucleotides lacking 5' phosphate groups.

2.4.3 Agarose Gel Electrophoresis

Following digestion, PCR-amplified inserts and recipient plasmid vector DNA were resolved using agarose gel electrophoresis. Agarose gels were made as follows: between 0.8 and 1% agarose (Eurogentec) was dissolved in 1x TBE (88.9mM Boric Acid, 2.49mM EDTA and 88.9mM Tris-Base in distilled water), heated to 100^0C, poured into a casting container and allowed with gel comb inserted. Digested product was mixed with 6x gel loading dye (30%

v/v glycerol, 0.25% w/v bromophenol blue, 0.25% w/v xylene cyanol) and loaded on to the gel; an appropriate volume of 1kb plus ladder (Invitrogen) was loaded into one of the wells.

The gel was run at 80 V in a Flowgen tank containing 1x TBE for an appropriate amount of time. Following completion of the run, the gel was soaked for at least 15 minutes in a bath of distilled water containing 1-5µl 10mg/ml ethidium bromide (Fisher Scientific). Thereafter the DNA was visualised under UV light. Insert bands of correct size were excised and DNA extracted using the QIAquick Gel Extraction kit (Qiagen) as per manufacturer's instructions.

2.4.4 Purification of Vector and Insert DNA

Gel extracted inserts and cut, capped vector DNA were purified using the High Pure PCR product purification kit (Roche), as per manufacturer's instructions. Purified product samples were then made up to a 200µl total volume using DEPC treated nuclease free water (Ambion), and then diluted 1:1 with phenol: chloroform: isoamyl alcohol 25:24:1 pH8 (Sigma). The solution was vortexed for 15 seconds and centrifuged at 16000 x g for 3 minutes. The upper layer containing DNA (~200 µl) was moved to fresh tube; the remaining phenol was diluted 1:1 with fresh DEPC water, and the process was repeated in order to obtain a total volume of 400µl DNA in nuclease free water.

The DNA was then ethanol precipitated by adding 2.5 volumes of 100% ethanol and 1/10 volumes of 3M Sodium Acetete pH 5.2, followed by freezing at -20^{0}C overnight. Next day, the solution was centrifuged at 16000 x g for 15 minutes at 4^{0}C. The DNA pellet was washed in 70% ethanol and allowed to dry at room temperature. DNA pellet was resuspended in clean DEPC treated water and the DNA concentration was determined using a Nanodrop spectrophotometer (Thermo Scientific).

2.4.5 Ligation of Inserts into Plasmid Vectors

The quantity of vector and insert DNA to be used in the ligation reaction was determined using the following calculation: ((ng of vector × kb size of insert) / kb size of vector) x molar ratio of insert:vector = ng of insert. Ligation was performed using the T4 DNA Ligase kit (Promega). A 10µl total reaction volume with 1x ligation buffer and 1U T4 DNA ligase. Ligation mix was incubated for 2-3 hours at room temperature, or overnight at 4^0C.

2.4.6 Bacterial Transformation with Plasmid

50% of ligation mix or 500ng plasmid DNA was transformed into either DH5α or One Shot Stabl3 chemically competent *E. coli* cells (both from Invitrogen). Stabl3 cells were used for cloning of lentivirus plasmids due to their ability to reduce the frequency of unwanted homologous recombination events between the long terminal repeats.

Half an aliquot of either DH5α or Stabl3 cells was used per transformation. Cells were defrosted on ice and a quantity of DNA was added as above. In all cases a DNA-negative control was used; where DNA was derived from a ligation reaction, an aliquot of T4 DNA Ligase untreated DNA was included to control for inefficient digestion / contamination of ligation reagents.

Cells and DNA were incubated on ice for 30 minutes and then heat shocked at 42^0C for a maximum of 90 seconds. Cells were allowed to recover on ice for 2 minutes before 1ml of LB broth (25g/L, Fisher Scientific) was added, after which cells were incubated for 1 hour at 37^0C on a shaker. Cells were centrifuged at 16000 x g for 60 seconds and supernatant was discarded. Cells were resuspended in a small volume of LB broth and spread onto 100mm

plate containing LB Agar (379/L, Fisher Scientific) and 100µg/ml ampicillin (Roche). Plates were then incubated at 37^0C overnight. Prior to use both LB broth and LB agar were sterilised in an autoclave and aseptic technique was used throughout.

2.4.7 Growth of Bacterial Cultures

Several colonies (individual clones) were picked and grown overnight in a shaking incubator at 37^0C, in 3ml LB broth containing 100µg/ml ampicillin. Plasmid DNA was extracted from overnight cultures using the QIAprep Spin Miniprep kit (Qiagen), according to manufacturer's instructions. Desired recombinants were identified using restriction enzyme digestion (as above) and DNA sequencing (see section 2.6, later). Correct clones were grown up in 400ml LB broth with 100µg/ml ampicillin at 37^0C overnight in a 4x volume conical flask. Plasmid DNA was extracted using a Qiagen Plasmid Maxi kit, as per manufacturer's instructions, and DNA concentration was determined using a nanodrop spectrophotometer. Plasmid DNA was then diluted as required in nuclease free water.

2.5 Generation of BL Lines Transduced with Lentiviral Vectors

2.5.1 Preparation of Lentivirus Stocks

293FT cells were split into 100mm plates and grown overnight in media without G418, until a confluence of 70-90% was reached. 293FT cells were transfected with 4µg lentivirus plasmid, 2µg envelope plasmid, pMD2G, and 6µg packaging plasmid, psPAX2, as follows: plasmid/packaging DNA and 26 µl Lipofectamine 2000 (Invitrogen) was added to separate 1.5ml aliquots of Opti-MEM® reduced serum media (Gibco), incubated 5 minutes at

RT, mixed and incubated 20 minutes at RT, added to 293FT cells and left overnight at 37°C. The next day, Opti-MEM® media was replaced with DMEM media (Invitrogen), supplemented with 10% heat inactivated BCS and 1% pyruvic acid. The virus-containing culture supernatant was harvested after 3 days, passed through a 0.45µm filter and stored at -80°C until required.

2.5.2 Spin Infection of BL Lines with Lentivirus

Bl41 cells ($1x10^5$) were incubated at 37°C for 30 minutes with lentivirus (4ml) and 6µg/ml polybrene (Sigma). Cells were then centrifuged for 2 hours (28-30°C) at 2200 RPM (Heraeus 8155 rotor) and plated out in 24 well plates with fresh media. GFP was analysed by FACS 48-72 hours post infection (see section 2.7, later). Infection with siRNA lentivuruses (Santa Cruz biotechnology) was selected using 10µg/ml puromycin (Invitrogen) after 2 passages in culture.

2.6 Sequencing of BHRF1 and BALF1

All sequencing reactions were performed centrally by the Functional Genomics and Proteomics Services (School of Biosciences, University of Birmingham), using an automated Applied Biosystems 3730. 100ng of template DNA was added to 3.2pmol primer and made up to a total volume of 10ul using deionised water. Several sequencing reactions were using the original forward and reverse PCR primer and lentivirus specific sequencing primers (see Table 2.2) including PAC1 FTGW F (sequences forward from Pac1 site across insert in FTGW), TREX F (sequences forward across insert from within TREX promoter in FTGW), and PAC1 R

(sequences backwards across insert in FH1T(gene)UTG and FTGW) (see Table 2.2 for sequencing primers).

2.7 FACS and Cell Sorting

In order to test for the efficiency of lentivirus transduction, as well as stable maintenance of lentivirus DNA, cell lines were assessed for GFP and HA-tagged BHRF1 expression. To assess GFP expression, cells were centrifuged at 450 x g for 5 minutes, washed in PBS and resuspended in 100µl PBS. Measurements were performed using an Accuri C6 flow cytometer (BD Biosciences). Where appropriate, cells were sorted for high GFP intensity using a MoFlo cell sorter (Dako).

To assess the expression of HA-tagged BHRF1 expression, cells were first fixed overnight at 4°C using 1ml IC Fixation Buffer (Invitrogen). The next day, cells were centrifuged at 450 x g for 5 minutes, and the IC Fixation Buffer aspirated. Cells were resuspended in 0.2% Triton X-100 made in PBS, and incubated on ice for 30 minutes to allow for effective cell permeabilization. Subsequently, cells were washed in PBS and incubated for 1 hour at 37^0C with anti-HA antibody (Roche) diluted 1/500 in EBV-negative human serum. Cells were washed again in PBS and incubated at 37^0C with the appropriate APC-conjugated secondary antibody (1/1000) (Stratech Scientific Ltd). Cells were washed one last time and measured using an Accuri C6 flow cytometer.

2.8 Apoptosis Assays

Approximately $2x10^6$ cells were plated out in 24 well plates in BL media (see section 2.1.2), and induced with 1µg/ml doxycycline hyclate (Dox) (Sigma Aldrich). For each sample, a

matching Dox untreated sample was also plated out. After 48 hours, an aliquot of cells was taken and diluted 1:1 with 0.4% trypan blue (Sigma Aldrich), and 10µl loaded into a TC10 system dual chamber counting slide (BioRad). Cell number and percentage viability were measured using a TC10 automated cell counter (BioRad). A 90% and 70% viability cut-off for Akata- and BL41-derived lines respectively was set, with samples below this threshold being discarded.

Induced lines were diluted in BL media to a concentration of $3x10^5$ cells/ml, and $3x10^4$ cells plated out, in triplicate, into a flat bottomed 96 well plate. Cells were diluted 1:1 with normal BL media, BL media with Dox only, BL media with ionomycin only or BL media with Dox and ionomycin. Note that ionomycin was added to a final concentration of 2µg/ml for Akata- and 0.5µg/ml for BL41- derived cell lines. Plates were incubated for 48 hours.

Live cells were stained in the plate with Syto17 (Invitrogen) at a final concentration of 50nM and incubated at 37^0C for 1 hour. Plates were then put on ice and 0.5ng Propidium Iodide (PI) (Invitrogen) was added to each well to stain for dead cells. Single and unstained samples for Syto17 and PI were also included to aid with colour compensation. Plates were maintained on ice and readings for each well were taken for 10000 cells, using an Accuri C6 flow cytometer (BD Bioscience).

Syto17 stains only live cells and is detected in FL4, PI is membrane impermeant and excluded from live cells; it is detected in FL3. Live cells were defined as Syto17 positive and PI negative, early apoptotic cells as Syto17 negative and PI negative, and late apoptotic or dead cells as Syto17 negative and PI positive.

2.9 Co-IP Assays

Approximately 10 x 10^6 cells were harvested by centrifugation at 450 x g for 5 minutes, washed in PBS and lysed in 500 µl 1% TX-100 Onyx buffer (20mM Tris-HCl, pH7.4; 135 mM NaCl; 1.5mM MgCl2; 1mM EGTA; 1% Triton-X 100; 10% glycerol) along with protease inhibitors (Roche)(1 tablet per 50ml buffer) for 30 minutes on ice. The mix was centrifuged at 13000 x g for 10 minutes, the debris-containing pellet discarded, and the protein-containing lysate harvested. Sepharose and Protein G beads (Sigma) were washed 4 times in 1ml lysis buffer and diluted to make a 1:1 slurry. To reduce non-specific binding of proteins to antibodies, cell lysate was pre-cleared; briefly, a volume of cell lysate containing protein from 5 x 10^6 was added to 50µl Sepharose Beads and incubated on a wheel for 1 hour at 4°C. Subsequently, the lysate-beads mix was centrifuged at 13000 x g for 30 seconds, the beads discarded and the supernatant retrieved. The lysate was then incubated with HA.11 monoclonal antibody (Covance) on a wheel, overnight at 4 ^{0}C. Afterwards, 50µl Protein G beads were added to the lysate and incubated on a wheel for 1 hour at 4°C. The beads were spun down as before and the lysate discarded. The beads were washed 4 x in 1ml Onyx buffer (samples were mixed by manually turning the sample tube) and protein eluted from the beads by boiling in 2 x Urea buffer containing β-mercaptoethanol. Protein-protein complexes can be subsequently assessed using western blot as described above (see section 2.3).

2.10 Immunofluorescence and Confocal Microscopy

Cells were harvested by centrifugation at 450 x g for 5 minutes, and washed 3 times with PBS. Cells were fixed in 2-4% paraformaldehyde made in PBS (15 Minutes at RT), and spun onto a poly-l-lysine slides (sigma) via a cytocentrifuge. The slides were washed with 100mM Glycine buffer, in PBS, to remove background fluorescence and permeabilized with 0.5%

TritonX-100 made in PBS for 15 minutes. The cell monolayer blocked for 1 hour at 37°C in 1% BSA in PBS and then was washed 3 times in PBS. Primary and secondary antibody binding was performed at 37°C. Approximately 100µl primary cellular localization antibody anti-HA (rat 1/1000, Roche), CoxIV (mitochondria, rabbit polyclonal, 1/500, abcam, ab16056), or Calnexin (ER, goat polyclonal, 1/500, abcam, ab93355) was dispensed over the slide and incubated for 60 minutes or overnight at 4°C and washed 5 times in agitated PBS. Incubated with the appropriate alexa fluor secondary antibody (life technologies) (594, red, or 488, green, 1/500) at 37°C for 60 minutes, and washed as before in PBS. Nucleus was stained using DAPI (blue). Slides were viewed on LSM510 Zeiss Confocal microscope and co-localisation was determined statistically using overlap coefficients (303).

3. Making lentiviruses to express BHRF1

3.1 Introduction

In order to determine how BHRF1 is able to interact with the cellular machinery to protect cells from apoptosis, a system was used in which the function of BHRF1 can be studied, in isolation, in the background of EBV negative Burkitts lymphoma. This system will also be useful when looking at the interactions between BHRF1 and the cellular BCL-2 homologues.

We chose to express BHRF1 using a lentivirus as these are able to stably integrate into the genomes of proliferating and non-proliferating cells and provide long term gene expression.

The chosen lentiviral system, TREX(gene)UTG (see Figure 3.1), was designed by Dr. Marco Herold, modified from a similar vector that he originally published (286). The essential features of this new vector are constitutive expression of GFP, which will prove beneficial when assessing infection efficiency and sorting of infected cells, and a tetracycline inducible promoter, enabling assays to be performed on identical lines in the presence or absence of gene expression.

The TREX(gene)UTG lentivirus system was used to express BHRF1 in order to obtain inducible and reversible expression of BHRF1 in an EBV negative background. This would exclude any contribution to the anti-apoptotic phenotype by other EBV gene products such as the EBNA3s (230).

The generation of TREX(gene)UTG vectors for the expression of protein coding genes is a two-step process, as described below for the generation of BHRF`1 expressing vectors.

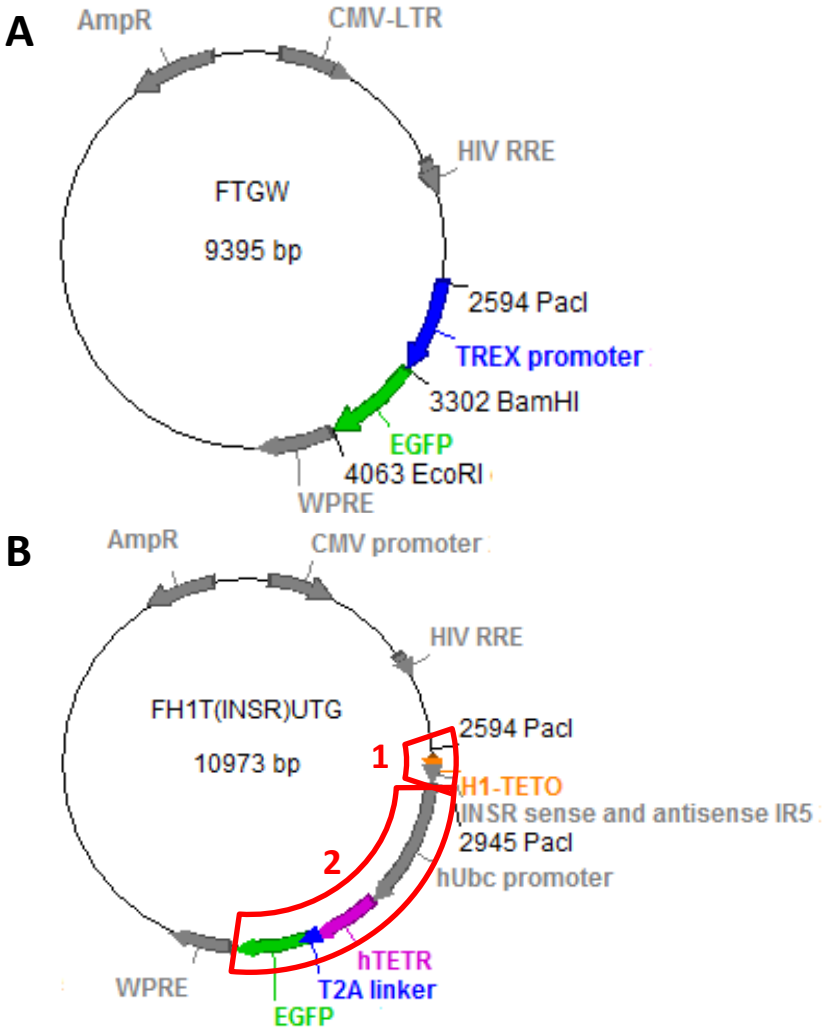

Figure 3.1: Map of original vector plasmids. **(A)** FTGW expresses eGFP under the control of a pol II tetracycline inducible promoter, TREX**.** There is no Tet repressor present so the TREX promoter is constitutively active. When the gene of interest is inserted between BamH1 and EcoR1 a segment containing GFP is lost. **(B)** FH1t(INSR)UTG plasmid with two expression cassettes highlighted in red. Cassette 1 containing pol III H1TetO promoter and IR5 insert is downstream of TATA box and between two Pac1 sites (2594 and 2945). Cassette 2 contains TetR and eGFP downstream of a constitutively expressed Ubiquitin C promoter. During the cloning protocol, cassette 1 is removed and replaced with a cassette containing the gene of interest downstream of the TREX promoter from the FTGW vector. Cassette 2 is maintained. Both vectors were designed and supplied by Marco Herold (286)

3.2 Establishing HA-BHRF1 in FH1t-UTG lentiviral system

We originally received two lentivirus vectors from Marc Herold, FTGW and FH1t(INSR)UTG (Figure 3.1). The FH1t(INSR)UTG vector contains a H1 Pol III promoter used to express shRNAs for RNA interference (RNAi) (304). For expression of mRNA for protein coding genes such as BHRF1, a Pol II promoter is required (305). For insertion of BHRF1 alongside a Pol II promoter, we employed an intermediate step using the second lentiviral vector, FTGW. The structure of FTGW is unpublished but is very similar to that of FUGW (306). FTGW contains a Pol II TREX promoter, with a tet operator for Dox inducible expression, which drives the expression of GFP (Figure 3.1A). The TREX promoter is constitutively active, despite the tet operator, due to the absence of a tetR gene. To express BHRF1 (the gene of interest) from the TREX pol II promoter we replaced GFP with a DNA fragment created using polymerase chain reaction (PCR).

In the second step of the process, we removed the H1 promoter and INSR segment from the FH1t(INSR)UTG vector using restriction digestion at internal Pac1 sites. This was replaced with the TREX promoter and BHRF1 fragment from the FTGW plasmid. This segment was also removed using Pac1, one internal site and one introduced with the BHRF1 PCR product. This procedure is described in more detail below.

The final product is the FTGW(BHRF1)UTG plasmid. The construct contains two cassettes; the TREX-gene cassette (highlighted in Figure 3.2A) and the UbiquitinP-TetR-T2A-eGFP cassette. In the second cassette the T2A peptide has been placed between codon-optimised TetR (Tet repressor) (307) and eGFP to link the two and ensure expression of both products. TetR and GFP mRNA are transcribed as one length, joined by T2A, which contains a cleavage site, so GFP and TetR are separated after translation, but expressed equally well (308).

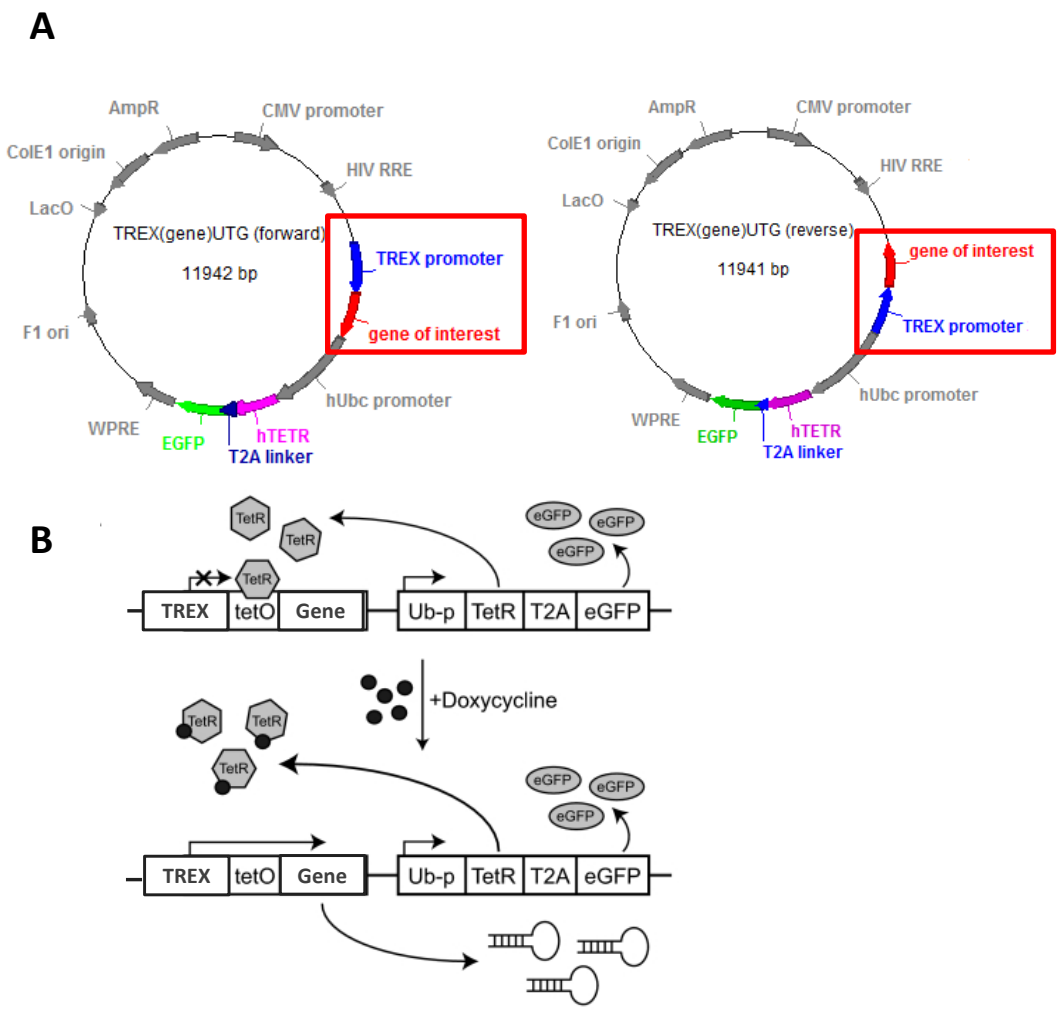

Figure 3.2: Map of final vector plasmids and method of tetracycline inducible expression. **(A)** FH1t(gene)UTG plasmid with gene of interest expression cassette highlighted in red. Cassette containing pol II TREX promoter and gene of interest between two Pac1 sites. This cassette was taken from an intermediary vector, in order to insert a pol II promoter, and can insert in a forward or reverse, or sense or anti-sense, orientation in relation to the vector backbone. A second cassette contains TetR and eGFP downstream of a constitutively expressed Ubiquitin C promoter and connected by a T2A peptide. The viral RNA genome is transcribed from a pol II CMV promoter and rev dependent nuclear export of the genome is mediated by the HIV rev response element (HIV RRE). The wood-chuck hepatitis virus post-transcriptional regulatory element (WPRE) helps to increase transgene expression. **(B)** Tetracycline inducible expression of gene of interest. eGFP and TetR are expressed constitutively from the ubiquitin C promoter. In the absence of Doxycycline (a tetracycline derivative) TetR binds and inactivates TetO to prevent gene expression. Doxycycline binds TetR and releases TetO so the gene can be transcribed from the TREX promoter. (286)

The first cassette consists of the TREX promoter (Pol II) and Tet regulated operator (TetO) downstream of the TATA box, followed by BHRF1 (307).

Upon infection with this lentiviral vector eGFP and TetR are constitutively expressed from the Ubiquitin C promoter. Expression of TetR blocks transcription from the H1-TetO promoter in the absence of Dox by binding and inhibiting TetO. In the presence of Dox, Dox binds to TetR and inhibits its localisation to TetO, enabling transcription from the TREX promoter and expression of the gene of interest. (Figure 3.2B)

3.2.1 Tagging of BHRF1 with haemagglutinin and generation of intermediate vectors

We thought it important to tag BHRF1 as the only BHRF1 antibody to work well in Western blot (5B11) performs very poorly in immunofluorescence (IF) and co-immunoprecipitation (Co-IP). A PCR reaction with specific primers was used to insert a Haemagglutinin (HA) tag onto the 5' end of the BHRF1 gene (HA-BHRF1), downstream of the ATG start codon. A 3' Pac1 restriction site was also inserted and the whole construct was then flanked by BglII and EcoR1 restriction sites on the 5' and 3' ends respectively. (Figure 3.3B) The PCR product was inserted into the multiple cloning site of commercial vector system (Promega), pGEM®-T easy (GenBank® Accession No. X65308), (Figure 3.3A) using A-tailing and blunt end cloning. Transformed colonies were identified through blue/white selection and sequenced using forward and reverse PCR primers and T7 commercial sequencing primer (alta biosciences). An untagged version of BHRF1 was also amplified by PCR at this point to provide a control to assess if the tag affected protein function.

A

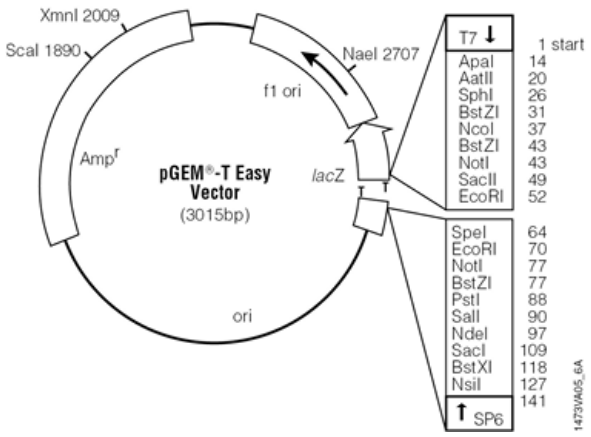

B

BglII Start Haemagglutinin tag

HA-BHRF1 Forward 5'– GCAGATCTACC**ATG**TACCCATACGATGTTCCAGATTACGCT GCCTATTCAACAAGGGAGATACTGTTAG - 3'

BHRF1 Forward 5 '- GCAGATCTACC**ATG**GCCTATTCAACAAGGGAGATAC - 3'

EcoR1 Pac1

BHRF1 Reverse 5'– AAGAATTCTTAATTAATTAGTGTCTTCCTCTGGAGATAAA TAAATAACTAC - 3'

Figure 3.3: Design of initial PCR product. (A) Vector map of commercial pGEM T easy vector from Promega (GenBank® Accession No. X65308). PCR products were inserted into the multiple cloning site after A-tailing, using blunt end ligation. The multiple cloning site falls within the lacZ gene leading to its disruption with the product insertion. In this way plasmids containing inserted PCR products can be picked by blue/white selection. (B) PCR primers used for addition of HA tag and restriction sites to wild type BHRF1. BglII restriction site was added to the 5' end of BHRF1 along with the HA tag, after the start codon, with the forward primer. A control with BglII but no HA tag was also made. Pac1 and EcoR1 restriction sites were added to the 3' end using the reverse primer. The same reverse was used for both tagged and control versions of BHRF1. The same primers were used for wild type and all mutant versions of BHRF1.

HA-BHRF1 was removed from pGEM®-T easy using the added BglII and EcoR1 restriction sites. The FTGW vector was digested with BamH1 and EcoR1 to remove a 761bp fragment containing the eGFP insert but leaving behind the TREX promoter. The HA tagged BHRF1 construct was ligated into this linearised vector using BamH1/BglII and EcoR1/EcoR1 complementary ends. This gave a construct containing the 5' HA-BHRF1 gene with 3' Pac1 site, all downstream of the TREX promoter and resulted in a construct referred to as FTGWHA-BHRF1 (Figure 3.4).

Before proceeding to clone the TREXHA-BHRF1 cassette in the final lentivirus backbone the ability of the TREX promoter to express BHRF1 was checked using the FTGWHA-BHRF1UTG vector. This was introduced into the 293T epithelial cell line by transient transfection and transduction (Figure 3.5). 293T cells were used as these tend to be very amenable to transfection and transduction and are an ideal line to use for preliminary experiments to ensure that expression is possible. Very high levels of BHRF1 mRNA and protein were expressed by both transfected and transduced 293 cells. BHRF1 mRNA expression was also seen in transduced BL41 cells but at levels much nearer those seen in Wp lines (Figure 3.5A). PSG5 BHRF1 was used as a transfection control and gave levels of mRNA and protein similar to those seen in Wp lines. It is clear that the TREX promoter has the ability to express BHRF1 mRNA and this is able to be translated. There is the potential for BHRF1 to be expressed at very high levels, although, from the levels of mRNA seen in transduced BL41 cells, this expression is likely to be much lower in EBV negative BL lines than in 293s.

3.2.2 Generation of final lentiviral product TREX(HA-BHRF1)UTG

The HA-BHRF1 downstream of the TREX promoter and Tet operator now forms a new cassette which was digested out of the FTGW vector with Pac1 enzyme to give a 1317bp

A

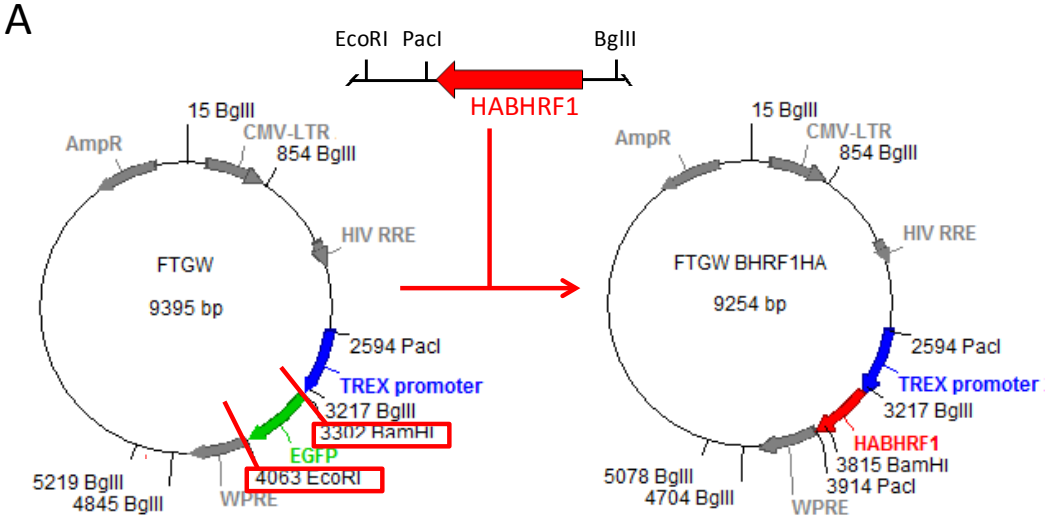

B

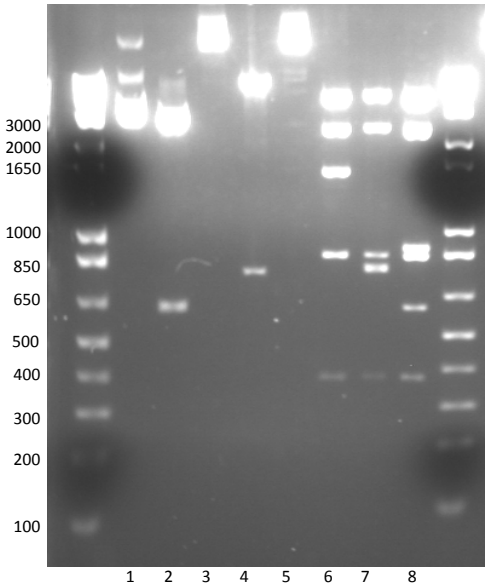

Lane	Plasmid	Digest	Size bp
1	pGEM T easy HA-BHRF1	-	3645
2	pGEM T easy HA-BHRF1	BglII / EcoR1	3015 and 630
3	FTGW	-	9395
4	FTGW	BamH1 / EcoR1	8634 and 761
5	FTGW HA-BHRF1	-	9254
6	FTGW	BglII / BamH1	4177, 2363, 1543, 839, 374, 85 and 14
7	FTGW BamH1/ EcoR1 cut	BglII / BamH1	4191, 2363, 839, 782, 761, 374, 85 and 14
8	FTGW HA-BHRF1	BglII / BamH1	4191, 2363, 889, 839, 598 and 374

Figure 3.4: Cloning BHRF1 into the intermediate vector: (A) FTGW vector was linearised by digestion with BamH1 and EcoR1 restriction enzymes to remove a fragment of 761bp containing GFP. HA-BHRF1 was removed from pGEMT by digestion with the BglII and EcoR1 restriction sites that were introduced with the PCR primers. This BHRF1 fragment was then inserted into the linearised vector using the complimentary EcoR1/EcoR1 and BamH1/BglII sites. (B) Digestion products of various vectors with and without BHRF1. To indentify correct ligation products, mini-prepped clones were digested with BamH1 and BglII. These enzymes were chosen due to an appropriate number of sites and range of digestion product sizes. There is a BamH1 site within the BHRF1 fragment so with correct fragment insertion a new BamH1 site is added to the vector. These digests enabled identification of whole undigested plasmid, linearised plasmid and FTGW-HABHRF1 plasmid in which ligation has been successful.

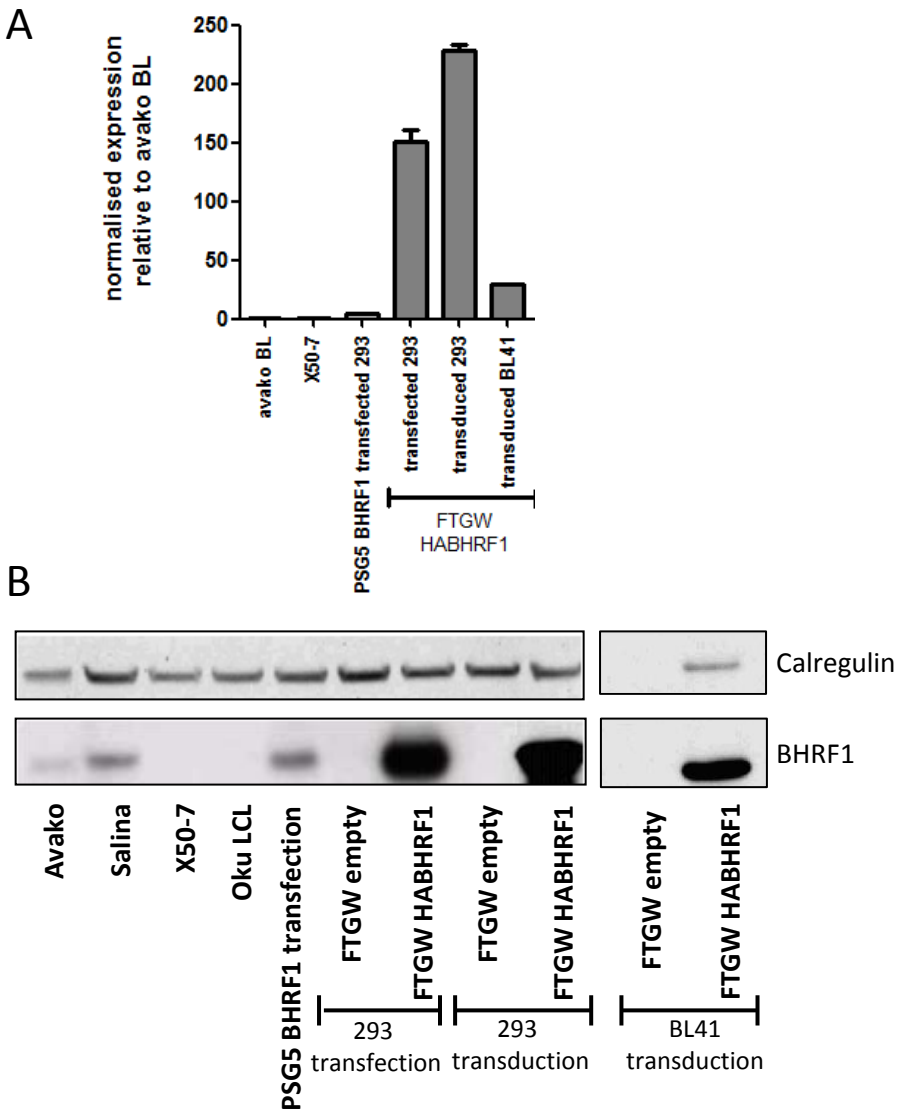

Figure 3.5: Checking HABHRF1 expression from the FTGWHABHRF1 plasmid. Expression of the HABHRF1 PCR fragment was checked in the FTGWHABHRF1 plasmid, with BHRF1 expressing BL and LCL lines as positive and negative controls. Lentivirus plasmids were introduced into the 293 epithelial cell line by transient transfection and transduction. (A) Transfected and transduced 293 cells express high levels of BHRF1 mRNA. Transduced BL41 EBV negative BL expresses much lower levels of BHRF1. PSG5 BHRF1 plasmid was used as a transfection control and gives more physiological levels. (B) BHRF1 protein is over-expressed in transfected and transduced 293s relative to physiological levels in Avako and Salina Wp BL. This protein expression corresponds to the levels of mRNA seen in (A).

sized fragment. The FH1t(INSR)UTG vector was also digested with Pac1 to remove the shRNA insert and H1tTetO, a 351bp sized fragment in total. The FTGW fragment containing HA-BHRF1 and TREX promoter was ligated into FH1t to give TREX(HA-BHRF1)UTG, in which the HA tagged BHRF1 construct should be expressed from the TREX promoter in a Dox regulated manner. (Figure 3.6)

Because the TREX HA-BHRF1 fragment has Pac1 restriction sites on both ends it is possible for it to insert in either the forward or reverse orientation in respect to the lentiviral backbone. The orientation of the fragment could affect expression and inducibility. For example, genes in the forward orientation could be subject to read-through from promoters upstream of the inserted cassette leading to expression in the absence of Dox. However, the reverse orientation could result in reduced stability and translation of mRNA and hence lower protein expression due to the lack of a downstream polyadenylation signal (309). The orientation of the inserted cassette can be determined through digestion with BamH1 (present within BHRF1 sequence) and BglII which give differently sized fragments depending on orientation. (Figure 3.6B) This can be confirmed during the sequencing of the final TREX(HA-BHRF1)UTG plasmid by identifying the orientation of the cassette in relation to the external primer.

3.2.3 Generation of BHRF1 mutant lentiviruses

Eight mutants of BHRF1 were developed by Marc Kvansakul. These mutants all contained a single base change leading to an amino acid substitution within the BH3 binding domain of BHRF1 (see chapter 4 for full description). They were originally received from Marc Kvansakul in the pGAL-trp vector from which I obtained the BHRF1 sequences. I performed cloning for each mutant as described above (Sections 3.2.1-2). As the base change was fairly

A

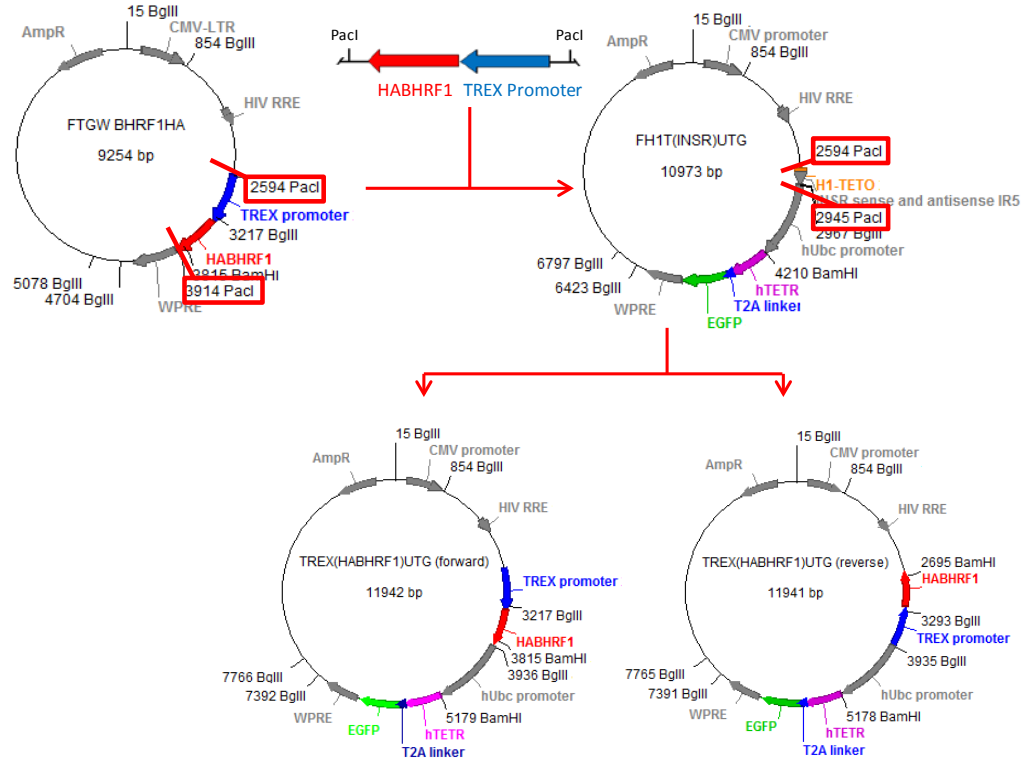

B

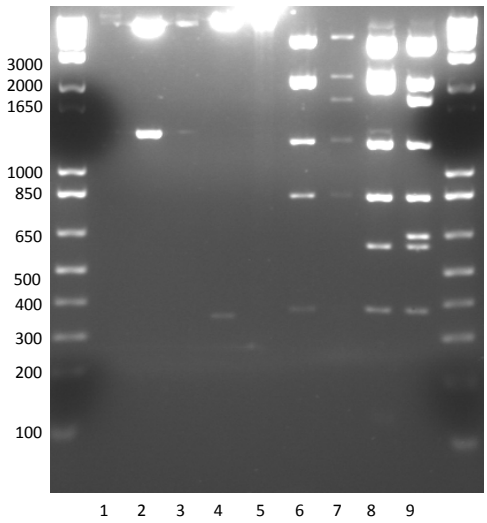

Lane	Plasmid	Digest	Size (bp)
1	FTGW HA-BHRF1	-	9254
2	FTGW HA-BHRF1	Pac1	7934 and 1320
3	FH1t (INSR)UTG	-	10973
4	FH1t(INSR)UTG	Pac1	10622 and 351
5	TREX(HABHRF1)UTG	-	11942
6	FH1t (INSR)UTG	BglII / BamH1	4191, 2213, 2113, 1243, 839 and 374
7	FH1t (INSR)UTG Pac1 cut	BglII / BamH1	4191, 2213, 1740, 1243, 839, 374, 351 and 22
8	TREX(HABHRF1)UTG forward orientation	BglII / BamH1	4191, 2363, 2213, 1243, 839, 598, 374 and 121
9	TREX(HABHRF1)UTG reverse orientation	BglII / BamH1	4191, 2213, 1841, 1243, 839, 642, 598 and 374

Figure 3.6: Production of final lentivirus vector. (A) After checking the insertion, HABHRF1 FTGW was digested with Pac1 restriction enzyme. It now contains two Pac1 sites as one was added with the insertion of the HABHRF1 fragment. This digest removes a 1.32kb fragment containing the TREX promoter and HABHRF1. This was extracted from an agarose gel and purified. The FH1T(INSR)UTG plasmid was also digested with Pac1 to remove a 351bp fragment containing the H1 promoter and INSR sequences. The TREX-HABHRF1 fragment was ligated into the linearised vector to give a vector labelled TREX(HABHRF1)UTG. Due to the ligation into two Pac1 sites the TREX-HABHRF1 cassette can insert in either the forward or reverse orientation. (B) Vector digests. 500ng of each plasmid was digested with the various restriction enzymes used in the cloning procedure. Correct clones were again indentified by digestion with BamH1 and BglII. Differences in fragment sizes allowed identification of undigested vector, linearised vector and plasmid with TREX-HABHRF1 insertion. They also allow differentiation between fragments inserted in forward and reverse orientations. For example; the reverse orientation gives a distinctive doublet of 642 and 598bp, between the 500 and 650bp marker bands, as compared to a single band on 598 in the forward orientation. The insertion and orientation of the fragments was confirmed by sequencing with TREX (within the TREX promoter), Pac1F (Pac1 site within vector) and Pac1R (Pac1 site from fragment) sequencing primers.

central in the BHRF1 sequence the same PCR primers as for wild type were used. The presence of the mutation was checked by sequencing prior to cloning and after cloning was complete.

3.3 Generation of stably infected cell lines

3.3.1 Production of lentivirus stock

After confirmation by sequencing, the final TREX(HA-BHRF1)UTG lentivirus was bulked up in the Stabl3 chemically competent *E.coli* strain (Invitrogen), which is designed specifically for the cloning of unstable inserts and reduce the frequency of homologous recombination of the long terminal repeats (LTRs) found in lentiviruses. Plasmid DNA was then removed and purified.

The HEK 293FT cell line was used for the production of lentiviruses along with the addition of psPAX2 packaging plasmid and the pMD2.G envelope plasmid, together making a 2nd generation system. At the same time, lentivirus was made using an empty control vector, FH1t(empty)UTG, in which the shRNA insert was removed.

3.3.2 Stably infecting cell lines

Two EBV negative BL lines, BL41 and BL2, were transduced with control, HA-BHRF1 and mutant BHRF1 lentiviruses via the spin infection method. Approximately one week post transduction the GFP expression of transduced lines was assessed by FACS (Figure 3.7A). The initial levels of GFP expression varied widely depending on which virus (for example; empty, wild type or different mutants) was used. BL41 was also much easier to infect than BL2, which, despite having the apparent advantage of being negative for BIM, seemed to be less

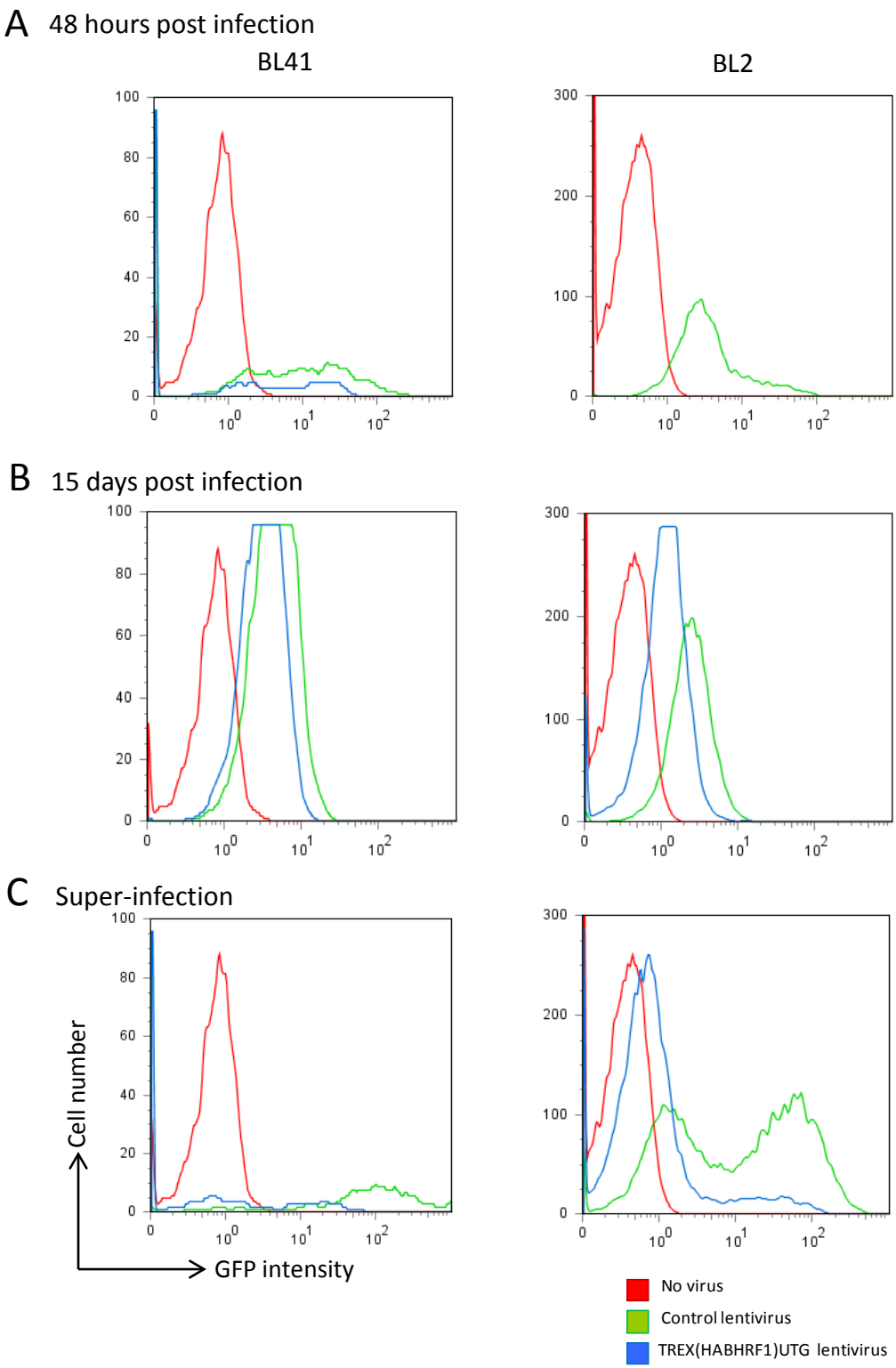
A
48 hours post infection
BL41
BL2
B
15 days post infection
C
Super-infection
Cell number
GFP intensity
No virus
Control lentivirus
TREX(HABHRF1)UTG lentivirus

Figure 3.7: GFP levels in BL41 and BL2 lentivirus transduced lines. Lines were transduced by spin infection with control and HABHRF1 lentivirus. The virus expresses GFP constitutively and this can be measured by flow cytometry. (A) 48 hours post infection cells were between 60 and 80% positive when compared to the uninfected GFP negative lines. Transduction of BL2 lines in particular was not well tolerated to the extent that there were not enough BL2 cells infected with TREX(HABHRF1)UTG to measure by FACS after 48h, although transduced cells later grew out after ficoll gradient purification. (B) 15 days post transduction, the intensity of GFP expression had dropped, the average intensity reduced by a factor of 10. However the percentage of GFP positive cells remained similar. (C) In order to increase the GFP intensity, a round of super-infection was performed. This resulted in two populations, one was the original GFP intensity in which no super-infection had occurred, the other was a small population which had taken up a second round of virus. The GFP intensity of the second population had risen by at least a factor of 10.

tolerant of the transduction procedure. Levels of GFP also fell over time. Specifically, while the percentage of GFP positive cells remained between 60 and 80%, GFP intensity fell by a factor of 10. This indicates that much of the GFP expression seen in the first few days post infection was derived from virus that had not stably integrated and was subsequently lost (Figure 3.7B).

Initial rounds of transduction only resulted in partial infection of BL41 and BL2. A round of super-infection was subsequently performed which resulted in two populations, one of the original GFP intensity and another with a mean intensity around 100 times higher (Figure 3.7C). This was followed by sorting for the top 50% intensity of GFP expression in the highest peak using a MoFlo cell sorter. Sorting returned 100% GFP positive cells with a stable mean GFP intensity 100 times higher than the original 1st round of infection (Figure 3.8). After induction with the tetracycline derivative doxycycline (Dox), these sorted lines expressed physiological levels of BHRF1, comparable to those seen in the Wp restricted line Salina (Figure 3.9). The same cells cultured in parallel in the absence of Dox, did not express detectable levels of BHRF1, although they later became leaky with extended time in culture.

3.4 Assessing BHRF1 expression and function

Over a series of experiments, protein expression of non tagged BHRF1 and HA-BHRF1 in the forward and reverse cassette orientation was found to be broadly similar. Expression levels were also comparable to those seen in Salina, a Wp restricted BL line which expresses BHRF1 at high levels, and so were physiologically relevant, and both HA-tagged and untagged BHRF1 expression were tightly regulated by Dox (Figure 3.9).

The ability of BHRF1 to protect from apoptosis was assessed, in the first instance, using a simple FACS assay. Cells were cultured either in the presence or absence of Dox for 48 hours,

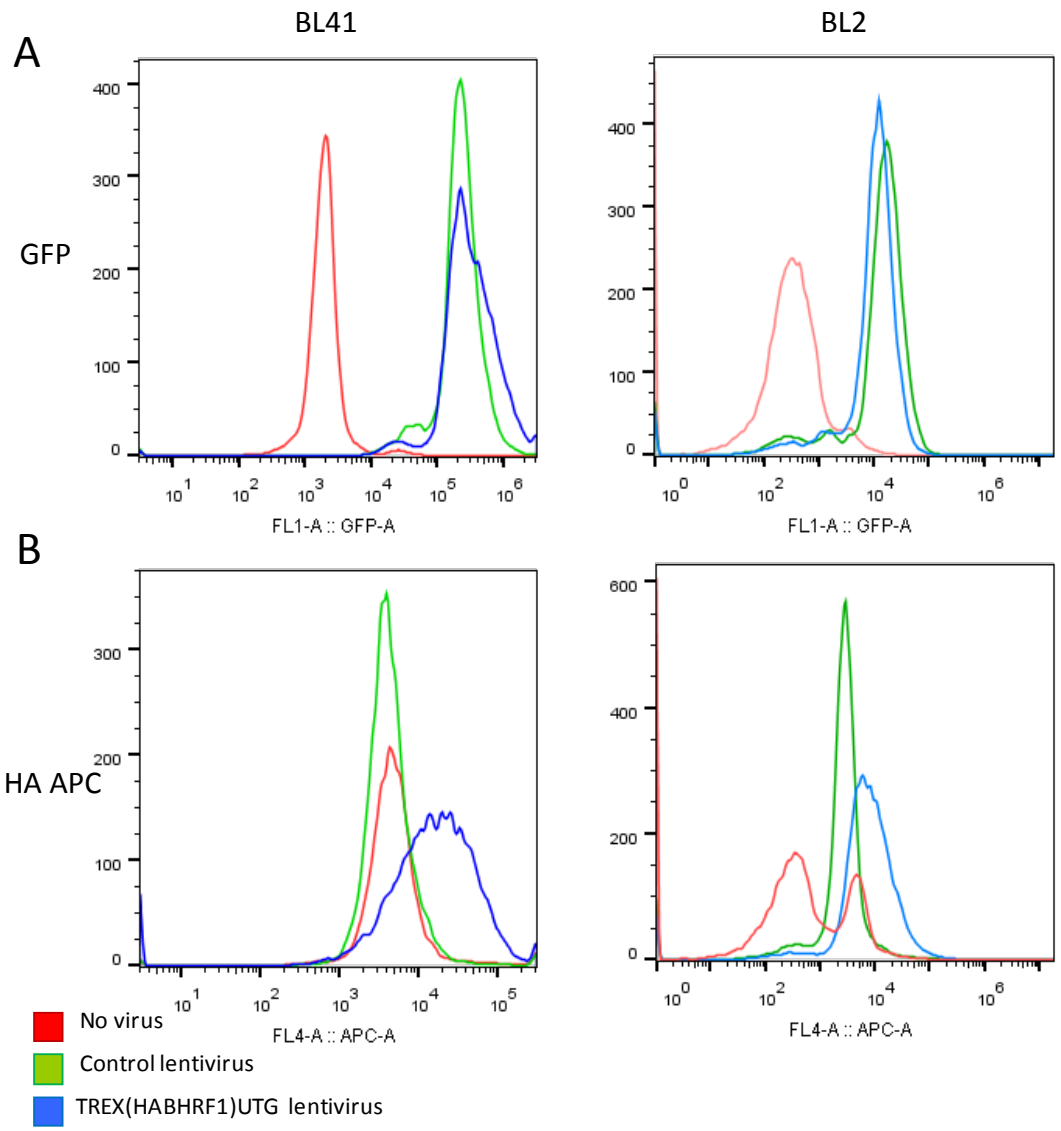

Figure 3.8: Expression levels after sorting: (A) After super-infection the top 50% of the most intense GFP peak were sorted for GFP. After cells had recovered they were re-assessed for GFP expression. Average GFP intensity of BL41 and BL2 lines was now stably 10x that of the original transductions. The differences in the scale of GFP intensity between (A) and Figure 3.7 are due to a change in the flow cytometer used. As these readings are purely relative, the values depend on the intensity of the laser. However, using the parental GFP negative controls a comparison can still be made. (B) Levels of HA expression determined using APC staining. HABHRF1 expression, induced with 1µg/ml Dox for 48h, were 10x higher in BL41 and 5x higher in BL2 than the empty vector and no virus parental control. The double peak, as with no virus control in BL2, was occasionally seen and is due to non specific background staining with the APC secondary antibody.

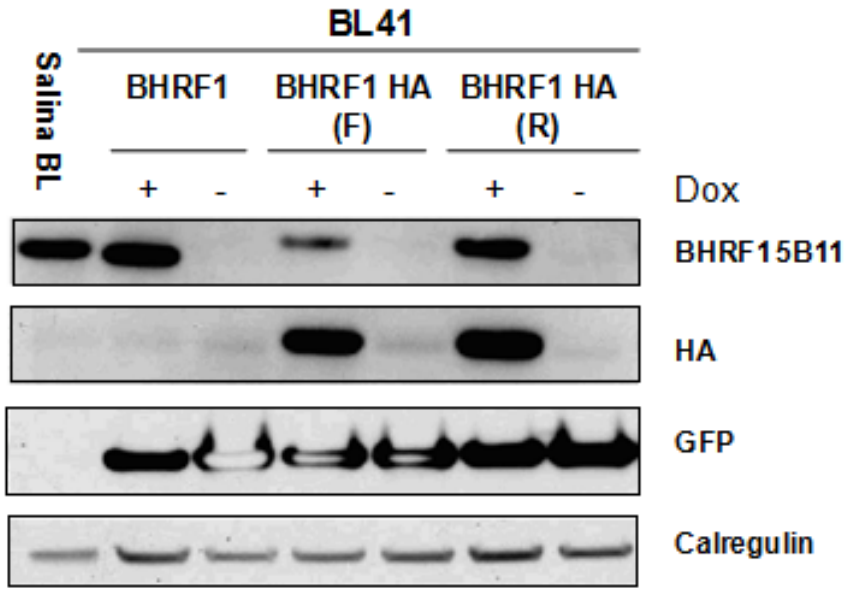

Figure 3.9: Dox induced expression of BHRF1 protein. BL41 lentivirus lines were induced with 1µg/ml Dox for 48h and assessed for expression using antibodies to BHRF1 (5B11) and HA. All lines expressed similar levels of GFP. HABHRF1 expression in forward and reverse cassette orientations was equal to non HA tagged protein over a number of experiments.

and subsequently were treated with either 0, 0.75 or 1.5 μg/ml ionomycin for 48 hours. Cells were harvested and stained with propidium iodide (PI) to enable identification of dead cells. Un-induced lines (without the addition of Dox) gave very similar levels of death as the BL41 parental line (Figure 3.10). BHRF1 is known to confer an anti-apoptotic phenotype at very low levels of protein expression, too low for detection by Western blot (101). Expression from the TREX promoter is highly inducible, in my experiments no BHRF1 associated protection was initially seen in the un-induced lines.

To confirm that HA-BHRF1 is able to protect from apoptosis at similar levels to endogenous BHRF1 from a variety of lines, we used four cytotoxic drugs, which act upon the intrinsic apoptosis pathway; ionomycin, anti-IgM, etoposide and roscovitine (see section 4.5), to induce death in a panel of Wp BL lines alongside the HA-BHRF1 expressing BL41 line (Figure 3.11). BL41 parental was used as a BHRF1 negative control. We found that HA-BHRF1, expressed by the inducible lentivirus system in BL41, protected against apoptosis to similar levels as endogenous BHRF1 expressed in Salina, Oku and Avako BL. This was the case with all four drugs tested.

Levels of apoptosis protection conferred by HA-tagged and untagged BHRF1 were very similar to those seen in Salina, so the HA tag clearly does not affect this function. To confirm that HA-BHRF1 was still able to localise to the mitochondrial membrane, confocal microscopy was performed using antibodies against the HA tag and COXIV (a mitochondrial membrane marker) to assess their co-localisation. (Figure 3.12) It is known that BHRF1 is localised on the mitochondrial membrane but there are reports that it can also localise to the endoplasmic reticulum and nuclear envelope. (310) Localisation to the mitochondrial membrane was seen in our assay (Figure 3.12), as well as a small amount of co-localisation with the endoplasmic reticulum marker calnexin (data not shown), although we were not

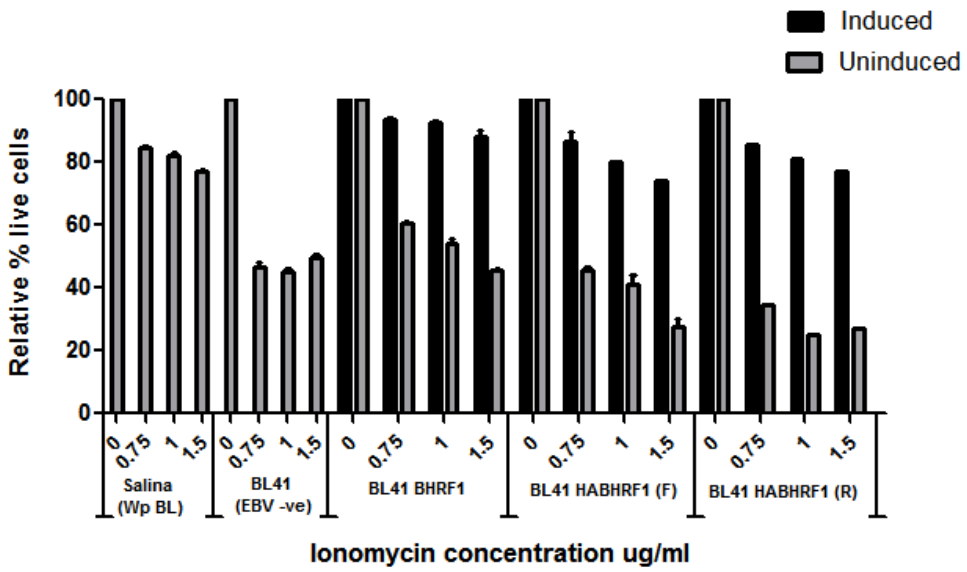

Figure 3.10: Effect of HA tag and cassette orientation on the function of BHRF1. The anti-apoptotic phenotype of BL41 BHRF1 expressing lines, with Salina-BL and parental BL41 as positive and negative controls respectively. Induced (1ug/ml dox 48h) and uninduced lines were treated with various ionomycin concentrations for 48h. Cells were harvested and stained with Propidium iodide (PI). GFP (FL1) and PI (FL4) were measured by flow cytometry. Drug treated live green cells (GFP +ve PI –ve) were normalised to untreated live green cells.

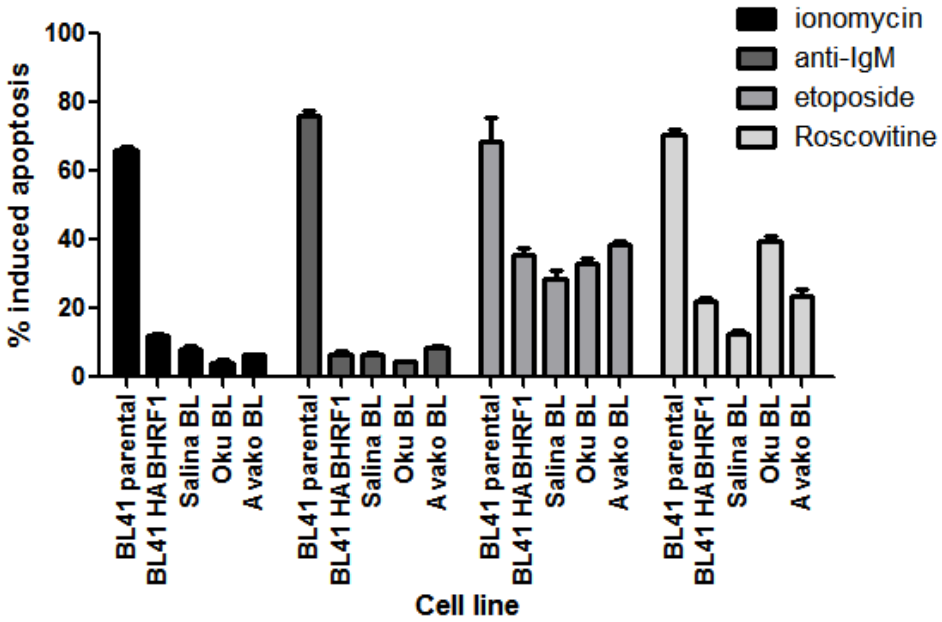

Figure 3.11: BL41 BHRF1 expressing lines protect from apoptosis as well as Wp lines. BL41 HABHRF1 lines were induced with dox. Apoptosis was induced through incubation of cells with four cytotoxic drugs; 1ug/ml ionomycin and 6ug/ml anti-IgM for 72 hours and 2.5ug/ml etoposide and 20ug/ml roscovitine for 48 hours. Values are from three independent experiments.

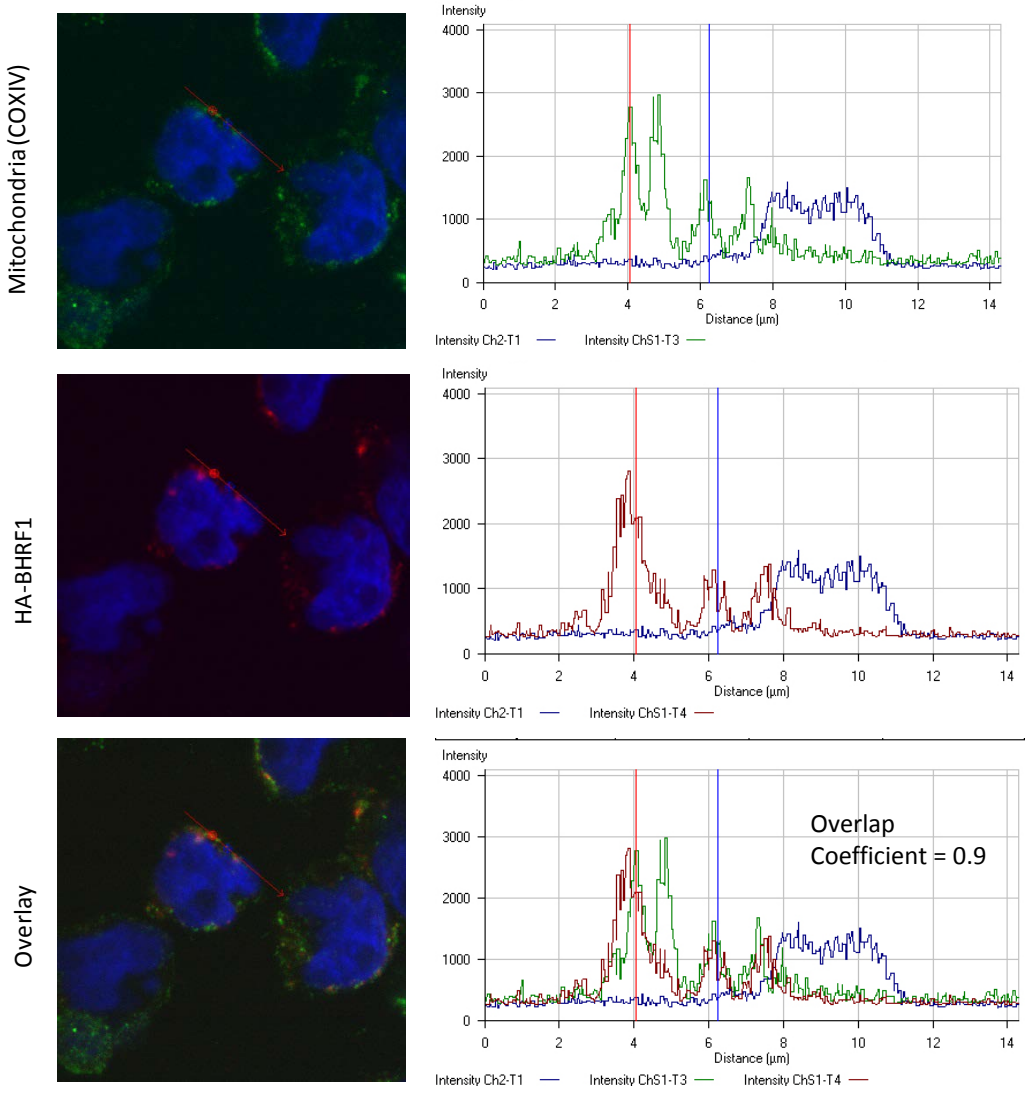

Figure 3.12: HABHRF1 localises to the mitochondria. The co-localisation of the HA tag of HABHRF1 (red) and a mitochondrial marker, COXIV (green) was looked at using confocal microscopy. When two spots were seen to overlap, profile and histogram software on the confocal were used to analyse the degree of co-localisation. A line is drawn to bisect the points of interest and the fluorescence intensities along that line are given for all fluorophores. If the peaks of intensity for two points coincide then there is probable co-localisation. This can also be shown statistically using overlap coefficients (303) which calculate the degree to which pixels from each image co-localise irrespective of signal intensity or photo bleaching. The overlap coefficient for HA/CoxIV was 0.9 (complete overlap = 1).

able to find any nuclear localisation. However, the microscopy was hampered by the extremely small size of BL cells which makes identifying co-localisation difficult.

The localisation studies, along with the apoptosis assays, indicate that BHRF1 function is not affected by the HA tag and that BL41 cells infected with TREX(HA-BHRF1)UTG are a good model in which to study BHRF1 function.

3.5 Discussion

3.5.1 Establishing a lentivirus system for inducible expression of BHRF1

In order to stably infect EBV negative BL cells I used an inducible lentivirus system developed by Herold *et al.* (286). Lentiviruses are useful in that they can infect dividing and non-dividing cells and deliver sustained gene expression through integration into the host genome. Lentivirus infection is superior to transient transfection for a variety of reasons, including more stable and less variable levels of gene expression. Additionally, the use of lentiviruses circumvents the need for possibly cytotoxic transfection reagents and any drugs that may potentially be needed for selection. This particular lentivirus also has the benefit of a TREX tetracycline inducible promoter, enabling expression to be tightly regulated. The TREX system has advantages over other models. For example, there is a less direct model in which a fusion protein consisting of the tet repressor and VP16 activating domain is used (311). In the absence of tetracycline the fusion protein binds to a tet operator sequence adjacent to a simple CMV promoter which is activated by VP16 to induce transcription. When tetracycline is added, the tet repressor is prevented from binding the operator and VP16 is no longer in contact with the promoter, causing transcription to cease (311). This system requires constant tetracycline addition to prevent transcription, needed if the gene of interest is toxic

to the cells, and may result in leaky expression if tetracycline is not added at a high enough concentration. Induction of expression by withdrawal of tetracycline is also slower than by addition. If the protein of interest has a long half life and is likely to remain in the cell after transcription has stopped the new phenotype may also be difficult to ascertain. VP16 also has the potential to activate other promoters, interfering with the phenotype.

The TREX system overcomes these problems in that transcription is induced, rather than repressed, by addition of tetracycline. However, we have still found this promoter to be slightly leaky in the absence of tetracycline, or its derivative doxycycline (Dox). This was not apparent when the cell lines were used for experiments but became particularly noticeable in lines of high passage, or cells that had undergone crisis such as storage in nitrogen. Due to the highly protective nature of BHRF1 there is most likely a selection advantage over time, or during periods of crisis, for any cells that express BHRF1 in the absence of Dox.

BHRF1 mRNA and protein were expressed from the FTGWHA-BHRF1 vector at very high levels in 293 epithelial cells (Figure 3.6). The high expression levels may have been due to a combination of 293s being highly amenable to transfection and infection, and the constitutive expression from the TREX promoter in this plasmid. This would allow BHRF1 mRNA and protein to build up in the cells. Transduction of FTGWHA-BHRF1 into BL41 EBV negative BL line gave mRNA levels closer to those seen in Wp-restricted BLs due to the apparent resistance of this line to infection.

During the first few days after initial transduction of BL41 and BL2 with TREX(HA-BHRF1)UTG, a large percentage of cells expressed high intensities of GFP. However, after the first few days the intensity of the GFP expression began to fall and had to be boosted by rounds of super-infection. (Figure 3.7) This is most likely due to partial integration of the lentivirus, with any virus that has not integrated being lost over time and subsequent rounds

of cell division. After sorting for cells expressing a high intensity of GFP, levels of expression became much more stable over time.

BL2 was more difficult to infect to a high level of GFP intensity than BL41 and persistently express lower levels of BHRF1 than BL41, even after sorting. This may be due to the sensitivity of the cells to adverse conditions and decreased tolerance of the transduction procedure leading to the death of any cells that have been highly infected. It is also known that, depending on the area of insertion into the genome, promoter silencing in lentiviruses can occur due to DNA methylation and other epigenetic modifications (312). It has been found with this vector system that some genes cannot be expressed (personal correspondence, G. Kelly, October 2010) which could be due to epigenetic promoter changes and may explain the inefficiency of expression in BL2.

3.5.2 BHRF1 function is not affected by the HA tag or cassette orientation

Once BL41 cells were transduced with TREX(HA-BHRF1)UTG, and were stably expressing a high level of GFP, various lines were tested to check the phenotype of BHRF1. (Figure 3.9)

The orientation of the TREX-HA-BHRF1 cassette could affect the control, and efficiency, of BHRF1 expression. The forward, or sense, and the reverse, or anti-sense, orientations of the cassette both have their pros and cons. Insertion in the forward orientation could result in promiscuous expression of BHRF1 due to read-through from the upstream viral CMV promoter. Alternatively reverse orientation may be detrimental due to our decision not to include an internal polyA sequence in the cassette. This was decided because of the risk that introducing a new polyadenylation signal could severely reduce the viral titre due to

premature termination during virus replication. However, a polyA tail is required for efficient production of mRNA as it aids in export from the nucleus and affects stability in the cytoplasm. The PolyA sequence is also particularly important for coding mRNAs in that it may improve recognition by the ribosomes and hence translation (312, 313). Because of the risk of truncation, lentivirus backbones now often contain an alternative to a polyA sequence just upstream of the 3'LTR to aid in stabilising of the viral RNA. In the case of FTGW and FH1t(INSR)UTG this is the Woodchuck hepatitis-virus Post-transcriptional Regulatory Element (WPRE). This can also help to stabilise mRNAs from the expression cassettes if they are in the sense orientation in relation to the WPRE.

BHRF1 was HA tagged by PCR in order to aid in both protein detection and additional assays such as co-immunoprecipitation (Co-IP) and confocal microscopy. The only monoclonal BHRF1 antibody we have found to work well in Western blot (5B11) performs very poorly when used in immunoflourescence (IF) and Co-IP, and for this reason it was highly desirable that a tagged form of BHRF1 be used.

When adding a tag to a protein coding sequence, there is the potential that protein folding and hence function could be affected. The HA tag was inserted at the N terminal end immediately after the start codon. This was due to a C terminal hydrophobic domain which localises the protein to intra-cellular membranes, mainly the outer mitochondrial membrane similarly to BCL-2 (46, 103).

The N terminus of BHRF1 contains the α1 helix, within four codons of the transcription start site, which is homologous to the BH4 domain in cellular BCL-2 proteins (46). It could potentially interfere with folding at this site, especially if the α1 helix is internalised within the protein structure. However, the BH4 domain has been shown not to be well conserved between cellular BCL-2 homologues, leading to the conclusion that it is not important for

function. The binding groove of BHRF1 also does not start until the α2 helix, quite a way downstream of α1 and so is unlikely to be affected by additions at the N terminus (104). (Figure 1.7)

The effect of the HA tag and orientation of the expression cassette on BHRF1 function and expression was tested by measuring BHRF1's ability to protect from cell death induced by ionomycin, a common apoptosis inducing drug. BHRF1 expression was not affected by the orientation of the expression cassette and the HA tagged protein functioned just as well as the un-tagged version regardless of orientation. (Figure 3.9) Both tagged and untagged proteins provided similar levels of protection to those seen in Salina, a Wp restricted BL line expressing high levels of BHRF1, showing that the protein performs naturally, despite the absence of the surrounding elements of the EBV genome, and that the HA tag does not significantly affect protein folding. HA-BHRF1 protected BL41 lines from a variety of cytotoxic drugs to similar levels as endogenous BHRF1 expressed in Salina, Avako and Oku-BL Wp restricted Burkitts (Figure 3.11). HA-BHRF1 is also able to localise to the mitochondrial membrane, an ability central to its function (310).

Overall, this demonstrates that the TREX(HA-BHRF1)UTG lentivirus is a good system for artificially expressing BHRF1 in EBV negative BL lines. It is tightly inducible, with marked difference in expression and phenotype between induced and un-induced lines. Physiological levels of BHRF1 expression have been achieved and this system can now be used to study aspects of BHRF1 function and interaction with other BCL-2 homologues.

4. BHRF1 binding groove mutations and their ability to protect from apoptosis

4.1 Introduction

In earlier sections we discussed the structure of BHRF1 in relation to cellular BCL-2, and the way in which its function relates to the highly conserved BH3 binding groove.

We have acquired eight different functional mutants of BHRF1 from Dr. Kvansakul which have been previously characterised using isothermal titration calorimetry (ITC) and yeast expression as described in Dr. Kvansakul's recent paper (104). These contain point mutations all within the conserved BH3 binding groove of BHRF1. The binding groove is encoded within the 1st BH domain and is essential for the binding of BHRF1 to the BH3 domains of pro-apoptotic homologues. By changing one or two nucleotides within the groove, and hence causing an amino acid substitution, we can affect the ability of BHRF1 to bind certain pro-apoptotic BCL-2 homologues such as BIM, PUMA, BID, BAX and BAK.

The ability of BHRF1 to bind the BH3 domains of certain pro-apoptotic BCL-2 homologues should affect its ability to protect from apoptosis. According to the various models for cellular BCL-2 homologue interaction, a loss of binding to pro-apoptotic homologues should lead to an increase in apoptosis as BHRF1 would no longer be able to hold BAX and BAK inactive or sequester the BH3-only proteins.

So far these mutants have only been characterised in a yeast based expression system. In order to gain a more accurate picture of BHRF1 binding properties *in vivo* the mutants must first be expressed in a B cell system and characterised *in vitro.* To be able to tease out how the changing ability of BHRF1 to bind various BCL-2 homologues results in differing levels of

protection from intrinsic apoptosis, the mutants were ectopically expressed in EBV negative BL backgrounds using the inducible lentivirus vector characterised in the preceding chapter.

4.2 BHRF1 binding groove mutations

The amino acid candidates for mutation were determined by Kvansakul *et al.* through structural analysis of BHRF1 bound to BIM and BAK (104) and from an extensive review of the literature.

The mutants were originally characterised in a yeast based expression system by Mark Kvansakul. Previously this group characterised the ability of a C-terminally truncated form of BHRF1 to bind the BH3 domains of pro-apoptotic BCL-2 homologues; BIM, PUMA, BID and BAK, with varying levels of affinity, using isothermal titration calorimetry (ITC) (104). These findings were further corroborated using co-immunoprecipitation of full length BHRF1 and pro-apoptotic BCL-2 homologues in a mammalian cell background. They also confirmed these results using a yeast based expression system, where death is induced by the over-expression of BAX and BAK (method described in (104) and (314)). This kind of system is useful in that it removes any effects due to the presence of cellular BCL-2. Yeast does not contain any known BCL-2 homologues or undergo apoptosis. However, in the budding yeast *Saccharomyces cerevisiae expression of BAX and BAK induces a form of caspase mediated cell death (315). An artificial intrinsic apoptotic pathway can then be reconstituted in yeast to test the ability of certain BCL-2 homologues to protect from BAX/BAK mediated cell death.*

The ability of BHRF1 to bind the BH3 domains of BIM, PUMA, BAX, BAK and BID was altered by mutating a single amino acid within the binding groove. Changes to amino acids within the BHRF1 binding groove can affect the ability of BHRF1 to bind the BH3 domain of cellular BCL-2 homologues. For example, changing the R100 amino acid has been shown to prevent

the formation of a conserved salt bridge with amino acids D67 and D83 on the BIM and BAK BH3 domain respectively, hence reducing the ability of BHRF1 to bind BIM and abolishing its ability to bind BAK (104, 109).

The locations of the main mutated amino acids are shown in Figure 4.1A, which shows the structure of BHRF1 bound to the BH3 domain of BAK. The binding groove of BHRF1 falls between the α3 and α5 helix (Figure 4.1B) and the amino acid changes cluster in this area. Table 4.1 shows the nucleotide changes which lead to specific single amino acid substitutions. The mutant name refers to the amino acid change and the location within the sequence, e.g. T68G gives T (threonine) to G (glycine) at location 68. The mutants will be referred to in this manner from here onwards. In Table 4.1 the base changes are highlighted in red and lead to amino acid substitutions which, in some cases, results in significant changes in amino acid properties, for example, R93D and R100D substitutes a positively to a negatively charged side chain and T68G substitutes a polar (hydrophilic) to a non-polar (hydrophobic) residue.

So far, these mutants have only been characterised using ITC and expression in a yeast based system. Table 4.2 shows the binding data of the various mutants as found by Mark Kvansakul using ITC. This technique gives a dissociation constant (K_d) which is used to describe the affinity between a ligand (BH3 domain) and a protein binding domain (BHRF1 binding groove). It is given as the molar concentration of the ligand at which the binding site on the protein is half occupied. The smaller the dissociation constant the tighter the binding between ligand and protein, i.e. the higher the affinity, the lower the concentration of ligand needed to saturate the protein binding site.

The individual mutations cause the ability of BHRF1 to bind BH3 peptides from BIM, PUMA, BID, BAK and BAX to vary widely. For example, the R100D mutation causes the complete loss

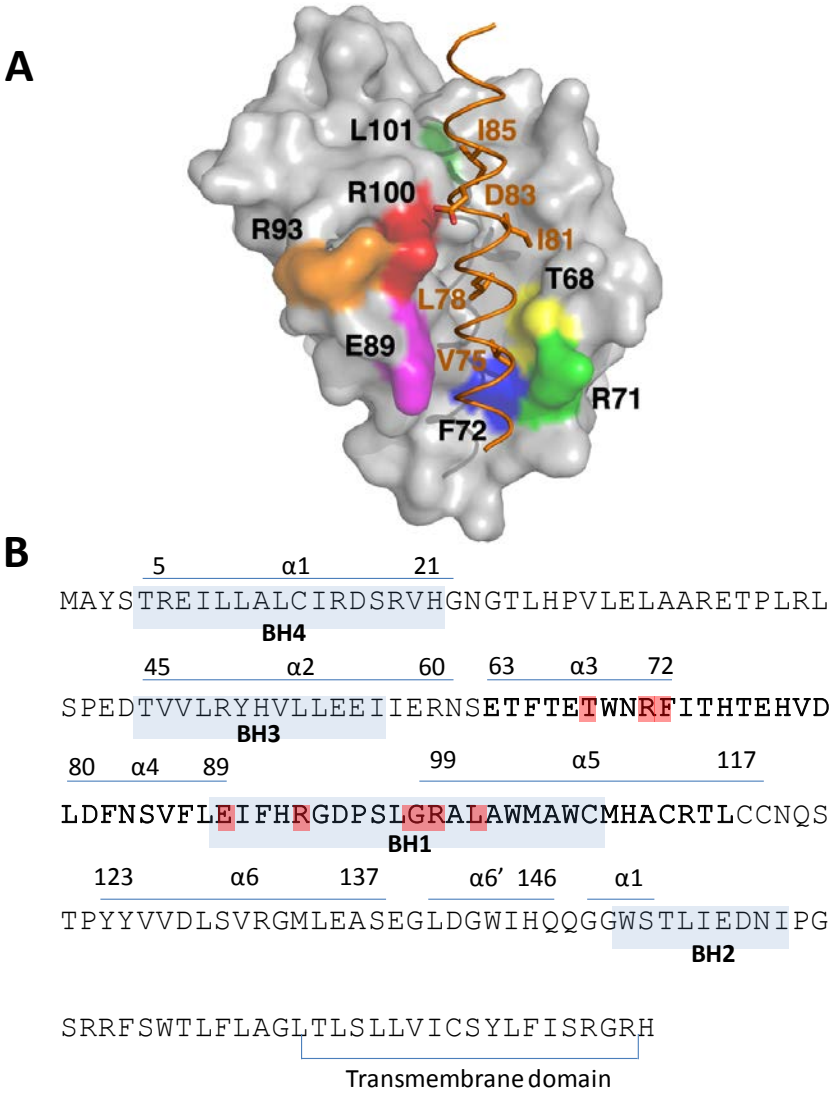

Figure 4.1: Locations of mutations within the BHRF1 binding groove. (A) Locations of amino acids to be mutated. Diagram shows the structure of BHRF1 bound to the BH3 domain of BAK (orange helix). Amino acids to be mutated are labelled in black and locations are highlighted in colour. G99 amino acid was also chosen for mutation but is located on the reverse of BHRF1 as it is shown in this orientation. From (104). (B) BHRF1 amino acid sequence. BHRF1 binding domain (bold) is located between the α3 and α5 helixes and includes the BCL-2 homology domain 1 (BH1). Amino acids which will be mutated and are important for BCL-2 homologue binding are highlighted in red. (Adapted from (46))

Mutant name	DNA mutation	Amino acid change
T68G	ACT > **GG**T	Threonine 68 to glycine
R71W	AGA > **T**G**G**	Arginine 71 to tryptophan
F72W	TTT > T**GG**	Phenylalanine 72 to tryptophan
E89G	GAG > G**G**G	Glutamic acid 89 to glycine
R93D	CGT > **GA**T	Arginine 93 to aspartic acid
G99A	GGG > G**C**G	Glutamic acid 99 to alanine
R100D	CGC > **GA**C	Arginine 100 to aspartic acid
L102I	TTG > **A**T**T**	Leucine 102 to isoleucine

Table 4.1: BHRF1 mutants and amino acid changes. Base changes within BHRF1 change amino acids within the groove which binds the BH3 domain of pro-apoptotic BCL-2 homologues. The amino acid candidates for mutation were determined by Kvansakul *et al.* 2010, through structural analysis of BHRF1 bound to BIM and BAK and through the literature. (104)

Mutant	BIM	BAX	BAK	PUMA	BID
WT	**18±2**	**1400±184**	**150±69**	**70±4**	**109±1**
T68G	9±1 (up 2x)	NB	491±129 (down 3x)	309±200 (down 4.5x)	102±2 (no change)
R71W	25±3 (no change)	288±6 (up 5x)	94±1 (up 1.5x)	n/a	132±4 (no change)
F72W	NB	NB	NB	282±46 (down 4x)	NB
E89G	930±6 (down 51.5x)	6050±637 (down 4x)	NB	604±117 (down 8.5x)	315±8 (down 3x)
R93D	10±2 (up 1.5x)	2340±481 (down 1.5x)	731±52 (down 5x)	78±6 (no change)	NB
G99A	83±21 (down 5x)	NB	4400±1970 (down 29.5x)	177±16 (down 2.5x)	NB
R100D	275±75 (down 15.5x)	NB	NB	394±95 (down 5.5x)	NB
L102I	13±3 (no change)	NB	180±58 (no change)	33±21 (up 2x)	34±6 (up 3x)

Table 4.2: Binding affinities of BHRF1 mutants to cellular BCL-2 homologues. Given as dissociation constant (K_d) found using isothermal titration calorimetry (ITC) with a C terminally truncated form of BHRF1 and the BH3 domains of BCL-2 homologues. K_d is given in nM which represents the concentration of ligand needed to occupy 50% of the protein binding sites. The higher the concentration, the less strongly the ligand binds. NB represents cases in which no binding occurs. Fold change in the strength of binding of mutant compared to WT is given in brackets. Data from Mark Kvansakul.

of binding to BAK, BAX and BID, and the binding to BIM and PUMA to reduce by 15 and 5 fold respectively (Table 4.2). F72W completely loses binding to every BCL-2 homologue tested, except for PUMA, for which the binding affinity is reduced 4 fold. G99A also has reduced binding to BIM and PUMA (a 4.5 and 2.5 fold reduction respectively), has lost binding to BID and BAX and has negligible binding to BAK (Table 4.2).

ITC also has the limitations of looking only at peptides in solution, which may not be physiologically relevant. Whilst this data is informative, it is difficult to truly determine the effect that each mutation will have on the ability of BHRF1 to protect from apoptosis in a physiological setting, such as a lymphoma cell.

To determine how loss or improvement of BHRF1 binding to certain BCL-2 homologues affects the function of BHRF1 these mutants need to be investigated in a more physiological system.

4.3 Expressing mutants of BHRF1 in EBV negative BL cell lines

To investigate the interaction of BHRF1 and the various BHRF1 mutants with cellular BCL-2 homologues the HA tagged wild type and mutants were cloned into the dox-inducible lentivirus system described in chapter 3. This then enabled the stable infection of BL41 and BL2 EBV negative lines so that their function could be assayed in the absence of other viral factors that could contribute to the degree of apoptosis protection. As in section 3.3.2, the BHRF1 mutants were transduced into BL41 and BL2 cells, over rounds of infection and super-infection, and then sorted for the top 50% GFP intensity.

In this vector system, GFP along with the tet repressor, is expressed constitutively from an independent promoter, and so is a useful marker for levels of transduction. The GFP intensities of the BL41 (Figure 4.2) and BL2 (Figure 4.3) BHRF1 mutant lines are all similar to

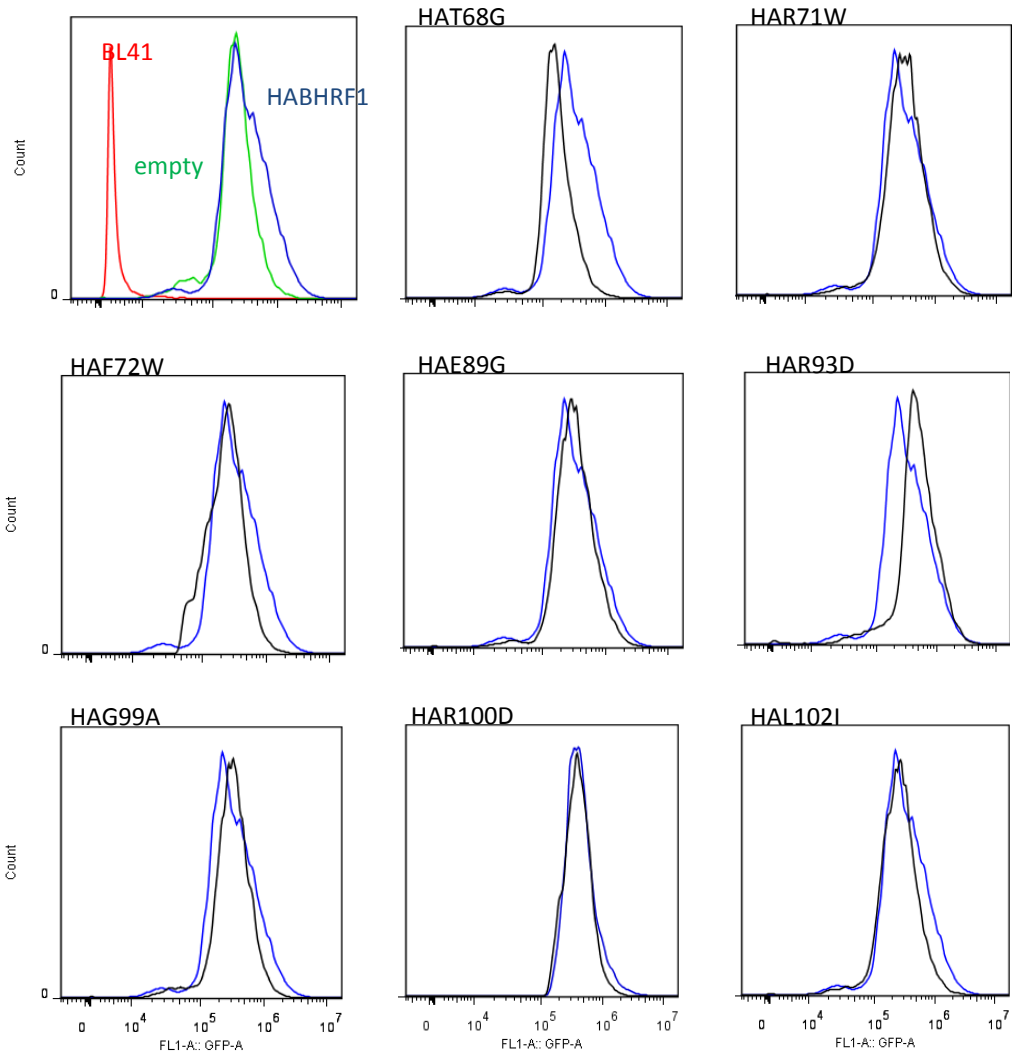

Figure 4.2: GFP levels in BL41 lines sorted for the top 50% of GFP intensity. The first plot shows uninfected GFP negative parental BL41 (red) compared the levels of GFP in the empty (green) and BHRF1 wild type (blue) lentivirus infected BL41 lines. The next eight plots show the levels of GFP named mutant (black) compared to wild type BHRF1 (blue). GFP expression in generally similar between the mutants and BHRF1 wt except for in two mutants (HAT68G and HAR93D).

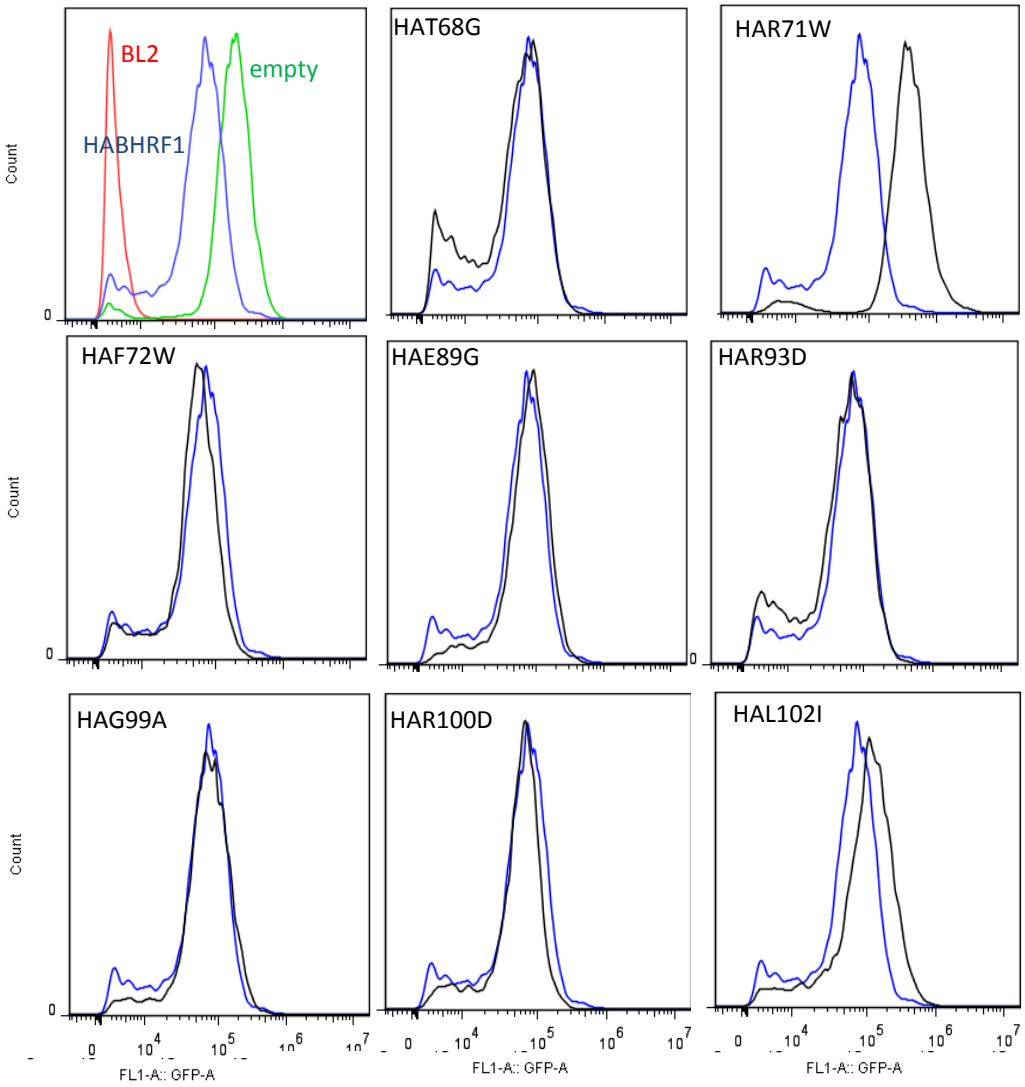

Figure 4.3: GFP levels in BL2 lines sorted for the top 50% of GFP intensity. As in figure 4.2 the first plot shows uninfected GFP negative parental BL2 (red) compared the levels of GFP in the empty (green) and BHRF1 wild type (blue) lentivirus infected BL2 lines. The next eight plots show the levels of GFP named mutant (black) compared to wild type BHRF1 (blue). GFP expression is again similar between the mutants and BHRF1 wt except for in HAR71W. This mutant later underwent a second round of sorting to bring the GFP levels down to those seen in the other mutants and wt. Generally all GFP levels were lower than those seen in BL41 lines which reflects the nature of BL2 to be less tolerant of virus transduction.

the BHRF1 wt, with the only significant exceptions being BL2 + HA-BHRF1 R71W and BL41 HA-BHRF1 F72W and R93D. If the difference in GFP intensity translates into difference in protein expression, levels can be altered by Dox titration.

The level of GFP intensity in BL2 lines is generally lower than BL41 lines. This correlates with what was seen in Figure 3.8 and was discussed in section 3.5.1. The HA levels were measured by FACs using HA-APC staining, and are given as the percentage of GFP positive cells which are also HA positive (Figure 4.4Ai and Bi) and the mean fluorescence intensity (MFI) of APC staining in cells which are also GFP positive (Figure 4.4Aii and Bii). Percentages of HA staining were fairly stable in BL41 lines but were more variable between the mutants in BL2. They varied between 71% and 93% in BL41 (Figure 4.4Ai) and 24% and 61% in BL2 lines (Figure 4.4Bi).

BL2 expression of HA tagged BHRF1 and mutants is around 2–3 fold lower than BL41 (Figure 4.4Aii and Bii). This is confirmed in Figure 4.5 in which western blotting has been used to measure BHRF1 protein expression. There is some, but not complete correlation, between Figure 4.5 and Figure 4.4Aii and Bii. For example, BL41HAR93D has a high MFI and protein is highly expressed; however, BL2 R71W has a low MFI but higher protein levels. This may be due to variable levels of death in the cells to be harvested for protein. In the case of protein samples all cells are taken regardless of viability whereas with FACs, only the live population is measured. However, it could also be due to the nature of cell staining for flow cytometry which can be influenced by conditions such as fixation, antibody concentrations and background fluorescence. Levels of BHRF1 expression in BL2 lines are approximately 50% lower than in BL41 by Western blot. Expression levels in BL41 lines are similar to the physiological levels of BHRF1 seen in Salina Wp BL. Although the BL2 levels are lower than this it is known that very little BHRF1 expression is needed to see a phenotype. This lower

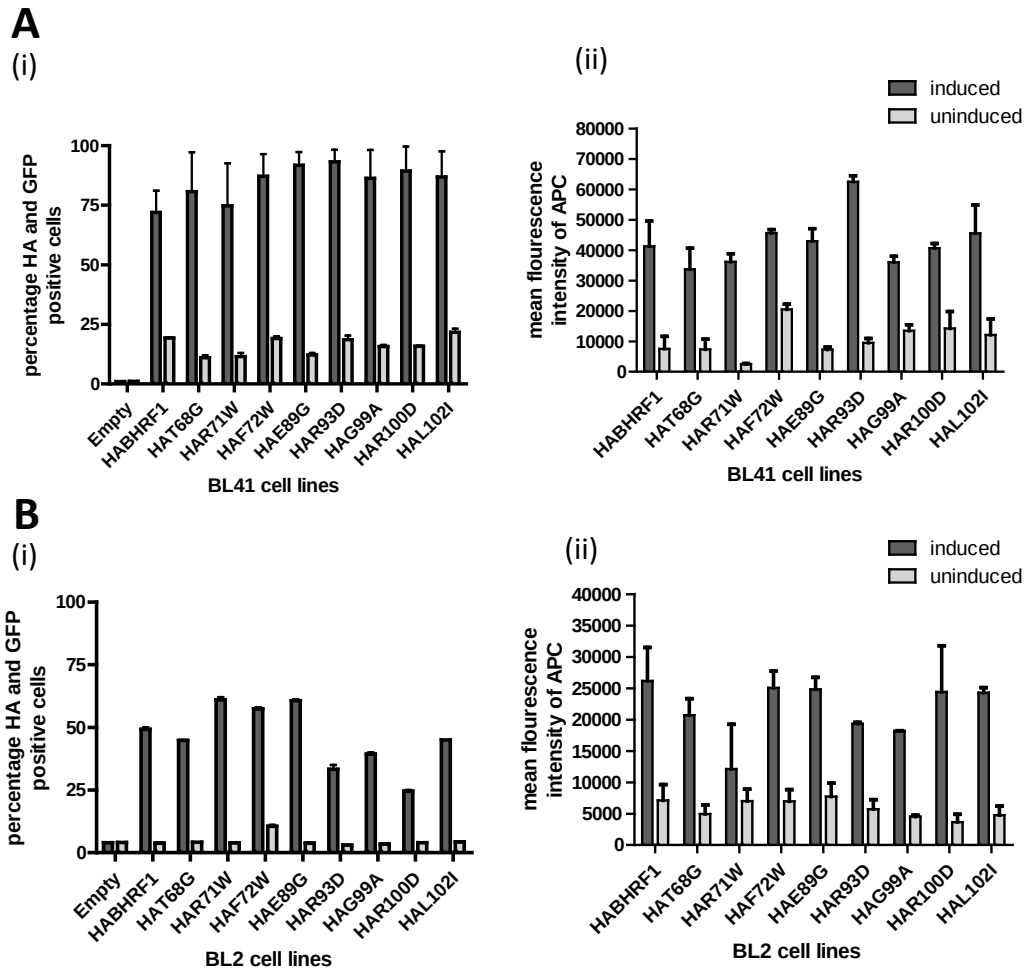

Figure 4.4: HA levels in (A) BL41 and (B) BL2 lines stained with APC, expressed as percentage of HA positive, GFP positive cells. (Ai) Induced HA positive cells in BL41 vary between 71% and 92%, with staining in un-induced lines being around 10 to 20% as expression is slightly leaky. (Bi) Levels of HA in BL2 lines are lower than BL41 but more tightly regulated. (Aii and Bii) mean fluorescence intensity (MFI) of induced and uninduced BL41 and BL2 lines respectively. MFI for APC in cells which are also GFP positive.

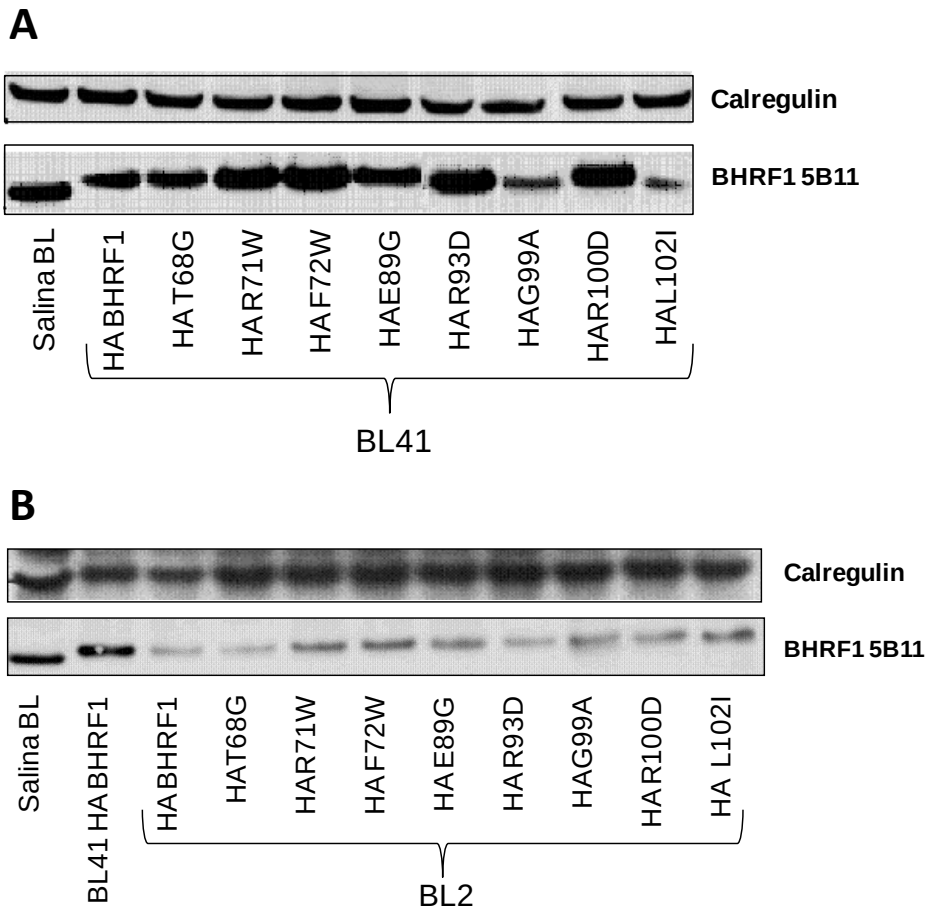

Figure 4.5: BHRF1 protein expression levels in BL41 and BL2 lines. BHRF1 protein expression was measured using the 5B11 BHRF1 antibody. (A) levels of BHRF1 in BL41 lines compared to Salina Wp BL. Lines were induced with concentrations of Dox between 0.5 and 1 μg/ml. Levels of expression are similar to Salina and so should have physiological levels of protection. (B) Levels of BHRF1 expression in BL2 lines compared to Salina BL and wt HABHRF1 in BL41. The protein expression in BL2 is around 50% lower than in BL2 but levels between the mutants are consistent which should improve the ease of interpretation.

level could actually be an advantage as it may allow more differentiation between the phenotypes of the different mutants if the lines are not saturated by high levels of BHRF1, giving very high levels of apoptosis protection.

Finally, the levels of HA expression in un-induced BHRF1 transduced BL41 lines are higher than the empty line (Figure 4.4A), indicating that there is some leaky expression from the TREX promoter. This is undetectable by Western blot but could affect the phenotype of the un-induced lines, as is known from LCLs, where only a very small amount of BHRF1 is required to exert a protective effect (101).

4.4 A Flow cytometry assay to assess levels of apoptosis

In order to determine the level of apoptosis protection conferred on BL41 and BL2 by mutated versions of BHRF1, an assay to accurately measure levels of drug induced apoptosis must be used. We decided to use a flow cytometry assay previously used by Kelly *et al.* in our group (101). This assay also has the advantage of distinguishing between populations of cells in the early and late stages of apoptosis. The assay uses two stains; Syto16 and propidium iodide (PI), to distinguish live and dead cells. Syto16, used by Kelly *et al,* is a green stain detected in the FL1 channel. As many of the cell lines used in our experiments were GFP positive we used Syto17, a red version of Syto16.

The Syto stains are membrane permeable molecules which are actively pumped into healthy cells and fluoresce when bound to DNA/RNA (316). Upon apoptosis, specifically the initiation of the caspase cascade which follows mitochondrial membrane permeablisation, there is a loss of Syto fluorescence, perhaps due to caspase mediated nucleic acid breakdown or chromatin condensation which may lead to a decrease in Syto binding sites (317).

P.I. is a red stain detected in FL2 and FL3, which fluoresces when bound to nucleic acids. It is impermeable to cell membranes and so only will only stain dead or dying cells in which the membrane has begun to break down.

Together, these two stains can differentiate between live (Syto17 positive, P.I. negative), early apoptotic (Syto17 negative/dim, P.I. negative) and late apoptotic/dead (Syto17 negative, P.I. positive). Figure 4.6A shows the gating used to define these populations, with Syto17 (FL4) on the X axis and P.I. (FL3) on the Y axis. The shift in population size, from mainly live to mainly late apoptotic/dead, can be seen in Figure 4.6B showing BL41 and Salina cell lines induced into apoptosis using ionomycin. Time points were measured over a period of 48 hours and indicate a pronounced shift towards the Syto17 negative, P.I. positive population, particularly in BL41 which is more sensitive to apoptosis. Interestingly, the early apoptotic (Syto17 negative/dim, P.I. negative) population remains relatively small over the full 48 hours. This population most likely represents the population described by Cohen *et al.* in which chromatin condensation has occurred but no DNA cleavage is observed (318). In thymocytes this population was observed to be at its highest 1 to 2 hours after treatment with 10μM etoposide, cells then progressed to apoptosis and DNA cleavage by 4 hours (318). This increase very early after drug treatment may explain why we don't see a larger Syto17 negative/dim, P.I. negative population, as the earliest time point in our assay was taken at 10 hours. Cohen *et al.* labelled these cells as pre-apoptotic whereas here they are referred to as early apoptotic. However, it is not known if this population are fated to die or if they can remain in this population or even revert to a normal live phenotype. Because it is ambiguous whether this population is genuinely apoptotic we decided to concentrate on the definitely live (Syto17 positive, P.I. negative) and late apoptotic/dead (Syto17 negative, P.I.

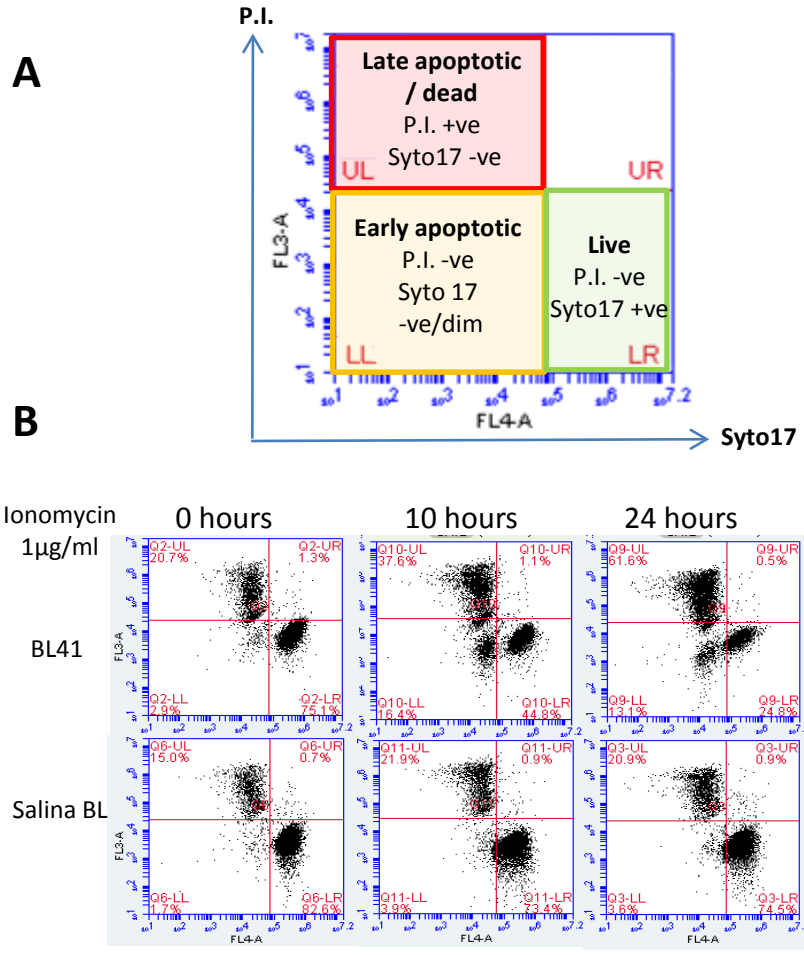

Figure 4.6: Flow cytometry assay to determine levels of apoptosis and to distinguish between late apoptotic, early apoptotic and live populations. Two stains were used to distinguish between live and apoptotic cells. Cells were stained with P.I. (propidium iodide) immediately before readings were taken. P.I. stains late apoptotic, or necrotic, cells. Cells were stained with syto17 one hour prior to taking readings. Syto17 requires uptake by active transport and so only stains live cells. (A) example gating of cells using Syto17 (X axis) and P.I. (Y axis) to give live (Syto17 positive, P.I. negative), early apoptotic (Syto17 negative/dim, P.I. negative) and late apoptotic (Syto17 negative, P.I. positive) populations. (B) Cell death in Salina Wp restricted BL and EBV negative BL41 lines induced by 1ug/ml ionomycin over a period of 48h. Over the various timepoints BL41 cells can be seen to move from the live Syto17 positive population, through early apoptosis and into P.I. positive late apoptosis. Salina undergoes very little apoptosis over the 48 hours due to the protective effect of EBV and maintains a background population of late apoptotic cells but very few cells enter early apoptosis.

positive). This should not change the overall pattern of death as the early apoptotic population remains consistently low between different drugs and cell lines.

4.5 Sensitivity of BHRF1 positive and negative BL41 and BL2 lines to Apoptosis inducing drugs

4.5.1 Ionomycin and anti-IGM

Cell death was induced using a variety of drugs which activate the apoptotic pathway. Initially we used the calcium ionophore, ionomycin. This induces influx of Ca^{2+} ions across the cell membrane to raise the level of intra-cellular calcium (319). Increase in intra-cellular Ca^{2+} ions is a well known inducer of apoptosis through various mechanisms including the activation of calmodulin, by binding to calcium, which then goes on to activate targets involved in apoptosis (320), and by activation of calcium dependent endonucleases (321, 322).

In order to resolve small differences in apoptosis protection conferred by different BHRF1 mutants we aimed to find a drug concentration that would give between 60 and 80% apoptosis in the most sensitive cell lines, namely empty and parental BL41 and BL2, and around 20% or less apoptosis in the most resistant lines, namely wild type BHRF1 infected BL41 and BL2. Parental lines, and Dox induced empty and HA-BHRF1, in a BL41 and BL2 background, were treated for 72 hours with 1–6μg/ml ionomycin. Cells were stained with Syto17 and P.I. and readings for 10000 cells were taken by BD Accuri flow cytometer (Figure 4.7A). Figure 4.7B shows that all concentrations of ionomycin used gave high levels of apoptosis in BL41 (above 80% in BL41 and BL41 empty lentivirus cell lines). In BL2 death was

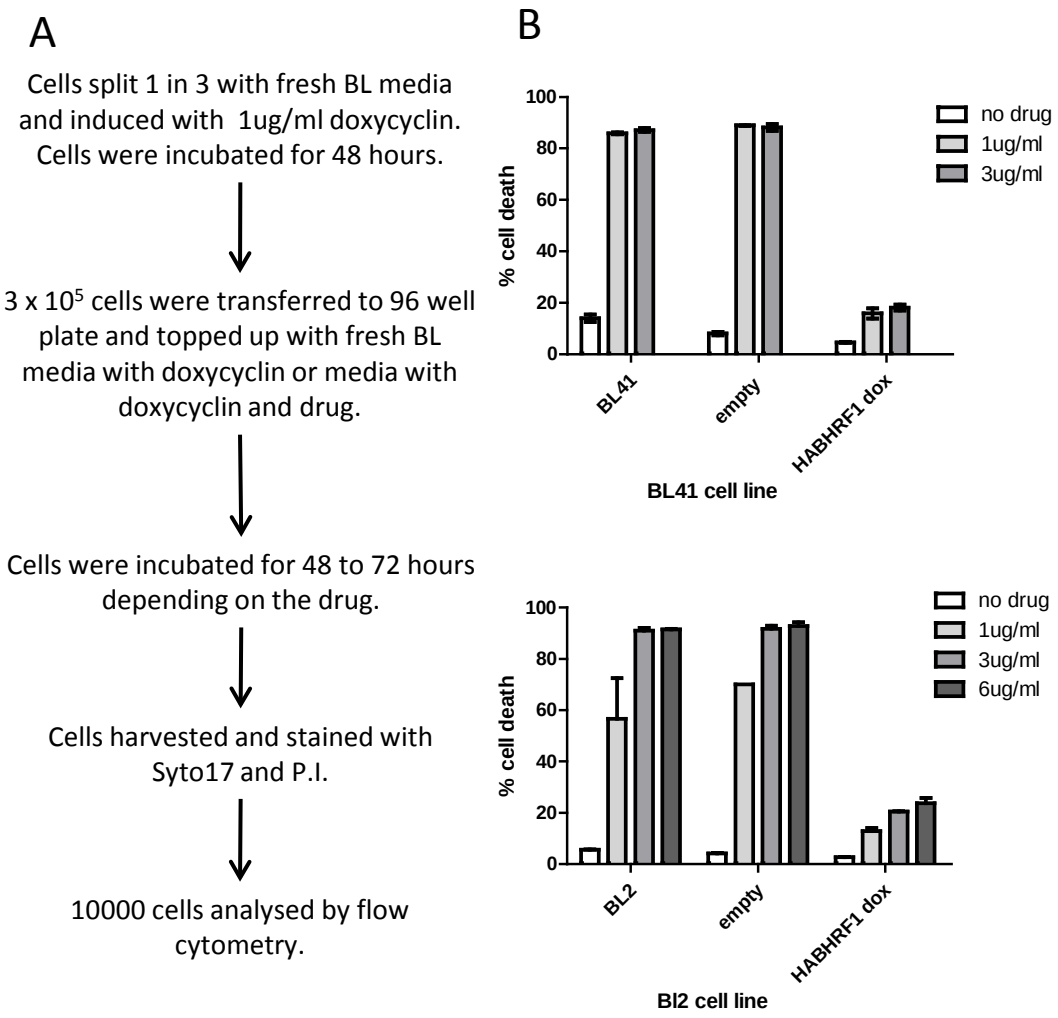

Figure 4.7: (A) Protocol of apoptosis assay. (B) Apoptosis assay to determine the concentration of ionomycin. Cells were incubated with drug for 72 hours and treated as in (A). Concentrations of 1ug/ml and 3ug/ml ionomycin were used on BL41, and 1ug/ml, 3ug/ml and 6ug/ml on BL2 cell lines, which proved more resistant to death. Parental, TREX(empty)UTG and TREX(HABHRF1)UTG infected lines were tested. Empty and HABHRF1 lentivirus infected lines were induced with dox. We aimed to find a drug concentration that would give between 60 and 80% apoptosis in empty and parental BL41 and BL2, and around 20% apoptosis in wild type BHRF1 expressing BL41 and BL2. From this data concentrations of 1ug/ml and 6ug/ml were used for BL41 and BL2 lines respectively.

still high but this cell line appears to be more resistant to apoptosis than BL41, perhaps because it lacks expression of one of the main pro-apoptotic BCL-2 homologues, BIM (290). There was around 58-70% apoptosis induced by 1µg/ml ionomycin in BL2 parental and empty lentivirus cell lines compared to above 80% death in BL41 lines treated with the same concentration. However, when the concentration was raised to 3ug/ml ionomycin staining showed similar levels of apoptosis in BL2 and BL41. Death was seen to increase with increasing drug concentration in BL2 but was so high in BL41 that no increase in death could be seen in the parental and TREX(empty)UTG vector lines although slight increases could be seen in HA-BHRF1 BL41 lines (Figure 4.7B). In both BL41 and BL2 lines the expression of HA-BHRF1, significantly increased the protection from apoptosis with around 20% apoptosis induced by the highest concentration of ionomycin in both backgrounds. In both BL41 and BL2, infection with the TREX(empty)UTG lentivirus had no affect on the apoptotic phenotype when compared to the parental cell line.

Based on these experiments we decided to use a concentration of 1µg/ml and 6µg/ml ionomycin for BL41 and BL2 respectively. The 6µg/ml concentration was used over the 3µg/ml as we suspected that higher levels of death in the HA-BHRF1 expressing lines would be needed to distinguish between small differences in the mutants.

Anti-IgM is another well known apoptosis inducing drug. Cross-linking with anti-IgM stimulates the B cell receptor on IgM positive cells. Activation of IgM causes generation of inositol trisphosphate (InsP3) which causes the release of Ca^{2+} ions from intra-cellular stores and apoptosis progresses through activation of caspases 2, 3 and 9 and in a similar manner as when activated by ionomycin (320, 323, 324).

In lines treated with anti-IgM, the presence of the TREX(empty)UTG lentivirus made no difference to apoptosis sensitivity when compared to the parental line (Figure 4.8). Again, the BL2 parental line is around 20% more resistant to apoptosis than the BL41 line.

A concentration of 6ug/ml and 10ug/ml anti-IGM was used for BL41 and BL2 respectively. This gives a similar level of apoptosis to ionomycin after 72 hours in BL41. However, in BL2 the levels of induced apoptosis are lower, around 60% in the parental and empty lines, although the levels of death in the HA-BHRF1 expressing lines still approach the desired level (20%). Hence, these levels are still within the useful range for determining differences between the apoptosis resistance of different cell lines.

4.5.2 Etoposide and Roscovitine

To examine BHRF1 mediated protection to apoptosis mediated by other mechanisms, we used etoposide and roscovitine, whose mechanisms are well characterised and which have previously been used to study EBV mediated resistance to apoptosis. (230, 325, 326).

Etoposide is a DNA topoisomerase inhibitor which activates p53 dependent apoptosis late in the cell cycle, at the G2/M checkpoint, after duplication of DNA (326). It acts by forming a complex with DNA and the topoisomerase II enzymes and prevents DNA religating; in doing so, it forms double stranded breaks in the DNA (327). Roscovitine is a selective cyclin dependent kinases (Cdk) inhibitor which induces apoptosis independently of the p53 pathway (328, 329). Increases in the concentration of etoposide and roscovitine cause a corresponding increase in the percentage of induced apoptosis (Figure 4.9A and B). Again, BL2 is more resistant to apoptosis and will require higher drug concentrations to give similar levels of death.

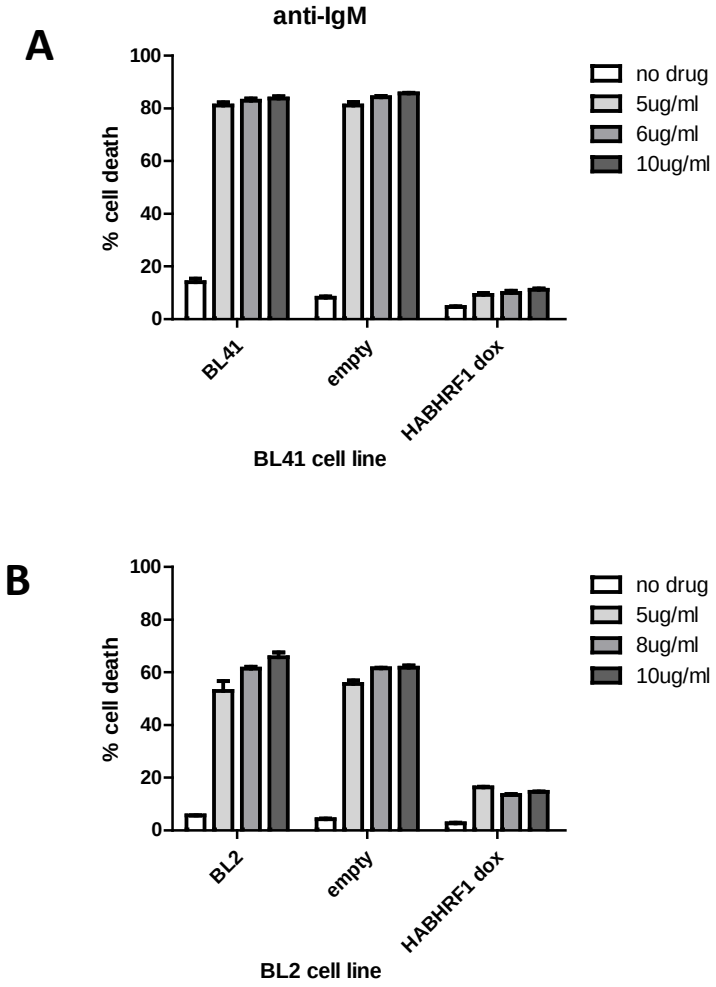

Figure 4.8: Determining concentrations for anti-IgM. Apoptosis assay was performed as in figure 4.7. Empty and HABHRF1 lines were induced with 1µg/ml dox. % cell death is the percentage of cells induced into late apoptosis by drug treatment. Cells were incubated with 5µg/ml, 6µg/ml and 10µg/ml anti-IGM for 72 hours. Apoptosis was induced in BL41 (A) and BL2 (B) cell lines. Based on this data concentrations of 6µg/ml and 10µg/ml anti-IGM were used for BL41 and BL2 respectively.

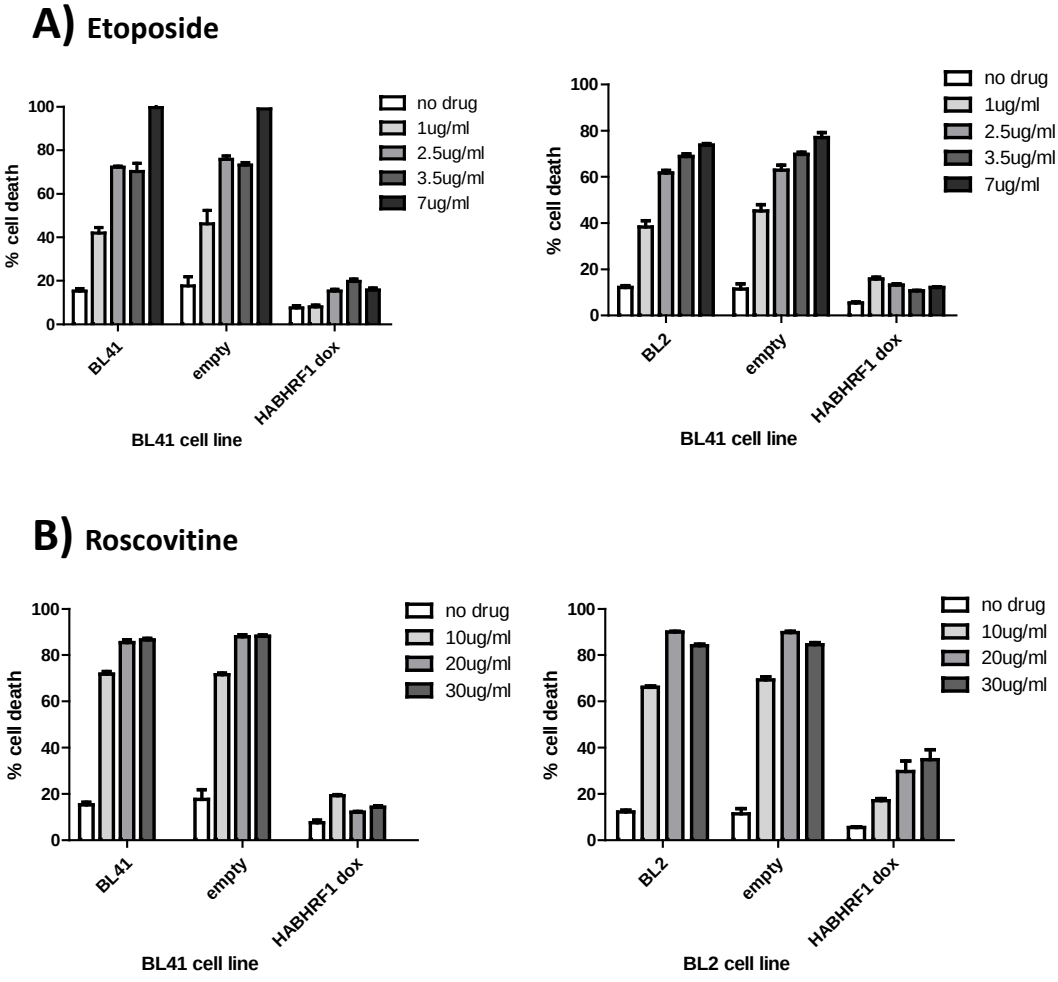

Figure 4.9: Determining concentrations for etoposide and roscovitine. Apoptosis assay was performed as in figure 4.7. Empty and HABHRF1 lines were induced with 1µg/ml dox. % cell death is the percentage of cells induced into late apoptosis by drug treatment. Cells were incubated with (A) 1µg/ml, 2.5µg/ml, 3.5µg/ml and 7µg/ml etoposide for 48 hours and (B) 10µg/ml, 20µg/ml and 30µg/ml roscovitine for 48 hours. Based on this data concentrations of 2.5µg/ml and 3.5µg/ml etoposide and 12ug/ml and 20ug/ml roscovitine were used for BL41 and BL2 respectively.

Cells were treated with roscovitine and etoposide for 48 hours instead of 72 hours as was used for anti-IgM and ionomycin. These time periods and initial concentrations had been tried and tested by other members of our group in similar cell lines (330), and were taken as a starting point. The dose response assays were then used to optimise the drug concentrations for our assays.

From these experiments we decided to use concentrations of 2.5ug/ml and 3.5ug/ml etoposide for 48 hours to induce death in BL41 and BL2 lines respectively. A concentration of 20ug/ml roscovitine was chosen for both BL41 and B2 lines which were incubated with drug for 48 hours. All of these concentrations gave between 60 and 80% apoptosis in the parental and empty lines, and between 10 and 20% apoptosis in the HA-BHRF1 Dox induced lines.

Figure 4.10 shows the same assays performed on un-induced HA-BHRF1 lines without dox which, therefore, should not express BHRF1. These lines are also slightly protected from apoptosis compared to the empty vector.

This data highlights that both BL41 and BL2 lines have leaky expression of HA-BHRF1 in the absence of Dox, and that this expression is functionally significant in that it can provide protection from apoptosis. This justifies our decision to exclude un-induced HA-BHRF1 lines from future assays.

4.6 The effect of mutated HA-BHRF1 on protection from apoptosis

To look at the effect that mutating BHRF1 has on its ability to protect from apoptosis we incubated BL41 and BL2 lines infected with wild type and mutant HA-BHRF1 expressing lentiviruses, induced with Dox, and then exposed to the four apoptosis-inducing drugs used

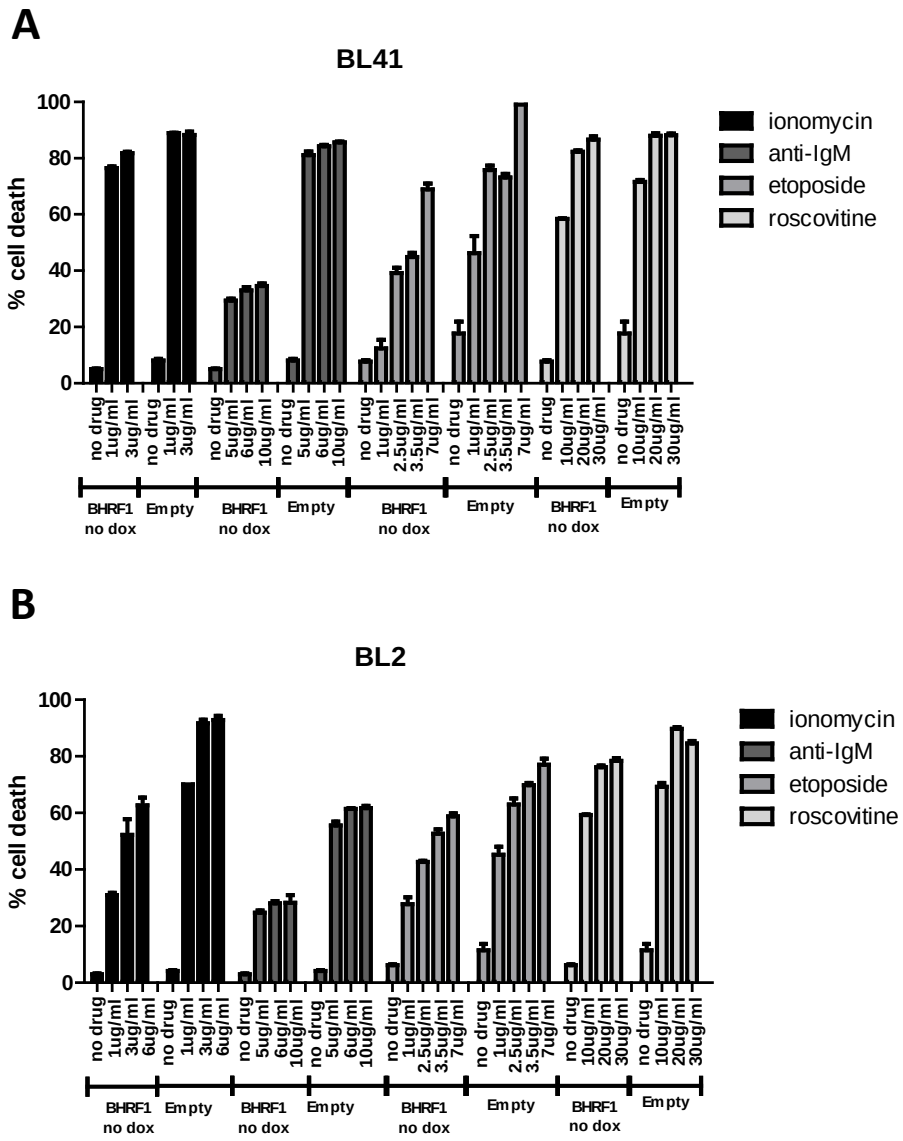

Figure 4.10: Leaky expression of HABHRF1 in uninduced lines. Lines not induced with dox still protect from apoptosis in a dose dependent manner in (A) a BL41 background and (B) a BL2 background compared to the empty vector control. Apoptosis assay was performed as in figure 4.7. % cell death is the percentage of cells induced into late apoptosis by drug treatment with ionomycin, anti-IgM, etoposide and roscovitine.

in Figures 4.7, 4.8 and 4.9. Cells were counted and assayed for viability prior to drug treatment using trypan blue and only cell cultures that were over 80% viable were used.

The levels of apoptosis were again measured using flow cytometry and staining with P.I. and Syto17. Any background levels of death were subtracted from death in the drug treated line to give levels of apoptosis induced with drug. The induced apoptosis was expressed relative to levels of apoptosis in the empty line so that death in the empty control equalled 1. Three technical replicates were taken for each cell background and each drug. An average was taken of the three replicates and a paired Student's T test was performed, with a 95% confidence interval, to determine whether the level of apoptosis induced in the mutants differs significantly from the wild type. Each experiment was performed at least three times and on different dates; averages of the technical replicates for each of the three experiments were taken and combined, an average of these three points was taken to give the mean of three experiments presented below.

4.6.2 Ionomycin and anti-IGM

BL41 and BL2 lines were treated for 72 hours with 1ug/ml and 6ug/ml ionomycin and 6ug/ml and 10ug/ml of anti-IGM respectively. Figure 4.11 shows three replicates of apoptosis assays with ionomycin in BL41 (left panels) and BL2 (right panels) HA-BHRF1 mutants.

As expected, HA-BHRF1 wild type has a significant level of protection from ionomycin-induced apoptosis compared to the empty lentivirus in both cell backgrounds.

The only mutants that show a mean of three experiments with significant changes in protection from ionomycin induced apoptosis, compared to wild type, are G99A and R100D (Figure 4.11). However, there are some changes in levels of apoptosis that are not significant

Ionomycin

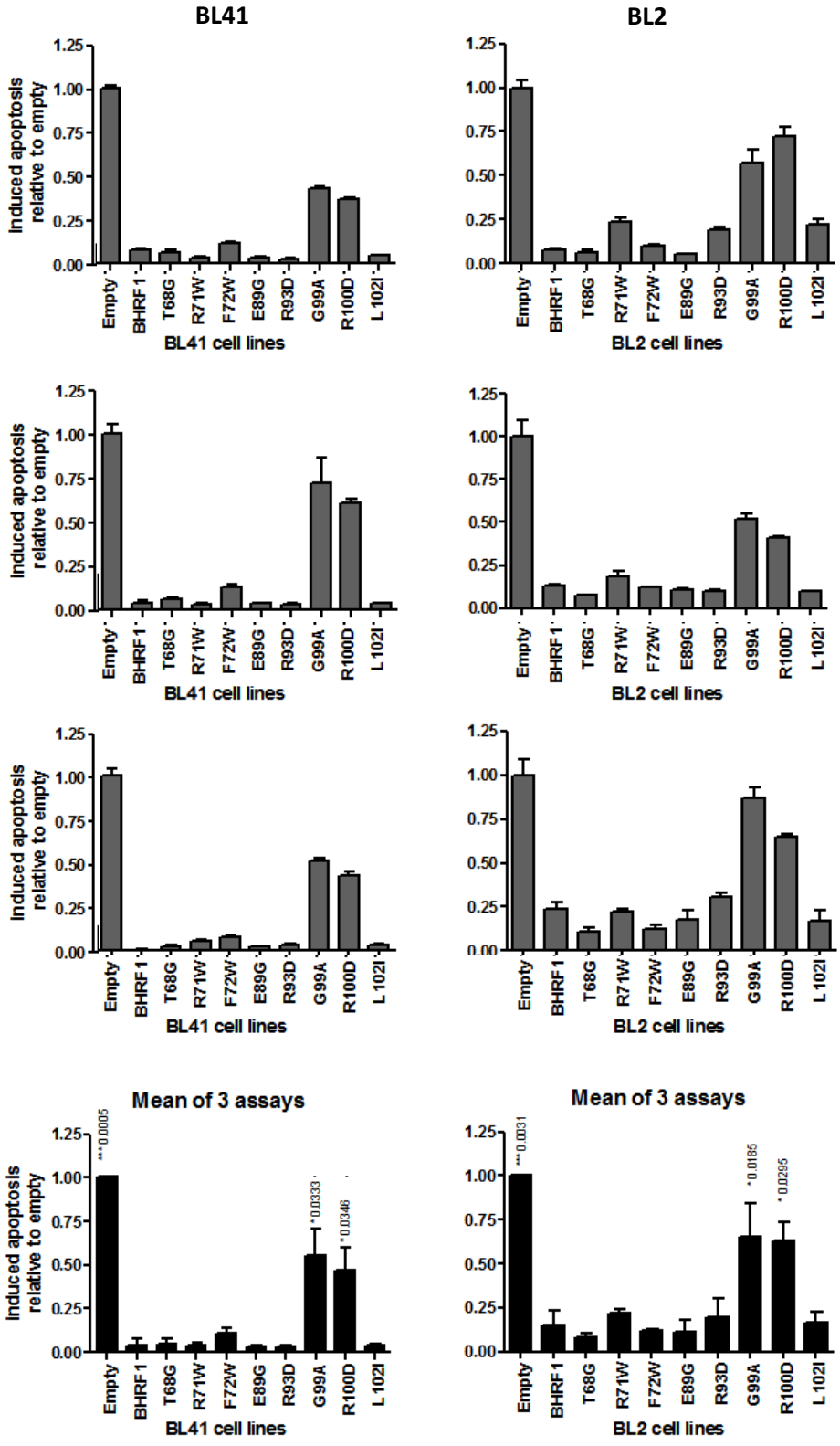
BL41
BL2
Induced apoptosis relative to empty
1.25
1.00
0.75
0.50
0.25
0.00
Empty
BHRF1
T68G
R71W
F72W
E89G
R93D
G99A
R100D
L102I
BL41 cell lines
BL2 cell lines
Mean of 3 assays
*** 0.0005
* 0.0333
* 0.0346
*** 0.0031
* 0.0185
* 0.0295

Figure 4.11: Apoptosis assays with ionomycin. 1μg/ml and 6μg/ml ionomycin were used to induce apoptosis in BL41 and BL2 empty, wild type BHRF1 and mutant BHRF1 expressing cell lines (dox treated). Lines were incubated with drug for 72 hours. Apoptosis is expressed as the percentage of cells induced into late apoptosis (above the background level of apoptosis with no drug) relative to the percentage of apoptosis in the empty line, so that the level of apoptosis in the empty line = 1. Three assays per drug were performed and an average of the three was taken. The significance of differences in relative apoptosis between wild type and mutant was tested with a paired T-test with a 95% confidence interval. When results were significant they were labelled on the graph.
Error bars represent the standard deviation of three technical replicates in each separate experiment. When the means were taken (black bars) error bars represent standard deviation three experimental replicates.

but are consistent over the three replicates. In BL41, F72W has lost some protection when compared to wild type, and R93D is frequently slightly more protected than wt BHRF1.

Although mutants in BL41 and BL2 have a similar ability to protect from apoptosis as wild type, this ability may be slightly decreased, in both mutants and wild type, in BL2. When comparing the levels of induced apoptosis relative to empty in a BIM positive (BL41) vs a BIM negative (BL2) background, two of the mutants, R71W and L102I, show a significant decrease in the ability to protect from apoptosis, relative to empty, in BL2 (*P*=0.004 and 0.0268 respectively). It may be that by losing the ability to bind BIM they have lost some of their survival advantage.

When anti-IgM cross-linking was used to induce apoptosis in a BL41 and BL2 there was a similar pattern of sensitivity to apoptosis, both between BL41 and BL2 lines and compared to the pattern of ionomycin induced death (Figure 4.12A). Like the lines treated with ionomycin, the G99A and R100D mutants were the most sensitive to apoptosis. However, when looking at the mean of three experiments in the BL41 background, this sensitivity was significantly different from wild type in the case of R1OOD, but G99A narrowly failed to reach significance (*P*=0.06).

In the BL2 background all mutants except for G99A and R100D show similar levels of resistance to anti-IGM induced apoptosis as wild type. There was no significant difference between the mutants in BL41 and in BL2.

4.6.3 Etoposide and Roscovitine

BL41 and BL2 lines were treated for 48 hours with 2.5ug/ml and 3.5ug/ml etoposide respectively (Figure 4.12B) or with 12ug/ml and 20ug/ml roscovitine (Figure 4.12C). The

(A) anti-IGM

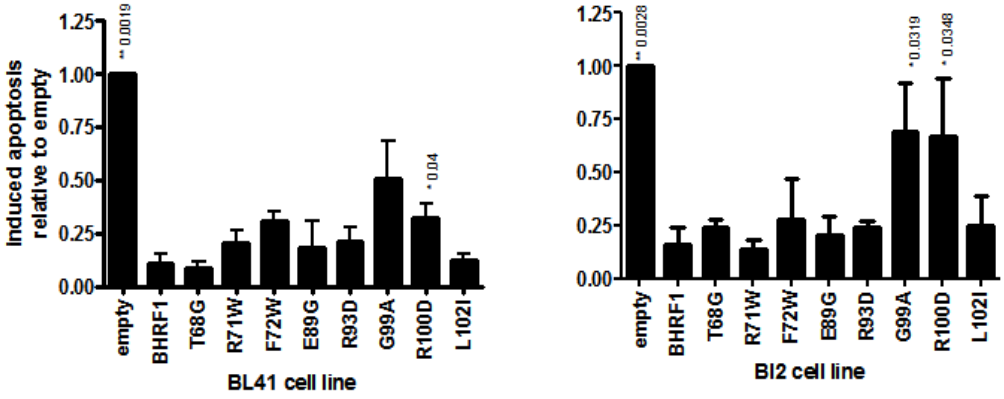

(B) Etoposide

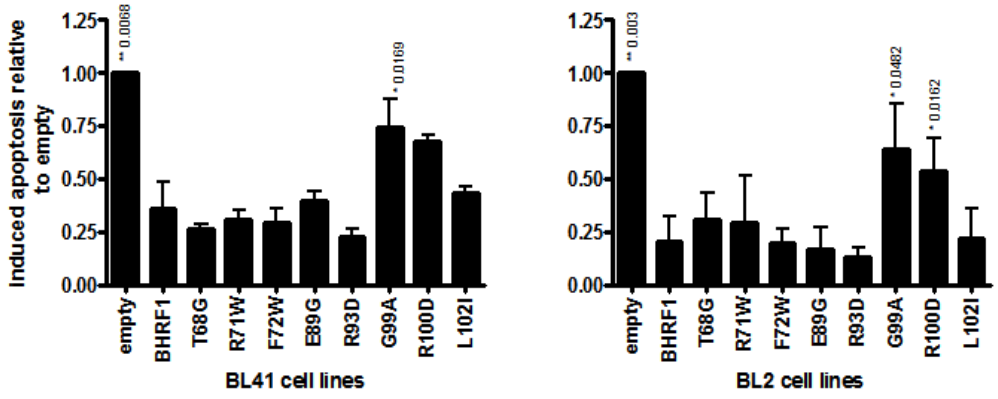

(C) Roscovitine

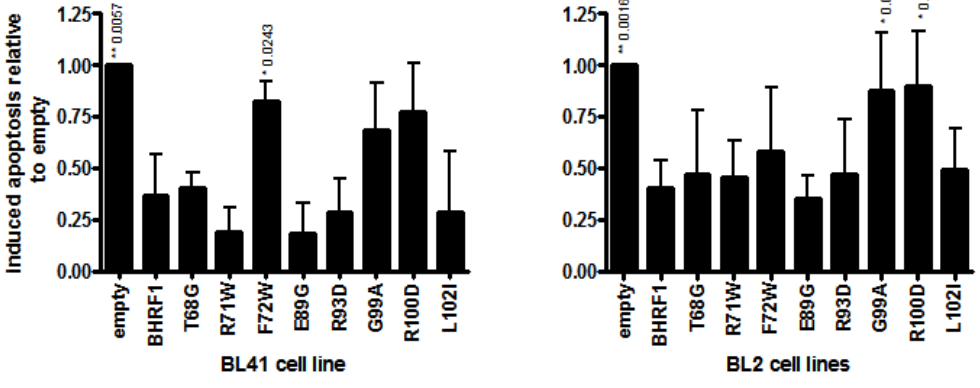

Figure 4.12: Apoptosis assays with anti-IGM, etoposide and roscovitine. (A) 6μg/ml and 10μg/ml anti-IGM (B) 2.5μg/ml and 3.5μg/ml etoposide and (C) 12μg/ml and 20μg/ml roscovitine, were used to induce apoptosis in BL41 and BL2 empty, wild type BHRF1 and mutant BHRF1 expressing cell lines. Lines were incubated with drug for 48 hours. Apoptosis was measured and analysed as in figure 4.12 and significance of differences between wild type and mutants was measured with paired T tests. Data is mean of three separate experiments.

percentage of mutant BHRF1 cells induced into apoptosis was expressed relative to the percentage apoptosis in the empty line.

When apoptosis was induced with etoposide (Figure 4.12B), G99A and R100D again lose protection from apoptosis. When the mean of three experiments is taken this increase in sensitivity is significant for both mutants in BL2 and for G99A in BL41, although R100D narrowly failed to reach significance (*P*=0.07).

G99A and R100D are also consistently more sensitive to roscovitine induced apoptosis. This is significant across the mean of three assays in BL2 but not in BL41 due to the high standard deviation (Figure 4.12C). In BL41 F72W also shows a significant difference to wild type across three assays and is much more sensitive to apoptosis induced by roscovitine than by any other drug. This difference is not as pronounced in BL2 background and is not significant.

4.6.4 BHRF1 G99A and R100D mutant protection

From these assays it appears that the mutants which most consistently affect BHRF1's ability to protect from apoptosis are G99A and R100D. The G99 and R100 amino acids both lie within the BH1 domain of BHRF1. From Table 4.2 it is clear that BHRF1 binding to various cellular BCL-2 homologues has been significantly decreased if not completely lost due to these mutations. G99A has completely lost binding to BAX and BID with binding to BIM, PUMA and BAK being decreased 4.5, 2.5 and 29 fold respectively. R100D has lost binding to BAX, BAK and BID. R100D binding to BIM has decreased 25 fold and there is also a 5.5 fold decrease in binding to PUMA. It is clear that a 25 fold reduction would have a huge impact but it is less clear if a 5.5 fold reduction may or may not make a large difference to binding ability.

These mutations decrease the ability of BHRF1 to protect from apoptosis induced by all four drugs tested. From Table 4.3 the percentage protection from apoptosis of G99A and R100D has decreased by around 30 to 50% in the case of each drug, in both cell backgrounds. G99A and R100D show a remarkably similar degree of loss of function, particularly considering differences in expression levels (Figure 4.5A).

The loss of protection in G99A and R100D is expected from the binding data which shows undetectable binding, or substantial decreases in binding, to all BCL-2 homologues analysed. However, from the binding data (Table 4.2) we could expect G99A to be more resistant to apoptosis than R100D due to a greater decrease in binding affinity for BCL-2 homologues conferred by the R100D mutation. From Figure 4.5 it can be seen that expression of HAR100D in BL41 is noticeably higher than HAG99A. This might possibly explain the apparent lack of difference in apoptosis protection between HAR100D and HAG99A in BL41. However, in BL2 there is no difference between expression of HAG99A and HAR100D (Figure 4.5) and the protection conferred by these mutants is similar when treated with all the drugs tested (Table 4.3).

4.6.5 BHRF1 F72W mutant protection

According to the binding data (Table 4.2) the F72W mutation causes the loss of binding to all BCL-2 homologues tested except for PUMA, which has decreased binding affinity by four fold. From this data we would expect F72W to have lost a lot of its protection from apoptosis. However, from the apoptosis assay data the F72W mutation provides similar protection as wild type BHRF1 in both BL41 and BL2 lines treated with ionomycin and etoposide (Table 4.3). In anti-IgM treated BL41, F72W is consistently less protective than wild type BHRF1 in all three assays, although this did not reach significance. The average

	Ionomycin		Anti-IGM		Etoposide		Roscovitine	
	BL41	BL2	BL41	BL2	BL41	BL2	BL41	BL2
BHRF1	95.9%	85.3%	89%	83.7%	64.3%	79.9%	63.7%	59.9%
F72W	89.3%	88.3%	69.2%	71.9%	70.3%	80.6%	17.7%*	42.2%
R93D	96.9%	80.2%	79.2%	75.7%	77.1%	87.1%	71.6%	53%
G99A	44.7%*	34.8%*	49.4%	30.6%*	25.6%*	35.9%*	31.8%*	12.3%*
R100D	53.2%*	37.3%*	67.4%*	32.9%*	32.6%	46.6%*	22.8%*	10.4%*

Table 4.3: Protection from apoptosis conferred by BHRF1 and mutants. Protection is expressed as a percentage relative to empty in which the percentage protection is 0%. 100% protection would indicate that only the background level of cell death was present and that no apoptosis had been induced by drug treatment. BL41 and BL2 lines were treated for 72h with 1µg/ml and 6µg/ml ionomycin, and 6µg/ml and 10µg/ml anti-IGM, respectively. They were treated for 48h with 2.5µg/ml and 3.5µg/ml etoposide and 20µg/ml roscovitine. A number of BHRF1 mutants, showing consistent changes in apoptosis protection over several experiments, were picked out for further study. In each case these values are the mean of three separate experiments.
Mutants in which the level of protection from apoptosis in significantly different from BHRF1 wild type are indicted by an *.

percentage protection from apoptosis in F72W is similar to the protection conferred by R100D, around 20% lower than the wild type. In anti-IGM treated BL2 F72W mutation gives more similar protection to wild type BHRF1. This could indicate that BL2 is more PUMA dependent than BL41 due to the loss of BIM.

In roscovitine treated BL41 lines the F72W mutation does cause a significant and large increase in the sensitivity to apoptosis, and reduces protection from apoptosis by 46%. This is similar to the loss of protection seen with R100D, the other mutant which consistently causes a large loss of protection and has lost binding to BAX, BAK and BID (Table 4.2). However, R100D has retained a small amount of binding to BIM.

When apoptosis is induced with roscovitine, F72W retains ability to protect in BL2 but not in BL41. This is most likely because, without any expression of BIM, BL2 is more dependent on PUMA to induce apoptosis.

4.7 The levels of most cellular BCL-2 homologues are not affected by the expression of mutated BHRF1

The sensitivity of cells to apoptosis can be influenced by the overall levels of the members of the pro and anti-apoptotic cellular BCL-2 family proteins. Therefore this needs to be considered when looking at the effect of expressing the viral BCL-2 homologue, BHRF1, in cells. The protein levels of cellular BCL-2 homologue may have the potential to affect the apoptosis sensitivity of the BHRF1 expressing cell lines. Cellular BCL-2 homologue levels may also have an effect on the function of BHRF1, since it works through interacting with these proteins.

From Figure 4.13 it can be seen that the expression of most BHRF1 mutants does not affect the levels of the majority of the cellular BCL-2 family proteins. An exception to this is BIM, a

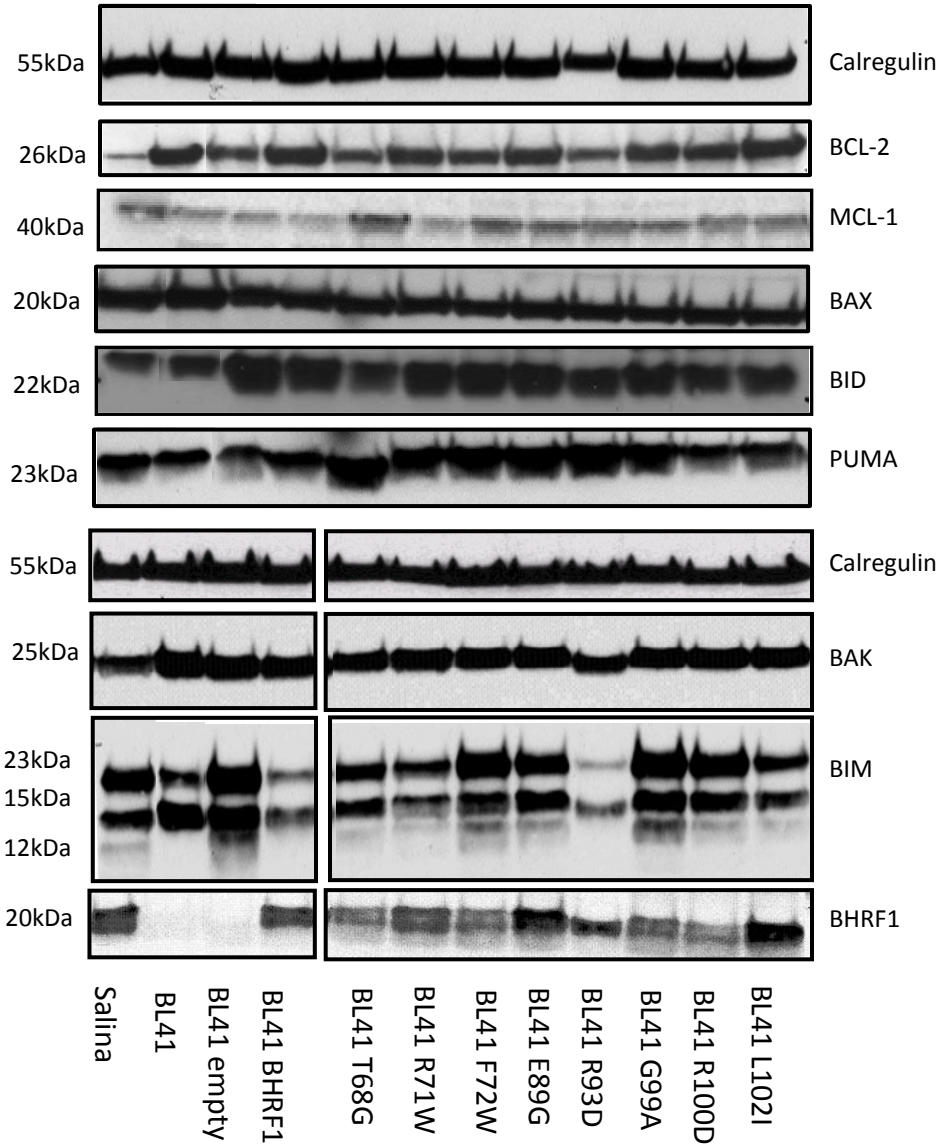

Figure 4.13: Levels of cellular BCL-2 homologues in BHRF1 wild type and mutant expressing BL41 lines.
Expression of BCL-2 homologues in BL41 empty, BHRF1 wild type and BHRF1 mutants compared to BL41 parental and Salina Wp BL. Some blots were manipulated to remove a duplicated well.

pro-apoptotic BH3 only homologue, and known binding partner of BHRF1. The levels of BIM protein in BL41 fall in the presence of wild type BHRF1 compared to empty lentivirus. This can also be seen in some of the mutants; R71W, R93D and L102I. From the binding data (Table 4.2) all these mutants have strong binding to BIM, with a dissociation constant of between 10 and 25 Kd, compared to wild type with 18 Kd. It is interesting that, from the binding data, T68G should bind strongly to BIM (with dissociation constant of 9 Kd) yet there is no reduction in the BIM levels seen in the T68G infected cell line when compared with mutants such as F72W and R100D, which should have very low binding to BIM. This pattern is followed by BL41 cell lines transduced on different dates (Figure 4.14). The levels of BIM are significantly higher in the BL41 parental and BL41 empty lines. This is also the case for F72W, G99A and R100D mutants which bind weakly to BIM and show higher BIM levels by Western blot. Lower BIM levels are seen in R93D and wild type, which bind strongly to BIM; however, at the time T68G was not included in the selection of cell lines.

A denaturing gel was used and hence, these differences in BIM level are most likely not due to direct binding to BIM but may alter BIM levels by some indirect mechanism.

4.8 Co-immunoprecipitation does not show BHRF1 binding to most BCL-2 homologues

Figures 4.15 and 4.16 relate to the co-immunoprecipitation of BHRF1 and the cellular BCL-2 homologues. BL41 cells expressing wild type or mutated BHRF1 were induced with Dox. Pellets were harvested and 10 million cells were lysed with 1% Triton X-100 Onyx buffer. Figure 4.15 shows the protein expression in the lysed lines prior to co-immunoprecipitation. BIM shows the same pattern of expression levels as seen in Figure 4.13.

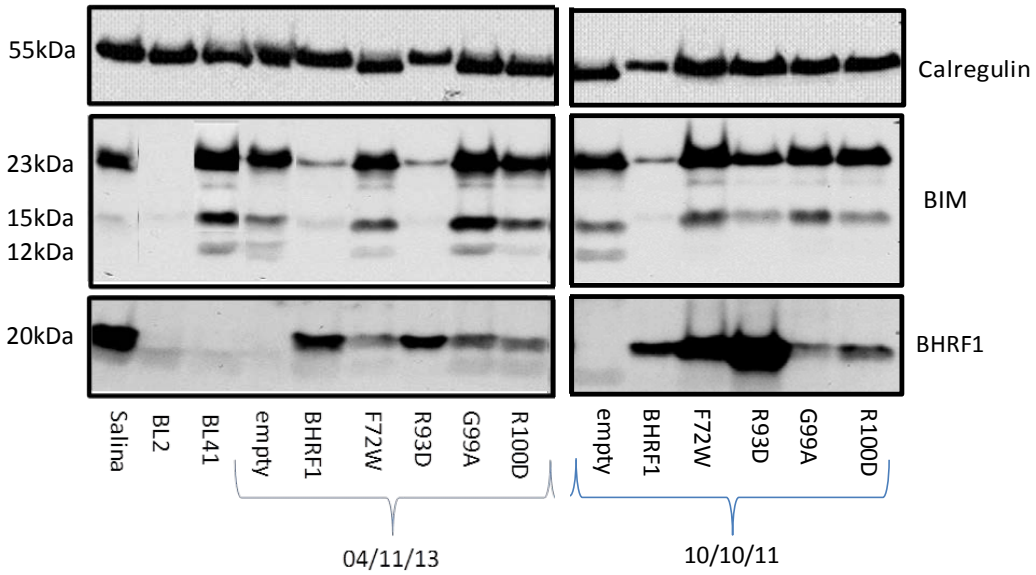

Figure 4.14: Levels of cellular BIM BCL-2 homologue is reduced by strong binding to BHRF1. Blots are shown for two separate sets of cell lines made on two different dates. Protein was recovered for each set of lines, run on Western blot and blotted for antibodies specific to BIM, BHRF1 and calregulin. Positive controls; BL41 and Salina, were included in the panel. BIM negative BL2 was used as a negative control for BIM.

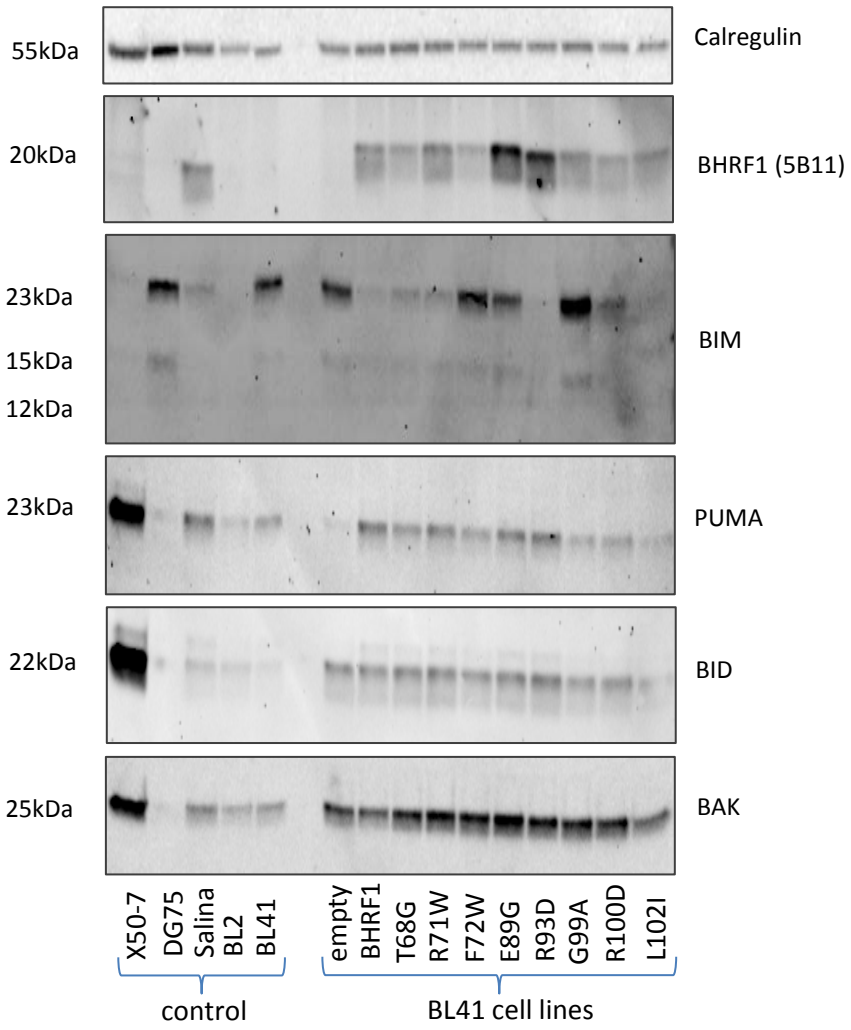

Figure 4.15: Lysates of lines used for Co-IP. 10 million cells were lysed in 1% Triton X-100 Onyx buffer. The lysate from the equivalent of 3 x 10^5 cells was used for Western blot to determine the expression of cellular BCL-2 homologues. The rest of the lysate was reserved for the Co-IP experiments. X50-7 LCL, Salina Wp and DG75, BL2 and BL41 EBV negative lines were lysed under the same conditions and used as controls.

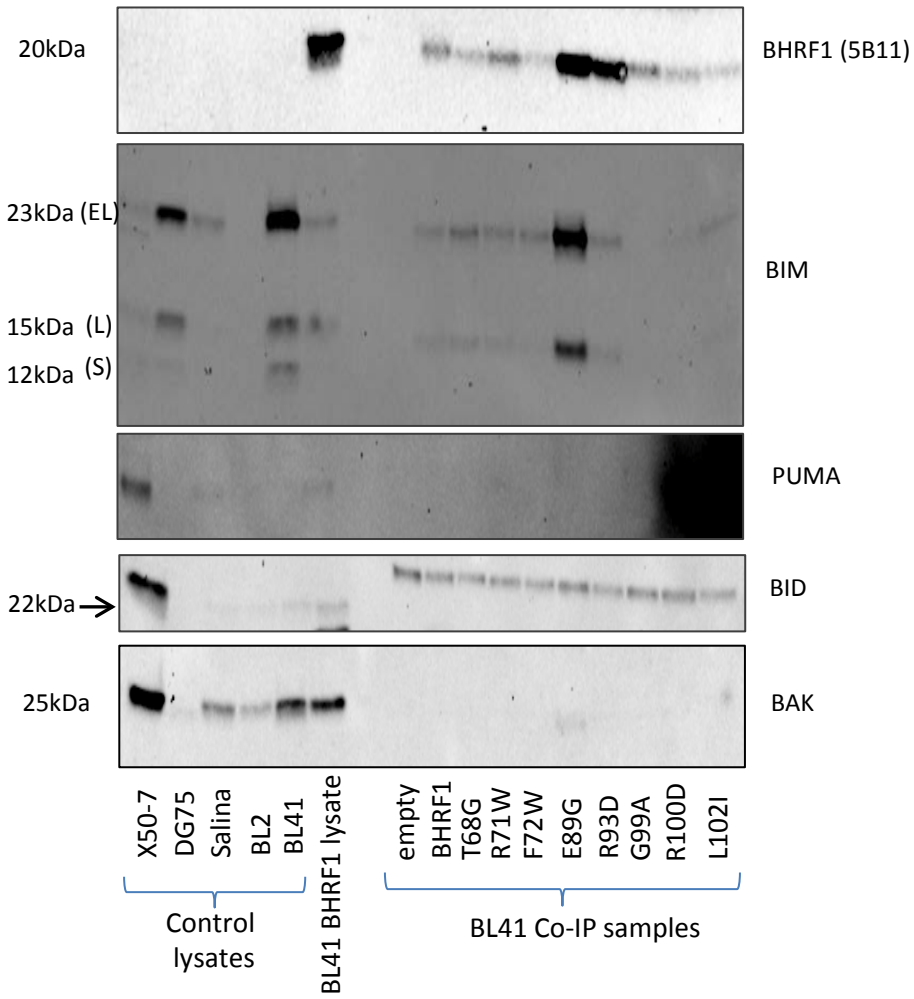

Figure 4.16: Co-IP of HABHRF1 and HABHRF1 mutant expressing BL41 lines. 10 million cells were lysed in 1% Triton X-100 Onyx buffer. BHRF1 was immuno-precipitated using anti-HA antibody. The protein was eluted by boiling in urea buffer. Protein from the Co-IP of 3 million cells was used for each gel. Lysates of X50-7 LCL, Salina Wp DG75, BL2 and BL41 EBV negative lines and HABHRF1 were used as a control. Protein in the BID blot is non-specific, running very close to the size of BID. True BID protein was only seen in the BHRF1 and parental BL41 lystate samples, the size is indicated by an arrow.

A Co-IP using an anti-HA antibody bound to protein G beads was performed on the lysate from 10 million cells and protein from the equivalent of 3 million cells was run on a Bis-Tris gel for Western blotting (Figure 4.16). The results of the Co-IP indicate that BHRF1 does interact with BIM and that this is also the case for most of the mutants. As expected BHRF1 wild type, T68G, R71W and R93D all bind BIM. Considering the amount of HAR93D bound by the beads and the indication of strong binding given by the dissociation constant of 10Kd (see Table 4.2), we might expect R93D to have bound more BIM compared to the wild type and other mutants. However, these levels, and those of T68G and R71W, appear similar.

Two unexpected results come from F72W and E89G. From the dissociation constants (Table 4.2) the F72W mutation has caused total loss of the ability to bind BIM. This is clearly not the case as there is a similar level of BIM protein precipitated using HAF72W as there is using the HA tagged wild type BHRF1. From the ITC data E89G should also have very weak binding to BIM, with a Kd of 930 vs 18 for wild type BHRF1. However, although there was a large amount of HAE89G protein in the lysate and bound by the HA beads, there is also a lot of BIM protein precipitated. This is most obvious when compared to R93D. This mutant was precipitated with HA antibody at a similar level to E89G and should bind BIM strongly (with a Kd of 10). However, significantly more BIM is precipitated with E89G than with R93D. When we look at the BIM levels in the lysate, it can be seen that these lower levels of precipitation are not due to weak binding but to the barely detectable levels of BIM in the R93D line. Despite these extremely low levels, R93D BHRF1 co-immunoprecipitated detectable levels of BIM, indicating strong binding.

While the strength of binding between BIM and E89G and F72W BHRF1 is not as high as between BIM and wild type or R93D BHRF1, it is still higher than indicated by the binding table.

There was no precipitation of BHRF1 with any of the other BCL-2 homologues. This was surprising as it is known that BHRF1 binds PUMA and BAK (109). The levels of BHRF1 in our assay were comparable to those seen in Wp restricted BLs, and yet at these physiological levels no binding to PUMA, BID or BAK was observed. The Co-IP assay was very difficult to perform consistently and to interpret, especially considering that there were often low and variable expression levels of wild type and mutated BHRF1. Over several assays attempted, using several different methods, we were able to see BIM precipitated but no other BCL-2 homologue precipitation was evident.

4.9 The effect of repression of BCL-2 homologues on BHRF1's ability to protect from apoptosis

Although we did not find any binding to PUMA or BAK with our Co-IP assay, this binding has previously been reported by others (109). However, other Co-IP assays were usually performed in lines artificially expressing high levels of BCL-2 homologues or BHRF1, or in cell types other than human B cells(84, 104, 109). In our assays both HA-BHRF1 and the BCL-2 homologues were expressed at physiological levels. It may be that our assay is not sensitive enough to pick up the low levels of immunoprecipitation seen with physiological levels of BHRF1. However, these interactions may still have a functional role despite us being unable to detect them. To investigate if BHRF1 function relies on the presence of individual BCL-2 homologues, and how mutation affects BHRF1 function, BIM, PUMA, BAX and BAK were repressed individually using short hairpin RNAs (shRNAs). These shRNA plasmids were bought as commercial constructs from Santa Cruz Biotechnology Inc, and hence the shRNA sequences are unknown. The products consisted of a pool of three to five lentiviral plasmids encoding target specific 19-25 (plus hairpin) nucleotide sequences designed to knockdown

target gene expression. These lentiviruses were transduced into wild type and mutant BHRF1 expressing BL41 lines. Stably transduced lines were selected using 10ug/ml puromycin and constitutively expressed shRNAs, leading to repression of target expression. A scrambled shRNA expressing lentivirus, containing a sequence which will not lead to the specific degradation of any cellular message, was used as a negative control for knockdown.

Figure 4.17 shows the knockdown with BIM, PUMA, BAX and BAK in several BHRF1 mutant BL41 lines, compared to the scrambled shRNA control lines (Figure 4.17 A-D respectively). Overall, good knockdown was achieved. PUMA and BAX were knocked down to undetectable levels in all mutants and BIM knockdown was complete for BIM-S and BIM-L isoforms, whereas expression was of BIM-EL was significantly reduced. Knockdown of BAK was only partial, but expression was significantly lower in all mutants when compared to the scrambled shRNA control (Figure 4.16D). Unfortunately, we did not have sufficient time to achieve knockdown of BID.

The ability of BHRF1, and its mutants, to protect against cell death in lines negative for BIM, PUMA, BAX or BAK, was assessed using the apoptosis assay described in section 4.4. Apoptosis was induced using ionomycin, anti-IGM, etoposide and roscovitine. Induced apoptosis in the shRNA lines, with knockdown of BCL-2 homologues, was expressed relative to the levels of induced apoptosis in the scrambled shRNA control lines. This gives the change in apoptosis protection resulting from the knockdown of specific BCL-2 homologues.

A

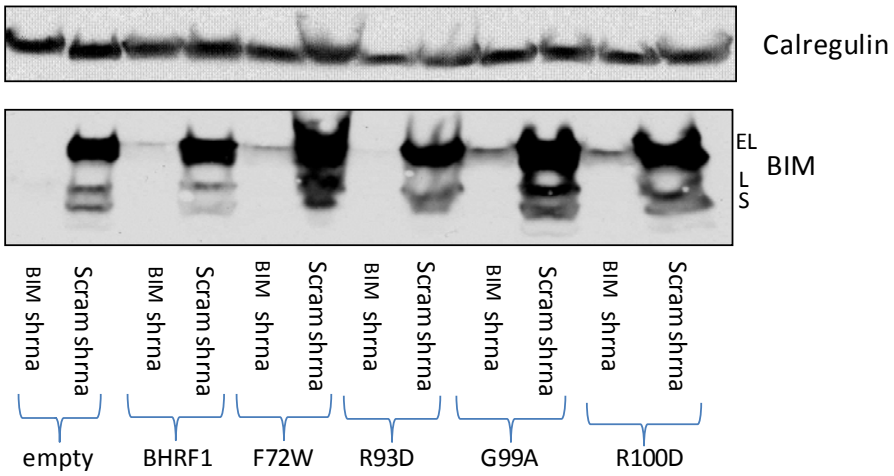
Calregulin
EL
L
S
BIM
BIM shrna
Scram shrna
empty
BHRF1
F72W
R93D
G99A
R100D

B

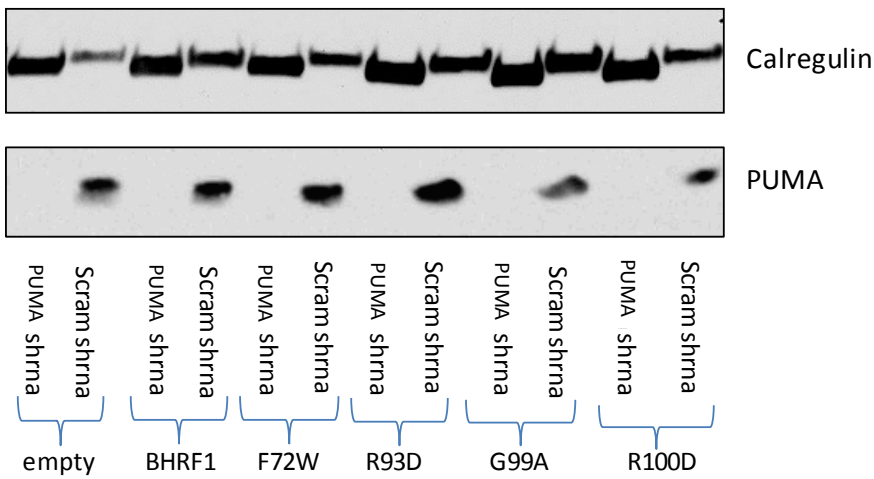
Calregulin
PUMA
PUMA shrna
Scram shrna
empty
BHRF1
F72W
R93D
G99A
R100D

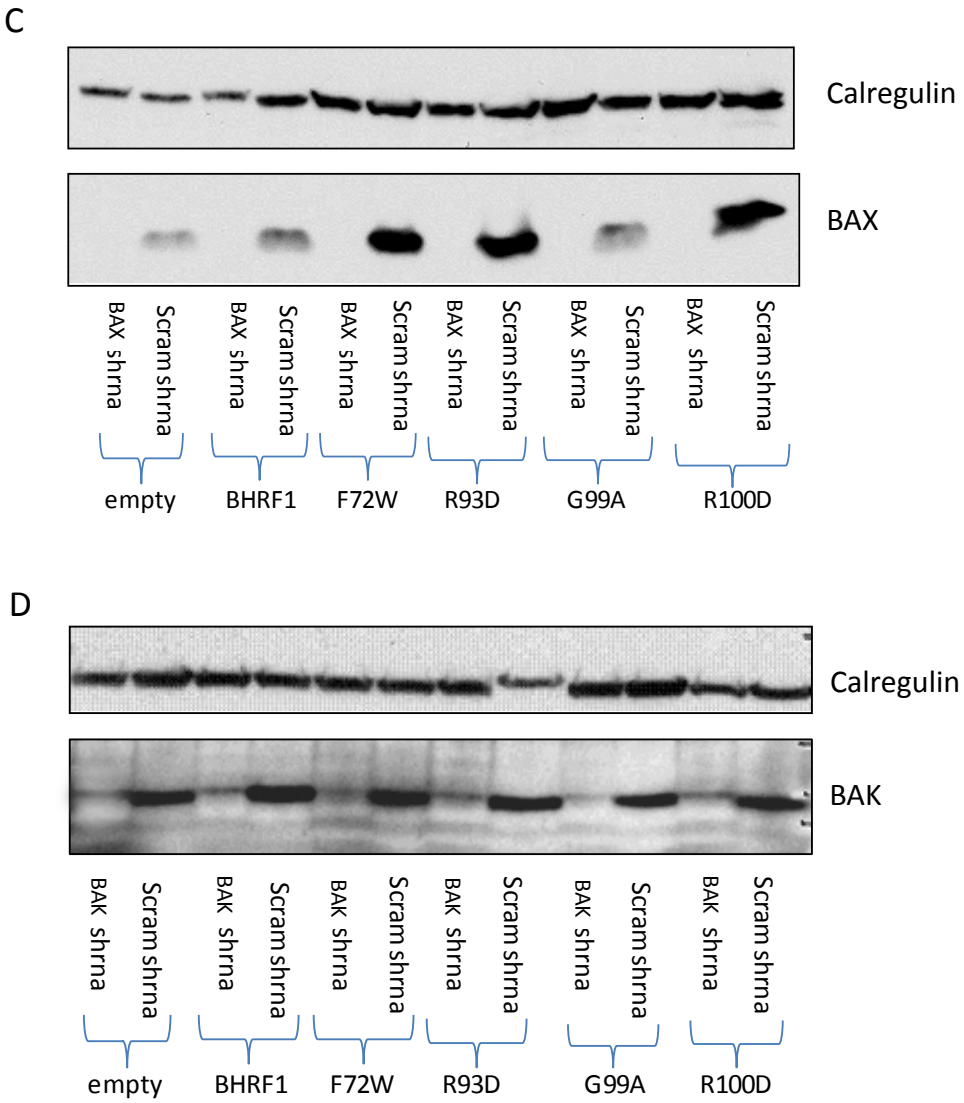

Figure 4.17: Knockdown of BCL-2 homologues with shRNA lentiviruses. BHRF1 mutant expressing BL41 lines were infected with lentiviruses containing BIM, PUMA, BAX and BAK BCL-2 homologues. A lentivirus containing a scrambled shRNA was used a control and repression of BCL-2 homologues was assessed with Western blot. BIM, PUMA, BAX and BAK shRNAs blots are shown in A to D respectively.

4.9.1 Mutant BHRF1 expressing lines with and without scrambled shRNA give a similar pattern of apoptosis protection

Figure 4.18 compares the levels of induced apoptosis in BL41 BHRF1 mutant lines used previously (BL41) and BL41 BHRF1 mutant lines with scrambled shRNA (Scram shRNA). The scrambled shRNA lines should give similar results to the BL41 BHRF1 mutant parental lines. The patterns of protection between the mutants are similar, as are levels of apoptosis induced by all drugs. The empty BL41 and BL41 scrambled shRNA lines give between 60 and 80% death with all drugs used, levels which were also seen in previous apoptosis assays. Apoptosis levels vary slightly when death is induced with anti-IGM, with levels of induced apoptosis being around 10% lower in scrambled shRNA lines. However, scrambled shRNA lines follow the same pattern of loss or gain in protection as BL41 lines, dependent upon the mutation.

4.9.2 Knockdown of BIM, PUMA, BAX and BAK changes the ability of some BHRF1 mutants to protect from apoptosis

The sensitivity to induced apoptosis of the various BCL-2 homologue knockdown lines is shown in Figure 4.19 to 4.23. Figure 4.19 shows the levels of apoptosis, induced by four drugs in the BL41 empty lines expressing scrambled, BIM, PUMA, BAX or BAK shRNAs. These levels can be variable, especially when apoptosis is induced with anti-IgM and roscovitine which have lost much of their ability to induce apoptosis in PUMA and BAK negative lines. Because of this variability, the mutants were expressed relative to the corresponding knockdown line containing the BHRF1 negative (empty) vector. Figures 4.20 to 4.23 show

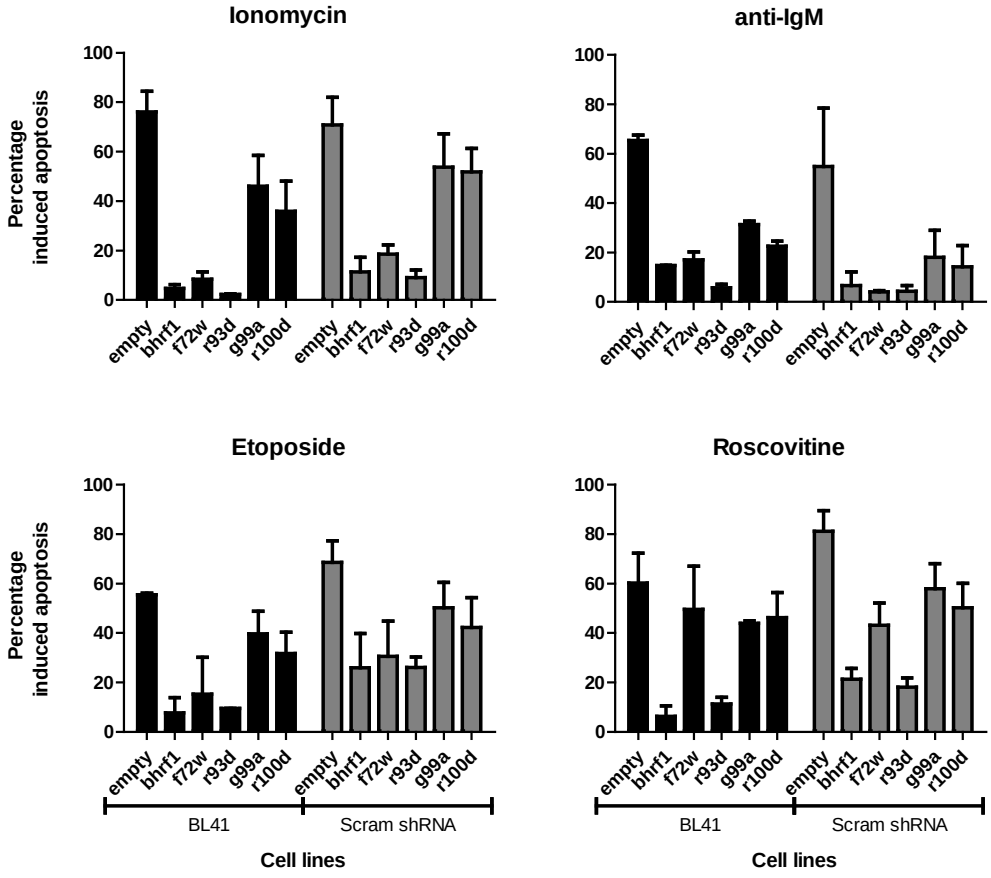

Figure 4.18: BHRF1 mutant lines protect at similar levels with and without scrambled shRNA. Comparison of BL41 BHRF1 mutant lines (BL41) and BL41 BHRF1 mutant lines expressing scrambled shRNA (Scram shRNA). The mean of three assays, in which apoptosis was induced using four different drugs. Death was induced with 1µg/ml, 6µg/ml, 2.5µg/ml and 12µg/ml of ionomycin, anti-IgM, etopside and roscovitine respectively. Percentage of induced apoptosis is given as percentage of late apoptosis in the drug treated lines minus the background level of late apoptosis in the untreated lines. Cells in untreated were always above 85% viable. Mean and standard deviation are from three experimental replicates.

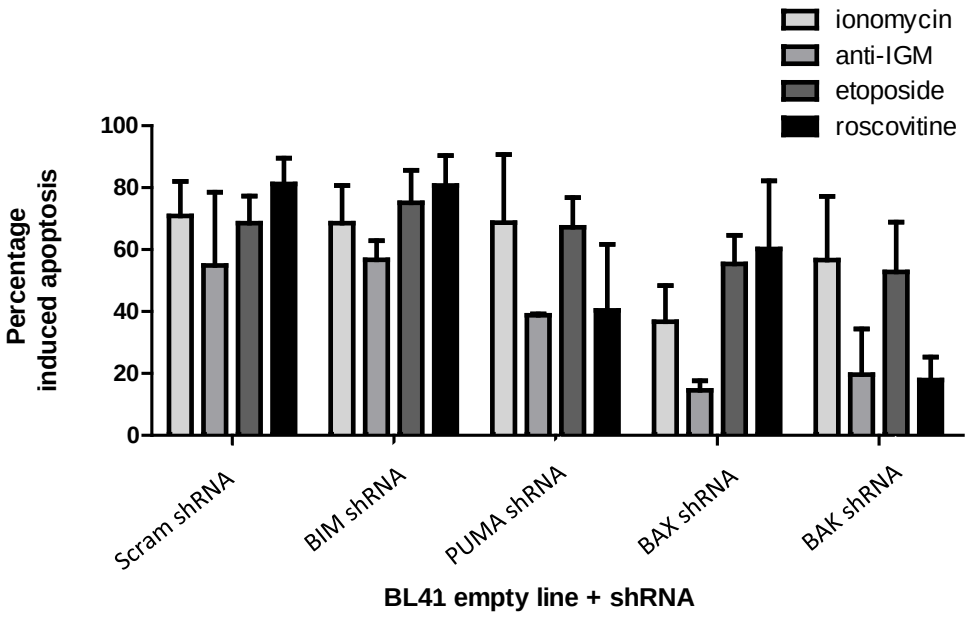

Figure 4.19: Percentage apoptosis induced in BL41 empty lines expressing BCL-2 homologue shRNAs. Percentage of apoptosis induced by ionomycin, anti-IGM, etoposide and roscovitine in empty control BL41 lines expressing BIM, PUMA, BAX , BAK and scrambled control shRNAs. Death was induced with 1µg/ml, 6µg/ml, 2.5µg/ml and 12µg/ml of ionomycin, anti-IgM, etopside and roscovitine respectively. Data is un-normalised and mean and standard deviation of three experimental replicates.

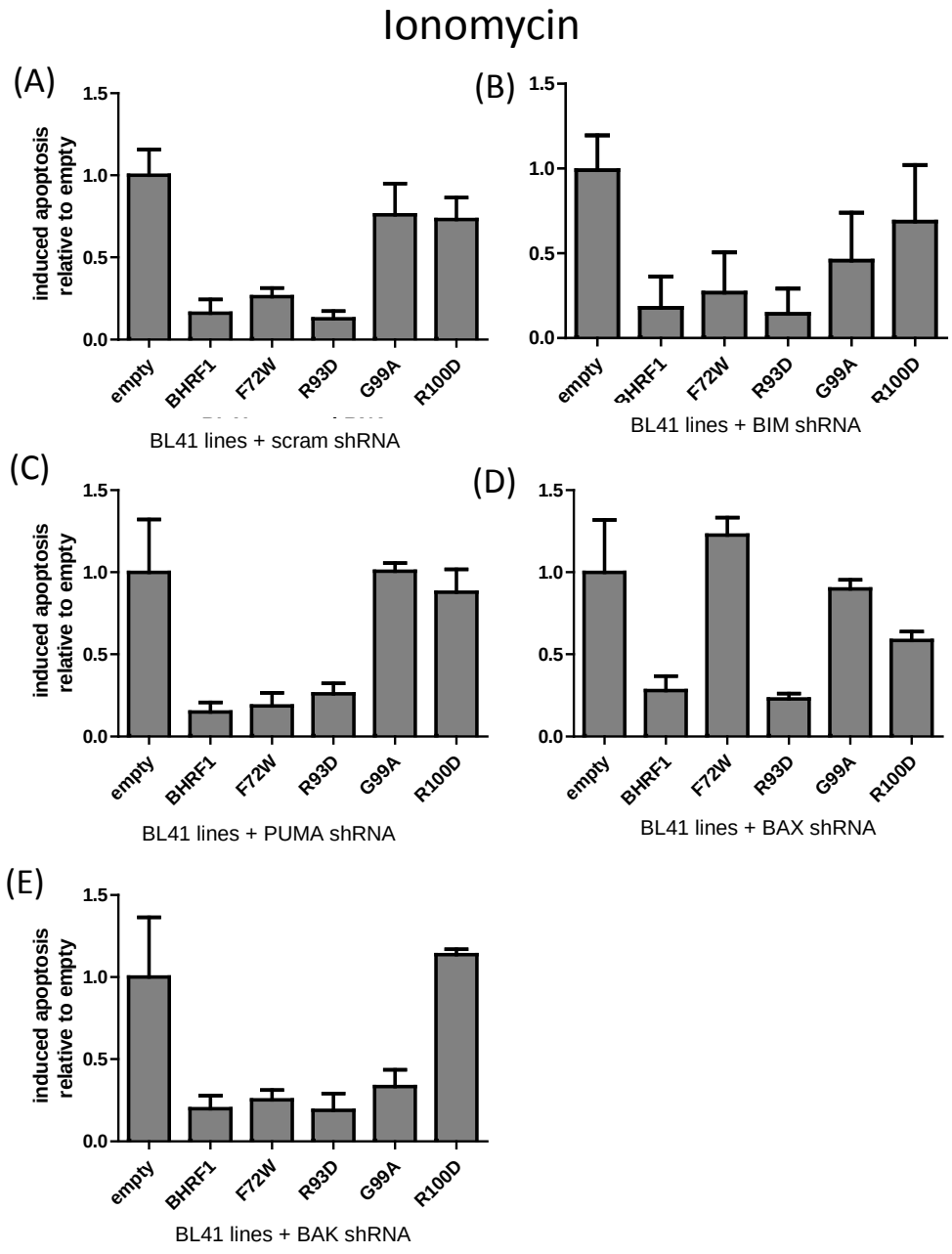

Figure 4.20: Ionomycin induced apoptosis in BHRF1 wild type and mutant expressing lines with BCL-2 homologue knockdown. BIM, PUMA, BAX and BAK were knocked down in the BL41 BHRF1 empty, wild type and mutant lines, using shRNA expression. Ability of these lines to protect from apoptosis was tested using 1µg/ml ionomycin. Data is expressed as level of induced apoptosis relative to empty. Scrambled (A), BIM (B), PUMA (C), BAX (D) and BAK (E) lines are shown separately. Data is mean and standard deviation of three experimental replicates.

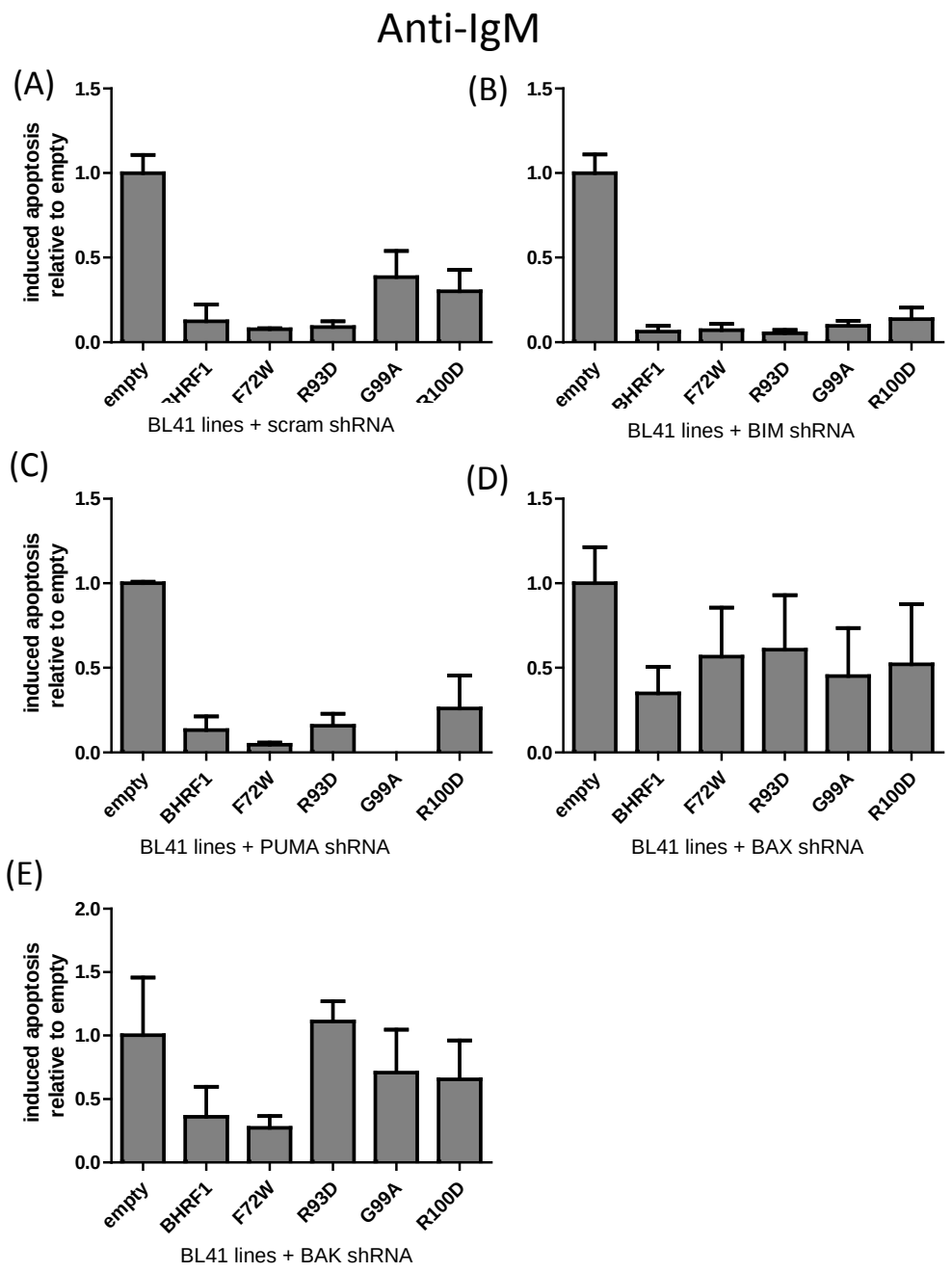

Figure 4.21: Anti-IgM induced apoptosis in BHRF1 wild type and mutant expressing lines with BCL-2 homologue knockdown. BIM, PUMA, BAX and BAK were knocked down in the BL41 BHRF1 empty, wild type and mutant lines, using shRNA expression. Ability of these lines to protect from apoptosis was tested using 6µg/ml anti-IgM. Data is expressed as level of induced apoptosis relative to empty. Scrambled (A), BIM (B), PUMA (C), BAX (D) and BAK (E) lines are shown separately. Data is mean and standard deviation of three experimental replicates. G99A PUMA shRNA line (C) was not tested because of problems with cell viability.

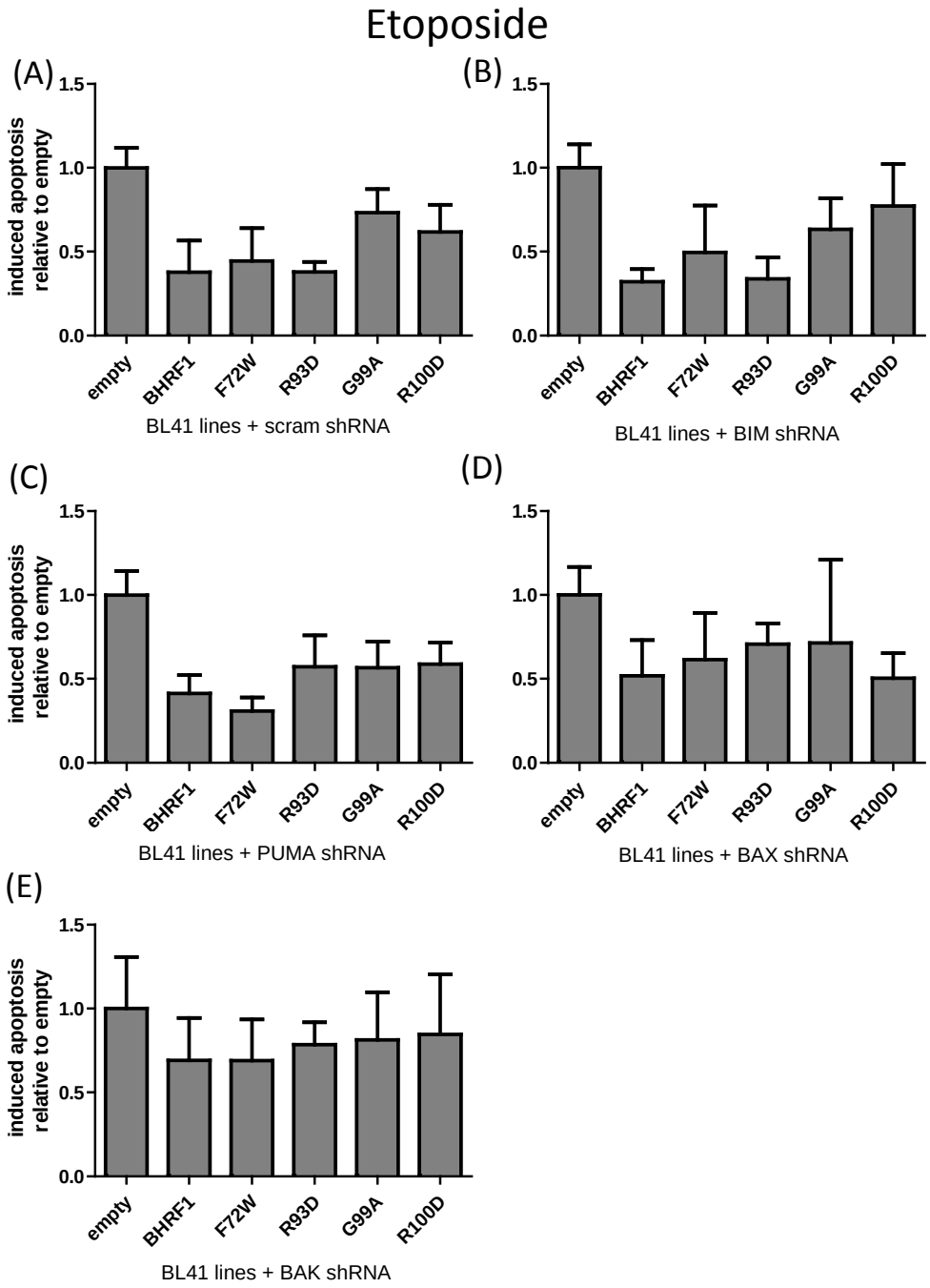

Figure 4.22: Etoposide induced apoptosis in BHRF1 wild type and mutant expressing lines with BCL-2 homologue knockdown. BIM, PUMA, BAX and BAK were knocked down in the BL41 BHRF1 empty, wild type and mutant lines, using shRNA expression. Ability of these lines to protect from apoptosis was tested using 2.5µg/ml etoposide. Data is expressed as level of induced apoptosis relative to empty. Scrambled (A), BIM (B), PUMA (C), BAX (D) and BAK (E) lines are shown separately. Data is mean and standard deviation of three experimental replicates.

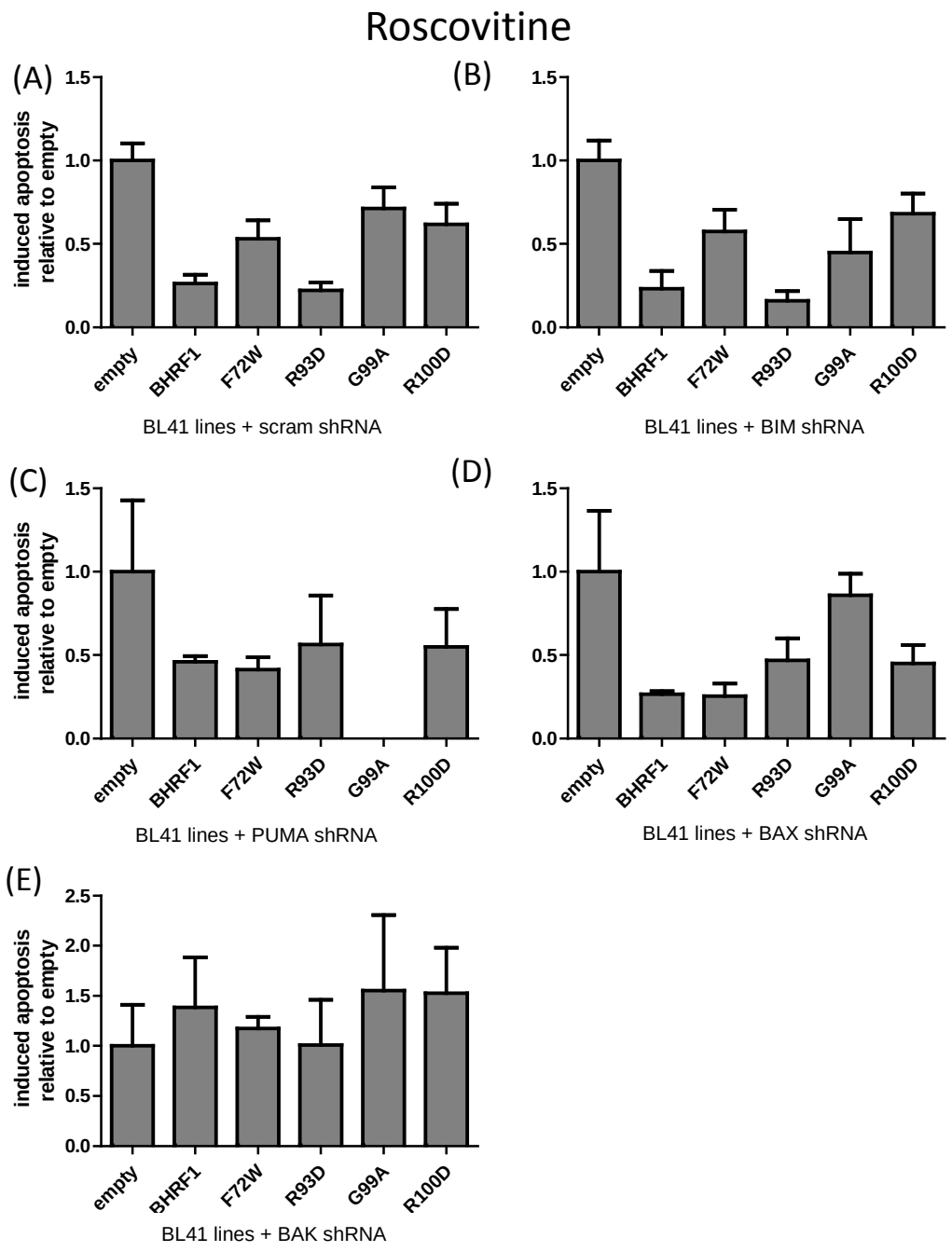

Figure 4.23: Roscovitine induced apoptosis in BHRF1 wild type and mutant expressing lines with BCL-2 homologue knockdown. BIM, PUMA, BAX and BAK were knocked down in the BL41 BHRF1 empty, wild type and mutant lines, using shRNA expression. Ability of these lines to protect from apoptosis was tested using 12µg/ml roscovitine. Data is expressed as level of induced apoptosis relative to empty. Scrambled (A), BIM (B), PUMA (C), BAX (D) and BAK (E) lines are shown separately. Data is mean and standard deviation of three experimental replicates. G99A shRNA was not tested with PUMA shRNA (C) because of problems with cell viability.

levels of apoptosis in shRNA expressing lines (A to E) relative to the level of apoptosis in the empty vector. Apoptosis was induced by a different drug in each Figure.

BIM shRNA lines provide very similar patterns of protection to scrambled shRNA (Figures 4.20 to 4.23 A and B) lines, and hence, BL41 BHRF1 lines without shRNA lentivirus. This agrees with the result seen in BIM negative BL2 expressing BHRF1 mutants (see Figures 4.11 and 4.12). However, assays performed with other shRNAs do show deviation from this standard pattern of protection.

The data can be more easily analysed if it is also expressed relative to the levels of apoptosis in the corresponding scrambled shRNA line. This indicates any changes in levels of apoptosis that may result from the knockdown of cellular BCL-2 homologues.

Figures 4.24 to 4.27 show the change in levels of induced apoptosis, normalised to empty vector, in the shRNA expressing lines compared to the scrambled shRNA. Data was expressed relative to empty, as in Figures 4.20-4.23, and then normalised to apoptosis levels in the scrambled shRNA to give the change in apoptosis due to the knockdown of each BCL-2 homologue, with no change being equal to 1. This means that the increase or decrease in apoptosis due to BCL-2 homologue knockdown can be seen clearly.

A t-test with a 95% confidence interval was performed to determine if apoptosis in the BCL-2 shRNA expressing lines were significantly different from the corresponding scrambled control lines. Because of the nature of the experiments, (inducing apoptosis simultaneously in a variety of cell lines) there was often variation in the absolute level of induced apoptosis in assays performed on different dates. This led to high standard deviations in some cases so not every change in apoptosis level was statistically significant.

The data from Figures 4.24 to 4.27 has been summarised in Figure 4.28 to aid comparison.

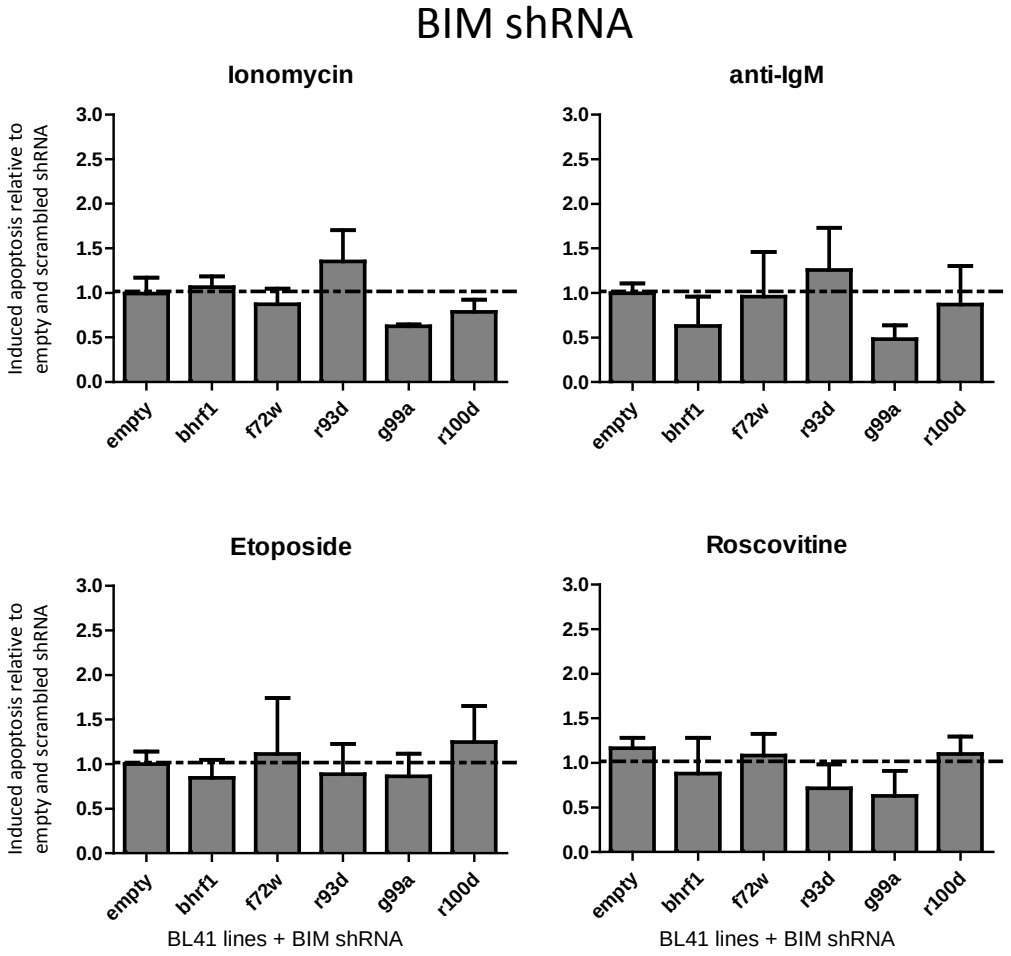

Figure 4.24: Apoptosis induced in BHRF1 mutant lines with BIM knockdown. BIM was knocked down in the BL41 BHRF1 empty, wild type and mutant lines, using shRNA expression. Ability of these lines to protect from apoptosis was tested using 1µg/ml ionomycin, 6µg/ml anti-IGM, 2.5µg/ml etoposide and 12µg/ml roscovitine. Data was expressed relative to empty, as in Figure 4.19-4.22, and then normalised to apoptosis levels in the scrambled shRNA to give the change in apoptosis due to the knockdown of BIM, with no change being equal to 1. Level of apoptosis in the scrambled lines are indicated as 1 by the dotted line. Mean and standard deviation is of three experimental replicates. A t-test with a 95% confidence interval was performed to determine significant changes from the level of apoptosis in the scrambled due to BIM knockdown. * = significant (*P*=0.05-0.01), ** = very significant (*P*=0.01-0.001), *** = extremely significant (*P*=0.001-0.0001)

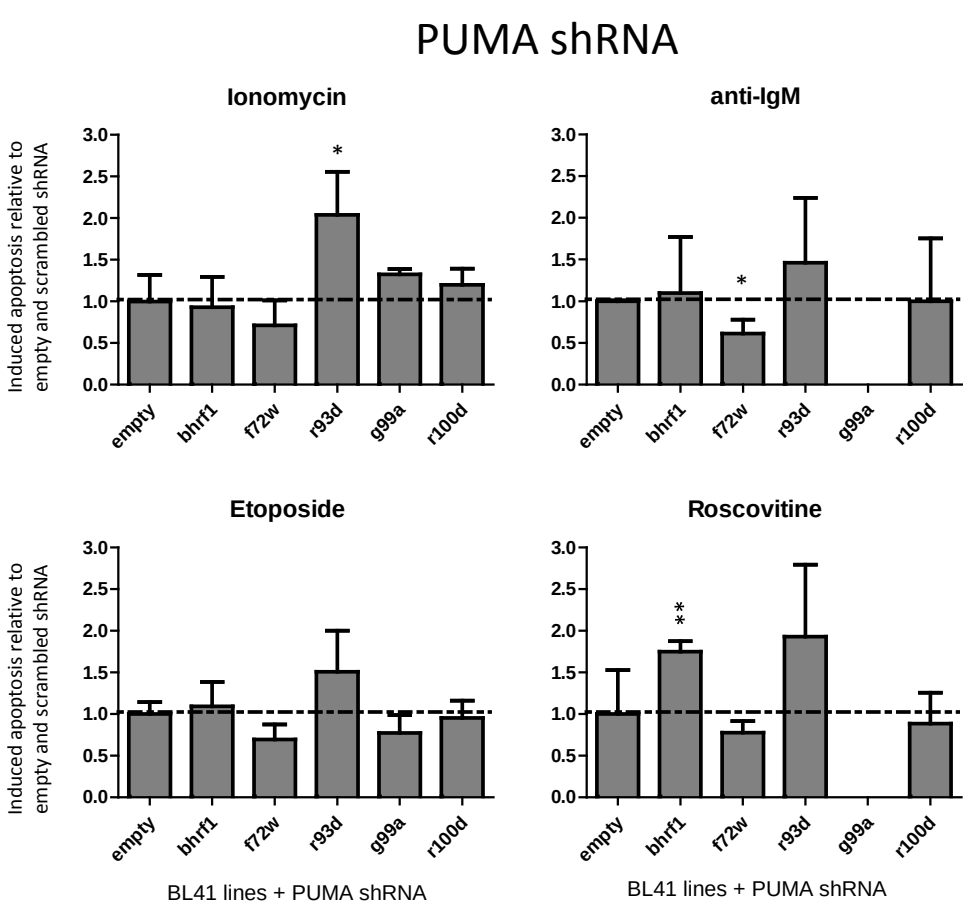

Figure 4.25: Apoptosis induced in BHRF1 mutant lines with PUMA knockdown. PUMA was knocked down in the BL41 BHRF1 empty, wild type and mutant lines, using shRNA expression. Ability of these lines to protect from apoptosis was tested using 1µg/ml ionomycin, 6µg/ml anti-IGM, 2.5µg/ml etoposide and 12µg/ml roscovitine. Data was expressed relative to empty, as in Figure 4.19-4.22, and then normalised to apoptosis levels in the scrambled shRNA to give the change in apoptosis due to the knockdown of PUMA, with no change being equal to 1. Level of apoptosis in the scrambled lines are indicated as 1 by the dotted line. Mean and standard deviation is of three experimental replicates. G99A shRNA was not tested with anti-IgM or roscovitine because of problems with cell line viability. A t-test with a 95% confidence interval was performed to determine significant changes from the level of apoptosis in the scrambled due to PUMA knockdown. * = significant (*P*=0.05-0.01), ** = very significant (*P*=0.01-0.001), *** = extremely significant (*P*=0.001-0.0001)

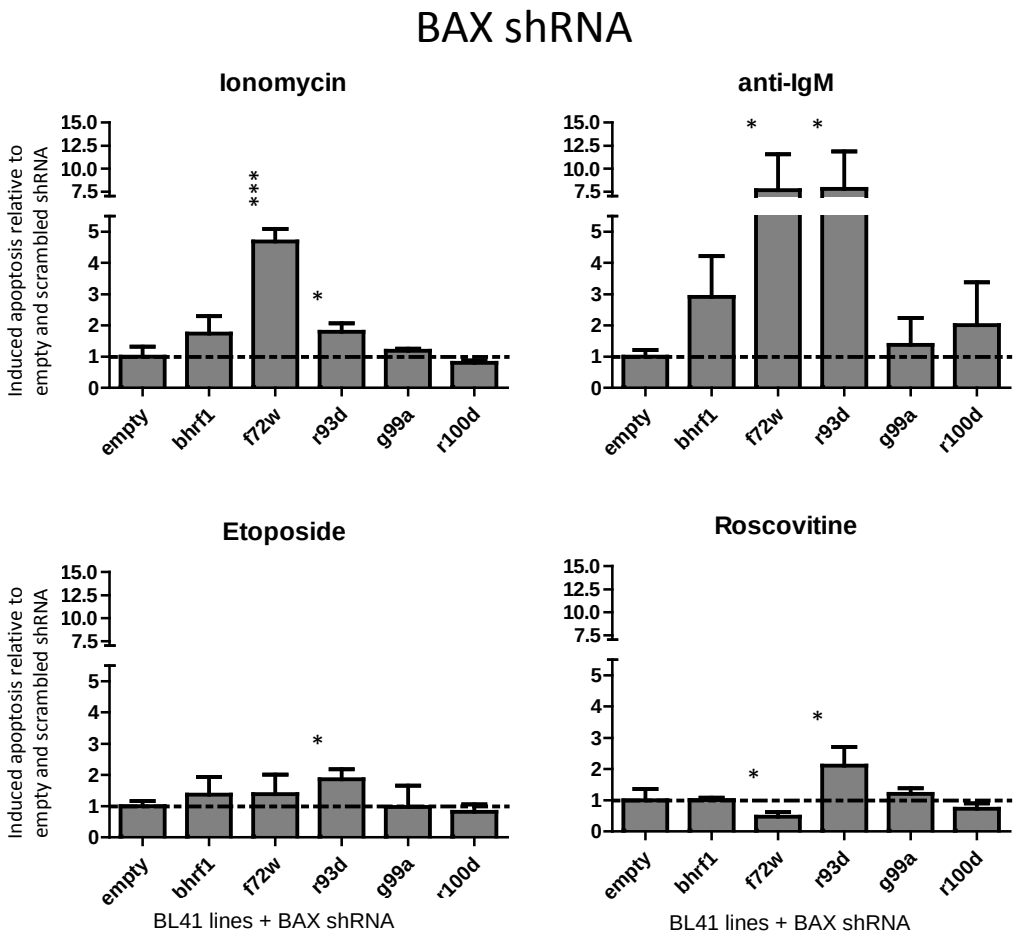

Figure 4.26: Apoptosis induced in BHRF1 mutant lines with BAX knockdown. BAX was knocked down in the BL41 BHRF1 empty, wild type and mutant lines, using shRNA expression. Ability of these lines to protect from apoptosis was tested using 1µg/ml ionomycin, 6µg/ml anti-IGM, 2.5µg/ml etoposide and 12µg/ml roscovitine. Data was expressed relative to empty, as in Figure 4.19-4.22, and then normalised to apoptosis levels in the scrambled shRNA to give the change in apoptosis due to the knockdown of BAX, with no change being equal to 1. Level of apoptosis in the scrambled lines are indicated as 1 by the dotted line. Mean and standard deviation is of three experimental replicates. A t-test with a 95% confidence interval was performed to determine significant changes from the level of apoptosis in the scrambled due to BAX knockdown. * = significant (*P*=0.05-0.01), ** = very significant (*P*=0.01-0.001), *** = extremely significant (*P*=0.001-0.0001)

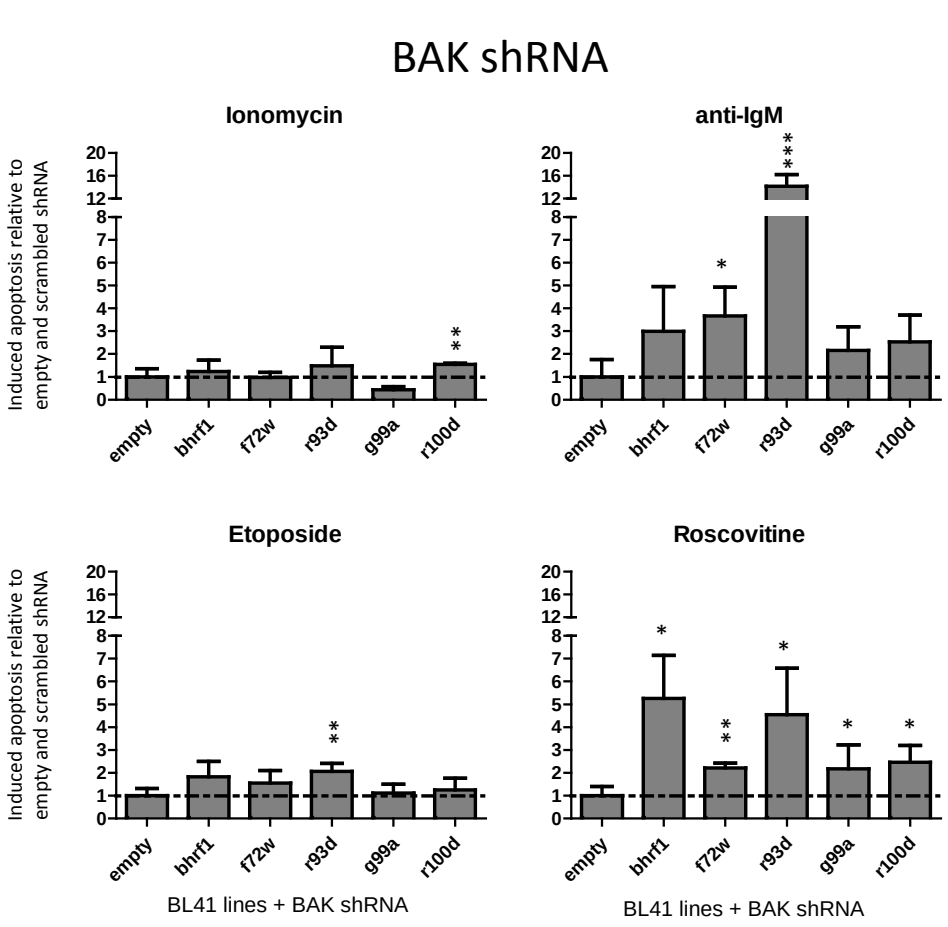

Figure 4.27: Apoptosis induced in BHRF1 mutant lines with BAK knockdown. BAK was knocked down in the BL41 BHRF1 empty, wild type and mutant lines, using shRNA expression. Ability of these lines to protect from apoptosis was tested using 1µg/ml ionomycin, 6µg/ml anti-IGM, 2.5µg/ml etoposide and 12µg/ml roscovitine. Data was expressed relative to empty, as in Figure 4.19-4.22, and then normalised to apoptosis levels in the scrambled shRNA to give the change in apoptosis due to the knockdown of BAK, with no change being equal to 1. Level of apoptosis in the scrambled lines are indicated as 1 by the dotted line. Mean and standard deviation is of three experimental replicates. A t-test with a 95% confidence interval was performed to determine significant changes from the level of apoptosis in the scrambled due to BAK knockdown. * = significant (*P*=0.05-0.01), ** = very significant (*P*=0.01-0.001), *** = extremely significant (*P*=0.001-0.0001)

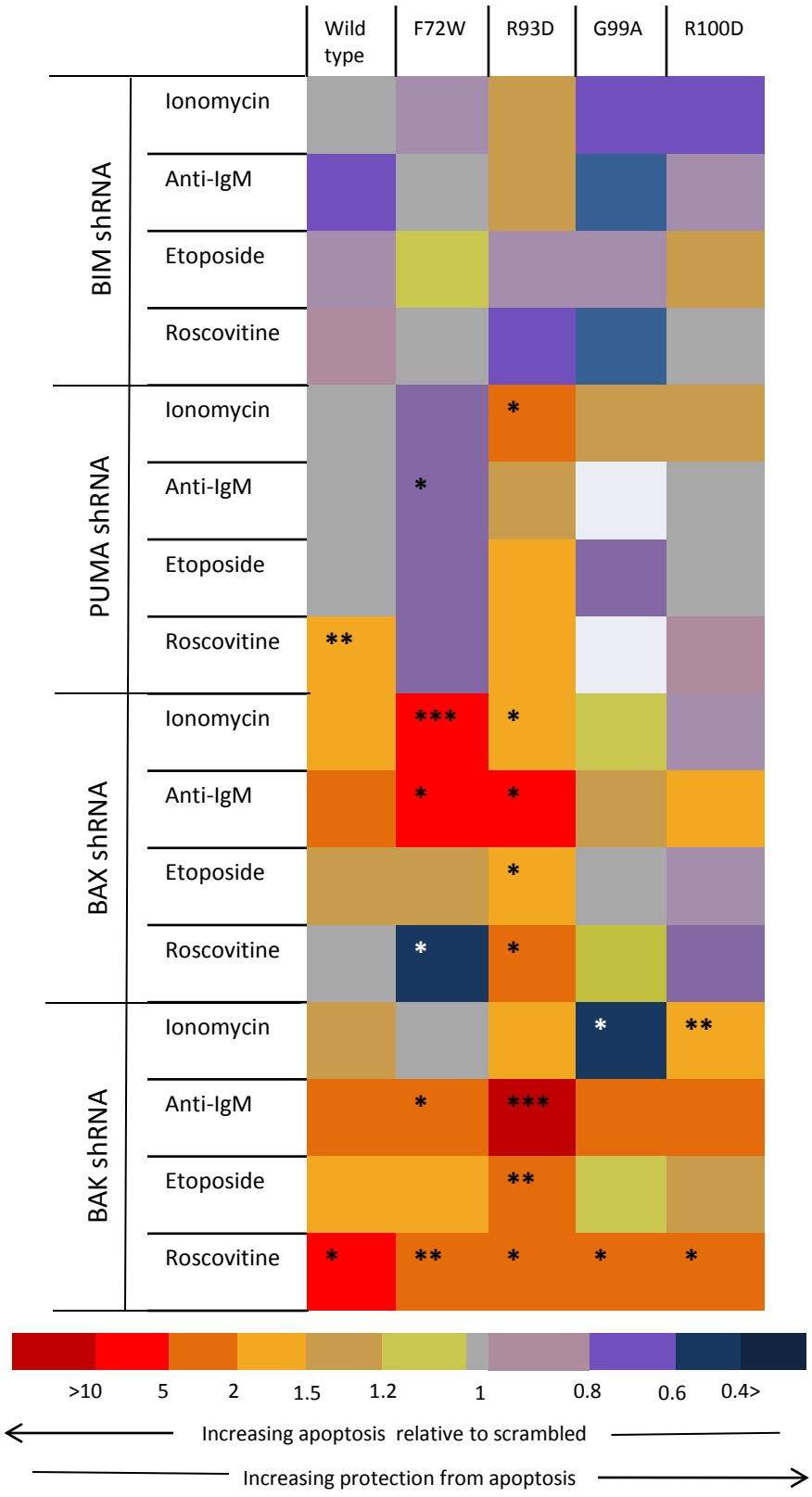
Wild type
F72W
R93D
G99A
R100D
BIM shRNA
PUMA shRNA
BAX shRNA
BAK shRNA
Ionomycin
Anti-IgM
Etoposide
Roscovitine
>10
5
2
1.5
1.2
1
0.8
0.6
0.4>
Increasing apoptosis relative to scrambled
Increasing protection from apoptosis

Figure 4.28: Heat map showing levels of apoptosis protection in BHRF1 mutant expressing BL41 lines with BCL-2 homologue knockdown. BIM, PUMA, BAX and BAK were knocked down in the BL41 BHRF1 empty, wild type and mutant lines, using shRNA expression. Ability of these lines to protect from apoptosis was tested using ionomycin, anti-IgM, etoposide and roscovitine. Data was expressed relative to empty and normalised to scrambled shRNA lines as in Figures 4.19 to 4.22. Change in apoptosis levels relative to those in scrambled are shown in colour where 1 (grey) is the same level of apoptosis as seen in scrambled lines. Red spectrum gives increase in apoptosis and decrease in protection, vice versa for blue spectrum. Significant differences from scrambled are indicated by * (P<0.05). * = significant (P=0.05-0.01), ** = very significant (P=0.01-0.001), *** = extremely significant (P=0.001-0.0001)

4.9.3 The effect of BIM and PUMA shRNA on protection

BIM knockdown (Figure 4.24) did not result in any significant changes from levels of apoptosis in lines with scrambled shRNAs. This was the case when apoptosis was induced with any of the four drugs. Although there appeared to be a general decrease in the apoptosis induced in G99A mutant line, this was not significant.

PUMA knockdown (Figure 4.25) resulted in no significant differences from scrambled lines when apoptosis was induced with etoposide. However, there was a significant decrease in apoptosis induced in f72W with anti-IGM. From the raw data (figure 4.19) anti-IGM induces generally less apoptosis in PUMA knockdown lines than in scrambled control (approximately 15% decrease in apoptosis in the empty line). There was a general increase in the apoptosis sensitivity of the PUMA knockdown R93D line, although this was only significant for ionomycin due to high standard deviations. Finally, there was also a very significant 2-fold increase in wild type BHRF1 apoptosis induced by roscovitine. This was despite the levels of cell death induced by the other drugs remaining equal to scrambled in wild type BHRF1 lines. Unfortunately we were unable to complete the panel of drugs for G99A BHRF1 + PUMA shRNA due to problems with the viability of this cell line which was eventually lost due to bacterial infection. Hence, only data for etoposide and ionomycin induced apoptosis are shown.

4.9.4 The effect of BAX and BAK shRNA on protection

Individual knockdown of both BAX and BAK leads to a drop in apoptosis induced in the empty lines (Figure 4.19). BAX or BAK knockdown decreased the levels of apoptosis induced

by all drugs, but particularly by ionomycin and anti-IgM (a drop of around 30% for both drugs compared to scrambled shRNA) (Figure 4.19).

Levels of apoptosis induced in G99A and R100D BAX shRNA lines remain similar to those seen with scrambled shRNA (Figure 4.26). However, there are significant decreases in protection when apoptosis is is induced in F72W with ionomycin and anti-IGM, and in R93D with all four drugs.

Wild type BHRF1 also shows a decrease in protection against ionomycin and anti-IGM induced apoptosis, although neither of these results are significant.

When BAK is knocked down BHRF1 and its mutants lose much of their ability to protect against etoposide and roscovitine induced death (Figures 4.22E and 4.23E). Levels of apoptosis in the BHRF1 and BHRF1 mutant lines approach the levels seen in the empty vector when apoptosis is induced with these two drugs.

In the case of roscovitine induced apoptosis, levels of death induced in the empty vector fall by approximately 60% when BAK is knocked down (Figure 4.19). This could decrease the differences in apoptosis level seen between BHRF1 and empty, a limitation that must be considered as it could artificially inflate any loss of protection when BHRF1 mutants are expressed relative to empty. However, etoposide induces around 60% apoptosis in the empty BAK shRNA line, yet there is still very little protection from etoposide induced apoptosis by BHRF1 or the mutants.

As with BAX shRNA, BAK shRNA expression causes R93D BHRF1 to consistently lose the ability to protect from apoptosis when compared to scrambled shRNA (Figure 4.27). This loss of protection ranges from significant to extremely significant when death is induced with roscovitine, etoposide and anti-IgM. With anti-IgM the loss of protection is extreme, with approximately a 12-fold increase in apoptosis compared to the scrambled shRNA line.

F72W BHRF1 significantly loses the ability to protect against roscovitine and anti-IgM induced apoptosis. BHRF1 wild type, G99A and R100D also significantly lose protection against roscovitine induced apoptosis, although, as mentioned above, this could be inflated by the general low levels of cell death induced by roscovitine in BAK knockdown lines. However, a significant loss of BAK shRNA R100D BHRF1 protection is also seen when apoptosis is induced with ionomycin, so this result could be valid.

4.10 Discussion

4.10.1 Isothermal titration calorimetry data may not be accurate in a physiological system

The binding affinity of BHRF1 and its mutants for cellular BCL-2 homologues BIM, PUMA, BAX, BAK and BID, was determined by Kvansakul *et al.* using isothermal titration calorimtery (ITC) (104). This was performed in solution using truncated proteins and BH3 domain peptides and so may not be accurate in a cellular system.

There may not always be a clear correlation between ITC generated thermodynamic data and protein-ligand binding in a physiological system. When Ladbury *et al.* compared thermodynamic data with structural information for protein-ligand binding they found that there was occasionally low correlation between thermodynamic data and structural data, especially when the protein was highly folded and contained a buried binding site. They go on to state that the thermodynamics of an interaction in isolation may not provide useful information in describing complex formation, but instead should be used as a guide and validated using other data (reviewed in (331)). The correlation between ITC data and binding in a cellular system has not been researched specifically in relation to BHRF1. However, the

BHRF1 protein does have a complex, highly folded structure which undergoes distinct morphologically changes when binding occurs (46) and so, while ITC is a useful tool when determining BHRF1-BCL-2 homologue interactions, we must also remember its limitations.

From our data, although the ITC data for the majority of mutants (Table 4.2) is supported by the co-immunopreciptiation data (Figures 4.15 and 4.16) and apoptosis assay data (Figures 4.11 and 4.12), there are some mutants for which the ITC data does not agree with our findings. The most pronounced of these are E89G and F72W.

The ITC data for these two mutants states that F72W has lost binding to all BCL-2 homologues tested except for PUMA, with which strength of binding has decreased 4-fold. E89G binds BIM, PUMA and BID but the strength of binding is decreased by 51, 8.6 and 2.8-fold respectively, with only negligible binding to BAX (Table 4.2).

When we look at the protection from apoptosis conferred by BHRF1 with a F72W or E89G mutation we would expect it to be low. In the case of F72W it should be similar, if not lower, than R100D. However, for both F72W and E89G, we see that protection is high and approaches that of wild type (Figure 4.11 and 4.12, Table 4.3).

The co-immunoprecipitation (Co-IP) data (Figure 4.16) shows F72W binding to BIM, which, although weaker than wild type, is definitely present. E89G appears to bind strongly to BIM. When you look at the levels of E89G BHRF1 in the lysate they are very high, but similar to those in R93D. From the ITC data (Table 4.2) R93D binds more strongly to BIM than wild type (18 vs 10Kd) and has similar level of binding to BIM as E89G, considering the low BIM levels in the R93D lysate. From the combination of the Co-IP and binding data we can be fairly sure that F72W and E89G bind more strongly to BIM than is indicated by the ITC data.

4.10.2 BHRF1 may affect the level of BIM protein

Western blots performed to measure the levels of BCL-2 homologues in the various BHRF1 mutant lines led to an interesting observation (Figure 4.14). The levels of BIM change dependent on the BHRF1 mutant. Wild type or mutated BHRF1 with strong binding to BIM by ITC and CoIP showed lower levels of BIM than the empty vector or mutants which bind BIM weakly (such as G99A and R100D). This effect was only seen with BIM and was consistent across cell lines made on different dates, particularly in the case of empty vector and wild type and R93D BHRF1 (Figure 4.14).

Desbien *et al.* saw an increase in BIM levels when cell were induced into apoptosis through cytokine withdrawal (109). This could explain the varying levels that we see. The mutants that are less protected, such as G99A and R100D, could be slightly more apoptotic than their well protected counterparts and hence, could show raised levels of BIM. However, before any assays were performed, including harvesting for protein, cells were tested for viability using trypan blue staining and were consistently found to be above 80% viable.

A second explanation could be that these variable levels of BIM are a result of complex formation with BHRF1 which could sequester free BIM. However, a denaturing gel was used for Western blots, which disrupts complexes and protein-protein interactions. Hence it is unlikely that the varying levels of BIM seen by Western blot would be due to free BIM being sequestered by BHRF1 as this should be released by denaturing during blotting.

EBNA3A and EBNA3C are known to down-regulate BIM at the transcriptional level (230). However, it has also been shown that infection of EBV negative BL lines with EBV can lead to lower levels of BIM protein due to phosphorylation of BIM by activated ERK (332).

Despite an extensive literature search we found no evidence that BHRF1 specifically, was able to down-regulate BH3-only BCL-2 homologues either at the transcriptional level or

through protein degradation. It could be that, as postulated by Desbien *et al,* BHRF1 induced a permanent conformational change in BIM before dissociating from binding (109). This conformational change could then lead to BIM degradation or a reduction in protein half-life.

4.10.3 BHRF1 may act through binding to BCL-2 homologues other than BIM

In our co-immunoprecipitation experiments (Figure 4.16) we were only able to observe binding of BHRF1 to BIM. However, the binding ITC data provided by Marc Kvansakul indicates that BHRF1 may also be able to bind BAX, BAK and BID.

Others have shown co-immunoprecipitation data in which BHRF1 binds to BAK and PUMA (84, 104, 109). These assays were not carried out in a BL system and were mainly performed in 293FT cells (104) or murine T (109) or B cells (84). They may also be performed on lines artificially expressing high levels of pro-apoptotic BCL-2 homologues (104). However, they do use a similar method to our assay.

BHRF1 must bind more homologues than BIM as it is still able to protect in a BIM negative system. It may be that, low levels of BCL-2 homologues in the lysate, together with the biochemical consequences of lysing cells and solubilising membrane complexes with detergent, have rendered our assay insufficiently sensitive to pick up binding of BHRF1 to PUMA and BAK. Because of these limitations, it may be valid to look for any functional changes in BHRF1 protection when BCL-2 homologues are removed from the system. These differences could indicate binding partners of BHRF1 that the Co-IP assay was not sensitive enough to pick up.

4.10.4 BHRF1 and its mutants protect from apoptosis induced by various cytotoxic drugs

In our apoptosis assays we showed that BHRF1, ectopically expressed from a lentivirus, in EBV negative lines BL lines has a similar protective effect to that seen in Wp restricted BL lines naturally expressing BHRF1 during latency (Figure 3.11).

We used four cytotoxic drugs which work through different pathways to induce apoptosis:

Ionomycin is a calcium ionophore which induces influx of Ca^{2+} ions across the cell membrane to raise the level of intra-cellular calcium (319). Increase in intra-cellular Ca^{2+} ions is a well known inducer of apoptosis through various mechanisms including the activation of calmodulin, by binding to calcium, which then goes on to activate targets involved in apoptosis (320), and by activation of calcium dependent endonucleases (321, 322). Ionomycin induces endoplasmic reticulum (ER) stress and appears to raise BIM levels preferentially over the levels of other BH3-only BCL-2 homologues such as BID and PUMA (333).

Anti-IgM crosslinking stimulates the B cell receptor on IGM positive cells. Activation of IgM causes generation of inositol trisphosphate (InsP3) which causes the release of Ca^{2+} ions from intra-cellular stores and apoptosis progresses through activation of caspases 2, 3 and 9, and in a similar manner as when activated by ionomycin (320, 323, 324). Hence, death will occur through both mitochondria dependent (intrinsic) and independent (extrinsic) pathways although the main BH3-only BCL-2 homologue involved in inducing apoptosis has been reported to be BIM (334).

Etoposide acts as a topioisomerase inhibitor. Topioisomerases modulate DNA topology to resolve knots and tangles in the DNA, by creating transient double strand breaks in the DNA backbone, spanned by a protinaceous bridge (335). Topioisomerase inhibitors convert

topioisomerase into physiological toxins and stabilise the transient breaks, this introduces high numbers of double strand breaks that are then converted into permanent breakages by the replication machinery. When these breaks are present at high enough levels they trigger the DNA damage response which may eventually lead to cell death by apoptosis (327). DNA damage leads to the activation of p53 by phosphorylation and cells eventually undergo apoptosis through activation of the BH3-only homologue PUMA.

Deletion of PUMA has been shown to protect cells against etoposide induced apoptosis (58), although this effect is not as complete as when p53 is lost or BCL-2 is overexpressed (336, 337). Although PUMA is the main mediator of DNA damage induced apoptosis (58) p53 may also induce apoptosis by activating NOXA, and possibly BID, BAX and BAK (338-342).

Roscovitine is a cyclin dependent kinase inhibitor which acts through both the p53 and NF-κB pathways (343). Activation of p53 can lead to cell cycle arrest and apoptosis, whereas activation of NF-κB is associated with survival through the prevention of caspase activation.

Roscovitine inhibits repression of p53 activation by MDM2 (344). Dey *et al.* found that roscovitine induced apoptosis through TNFα signalling and the extrinsic pathway (see Figure 1.1 for overview of extrinsic pathway) while, at the same time, down-regulating NF-κB and its target genes such as FLIP and BCL_{XL} (343).

NF-κB and FLIP repress caspase activation. NF-κB prevents activation of caspase 3 and FLIP represses activation of caspases 8 and 10. Caspase 3 activation leads to apoptosis through the extrinsic pathway. Caspases 8 and 10 activate caspase 3 and also induced cleavage of the BH3 only protein BID to activated t-BID. When BID is activated apoptosis can also progress through the intrinsic pathway (reviewed in (15)).

BHRF1 protected from apoptosis induced by all of these drugs (Figures 4.11 and 4.12). Interestingly, the pattern of protection conferred by the BHRF1 mutants did not change

depending on which drug was used. When death was induced by drugs which favour activation of different members of the BCL-2 homologue family, we might have expected more variation in the levels of protection conferred by mutants with disrupted binding to members of this family.

4.10.5 BHRF1 may act mainly through binding to BAK

It is known that BHRF1 is able to bind BAK, but recently attention has turned towards its ability to bind BH3-only homologues as the main means by which it represses apoptosis (104, 109, 345). However, from our data, with exception of F72W BHRF1, the ability of BHRF1 and its mutants to protect from a variety of cytotoxic drugs remains the same regardless of the particular pathway activated (Figures 4.11 and 4.12). These cytotoxic drugs induce apoptosis through the activation and up-regulation of different BH3-only BCL-2 homologues. As the mutants cause loss of binding to various BH3-only homologues depending on the mutation, we could expect their ability to protect from apoptosis to change depending on the drug used to induce apoptosis. However, regardless of the drug, the protection conferred by BHRF1 mutants, in relation to wild type and other mutants, is always similar (except for F72W BHRF1 discussed in section 4.6.5), (Table 4.3).

For this pattern to remain the same it is likely that BHRF1 is acting through the same binding partners regardless of the drug used. A possible candidate from the BH3-only family is BIM, a highly promiscuous BCL-2 homologue, activated by most cell death stimuli (346). Alternatively, binding to the BH3-only BCL-2 homologues may not be responsible for the large differences in apoptosis protection seen between wild type BHRF1 and some of its mutants (mainly G99A and R100D).

BHRF1 is known to bind BAK (109) and may be able to bind BAX. These proteins receive death signals propagated by activation of the BH3-only proteins and respond by forming pores in the mitochondrial membrane. If BHRF1 could prevent BAX and BAK from being activated, it could repress apoptosis regardless of which BH3-only proteins are active, by binding to just two BCL-2 homologues.

From the shRNA experiments, BAK knockdown has the greatest effect of all the BCL-2 homologues knockdowns tested. The levels of death in the empty vector shRNA lines (Figure 4.19) are lower, as expected, when BAX or BAK are knocked down. In ionomycin, anti-IgM and etoposide induced apoptosis, death most likely occurs through activation of both BAX and BAK as knockdown of one or the other does not change levels of death and they appear interchangeable. However, when death is induced with roscovitine, apoptosis occurs mainly through BAK rather than BAX, as levels of apoptosis drop when BAK is knocked down.

Knockdown of BAK causes significant loss of BHRF1 function when apoptosis is induced with roscovitine (Figure 4.27). This indicates that BHRF1 was protecting through binding to BAK and cannot protect as efficiently from apoptosis occurring through BAX despite the overall levels of death being lower. This loss of protection is not as significant when apoptosis is induced by the other drugs in BAK shRNA lines. This may be because death occurs equally through BAX and BAK when induced with these drugs and so differences in protection with and without BAK would not appear so large.

When BAX is knocked down there is a significant decrease in the ability of F72W and R93D BHRF1 to protect against anti-IgM, etoposide and roscovitine induced apoptosis (Figure 4.26). This may indicate that these two mutants are more able than wild type to bind BAX.

BAX knockdown does not significantly change the ability of wild type BHRF1 to protect from apoptosis. BHRF1 may not bind BAX but still has a somewhat protective effect when

mitochondrial membrane permeabilisation is occurring solely through this BCL-2 homologue. This may be due to its ability to prevent BAX activation by binding upstream BH3-only BCL-2 homologues.

This data indicates that BHRF1 may have its main effect by binding to BAK but may also prevent BAK and BAX activation though interaction with BH3-only BCL-2 homologues. Therefore, elucidating the BH3-only binding partners of BHRF1 may also be important for determining the way by which it exerts it protective effect.

4.11 Apoptosis protection by BHRF1 is not dependent upon binding to BIM

Although BHRF1 has been found to bind several pro-apoptotic cellular BCL-2 homologues (including PUMA, BAK and BID), binding to BIM is thought to be the main BCL-2 homologue through which BHRF1 exerts its anti-apoptotic effect (84, 109).

In our assays we expressed BHRF1, and its mutants, in both a BIM positive (BL41) and BIM negative (BL2) EBV negative Burkitt lymphoma line.

When apoptosis was induced with four cytotoxic drugs (ionomycin, anti-IGM, etoposide and roscovitine) higher doses were required to induce significant levels of apoptosis in the BL2 cell lines (Figures 4.7, 4.8 and 4.9). However, this is to be expected when one of the most promiscuous pro-apoptotic BH3-only BCL-2 homologues is removed from the system.

Despite BIM being one of the main binding partners of BHRF1 (84, 104, 109), the ability of BHRF1 to protect from apoptosis did not change between a BIM positive (BL41) and BIM negative (BL2) background (Figures 4.11 and 4.12). This result is supported by data from the BIM shRNA lines, where an shRNA was used to knockdown BIM expression. Protection

conferred by BHRF1 and its mutants did not change between the scrambled shRNA control lines and those containing BIM shRNA (Figure 4.24).

This indicates that BIM must be replaced by other cellular BCL-2 homologues which are also bound by BHRF1 in a very similar manner. The ability of BHRF1 to bind BIM is still important but may be replaced by binding to other BCL-2 homologues. These results indicate that there is some functional redundancy between the pro-apoptotic BCL-2 homologues. This result is supported by others who have remarked upon the redundancy of BH3-only BCL-2 homologues and have shown that, when one homologue is deleted, another often takes its place (347, 348). This seems a likely explanation when considering the importance of the process for disease prevention and the complexity of the pathway.

Viral BCL-2 homologues are important for the maintenance of virus infected cells and aid the virus during transformation and re-entry into lytic cycle by blocking death receptor signalling (108) and suppressing the apoptotic response. Although BHRF1 is not essential for transformation or re-entry into lytic cycle (349, 350) EBV contains a repertoire of apoptosis modulating proteins, such as LMP1 and the EBNA3s (see section 1.7), highlighting the importance of this process for the virus life cycle. Because of this need for apoptosis suppression BHRF1 may need to be more efficient, and efficiently bind a greater number of BH3-only proteins, than cellular anti-apoptotic BCL-2 homologues.

4.12 R100 and G99 are key amino acids for BHRF1's ability to bind cellular BCL-2 homologues

The ability of BHRF1 to bind cellular BCL-2 homologues is known to affect its ability to protect cells from apoptosis (109).

Several mutants of BHRF1, each containing a single mutated amino acid within the BH3 binding groove, were expressed in an EBV negative Burkitt lymphoma background, and their ability to protect these cells against apoptosis was tested.

Our apoptosis data indicates that the most essential amino acids relating to BCL-2 homologues binding and hence, protection from apoptosis, are R100 and G99. These amino acids are analogous to those required for hydrophilic interactions between BIM and BCL-XL (351). BHRF1 with a G99A or R100D mutation consistently loses protection from apoptosis in all apoptosis assays, regardless of drug or individual BCL-2 homologue knockdown (Figures 4.11, 4.12 and 4.20 to 4.23). Khanim *et al.* also mutated amino acids in the BH1 domain, including G99 and R100, and showed a loss of protection from *Cis*-platin (310). Desbien *et al.* 2009, a key paper for our work, mutated G99 and R100 to give G99A and R100A, which was found to lead to a decrease in BIM and BAK binding (109).

Desbien *et al.* favour BIM as the main cellular BCL-2 homologue through which BHRF1 acts. However, whereas they found that shRNA knockdown of BIM fully protected HT-2 mouse T cells from IL2 withdrawal induced apoptosis; we did not find this in B cells. Knockdown of BIM in BL41 slightly increased resistance to death induced by cytotoxic drugs but was not completely protective (Figures 4.19 to 4.24).

Desbien *et al.* found that G99A led to a reduced ability to protect both immature B cells from apoptosis induced by B cell receptor cross-linking, and a loss of HT-2 T cell protection from IL2 withdrawal. R100A retained some of its protective effect in HT-2 cells and was as effective as wild type in B cells. When they immunoprecipitated BHRF1 and the G99A and R100A mutants, using FLAG tagged whole proteins, they found that wild type and R100A bound BIM, but G99A did not. Binding of R100A to BIM-EL and L was found to be slightly

decreased and G99A almost completely lost binding to both BIM isoforms. Both mutations lost all binding to BAK. (109).

In our system G99A and R100D mutated BHRF1 have equally lost ability to protect from apoptosis, both in a BIM positive and BIM negative background. We also did not see any binding of R100D BHRF1 to BIM by co-immunoprecipitation (Figure 4.16), which correlates with the apoptosis assay results. This could be a result of the difference in amino acid substitution (R is replaced by a D in our assay, rather than an A) which could disrupt binding to a greater degree.

Desbien *et al.* conclude that BHRF1 prevents death through binding to BIM and not through BAK. However, they do see that BHRF1 binds only a small proportion of the total BIM within a cell. Desbien *et al.* suggest that BHRF1 could be binding a conformational subset of BIM. However, from our results the presence or absence of BIM makes no difference to protection from apoptosis, hence, BIM may not be the main BCL-2 homologue bound by BHRF1, explaining the low levels of binding.

4.13 BHRF1 mediated resistance to Etoposide induced death is independent of BIM and PUMA

Etoposide causes DNA damage which leads to the activation of p53 by phosphorylation (327), causing cells to undergo apoptosis through activation of the BH3-only homologue PUMA. Although PUMA is the main mediator of DNA damage induced apoptosis (58) p53 may also induce apoptosis by activating NOXA, BID, BAX and BAK (338-342).

When using a drug which induces DNA damage it is important to know the p53 status of the cell lines used, as p53 is often mutated or inactivated in cancer cell lines. Most BLs have aberrations in the p53 pathway, through either mutation of p53, deletion of p14ARF or over-

expression of MDM2. BL2 is known to have wild type p53 but over-expresses the p53 inhibitor MDM2 (275). Etoposide is able to phosphorylate p53 and prevent complex formation with MDM2 (352). Wade *et al.* also showed that BL41 is able to die by etoposide induced apoptosis (326) despite having a mutated form of p53 (353). However, activation of PUMA is p53 dependent (354). It has been found that, in p53 independent apoptosis induced by DNA damage, BID may be the main BH3-only BCL-2 homologue through which the apoptotic signal is propagated (355).

When apoptosis is induced with etoposide in BL2 cells there is no significant difference in the pattern of protection compared with other apoptosis inducing drugs (Figure 4.12). This indicates that, despite different pathways being activated, death is induced by similar BCL-2 homologues.

In BL41 lines treated with etoposide cells will die through p53 independent apoptosis mainly mediated by BID. If BID is the only BH3 only BCL-2 homologue which is active it explains why protection is generally lower, relative to empty, when apoptosis is induced with etoposide. From the ITC data, binding of BHRF1 to BID is generally weaker than binding to BIM (109 vs 18K_d) so BHRF1 may have less of a protective effect. This general decrease in protection is true for all mutants except G99A and R100D (which have weak binding to BIM and BID).

When PUMA is knocked down using shRNAs there is no significant change in protection against etoposide induced death conferred by BHRF1 or its mutants (Figure 4.25). The percentage of cell death induced by etoposide treatment also does not change between PUMA positive and PUMA knockdown BL41 empty lines. These results indicate that apoptosis induced by etoposide in BL41 is, indeed, independent of PUMA. If BHRF1 is not protecting BL41 lines from etoposide induced apoptosis by binding to PUMA then this effect is likely achieved through binding to other BCL-2 homologues such as BID.

4.14 F72W mutated BHRF1 significantly loses protection to roscovitine induced death in BL41 but not in BL2

Roscovitine is a cyclin dependent kinase inhibitor which acts through both the p53 and NF-κB and the extrinsic pathway (343). P53 activation leads to up-regulation of PUMA and activation of the extrinsic pathway leads to cleavage of BID to active t-BID.

It is through the intrinsic pathway that BHRF1 would have its protective effect. Both BL2 and BL41 are protected from roscovitine induced apoptosis by BHRF1 and many of its mutants. Again, the pattern of protective ability between the mutants is similar to that seen in other drugs, and is similar between BL41 and BL2 (Figure 4.11 and 4.12).

G99A and R100D significantly lose protection against roscovitine in BL2 and have greatly reduced protection in BL41. However, in BL41, F72W has significantly lost apoptosis protection to the extent that there is no significant difference in the apoptosis protection of F72W and G99A and R100D (Table 4.3). In contrast, in BL2 lines the protection provided by F72W is not significantly different from wild type, and is significantly more than the low protection provided by R100D (P=0.0099).

This is most likely because, BL2 contains wild type p53 alleles (275); roscovitine acts through both the intrinsic pathway and via activation of p53. In BL2 it can overcome the high levels of MDM2 to activate p53, and also down-regulate NF-κB. In BL41, in which p53 is mutated (353), it can only act through down-regulation of NF-κB and associated proteins. If this is the case, then BL2 would die by a similar pathway to that seen in etoposide and mainly through activation of PUMA. Death in BL41 would occur through the extrinsic pathway and the associated activation of the BH3 only protein BID, and in turn, activation of BAX and BAK.

F72W has no binding to BID by ITC. This would explain the low levels of protection from F72W BHRF1 in BL41 but not in BL2. It may be that, in the absence of BIM, BL2 is more dependent on PUMA than BL41. If BHRF1 F72W is able to bind PUMA strongly then it may have a more protective effect in BL2 than in BL41.

Mutants other than F72W, G99A, R100D and R93D have some degree of binding to BID by ITC. Apoptosis data supports this, except in the case of R93D. These mutants are able to protect from roscovitine induced death in both BL41 and BL2 and, therefore, must be able to bind both BIM and PUMA.

In conclusion, BIM binding was not found to be essential for death in B cells when apoptosis was induced by four different cytotoxic drugs acting through different pathways. Removing BIM from the system did not change the ability of wild type BHRF1 or any of the BHRF1 mutants to protect from apoptosis, indicating that this protection was mediated by binding to other BCL-2 homologues.

Only two BHRF1 mutants consistently lost protection from apoptosis, highlighting the importance of the G99 and R100 amino acids for BHRF1 binding. The loss of function of these two mutants was similar across all drugs used. These cytotoxic drugs induce apoptosis through activation of different BH3-only BCL-2 homologues but always act through BAX and BAK. Hence, as patterns of protection were constant regardless of drug and activated BH3-only protein, BHRF1 may be acting mainly through binding to BAK and BAX. Smaller differences between the mutants, which change when BCL-2 homologues are knocked down, may be due to binding of BH3-only BCL-2 homologues. When death is induced by DNA damage, protection by BHRF1 is not dependent on binding to PUMA, and may occur mainly through binding of BHRF1 to BID, BAK and BAX. When these BCL-2 homologues are not

bound strongly apoptosis may be mediated by other BH3-only proteins in a hierarchy of binding in which the BH3-only proteins have overlapping functions and a degree of redundancy.

5. BALF1, latency and protection from apoptosis

5.1 Introduction

EBV is the only γ-herpesvirus known to encode two viral BCL-2 homologues. Together these two homologues are essential for efficient B cell transformation but have been shown to be individually functionally redundant (98).

The first of these, BHRF1, has been extensively studied and is discussed in the previous chapters. However, very little is known about the second viral BCL-2 homologue, BALF1. Despite it being discovered in 1999 (96), there is still disagreement over the function of BALF1, to the extent that no consensus has yet been reached as to whether it is pro- or anti-apoptotic.

We first looked to see if BALF1, primarily a lytic protein, was expressed in latency in a similar manner to BHRF1. In order to try to elucidate the role of BALF1 in BL and apoptosis, we used the previously described dox inducible lentivirus system, made by Herold *et al*. (286), to express HA tagged BALF1 in EBV negative and Wp restricted BL lines.

5.2 BALF1 is expressed during latency

It is known that, similarly to BHRF1, BALF1 is important during B cell transformation, and together BALF1 and BHRF1 are essential for regulation of apoptosis during initial infection (98). Recently BHRF1 was also found to be expressed in latently infected BL cells (101). Similarly to BHRF1, expression of BALF1 was originally thought to be restricted to lytic cycle, but it is possible that BALF1 is also expressed during latency, either as an anti-apoptotic BCL-

2 homologue, similar to BHRF1 (96), or alongside BHRF1 in order to regulate its function (41).

We used qPCR to look for expression of BALF1 in EBV positive B cell lines with various latent profiles (Figure 5.1). A panel of seven latency I BL lines was used alongside five BL lines with Wp restricted expression. Eight lines with latency III expression were used, including two Lat III BL lines and 6 LCLs. Lat III BLs were defined as the product of a latency I BL line which has drifted into latency III as a result of the lack of immune surveillance in culture. LCLs are latency III lines produced from *in vitro* EBV-induced transformation of normal B cells. We also looked at BHRF1 expression in the same lines for comparison. The assays used the same standard DNA containing single cDNA copies of BALF1 and BHRF1, and so levels of detected mRNA can be directly compared.

As expected, the levels of BHRF1 are highest in the Wp restricted lines, with no expression in latency I and detectable but low levels of expression in the latency III lines. This agrees with the results of Kelly *et al.* when BHRF1 was first found to be expressed in Wp restricted latency (101). BALF1 is expressed at between 0 and 0.1 copies per copy of PGK (housekeeping control used for comparison), levels >10 fold lower than the levels of BHRF1 in the Wp BL lines. However, expression of BALF1 is at a similar level to that observed for BHRF1 in latency III lines and LCLs. It is known that BHRF1 is able to protect LCLs from apoptosis and has a protective effect at low levels undetectable by Western blot (101), so these levels may be high enough for BALF1 to have a functional role in these lines.

The pattern of BALF1 expression is much less restricted than that of BHRF1. BHRF1 expression in latency is restricted exclusively to Wp lines and, at low levels, latency III lines. BALF1 is expressed, albeit at lower levels, in the majority of cell lines tested.

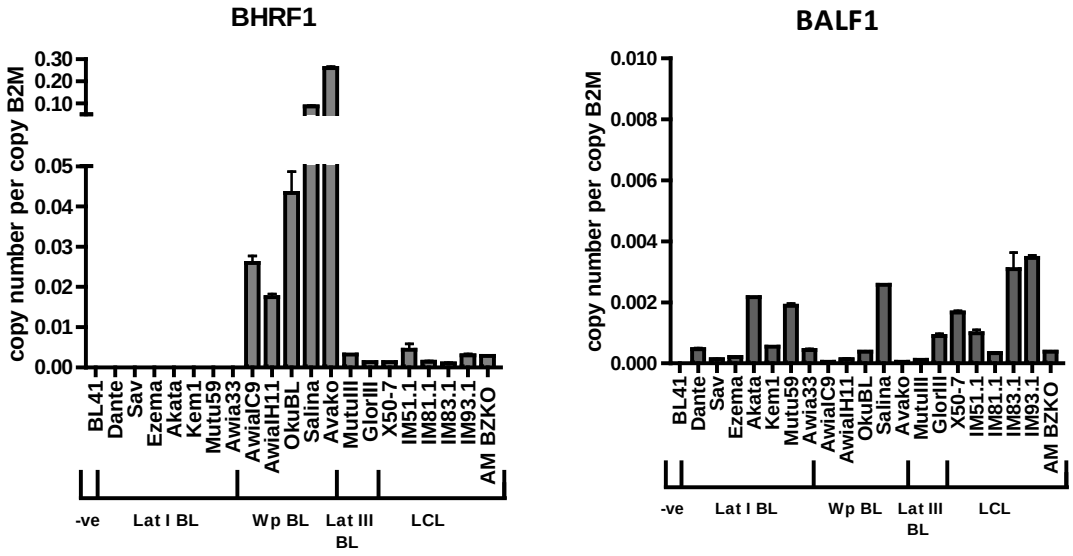

Figure 5.1: Levels of BHRF1 and BALF1 expressed in latent EBV positive cell lines. Levels of mRNA expression were measured using qPCR and a plasmid standard which gives absolute copy number. Levels were then normalised to cellular control (B2M). Levels of latent BHRF1 and BALF1 in individual lines can therefore, be directly compared. LCLs defined as a latency III lines produced from EBV infection *in vitro,* whereas Lat III BL are the result of a Latency I line drifting into latency III as a result of the lack of immune regulation. AMBZKO is an LCL negative for BZLF1, and, as such, must be 100% latent. Results are a mean of 3 technical replicates ±sd.

5.3 BALF1 is expressed in non B cell lines

As BALF1 is expressed across all forms of latency in B cell lines we used qPCR to look at expression in non B cell lines (Figure 5.2). We analysed BHRF1 expression for comparison.

Three lines of EBV positive T/natural killer (NK) cell origin were used, one originating from chronic active EBV (SNK10) and two others from T/NK cell lymphomas (SNK1 (295) and SNK6 (297, 298). SNT8 and SNT16 are T cell lymphoma lines which were established from a nasal T cell lymphoma (SNT8) (298) and peripheral blood from a case of chronic active EBV (SNT16) (297).

These T and NK lines were all EBNA1 and LMP1/2 positive but lacked expression of EBNA2 indicating that they display a latency II phenotype (297).

In addition to the T/NK cell lines, c666 (299), an EBV positive nasopharyngeal carcinoma line with an epithelial origin and latency II phenotype was tested. A gastric carcinoma cell line, infected *in vitro* with EBV (AGS + EBV) (300) was also tested. AGS + EBV has an epithelial cell origin and expresses a latency I pattern of EBV gene expression. Finally, the Hodgkin lymphoma line L591 (301, 302) was included in the analysis. This line has a latency III phenotype, in contrast with Hodgkin lymphoma *in vivo*.

As in Figure 5.1, BHRF1 shows expression restricted to B cell lines with a Wp or latency III pattern of gene expression but is not expressed in other forms of latency. Detectable expression is seen in Salina a Wp BL line, Mutu, a lat III B cell line and L591, a Hodgkin lymphoma line, also latency III. BHRF1 expression is not detectable in other cell types.

In contrast, BALF1 has more widespread expression. It is expressed at variable levels in all forms of latency, (latency I, II, III and Wp). Expression of BALF1 mRNA is not dependent on cell type, with expression seen in T/NK cells (particularly in SNK6), epithelial cells and B cells. Expression levels of BALF1 were similar to the levels of BHRF1 seen in Lat III lines and LCLs.

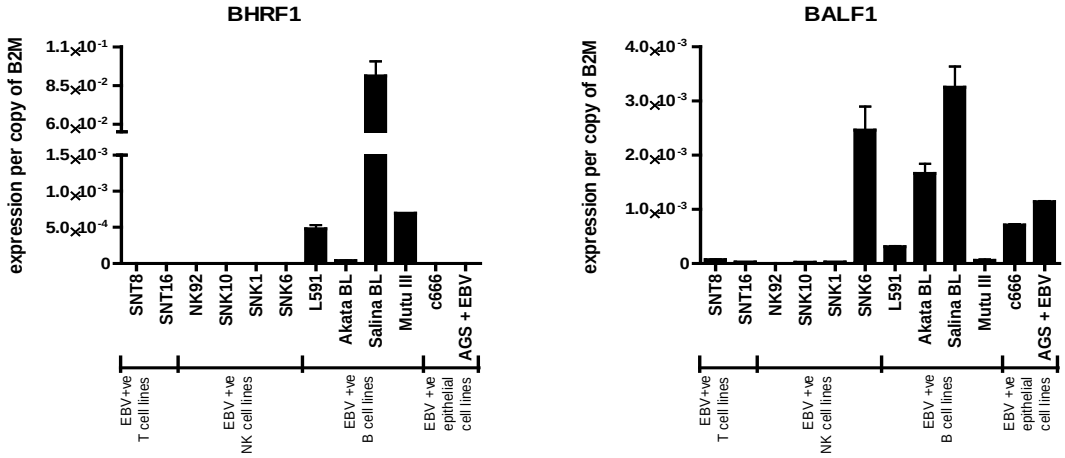

Figure 5.2: Levels of BHRF1 and BALF1 expression in latent EBV positive non-BL lines. Levels of BHRF1 and BALF1 were measured in two EBV positive Lat II T cell lines (SNT8 and SNT16), four EBV positive Lat II NK cell lines (NK92, SNK10, SNK1 and SNK6), two epithelial cell lines; one EBV positive Lat II nasopharyngeal carcinoma line (c666), and one EBV positive Lat I gastric carcinoma line (AGS+EBV). B cell lines used were two EBV positive Lat III lines, Mutu III and L591 (Hodgkin lymphoma line), one Lat I BL (Akata BL) and one Wp restricted BL (Salina BL).
Levels of mRNA expression were measured using qPCR and a plasmid standard which gives absolute copy number. Levels were then normalised to cellular control. Levels of latent BHRF1 and BALF1 in individual lines can therefor, be directly compared. Results are mean of 3 technical replicates ± sd.

5.4 BALF1 protects from apoptosis

Using the inducible lentivirus system described in Chapter 3, we expressed HA tagged BALF1 in the EBV negative BL41 cell line. This lentivirus constitutively expresses GFP as a marker for infection. EBV negative BL41 and the Wp restricted cell lines, Avako and Oku were transduced several times with empty control and HA-BALF1 lentiviruses and then sorted for the 50% highest GFP expressing cells. The GFP expression of these lines is shown in Figure 5.3. BL41 HABALF1 line was compared to the GFP expression of the BL41 HA-BHRF1 wild type used in earlier chapters. Despite several round of super-infection and sorting the GFP levels in BL41 HA-BALF1 lines are factor of 10 times lower than those in HABHRF1. In contrast, Avako and Oku BL were also transduced with HA-BALF1 and show higher levels of GFP expression, similar to those seen in BL41 HA-BHRF1. It is notable that Avako and Oku both express BHRF1 which could have a protective effect during transduction.

The protein expression of BALF1 transduced lines was tested using Western blot (Figure 5.4). As there is no antibody to BALF1, expression was determined using an antibody against the HA tag. The expression of HA tagged BALF1 is very high in the Avako and Oku Wp lines. However, in BL41 lines, although we can see low expression of HA tagged BHRF1, expression of HA-BALF1 protein was below the level of detection by blotting. Detection of HA-BHRF1 by the 5B11 anti-BHRF1 antibody, as opposed to the anti-HA antibody, shows much stronger expression (Figure 5.4B) indicating that the failure to detect HA-BALF1 may be partly due to the sensitivity of the anti-HA antibody. There may also be lower levels of transduction in the BL41 lines. It is known that BHRF1 can protect from apoptosis at levels of expression undetectable by Western blot (101). If BALF1 has a similar ability, a phenotype for BALF1

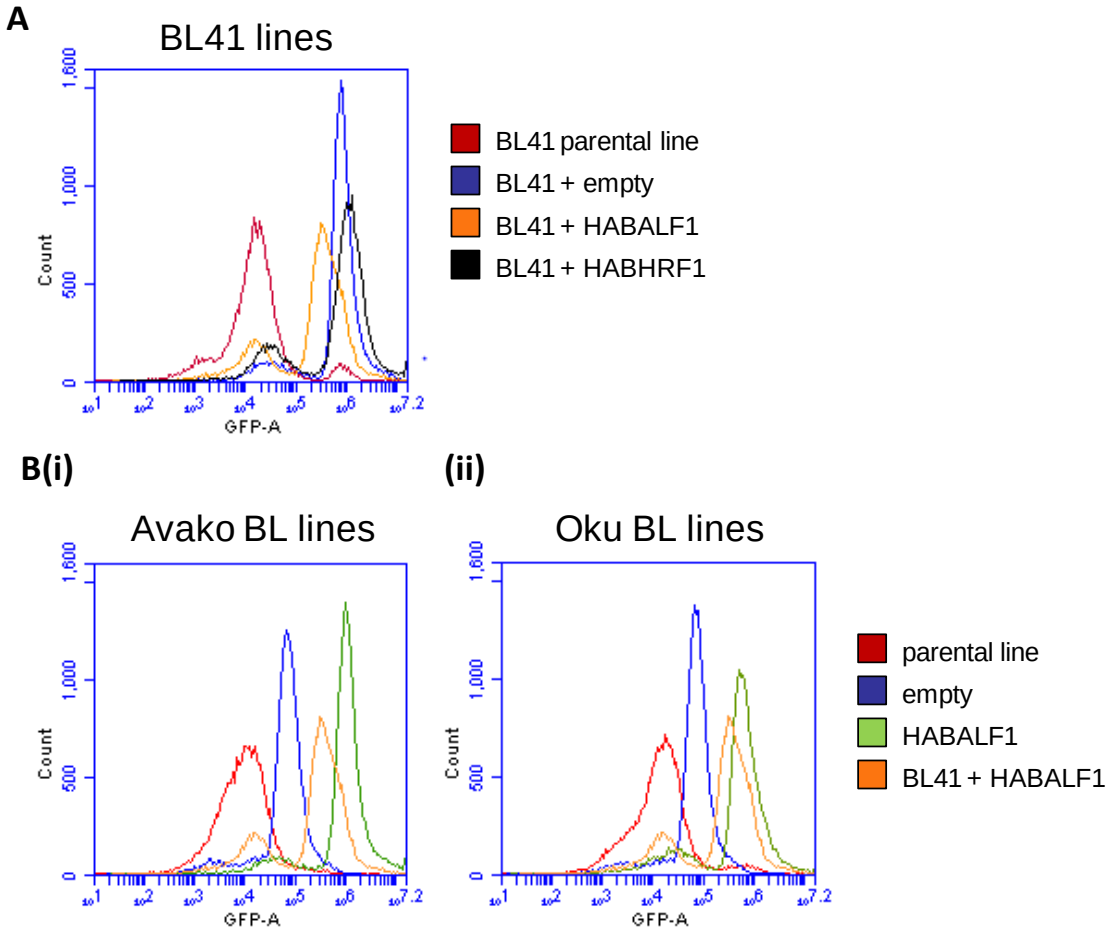

Figure 5.3: Levels of GFP expression in lentivirus transduced lines. EBV negative BL41 (A) and EBV positive, Wp restricted, Avako (Bi) and Oku (Bii) BL, were transduced with empty control and HABALF1 expressing lentivirus. This lentivirus (discussed in chapter 3) contains a GFP marker which is constitutively expressed. As described in chapter 3, the lentivirus transduced lines went through several rounds of super-infection and sorting. GFP expression was analysed by flow cytometry. GFP negative parental lines are shown in red, and empty control lentivirus lines in blue. In BL41 lines (A) BL41 HABALF1 (orange) and BL41 HABHRF1 (black) were compared. In Avako (Bi) and Oku (Bii) BL lines, the respective Wp line transduced with HABALF1 lentivirus (green) was compared to BL41 HABALF1 (orange).

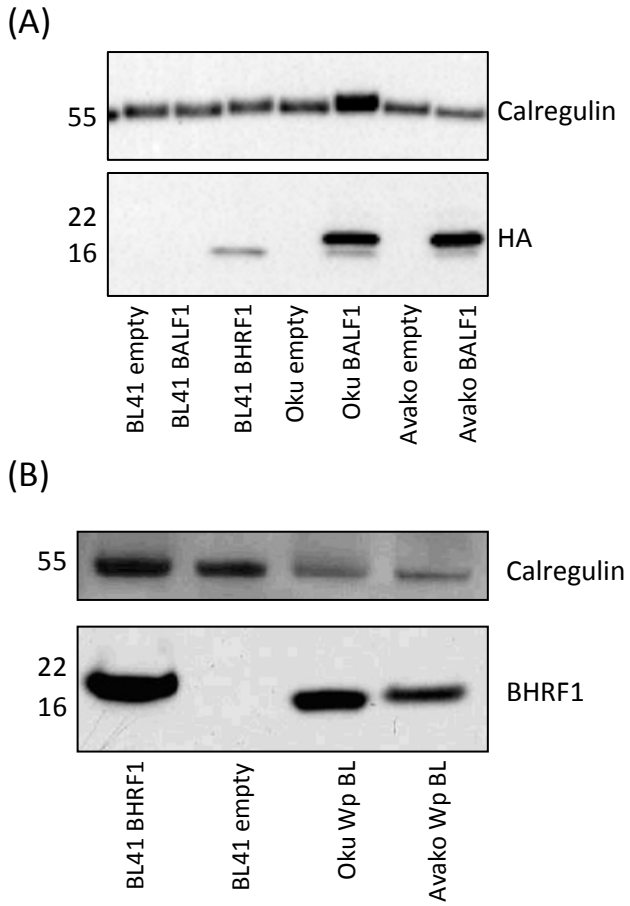

Figure 5.4: BALF1 protein expression. (A) BALF1 expression was measured using an anti-HA antibody to the HA tag, as there is no antibody available for BALF1. BALF1 was transduced into various lines using lentiviruses for stable expression. HABALF1 is expressed highly in Oku and Avako BL. HABALF1 is not detectable in BL41, however, HABHRF1 expression is also low. (B) BHRF1 expression in BL41, and Oku and Avako BL lines. There are similar levels of BHRF1 in BL41 lentivirus transduced line and Oku and Avako Wp despite the low expression of HA in the same BL41 BHRF1 line shown in (A).

mediated protection may be apparent despite our inability to detect BALF1 protein expression.

We induced protein expression with 1μg/ml dox for 48 hours and then induced apoptosis with four cytotoxic drugs; ionomycin, anti-IgM, etoposide and roscovitine, using concentrations of 1, 6, 2.5 and 12 ug/ml respectively. We then performed an apoptosis assay as described in section 4.4. Data was expressed as the amount of apoptosis induced by drug treatment, relative to the apoptosis induced in the corresponding empty vector cell line. *P* values with a 95% confidence interval were used to show significant differences between levels of apoptosis in the empty vector and BALF1 or BHRF1 expressing lines.

As can be seen in Figure 5.5, BALF1 significantly protects BL41 lines from apoptosis induced with all four cytotoxic drugs tested. Protection is similar to BHRF1 when death is induced with anti-IgM, etoposide and roscovitine. When death is induced with ionomycin the BL41 BHRF1 cell line is very highly protected, the BALF1 expressing line is less protected but levels of induced apoptosis are still significantly lower when compared to the empty control line. As HA-BALF1 was undetectable by Western blot, this data shows that, similarly to BHRF1, BALF1 can protect even when protein levels are so low as to be undetectable with the antibodies used.

5.4.1 BALF1 can protect Wp BL lines more than endogenous BHRF1 alone

Bellows *et al*. have previously shown that BALF1 may be able to abrogate the anti-apoptotic function of BHRF1 (41). To reinvestigate this we expressed HA tagged BALF1 in Oku and Avako Wp restricted BL lines which already express high levels of endogenous BHRF1. These

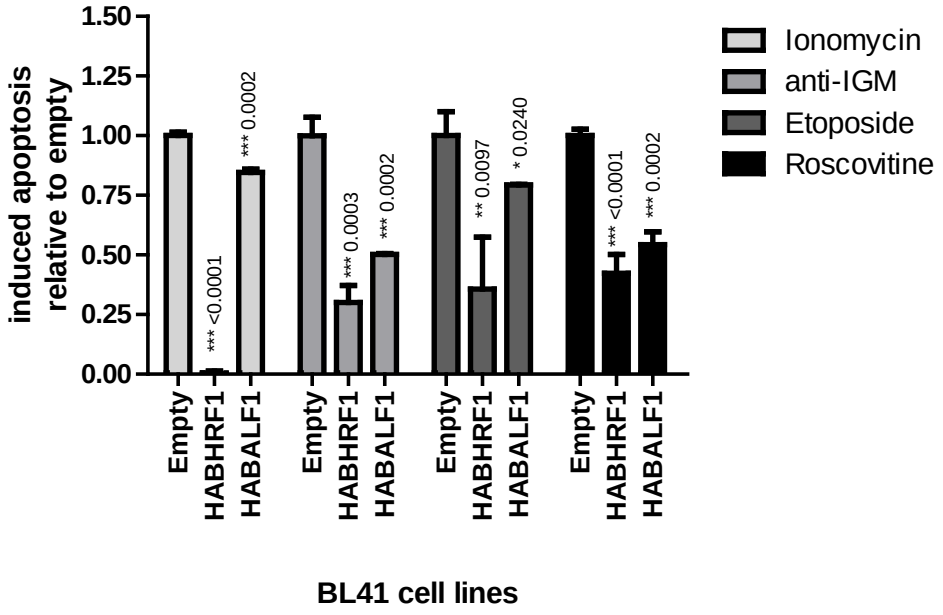

Figure 5.5: BALF1 protects from apoptosis induced by cytotoxic drugs. BALF1 protects BL41 cells to similar levels as BHRF1. Death was induced with 1ug/ml, 6ug/ml, 2.5ug/ml and 12ug/ml ionomycin, anti-IgM, etoposide and roscovitine respectively. Data is expressed relative to the respective empty lines. *P* values were considered significant if less than 0.05; * significant (*P*=0.01 to 0.05), ** very significant (*P*=0.001 to 0.01), *** extremely significant (*P*=0.0001 to 0.001), and show difference in apoptosis level from empty vector control. Data is the mean of three technical replicates ±sd.

lines were induced into apoptosis using the four cytotoxic drugs referred to in the previous section. Again, apoptosis was expressed as induced death relative to the apoptosis induced in the empty control line. *P* values showing significant differences in death between BALF1 and empty lines are given with a 95% confidence interval (Figure 5.6).

Overexpression of BALF1 significantly increases the anti-apoptotic protection in both Oku and Avako Wp BLs against all four drugs tested. BALF1 expression reduces death by around 10% in anti-IgM and etoposide treated Oku and Avako and in ionomycin treated Oku. There is a greater protection of around 30–60%, or over, in BALF1 expressing Avako lines treated with ionomycin, and both Oku and Avako lines treated with roscovitine.

5.5 BALF1 shows similarity to important domains in BHRF1 and BCL_{XL}

Multiple sequence alignment was performed of BALF1, BHRF1 and BCL_{XL} (Figure 5.7). The BHRF1 amino acids which have been mutated in this thesis are highlighted in red and important amino acids for binding of BCL_{XL} and BH3 domains, as found by Lama and Sankararamakrishnan (356) (R139, Q111, E129 and L130), are highlighted in blue. The BH3 domains, α-helices, and BH3 binding domain of BHRF1, as found by Huang *et al*. (46), are also shown.

BALF1 shows homology to BHRF1 and BCL_{XL} in the BH4 and BH1 domains but not in the BH2 or BH3 domains. The sequence corresponding to the trans-membrane domain of BHRF1 and BCL_{XL} is also poorly conserved and may be partially truncated. BALF1 not only shows homology to the BH domains, but also some of the individual amino acid residues important for BHRF1 and BCL_{XL} binding to BH3 domains. BALF1 shows homology to R71 of BHRF1, which is also analogous to Q111 in BCL_{XL}. There is no homology to BHRF1 E89 but there is to the residue next to it; I90 which is analogous to BCL_{XL} L130, also important for BH3 binding

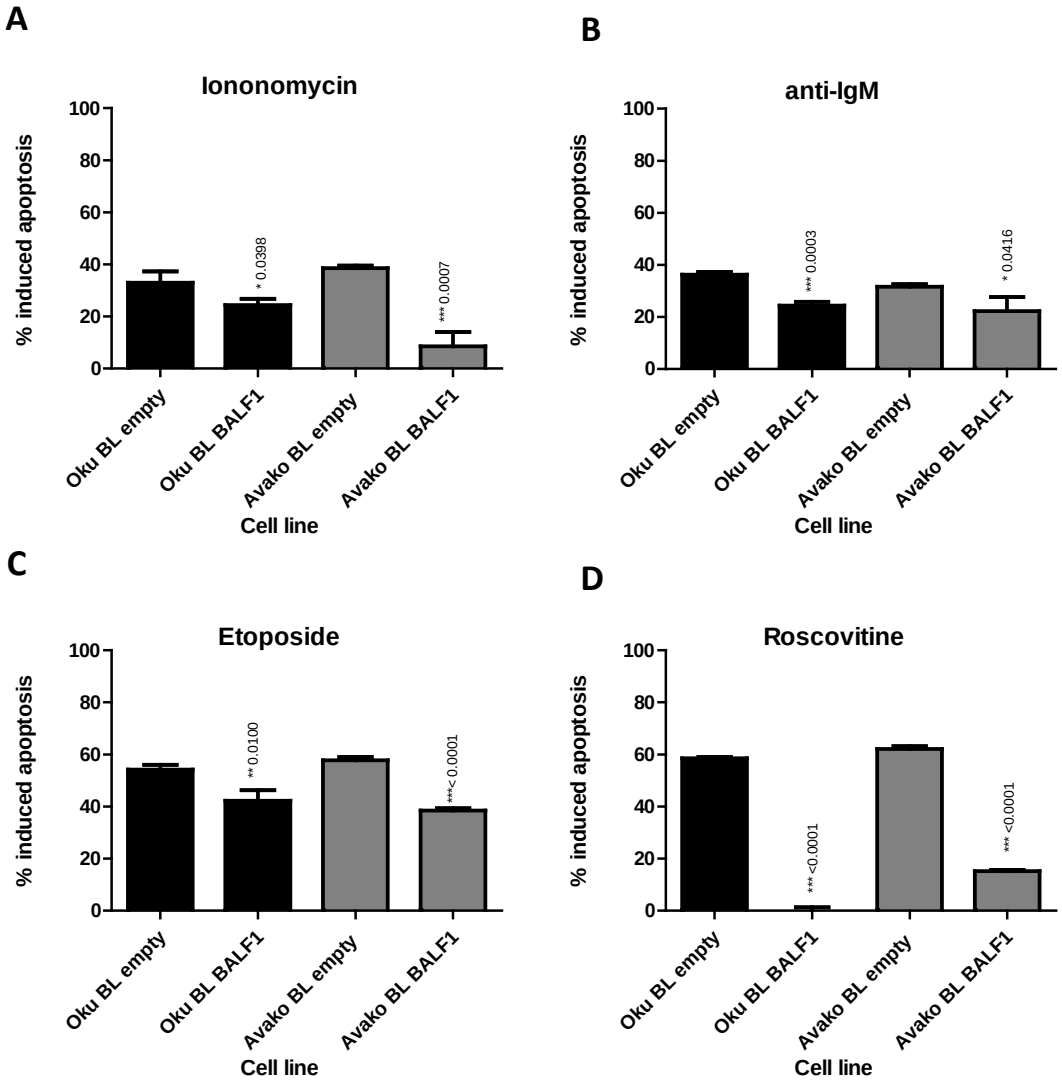

Figure 5.6: BALF1 and BHRF1 protect from apoptosis. BALF1 protects Wp BL lines to a greater extent than endogenous BHRF1 alone. Data is expressed relative to the respective empty lines. *P* values were considered significant if less than 0.05; * significant (*P*=0.01 to 0.05), ** very significant (*P*=0.001 to 0.01), *** extremely significant (*P*=0.0001 to 0.001), and show difference in apoptosis level from empty vector control. Data is the mean of three technical replicates ±sd.

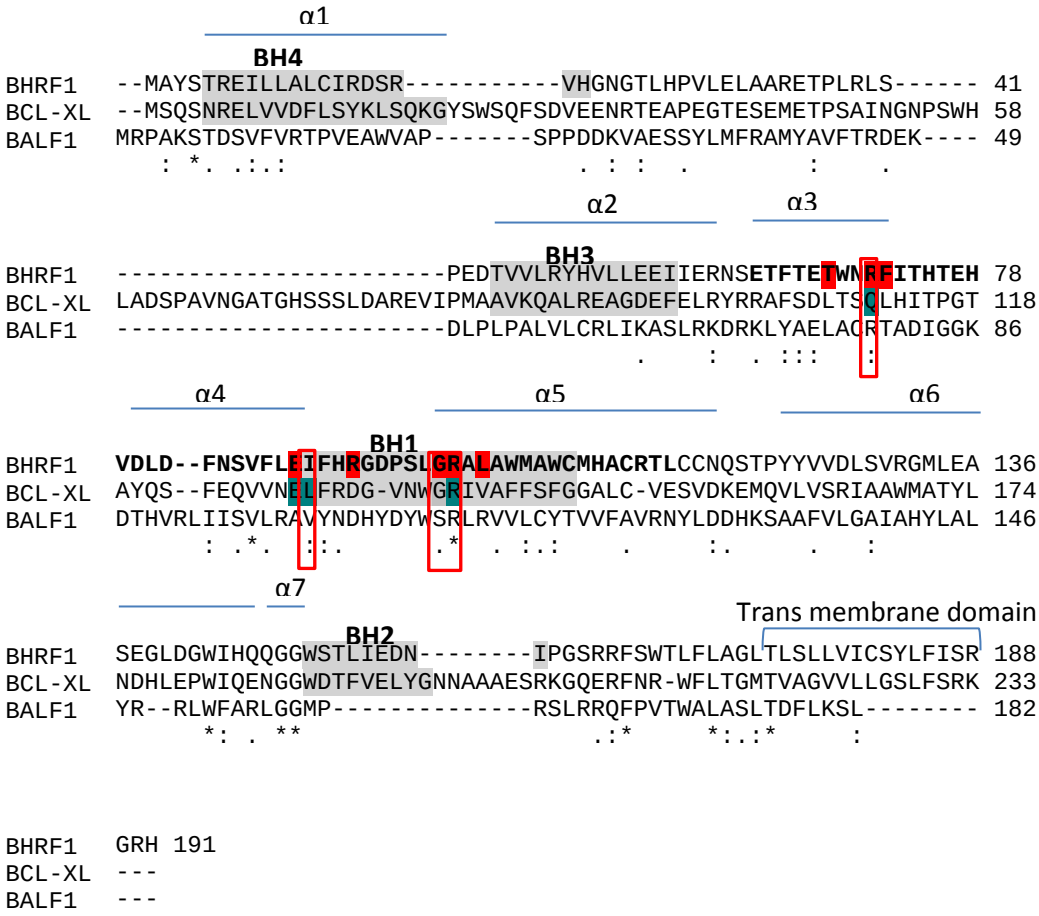

Figure 5.7: BALF1 is homologues to BHRF1 and BCL_{XL}. BALF1, BHRF1 and BCL_{XL} were aligned using multiple sequence alignment. Bcl2 homology domains of BHRF1 are highlighted in grey, BHRF1 α-helices are also shown and the BHRF1 binding domain is shown in bold (46). BHRF1 amino acids mutated in this thesis are highlighted in red. Important amino acids for the interactions of BCL_{XL} with BH3 domains, as found by (354), are highlighted in blue. Important residues which show homology are highlighted with a red box. * = a fully conserved residue, : = partial conservation with strongly similar properties, . = partial conservation with similar properties.

(356). Interestingly, the two BHRF1 residues which we have shown to be highly important for BH3 binding (see section 4.12); G99 and R100, also show a degree of conservation in BCL_{XL} and BALF1, with R100 showing total conservation across the three proteins. BHRF1 R93, an amino acid whose mutation to D93 did not cause BHRF1 to lose the ability to bind BH3 domains, is not conserved. However, both BCL_{XL} and BALF1 have aspartic acid (D) at the corresponding location, which may explain why the R93D mutation had little affect on the function of BHRF1.

5.6 Discussion

BALF1 was first characterised in 1999 by Marshall *et al.* (96) and was found using a homology search of the EBV genome with BCL_{XL} as a comparison. Marshall *et al.* found that BALF1, transfected into HeLa cells, could protect against apoptosis induced with anti-Fas antibody, interferon gamma and the topioisomerase inhibitor, camptothecin, to similar levels as BCL_{XL}. They also found that BALF1 co-immunoprecipitated with BAX and BAK, indicating that it functioned in a similar manner to BHRF1 (96).

Altmann and Hammerschmidt have shown that expression of either BHRF1 or BALF1 are essential for efficient transformation, but that they are interchangeable (98). This indicates that BALF1 may have a similar function to BHRF1.

Bellows *et al.* were the next to publish work focusing on the function of BALF1 (41). In contrast to Marshall *et al.* they failed to find an anti-apoptotic function for BALF1, and found that BALF1 did not protect epithelial cells against Sindbis virus induced death. They also found that BALF1 expression conferred no protection to DG75 cells induced into apoptosis through BAX over-expression. They tested both BALF1 and BALF0 (initiated at different methionines in the same reading frame within the BALF sequence) co-transfected into CHO

cells with BHRF1 or Kaposi's sarcoma virus vBCL-2; KSBCL-2. BALF1 and BALF0 were found to antagonise BHRF1 and KSBCL-2 and prevent them from protecting from apoptosis induced by BAX over-expression. BALF1, but not BALF0, was found to precipitate with BHRF1 and KSBCL-2, but not $BCL_{XL.}$ However, they did not see co-localisation of BHRF1 and BALF1. Whereas BHRF1 localises to the mitochondrial membrane BALF1 was found to be localised in the cytosol (41). From Figure 5.7 showing a multiple alignment of BHRF1, BCL_{XL} and BALF1, it is clear that, unlike BHRF1 and BCL_{XL}, BALF1 has a truncated transmembrane domain. This is the domain that localises anti-apoptotic BCL-2 homologues to the mitochondrial membrane so, without it, it is likely that BALF1 would be localised in the cytosol.

Unlike Bellows *et al.* (41) we did not find that BALF1 antagonised the function of endogenous BHRF1 but instead increased the protection of Wp lines from apoptosis. Our findings agree with those of Marshall *et al*. (96) and the recent paper by Hsu *et al*. (357). Hsu *et al.* found that BALF1 could protect 293 cells from serum starvation and increased cell survival through inhibition of apoptosis and not cell cycle progression (357). Hsu *et al.* also found that BALF1 promotes tumour formation in nude mice and promotes metastasis.

We also found that BALF1 had an anti-apoptotic effect, although not as strong as that of BHRF1. However, in our assays, BALF1 provided protect from apoptosis despite us being unable to detect HA-BALF1 protein expression with anti-HA antibody. However, we did achieve high levels of HA-BALF1 protein expression in Wp lines.

Good levels of GFP expression, and hence transduction, were much more difficult to achieve in BL41 using BALF1 lentivirus, as opposed to BHRF1 lentivirus. This appears to be a common problem, and difficulties in achieving stable clones with BALF1 expression were also experienced by Lee and Hope (111), although in contrast to our work, they did not find that BALF1 or BALF0 had a protective effect.

A difference between our work and published studies on BALF1 is that we are the only group who have stably expressed BALF1 using a lentivirus. Other studies expressed BALF1 using transient transfection of a variety of plasmid vectors such as pcDNA (357), pBABE (112) and pEGFP (96). One of the reasons we chose to use lentiviruses, as opposed to transient transfection, was that both transfection and transduction are disruptive processes and involve a loss of cell viability. However, unlike transfection, in which gene expression is transient and cells must be harvested quickly, stably transduced cells have long term gene expression. This means that we can allow the cells time to recover from the transfection process and regain viability, an advantage when performing cell death assays in already sensitive cell lines such as EBV negative BL. Some of the variation between BALF1 cell death assays in these papers could be due to variability caused by the transfection process. In the Bellows paper, in which BALF1 was shown to antagonise BHRF1 (41), it was not clear if a control was used in the co-transfection experiments. Co-transfection of two plasmids often results in reduced cell viability, if a control plasmid was not used this could explain the loss of viability in BALF1/BHRF1 transfected cells as opposed to cells transfected with BHRF1 alone.

Although our findings support those published in the literature, some caution is required when interpreting the results. The difficulty we found when transducing the BL lines with BALF1 lentivirus, and the subsequent rounds of sorting that were undertaken to achieve stable infection, may have had the unintentional result of selecting for cells with a more resistant phenotype. By its nature sorting subjects cells to apoptotic stimuli, and by growing up the few GFP positive cells returned we may have also been selecting for apoptosis resistance. An empty plasmid was included as an attempt to control for these factors, however, stable infection was not as difficult with this lentivirus as with that containing

BALF1. If BALF1 is in fact pro-apoptotic, explaining the difficulties in achieving good levels of expression, leaky expression from the lentivirus may drive cells towards apoptosis, with any cells remaining having a more apoptosis-resistant phenotype.

To support our results we could try to achieve transient transfection of BL lines with small BALF1 plasmids as performed in other studies looking at the function of BALF1. Although, for reasons discussed above, this method is not ideal for use with apoptosis assays, it could provide short-lived high levels of BALF1 expression without the need for sorting, and hence, remove some of the potential selection pressure. Another option may be to use custom shRNAs to knock down BALF1 in lines in which it is already expressed. We have shown that expression of BALF1 is promiscuously expressed in several forms of latency, however, expression levels are low, and so sensitive assays would be needed to detect knockdown and differences in apoptosis sensitivity. These techniques could allow us to answer the question of whether BALF1 is pro- or anti-apoptotic but stable cell lines may be needed before we can look at how BALF1's function relates to BHRF1.

With so little literature to compare it is still difficult to determine if BALF1 is indeed anti-apoptotic. However, the results of Bellows *et al.* have not been confirmed by other publications, or our own work. The majority of the work on BALF1 has found it to be anti-apoptotic (96, 112, 357) although a mechanism for this ability is unknown.

Our results confirm those of Cabras *et al.* 2005 who found that BALF1 was expressed during latency in BL and NPC samples (112). They showed that BALF1 was able to protect NIH3T3 against apoptosis induced with different serum concentrations, and maintained growth. We also found that BALF1 was expressed in a wide range of BL lines as well as lines from a non B cell background, including lines with an epithelial and NK/T cell origin (Figure 5.2).

BHRF1 is only expressed during latency in a select few cell types and not in NPC (358). Expression of high levels of latent BHRF1 in BL is not due to 'normal' EBV expression, but is instead due to a deletion which has gained more prevalence through providing a selection advantage (101). Although BHRF1 is found in latency III B cell lines and LCLs, it is not expressed in latency I or latency II, the forms of latency expressed in most EBV related malignancies. The physiological levels of BALF1 mRNA are similar to those of BHRF1 mRNA in LCLs and so may be high enough to provide a phenotype. Expression of low levels of BALF1 could, therefor, provide a protective effect in latency types which do not express BHRF1.

6.0 Conclusions and future work

In this thesis we investigated the mechanism by which the EBV encoded viral BCL-2 homologue, BHRF1, interacts with the cellular BCL-2 family of proteins to confer apoptosis protection in EBV negative BL cell lines. We also investigated whether the second vBCL-2 homologue, BALF1 is a pro- or anti-apoptotic protein.

Chapter 3 described how we expressed BHRF1 in EBV negative BL lines using the FTGW(insert)UTG lentivirus system to create stable, dox inducible, cell lines. These cell lines expressed physiologically relevant levels of BHRF1, similar to those observed in Wp restricted BL lines, and gave a similar protective phenotype.

The BHRF1 binding groove mutants were originally made by Marc Kvansakul and characterised using ITC in a similar manner as described in (104). We expressed them in an EBV negative BL background to look at BHRF1 binding ability in a cellular system.

Few papers have been published which specifically look at the key amino acids for BCL-2 homologue binding. There have been a small number of mutational studies performed on the BHRF1 binding groove (46, 104, 109) but these used a limited number of mutations. Studies into the binding of BHRF1 to the BH3 domains of various BCL-2 homologues have been performed but these are mainly in solution or use truncated peptides rather than whole proteins, and so may not be physiologically relevant (84, 104).

6.1 The interaction of BHRF1 with cellular BCL-2 homologues

Previous literature has indicated that BHRF1 acts mainly through binding to BIM (109). However, in this thesis we have shown that BHRF1 functions through a variety of BH3 only BCL-2 homologues and binding to BIM is not the sole critical interaction for BHRF1 function.

From the binding and the apoptosis assay data in chapter 4, we can postulate that BHRF1 interacts with cellular pro-apoptotic BCL-2 homologues in a hierarchy of binding, with others taking the place of those which are inactive or have been knocked down.

From the knockdown studies, BHRF1 appears to bind a hierarchy of BCL-2-homologues (Figure 6.1). BHRF1 appears to act mainly through BAK and the BH3-only protein t-Bid. Although BHRF1 binds strongly to BIM, binding to BIM is not essential for it to function as an anti-apoptotic protein, as knockdown of BIM does not change BHRF1's ability to protect from apoptosis induced by any of the cytotoxic drugs tested. BHRF1 was able to protect from death induced by DNA damage, but this was not dependent on the presence of PUMA and so protection may be more dependent on binding to BAK and t-BID. Although interactions with NOXA could play a role we did not look at this BH3-only homologue in our assays. Interactions between BHRF1 and PUMA or BAX are not essential for the anti-apoptotic activity of BHRF1, although the loss of binding to BIM, or BIM deletion, may make BHRF1 more dependent on binding to PUMA.

The activation of different drug pathways, which in turn activate different BH3-only BCL-2 homologues, does not change the protective ability of BHRF1 wild type or its mutants. Therefore, it is likely that BHRF1 acts mainly downstream of the BH3-only proteins. BHRF1 may be working through the multi-domain BCL-2 homologues BAX and BAK. As several publications (23, 104, 109) show BHRF1 binding to BAK but not to BAX, its action may mainly be to bind BAK and keep it inactive. However, we have also shown that BHRF1 is still partially protected from ionomycin and anti-IgM induced death when BAK is knocked down, indicating that it also working through other BCL-2 homologues, most likely the BH3-only homologues (Figure 6.1).

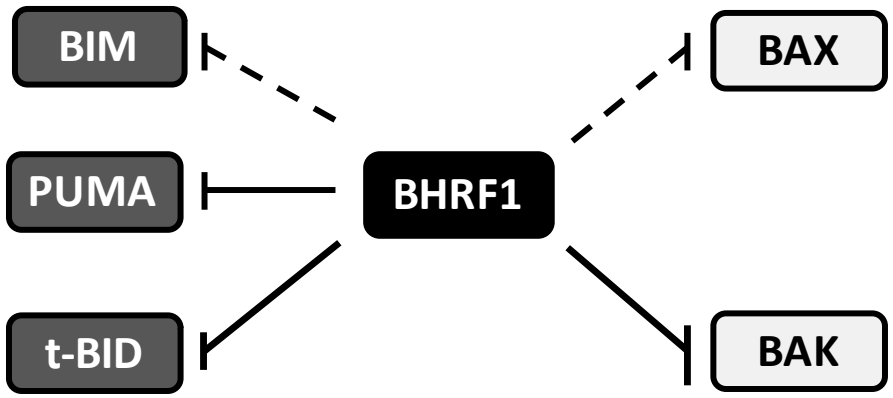

Figure 6.1: Impact of BCL-2 homologue binding on BHRF1 function. In our assays we found that binding to a hierarchy of BCL-2 homologues had varying degrees of impact on the function of BHRF1. Binding to BAK and BID had the greatest impact on BHRF1 function, followed by binding to PUMA, BIM and BAX, the loss of which did not greatly affect the function of BHRF1. Weight of lines represent the degree to which binding is needed for BHRF1 function.

Comparing the interactions of BHRF1 with the interactions of cellular anti-apoptotic BCL-2 homologues may help us determine how BHRF1 is able to protect from apoptosis (see Figure 1.4 and section 1.3.3). The pattern of BHRF1 binding to pro-apoptotic homologues appears to be most similar to BCL_{XL}. BCL_{XL} interacts with BIM, PUMA, t-Bid, BAK and BAX in a similar manner to BHRF1. BHRF1 has been shown to closely resemble BCL_{XL} in its structure and interactions, with around 32% sequence homology in its carboxy terminus (359), but much higher homology in its structure and folding (46, 104).

Recent research has moved away from BHRF1's interactions with BAX and BAK, and has focused on the BH3-only proteins, BIM in particular (109). However, here we have shown that BHRF1's interaction with BIM is not the sole critical interaction for BHRF1 to function. In fact the loss of BIM had no impact on the ability of BHRF1 to protect from apoptosis. From this research it is difficult to pin point one interaction with a sole cellular BCL-2 protein that is critical for BHRF1 function. However, our data suggests that it is BHRF1's ability to bind multiple cellular BCL-2 family proteins that allows it to provide high level protection from a diverse range of apoptotic stimuli. If we were to try to highlight any interactions then our data would suggest that the function of BHRF1 is much more reliant on the ability to bind other anti-apoptotic homologue such as BID and BAK than BIM. From our data, BHRF1 does not exert its anti-apoptotic effect through mainly binding to BIM, and more focus needs to be placed on binding to the other pro-apoptotic homologues if the system is to be properly understood.

6.2 Limitations and further experiments

We looked at the ability of BHRF1 to bind various BCL-2 homologues and protect from apoptosis in a BL background when eight of the key binding groove amino acids were

mutated. Kvansakul *et al.* had previously characterised the binding affinity of these mutants to five pro-apoptotic BCL-2 homologues; BAX, BAK, BIM, PUMA and Bid, using ITC.

While our data reliably showed that the key residues required for BHRF1 function are G99 and R100, and the ITC data showed that mutations at these sites causes loss or reduction in binding to the majority of BCL-2 homologues tested, we were unable to confirm this loss of binding by co-immunoprecipitation (Co-IP).

Our Co-IP assays provided good results for BIM but we were not able to detect binding of WT BHRF1 to other BCL-2 homologues. This therefore, made assessing the binding of the mutants to these cellular BCL-2 proteins impossible. There are a variety of factors that can affect the results of Co-IP assays including the concentration of proteins in the lysate, the sensitivity of the antibody and the type of buffer used to lyse the cells. In fact, the type and concentration of the detergent used in lysis can lead to variability between methods and may even induce dimerization (41, 360). Co-IP assays may also miss transient binding and the method may disrupt weaker interactions (361). In these experiments it is likely that the low, but physiological, levels of BHRF1 restricted the analysis. Therefore the Co-IP assays, did not provided sufficient information on the binding abilities of the BHRF1 mutants to all cellular BCL-2 family proteins to draw firm conclusions.

We therefore turned to the ITC data to assess the binding ability of the BHRF1 mutants. This method uses truncated proteins in solution, and we found the data to be useful, but not completely concordant with the results, in a cellular system. In most cases the ITC data was consistent with protective ability of the BHRF1 mutant, for example G99A and R100D consistently showed significant loss of binding to all cellular BCL-2 proteins tested. However, there were some discrepancies in which the protective phenotype of the mutant was at odds with the ITC data (e.g. F72W which protected almost as well as wild type but was

predicted by ITC to have lost or greatly reduced binding to the majority of BCL-2 homologues tested). Therefore it may be necessary to study these particular mutants in a different system in which we overexpress BHRF1 and carry out Co-IPs.

Since there are at least 11 BH3-only BCL-2 homologues which have been discovered so far (54) as well as the multi-domain pro death homologues BAX and BAK, it is maybe not surprising that we found that the ability of BHRF1 to function as an anti-apoptotic protein was not attributed to an interaction with only one cellular BCL-2 protein. Rather our data have shown that there is a degree of redundancy between the pro-apoptotic BCL-2 homologues. When we used siRNAs to knockdown of expression of some of these homologues we saw very little difference in the ability of BHRF1 to protect against apoptosis. In fact, there very little change to BHRF1's anti-apoptotic ability when BIM, a BH3-only BCL-2 homologue previously thought to be the main binding partner of BHRF1 (109), is knocked down, or when the BHRF1 protein is expressed in BIM negative lines. This indicates that BHRF1 can bind and neutralise an array of cellular BCL-2 pro-apoptotic proteins and thereby protect from a diverse range of apoptotic stimuli that induce the intrinsic pathway via different routes. It has been shown previously that BHRF1 can protect in BIM positive and negative lines (101, 110, 179) so BIM does not play an essential role in the anti-apoptotic function of BHRF1. From our knockdown studies, and the induction of apoptosis through different pathways, it is apparent that BHRF1 may act through binding to both BAX and BAK. Uren *et al.* found that anti-apoptotic BCL-2 homologues, including BHRF1, could protect from apoptosis induced by expression of BH3-only proteins that they could not bind, indicating a role in binding to BAX/BAK instead of BH3-only BCL-2 homologues (23).

To improve our ability to interpret the apoptosis assay data we could try the experiments in parallel in a less complex system. There are several systems that have been used to explore

the binding of BCL-2 anti-apoptotic proteins to the pro-apoptotic BCL-2 homologues. Many of these methods employ truncated peptides, representative of the binding domains of the BCL-2 homologues, and a substitute for initiation of apoptosis, such as liposome permeabilization (56), BH3 profiling and permeabilization of cell free mitochondria (20). These assays have similar disadvantages to those inherent in ITC, in that interactions are shown using truncated proteins in a cell-free system, and may give results that are not relevant inside the cell. A cellular system could possibly be developed in which no endogenous BCL-2 homologues exist, and the pathway could be reconstructed to the desired complexity. An assay which comes close to this involves reconstructing the intrinsic apoptosis pathway in yeast. This method was used by Kvansakul *et al.* alongside ITC (104) and was useful for circumnavigating the complications of having endogenous BCL-2 protein in the system and removed the need to use detergents which could disrupt binding (360). Although the budding yeast *Saccharomyces cerevisiae* does not undergo apoptosis or express any BCL-2 family members, overexpression of BAX and BAK is lethal and kills through the activation of permeabilization of mitochondrial membranes and impairment of mitochondrial biogenesis (315, 362). Full length BCL-2 homologue cDNAs can be cloned into yeast to test their ability to prevent BAX/BAK induced death. It has been shown that co-expression of BCL-2, MCL1, BCL_{XL} and A1 with BAX/BAK can protect yeast from death (315). Kvansakul *et al.* also showed that BHRF1 can protect from BAK, but not BAX, induced death in this system (104). It is possible to reconstruct the whole intrinsic apoptosis pathway in yeast, including anti-apoptotic and BH3-only BCL-2 homologues. This can be achieved by expressing BAX/BAK, BH3-only and pro-apoptotic BCL-2 homologues from inducible or repressible promoters so that expression can be induced by addition of galactose or dox, for example (362). In this way, expression of the various classes of the BCL-2 homologues can be

timed and levels of expression can be varied through titration of the inducing agent. Using this model, NOXA, BIF, BMF and BID have been shown to activate BAX/BAK indirectly by inhibition of BCL-2 and BCL_{XL} (362) and BIM has been shown to induce death through inhibition of BCL_{XL} (363).

In order to determine the binding abilities of the mutants, we could over-express them in the same EBV negative BL system using a different promoter and lentivirus system. While these high levels would not be physiologically relevant and would not yield useful apoptosis data, they might be high enough to detect binding by CO-IP.

It would be interesting to combine yeast assays with our apoptosis data from a BL background, and could help to confirm some of our observations of a hierarchy of BHRF1 binding to BCL-2 homologues. However, due to the high number of cellular BCL-2 homologues, which would all need to be expressed in conjunction with either BAX or BAK, a full panel of yeast assays would be a large undertaking, especially if we also wanted to include the BHRF1 mutants.

Another option would be to continue the knockdown studies. In this thesis we used a mix of commercial lentivirus plasmids (Santa Cruz Biotechnology Inc), expressing up to five different shRNAs sequences, to stably knockdown BIM, PUMA, BAX and BAK. These plasmids eventually gave good levels of knockdown but required several rounds of super infection and had the disadvantage of being drug selectable with no marker for expression. With more time we would have gone on to express several BCL-2 shRNAs in tandem to further simplify the system. Ideally we would also have included Bid in the panel of knockdowns. However, due to time constraints and issues with achieving good levels of knockdown we were unable to include it. As BHRF1 appears to favour binding to t-BID when death is

induced by several different drug pathways, it would be interesting to see the effect that removing BID from the system would have on BHRF1's ability to protect.

6.3 EBV and implications for the treatment of BL

As BHRF1 expression has been shown to render Eμ-myc mice resistant to treatment(104), the expression of BHRF1 could have implications for the treatment of BL.

BL is a highly aggressive B cell lymphoma characterised by a translocation, commonly between chromosomes 8 and 14, which leads to upregulation of the MYC oncogene (270, 364). C-Myc overexpression sensitises cells to apoptotic stimuli under unfavourable growth conditions (271). In the majority of BL cell lines and a significant percentage of BL biopsies, the pro-apoptotic effect is usually counteracted by mutation of the tumour suppressor p53, or elements of the p53 pathway (274, 275). In Eμ-myc mice (a model for BL) mutations in the p53 pathway are extremely common (365). EBV is also thought to have a role in suppressing MYC driven apoptosis, and can regulate apoptosis through a variety of mechanisms (see section 1.7.2 for details).

BL is one of the fastest growing malignancies, with a doubling time of around 25 hours, and so is treated aggressively with intensive combination chemotherapy (284, 366, 367). Despite being highly aggressive, BL is also sensitive to apoptosis as a result of the myc translocation, and chemotherapy can achieve remission, for at least a year, in 75–89% of paediatric patients and 47–86% of adults (284). For relapsed patients the prognosis is less optimistic, although around 25% of paediatric patients may achieve long-term survival with a combination of rituximab and haematopoietic stem cell transplantation (368). If first line treatment does not work or the tumour relapses then there are very few other treatment options available. Furthermore, many HIV positive individuals cannot tolerate the intense

chemotherapy required for BL and opt out of treatment. Therefore there is a need for new and targeted treatments for BL.

There is very little data on whether endemic and sporadic EBV have a different prognosis. They are histologically indistinguishable(369) and are currently both treated using the same chemotherapy regimes(284). Failure of first-line treatment results in poor prognosis in all forms of BL and relapse occurs in approximately 15–20% of patients.

It is not known if this subset of patients who fail to respond to treatment carry a version of EBV positive BL which harbours a Wp restricted form of EBV as opposed to the more common latency I form. Our data would strongly suggest that BLs that express BHRF1 are refractory to chemotherapy. The expression of BHRF1 during latency by Wp restricted EBV would result in a potent anti-apoptotic response. In Burkitt-like lymphomas (a form of B-cell lymphoma partway between BL and diffuse large B cell lymphoma, which may, or may not, have the *myc,* and other, translocations) it has been shown that possessing the c-myc translocation alongside an *IgH/BCL-2* fusion (which mimics BHRF1 over-expression in Wp restricted BL), increases resistance to treatment and drastically decreases patient survival (370, 371). In a study of 13 Burkitt-like lymphoma patients, with *myc* and *BCL-2* translocations, none survived beyond 7 months, despite aggressive chemotherapy (370).

In our work, we have seen a dramatic increase in cell survival upon treatment with apoptosis inducers when BHRF1 was expressed to physiological levels in EBV negative lines. Furthermore, these BHRF1 expressing EBV negative lines were equally well protected from apoptosis as their Wp restricted counterparts. This indicates that it is solely BHRF1 which gives Wp restricted BL its drug resistant phenotype.

Because BHRF1 may increase the apoptosis resistance of a cancer which requires highly aggressive chemotherapy, inhibition of BHRF1 could prove beneficial and may enable the

intensity of chemotherapy to be reduced in some cases. This could improve treatment outcomes in all subtypes of BL.

As many of the most treatment resistant cancers have been found to express high levels of the BCL-2 anti-apoptotic proteins, work is underway to find ways of suppressing their expression or inhibiting their function (reviewed in (372)). Inhibition of BCL-2 expression with antisense RNA has shown promise and one such compound, oblimersen sodium, has been tested in Phase III clinical trials(373, 374). However, doubt has been thrown over the mechanism of oblimersen, as CpG motifs, included the antisense RNA, activate toll-like receptor 9 and trigger an inflammatory response which also results in tumour cell killing (375).

BH3 mimetics have shown promise as BCL-2 inhibitors in recent years and could also be used to inhibit BHRF1. These target the protein-protein interactions of BCL-2 homologues. They mimic the BH3 domains of BH3-only homologues and bind to the hydrophobic cleft of anti-apoptotic BCL-2 proteins. The BCL-2 proteins are antagonised and release pro-apoptotic BCL-2 family proteins leading to cell death (reviewed in (376)).

One such BH3 mimetic, ABT-737, and its oral version ABT-263, inhibits BCL-2, BCL_{XL} and $BCL_{W,}$ but not MCL1 or A1 (377, 378). ABT-737 and ABT-263 have shown promising results in Phase I/II clinical trials but are less effective against cancers which express high levels of MCL1 and A1, tumours which initially respond well to ABT-737 have been shown to upregulate MCL1 and A1 expression after an extended period of treatment (379). In these cancers the effect of ABT-737 can be enhanced by inhibition of MCL1 and A1 using shRNAs (379) or through upregulation of BH3 only BCL-2 homologues which antagonise MCL1 and

A1, such as BIM and PUMA (reviewed in (380)). Hence, a combination of therapy types is likely to be beneficial.

Targeting widely expressed cellular BCL-2 proteins can lead to on-target toxicity in normal cells that are dependent on these proteins. For example platelets were severely affected by ABT-263 because they are dependent on BCL-XL for survival(381, 382). ABT-263 was redesigned to produce ABT-199 that is more effective against BCL-2 than BCL-XL and this toxicity was reduced (383).

An advantage of using BH3 mimetics to target a viral BCL-2 family protein such as BHRF1, is that higher doses of drug may be used because there should be no toxicity on normal cells. Despite its similarity to $BCL_{XL,}$ BHRF1 has been shown to be completely insensitive to ABT-737 (104). Hence, ABT-737 may not be as effective in BL.

When designing BH3 mimetics specific to BHRF1, data from our work could aid in determining basic requirements for the molecule. For example, we have shown the binding to the G99 and R100 amino acids in the BHRF1 hydrophobic groove is extremely important for the formation of BH3/BHRF1 complexes. Complex formation was not dependent on binding to the T68, R71, E89, R93, L102, and to some extent the F72, amino acids. Designing a compound with strong binding to these 6 amino acids, or increased affinity for G99 and R100, would drastically increase the strength of binding to BHRF1, outcompeting the BH3-only proteins and rendering BHRF1 inactive. We have also shown that BHRF1 binds strongly to BIM, although it may mainly act through BID and BAK. Basing any sequences on the BH3 domains of these proteins could be a good place to begin in the construction of a BH3 mimetic for BHRF1.

In a recent publication, Procko *et al.* have designed a BHRF1 mimetic, BINDI, using computational design with the BIM BH3 domain as a guide (384). The BIM BH3 domain was

grafted onto the BHRF1 binding groove and then surrounding residues of the BH3 domain, and scaffold protein, were modified, to provide optimal binding and fit. BINDI as been shown to have very high affinity and specificity for BHRF1, these levels of binding may be higher than any other drug, protein or peptide designed to bind BCL-2 homologues. In Ramos-AW cell lines (EBV positive, expressing low levels of BHRF1) BINDI induced cytochrome C release from mitochondria. However, there was also some affect of BINDI on mitochondria isolated from EBV negative Ramos, indicating that BINDI may retain some off target effect (384). Procko *et al.* also did not look at the effect of BINDI in Wp restricted BL which express higher levels of BHRF1 than LCLs of Lat BLs (101). However, they did show that BINDI, in combination with cyclophosphamide and bortezomib, was able to slow transformation and tumour progression in nude BALB/c mice with subcutaneous xenografts of Ramos-AW. BINDI extended survival to 24 days as opposed to 16 days with chemotherapy only (384). This research, although very preliminary as a treatment for BL, has shown that it is possible to computationally design proteins that will then have an *in vivo* effect. It will be interesting to see extended research on the properties of BINDI *in vitro* and *in vivo,* especially in relation to its ability to sensitise Wp restricted BL to treatment.

6.4 BALF1 and resistance to apoptosis

BALF1 is the second vBCL-2 homologue expressed by EBV and its function is still controversial.

Expression of either BALF1 or BHRF1 has been shown to be essential during transformation (98). However, it is not known if BALF1 is pro- or anti-apoptotic. There are reports that BALF1 has a pro-apoptotic function and may antagonise BHRF1 in a similar manner to the way in which cellular pro-apoptotic BCL-2 homologues antagonise their anti-apoptotic

counterparts(41). However, we found that BALF1 was able to protect BL cells from apoptosis, and increased the protection already conferred by BHRF1 expression. These results are supported by several other studies (96, 357).

Considering the wealth of published information on BHRF1, it is surprising that BALF1 is not better studied, especially considering the rarity of two BCL-2 homologues being expressed by the same virus. An extensive literature search revealed only 5 primary publications which explore the function of BALF1 (41, 96, 98, 112, 357). In an otherwise extensively studied virus there is a real dearth of information surrounding a protein which could have implications, not only for EBV biology, but also for EBV associated malignancy.

In part, this lack of information may be due to the absence of tools to assess BALF1's expression and function, such antibodies and siRNAs, for example, as well as the difficulty in achieving stable and long-term BALF1 expression (111). In our studies we used a lentivirus to express a HA tagged version of BALF1 in BL cell lines. This proved difficult to transduce into cell lines but once stable transduction was achieved, Wp restricted BL lines expressed HA-BALF1 to very high levels and we were able to see a protective effect in addition to that provided by endogenous BHRF1.

Unfortunately our experiments were limited by time constraints. However, these cell lines could provide a very useful resource for the study of BALF1 function. With the HA tag they enable easy detection of the BALF1 protein and can be used for co-immunoprecipitation and immunofluorescence assays. With expression of BHRF1 and BALF1 in the same system it could be interesting to look at their similarities and differences in terms of interactions with cellular BCL-2 homologues and their ability to protect against various cytotoxic drugs.

6.5 BALF1 expression and the implication for EBV related malignancy

We found that BALF1 was expressed in B cell lines during EBV latency. Unlike BHRF1, BALF1 mRNA was expressed during Wp restricted latency, latency I, and III. Due to the lack of any antibodies to BALF1, we were unable to look for BALF1 protein expression in these lines. However, BALF1 mRNA was expressed to similar levels as those of BHRF1 mRNA seen in LCLs, which is known to be high enough to affect phenotype (101).

BALF1 expression is not restricted to B cells. Cabras *et al.* showed BALF1 to be expressed in BL cell lines and NPC biopsies (112). In an extensive panel of cell lines we showed BALF1 to be expressed over a wide range of malignancies, and all forms of EBV latency.

This unrestricted pattern of expression means that BALF1 could potentially be much more physiologically relevant for EBV related malignancy than BHRF1, which has a restricted pattern of expression and is rarely found expressed in anything but Wp restricted BL and LCLs (101). Furthermore, BALF1 has been shown to increase tumour formation in nude mice, and cell movement and invasion in cell culture which could translate in increased metastatic potential(357). Hence, abrogation of the anti-apoptotic function of BALF1 would have implications for the treatment of all EBV related malignancies, not only BL. However, without the knowledge of how BALF1 achieves its effect, whether through interactions with cellular pro-apoptotic proteins as a vBCL-2 homologue as its sequence homology suggests(96), or through other mechanisms such as upregulation of transcription factors like NF-κβ, a known ability of BCL-2 (385) , it would be extremely difficult to design a treatment to repress BALF1's function. Further study into the basic function and binding of BALF1 could be very beneficial. There remains the opportunity for future research to have an extensive impact on the understanding of the virus and its associated malignancies.

7. References

1. Lodish H, Berk A, Zipursky S, Matsudaira P, Baltimore D, Darnell J. Cell Death and Its Regulation. Molecular Cell Biology. 4th edition. 4th ed. New York: W. H. Freeman; 2000.
2. Norenberg MD, Rao KV. The mitochondrial permeability transition in neurologic disease. Neurochem Int. 2007 Jun;50(7-8):983-97.
3. Galluzzi L, Brenner C, Morselli E, Touat Z, Kroemer G. Viral control of mitochondrial apoptosis. PLoS Pathog. 2008 May;4(5):e1000018.
4. Hanahan D, Weinberg RA. Hallmarks of cancer: the next generation. Cell. 2011 Mar;144(5):646-74.
5. Kang MH, Reynolds CP. Bcl-2 inhibitors: targeting mitochondrial apoptotic pathways in cancer therapy. Clin Cancer Res. 2009 Feb 15;15(4):1126-32.
6. Liao JB. Viruses and human cancer. Yale J Biol Med. 2006 Dec;79(3-4):115-22.
7. Kroemer G, Galluzzi L, Vandenabeele P, Abrams J, Alnemri ES, Baehrecke EH, et al. Classification of cell death: recommendations of the Nomenclature Committee on Cell Death 2009. Cell Death Differ. 2009 Jan;16(1):3-11.
8. Linkermann A, Green DR. Necroptosis. N Engl J Med. 2014 Jan 30;370(5):455-65.
9. Fan YJ, Zong WX. The cellular decision between apoptosis and autophagy. Chin J Cancer. 2012 Oct 10;31(11).
10. Rubinsztein DC, Codogno P, Levine B. Autophagy modulation as a potential therapeutic target for diverse diseases. Nat Rev Drug Discov. 2012 Sep;11(9):709-30.
11. Natkunam Y. The biology of the germinal center. Hematology Am Soc Hematol Educ Program. 2007:210-5.
12. Hacker G. The morphology of apoptosis. Cell Tissue Res. 2000 Jul;301(1):5-17.
13. Sayers TJ. Targeting the extrinsic apoptosis signaling pathway for cancer therapy. Cancer Immunol Immunother. 2011 Aug;60(8):1173-80.
14. Lavrik I, Golks A, Krammer PH. Death receptor signaling. J Cell Sci.2005 Jan 15;118(Pt 2):265-7.
15. Xu G, Shi Y. Apoptosis signaling pathways and lymphocyte homeostasis. Cell Res. 2007 Sep;17(9):759-71.
16. Luo X, Budihardjo I, Zou H, Slaughter C, Wang X. Bid, a Bcl2 interacting protein, mediates cytochrome c release from mitochondria in response to activation of cell surface death receptors. Cell. 1998 Aug 21;94(4):481-90.
17. Micheau O, Tschopp J. Induction of TNF receptor I-mediated apoptosis via two sequential signaling complexes. Cell. 2003 Jul 25;114(2):181-90.
18. Chang L, Kamata H, Solinas G, Luo JL, Maeda S, Venuprasad K, et al. The E3 ubiquitin ligase itch couples JNK activation to TNFalpha-induced cell death by inducing c-FLIP(L) turnover. Cell. 2006 Feb 10;124(3):601-13.
19. Ghiotto F, Fais F, Bruno S. BH3-only proteins: the death-puppeteer's wires. Cytometry A. 2010 Jan;77(1):11-21.
20. Letai A, Bassik MC, Walensky LD, Sorcinelli MD, Weiler S, Korsmeyer SJ. Distinct BH3 domains either sensitize or activate mitochondrial apoptosis, serving as prototype cancer therapeutics. Cancer Cell. 2002 Sep;2(3):183-92.
21. Huang DC, Cory S, Strasser A. Bcl-2, Bcl-XL and adenovirus protein E1B19kD are functionally equivalent in their ability to inhibit cell death. Oncogene. 1997 Jan 30;14(4):405-14.
22. Cory S, Huang DC, Adams JM. The Bcl-2 family: roles in cell survival and oncogenesis. Oncogene. 2003 Nov 24;22(53):8590-607.
23. Uren RT, Dewson G, Chen L, Coyne SC, Huang DC, Adams JM, et al. Mitochondrial permeabilization relies on BH3 ligands engaging multiple prosurvival Bcl-2 relatives, not Bak. J Cell Biol. 2007 Apr 23;177(2):277-87.
24. Nicholson DW. Caspase structure, proteolytic substrates, and function during apoptotic cell death. Cell Death Differ. 1999 Nov;6(11):1028-42.

25. Slee EA, Adrain C, Martin SJ. Serial killers: ordering caspase activation events in apoptosis. Cell Death Differ. 1999 Nov;6(11):1067-74.
26. Logue SE, Martin SJ. Caspase activation cascades in apoptosis. Biochem Soc Trans. 2008 Feb;36(Pt 1):1-9.
27. Luthi AU, Martin SJ. The CASBAH: a searchable database of caspase substrates. Cell Death Differ. 2007 Apr;14(4):641-50.
28. Acehan D, Jiang X, Morgan DG, Heuser JE, Wang X, Akey CW. Three-dimensional structure of the apoptosome: implications for assembly, procaspase-9 binding, and activation. Mol Cell. 2002 Feb;9(2):423-32.
29. Rodriguez J, Lazebnik Y. Caspase-9 and APAF-1 form an active holoenzyme. Genes Dev. 1999 Dec 15;13(24):3179-84.
30. Li H, Zhu H, Xu CJ, Yuan J. Cleavage of BID by caspase 8 mediates the mitochondrial damage in the Fas pathway of apoptosis. Cell. 1998 Aug 21;94(4):491-501.
31. Ellis HM, Horvitz HR. Genetic control of programmed cell death in the nematode C. elegans. Cell. 1986 Mar;44(6):817-29.
32. Tsujimoto Y, Gorham J, Cossman J, Jaffe E, Croce CM. The t(14;18) chromosome translocations involved in B-cell neoplasms result from mistakes in VDJ joining. Science. 1985 Sep 27;229(4720):1390-3.
33. Bakhshi A, Jensen JP, Goldman P, Wright JJ, McBride OW, Epstein AL, et al. Cloning the chromosomal breakpoint of t(14;18) human lymphomas: clustering around JH on chromosome 14 and near a transcriptional unit on 18. Cell. 1985 Jul;41(3):899-906.
34. Cleary ML, Smith SD, Sklar J. Cloning and structural analysis of cDNAs for bcl-2 and a hybrid bcl-2/immunoglobulin transcript resulting from the t(14;18) translocation. Cell. 1986 Oct 10;47(1):19-28.
35. Vaux DL, Cory S, Adams JM. Bcl-2 gene promotes haemopoietic cell survival and cooperates with c-myc to immortalize pre-B cells. Nature. 1988 Sep 29;335(6189):440-2.
36. Adams JM, Cory S. The Bcl-2 protein family: arbiters of cell survival. Science. 1998 Aug 28;281(5381):1322-6.
37. Vaux DL, Weissman IL, Kim SK. Prevention of programmed cell death in Caenorhabditis elegans by human bcl-2. Science. 1992 Dec;258(5090):1955-7.
38. Willis S, Day CL, Hinds MG, Huang DC. The Bcl-2-regulated apoptotic pathway. J Cell Sci. 2003 Oct;116(Pt 20):4053-6.
39. Nakayama K, Negishi I, Kuida K, Shinkai Y, Louie MC, Fields LE, et al. Disappearance of the lymphoid system in Bcl-2 homozygous mutant chimeric mice. Science. 1993 Sep;261(5128):1584-8.
40. Bouillet P, Cory S, Zhang LC, Strasser A, Adams JM. Degenerative disorders caused by Bcl-2 deficiency prevented by loss of its BH3-only antagonist Bim. Dev Cell. 2001 Nov;1(5):645-53.
41. Bellows DS, Howell M, Pearson C, Hazlewood SA, Hardwick JM. Epstein-Barr virus BALF1 is a BCL-2-like antagonist of the herpesvirus antiapoptotic BCL-2 proteins. J Virol. 2002 Mar;76(5):2469-79.
42. Foyouzi-Youssefi R, Arnaudeau S, Borner C, Kelley WL, Tschopp J, Lew DP, et al. Bcl-2 decreases the free Ca2+ concentration within the endoplasmic reticulum. Proc Natl Acad Sci U S A. 2000 May 23;97(11):5723-8.
43. Kirkin V, Joos S, Zornig M. The role of Bcl-2 family members in tumorigenesis. Biochim Biophys Acta. 2004 Mar 1;1644(2-3):229-49.
44. Brunelle JK, Letai A. Control of mitochondrial apoptosis by the Bcl-2 family. J Cell Sci. 2009 Feb 15;122(Pt 4):437-41.
45. Beverly LJ, Varmus HE. MYC-induced myeloid leukemogenesis is accelerated by all six members of the antiapoptotic BCL family. Oncogene. 2009 Mar;28(9):1274-9.
46. Huang Q, Petros AM, Virgin HW, Fesik SW, Olejniczak ET. Solution structure of the BHRF1 protein from Epstein-Barr virus, a homolog of human Bcl-2. J Mol Biol. 2003 Oct 3;332(5):1123-30.

47. Allagnat F, Cunha D, Moore F, Vanderwinden JM, Eizirik DL, Cardozo AK. Mcl-1 downregulation by pro-inflammatory cytokines and palmitate is an early event contributing to beta-cell apoptosis. Cell Death Differ. 2011 Feb;18(2):328-37.
48. Cimmino A, Calin GA, Fabbri M, Iorio MV, Ferracin M, Shimizu M, et al. miR-15 and miR-16 induce apoptosis by targeting BCL2. Proc Natl Acad Sci U S A. 2005 Sep 27;102(39):13944-9.
49. Calin GA, Dumitru CD, Shimizu M, Bichi R, Zupo S, Noch E, et al. Frequent deletions and down-regulation of micro- RNA genes miR15 and miR16 at 13q14 in chronic lymphocytic leukemia. Proc Natl Acad Sci U S A. 2002 Nov 26;99(24):15524-9.
50. Eis PS, Tam W, Sun L, Chadburn A, Li Z, Gomez MF, et al. Accumulation of miR-155 and BIC RNA in human B cell lymphomas. Proc Natl Acad Sci U S A. 2005 Mar 8;102(10):3627-32.
51. Liang Y, Nylander KD, Yan C, Schor NF. Role of caspase 3-dependent Bcl-2 cleavage in potentiation of apoptosis by Bcl-2. Mol Pharmacol. 2002 Jan;61(1):142-9.
52. Bellows DS, Chau BN, Lee P, Lazebnik Y, Burns WH, Hardwick JM. Antiapoptotic herpesvirus Bcl-2 homologs escape caspase-mediated conversion to proapoptotic proteins. J Virol. 2000 Jun;74(11):5024-31.
53. Cheng EH, Kirsch DG, Clem RJ, Ravi R, Kastan MB, Bedi A, et al. Conversion of Bcl-2 to a Bax-like death effector by caspases. Science. 1997 Dec 12;278(5345):1966-8.
54. Cory S, Adams JM. The Bcl2 family: regulators of the cellular life-or-death switch. Nat Rev Cancer. 2002 Sep;2(9):647-56.
55. Dai H, Pang YP, Ramirez-Alvarado M, Kaufmann SH. Evaluation of the BH3-only Protein Puma as a Direct Bak Activator. J Biol Chem. 2014 Jan;289(1):89-99.
56. Kuwana T, Bouchier-Hayes L, Chipuk JE, Bonzon C, Sullivan BA, Green DR, et al. BH3 domains of BH3-only proteins differentially regulate Bax-mediated mitochondrial membrane permeabilization both directly and indirectly. Mol Cell. 2005 Feb 18;17(4):525-35.
57. Youle RJ, Strasser A. The BCL-2 protein family: opposing activities that mediate cell death. Nat Rev Mol Cell Biol. 2008 Jan;9(1):47-59.
58. Villunger A, Michalak EM, Coultas L, Mullauer F, Bock G, Ausserlechner MJ, et al. p53- and drug-induced apoptotic responses mediated by BH3-only proteins puma and noxa. Science. 2003 Nov 7;302(5647):1036-8.
59. Puthalakath H, Strasser A. Keeping killers on a tight leash: transcriptional and post-translational control of the pro-apoptotic activity of BH3-only proteins. Cell Death Differ. 2002 May;9(5):505-12.
60. Puthalakath H, Huang DC, O'Reilly LA, King SM, Strasser A. The proapoptotic activity of the Bcl-2 family member Bim is regulated by interaction with the dynein motor complex. Mol Cell. 1999 Mar;3(3):287-96.
61. Egle A, Harris AW, Bouillet P, Cory S. Bim is a suppressor of Myc-induced mouse B cell leukemia. Proc Natl Acad Sci U S A. 2004 Apr;101(16):6164-9.
62. Ke F, Voss A, Kerr JB, O'Reilly LA, Tai L, Echeverry N, et al. BCL-2 family member BOK is widely expressed but its loss has only minimal impact in mice. Cell Death Differ. 2012 Jun;19(6):915-25.
63. Hunter JJ, Parslow TG. A peptide sequence from Bax that converts Bcl-2 into an activator of apoptosis. J Biol Chem. 1996 Apr;271(15):8521-4.
64. Gillies LA, Kuwana T. Apoptosis regulation at the mitochondrial outer membrane. J Cell Biochem. 2014 Apr;115(4):632-40.
65. Dewson G, Kluck RM. Mechanisms by which Bak and Bax permeabilise mitochondria during apoptosis. J Cell Sci. 2009 Aug 15;122(Pt 16):2801-8.
66. Dewson G, Kratina T, Sim HW, Puthalakath H, Adams JM, Colman PM, et al. To trigger apoptosis, Bak exposes its BH3 domain and homodimerizes via BH3:groove interactions. Mol Cell. 2008 May;30(3):369-80.
67. Kroemer G, Galluzzi L, Brenner C. Mitochondrial membrane permeabilization in cell death. Physiol Rev. 2007 Jan;87(1):99-163.

68. Korsmeyer SJ, Wei MC, Saito M, Weiler S, Oh KJ, Schlesinger PH. Pro-apoptotic cascade activates BID, which oligomerizes BAK or BAX into pores that result in the release of cytochrome c. Cell Death Differ. 2000 Dec;7(12):1166-73.
69. Antignani A, Youle RJ. How do Bax and Bak lead to permeabilization of the outer mitochondrial membrane? Curr Opin Cell Biol. 2006 Dec;18(6):685-9.
70. Czabotar PE, Westphal D, Dewson G, Ma S, Hockings C, Fairlie WD, et al. Bax crystal structures reveal how BH3 domains activate Bax and nucleate its oligomerization to induce apoptosis. Cell. 2013 Jan 31;152(3):519-31.
71. Gallenne T, Gautier F, Oliver L, Hervouet E, Noel B, Hickman JA, et al. Bax activation by the BH3-only protein Puma promotes cell dependence on antiapoptotic Bcl-2 family members. J Cell Biol. 2009 Apr 20;185(2):279-90.
72. Hsu YT, Wolter KG, Youle RJ. Cytosol-to-membrane redistribution of Bax and Bcl-X(L) during apoptosis. Proc Natl Acad Sci U S A. 1997 Apr 15;94(8):3668-72.
73. Kim H, Rafiuddin-Shah M, Tu HC, Jeffers JR, Zambetti GP, Hsieh JJ, et al. Hierarchical regulation of mitochondrion-dependent apoptosis by BCL-2 subfamilies. Nat Cell Biol. 2006 Dec;8(12):1348-58.
74. Willis SN, Fletcher JI, Kaufmann T, van Delft MF, Chen L, Czabotar PE, et al. Apoptosis initiated when BH3 ligands engage multiple Bcl-2 homologs, not Bax or Bak. Science. 2007 Feb;315(5813):856-9.
75. Du H, Wolf J, Schafer B, Moldoveanu T, Chipuk JE, Kuwana T. BH3 domains other than Bim and Bid can directly activate Bax/Bak. J Biol Chem. 2011 Jan;286(1):491-501.
76. Chipuk JE, Kuwana T, Bouchier-Hayes L, Droin NM, Newmeyer DD, Schuler M, et al. Direct activation of Bax by p53 mediates mitochondrial membrane permeabilization and apoptosis. Science. 2004 Feb;303(5660):1010-4.
77. Merino D, Giam M, Hughes PD, Siggs OM, Heger K, O'Reilly LA, et al. The role of BH3-only protein Bim extends beyond inhibiting Bcl-2-like prosurvival proteins. J Cell Biol. 2009 Aug 10;186(3):355-62.
78. Lessene G, Czabotar PE, Colman PM. BCL-2 family antagonists for cancer therapy. Nat Rev Drug Discov. 2008 Dec;7(12):989-1000.
79. Del Gaizo Moore V, Brown JR, Certo M, Love TM, Novina CD, Letai A. Chronic lymphocytic leukemia requires BCL2 to sequester prodeath BIM, explaining sensitivity to BCL2 antagonist ABT-737. J Clin Invest. 2007 Jan;117(1):112-21.
80. Henson ES, Gibson EM, Villanueva J, Bristow NA, Haney N, Gibson SB. Increased expression of Mcl-1 is responsible for the blockage of TRAIL-induced apoptosis mediated by EGF/ErbB1 signaling pathway. J Cell Biochem. 2003 Aug;89(6):1177-92.
81. Theodorakis P, Lomonosova E, Chinnadurai G. Critical requirement of BAX for manifestation of apoptosis induced by multiple stimuli in human epithelial cancer cells. Cancer Res. 2002 Jun;62(12):3373-6.
82. Gillissen B, Wendt J, Richter A, Richter A, Muer A, Overkamp T, et al. Endogenous Bak inhibitors Mcl-1 and Bcl-xL: differential impact on TRAIL resistance in Bax-deficient carcinoma. J Cell Biol. 2010 Mar 22;188(6):851-62.
83. Strasser A, Jost PJ, Nagata S. The many roles of FAS receptor signaling in the immune system. Immunity. 2009 Feb 20;30(2):180-92.
84. Flanagan AM, Letai A. BH3 domains define selective inhibitory interactions with BHRF-1 and KSHV BCL-2. Cell Death Differ. 2008 Mar;15(3):580-8.
85. Thomson BJ. Viruses and apoptosis. Int J Exp Pathol. 2001 Apr;82(2):65-76.
86. Han J, Sabbatini P, Perez D, Rao L, Modha D, White E. The E1B 19K protein blocks apoptosis by interacting with and inhibiting the p53-inducible and death-promoting Bax protein. Genes Dev. 1996 Feb 15;10(4):461-77.
87. Han J, Modha D, White E. Interaction of E1B 19K with Bax is required to block Bax-induced loss of mitochondrial membrane potential and apoptosis. Oncogene. 1998 Dec 10;17(23):2993-3005.

88. Cuconati A, White E. Viral homologs of BCL-2: role of apoptosis in the regulation of virus infection. Genes Dev. 2002 Oct 1;16(19):2465-78.
89. Galindo I, Hernaez B, Díaz-Gil G, Escribano JM, Alonso C. A179L, a viral Bcl-2 homologue, targets the core Bcl-2 apoptotic machinery and its upstream BH3 activators with selective binding restrictions for Bid and Noxa. Virology. 2008 Jun;375(2):561-72.
90. Goldmacher VS, Bartle LM, Skaletskaya A, Dionne CA, Kedersha NL, Vater CA, et al. A cytomegalovirus-encoded mitochondria-localized inhibitor of apoptosis structurally unrelated to Bcl-2. Proc Natl Acad Sci U S A. 1999 Oct 26;96(22):12536-41.
91. Arnoult D, Bartle LM, Skaletskaya A, Poncet D, Zamzami N, Park PU, et al. Cytomegalovirus cell death suppressor vMIA blocks Bax- but not Bak-mediated apoptosis by binding and sequestering Bax at mitochondria. Proc Natl Acad Sci U S A. 2004 May 25;101(21):7988-93.
92. Wang GH, Garvey TL, Cohen JI. The murine gammaherpesvirus-68 M11 protein inhibits Fas- and TNF-induced apoptosis. J Gen Virol. 1999 Oct;80 (Pt 10):2737-40.
93. Roy DJ, Ebrahimi BC, Dutia BM, Nash AA, Stewart JP. Murine gammaherpesvirus M11 gene product inhibits apoptosis and is expressed during virus persistence. Arch Virol. 2000;145(11):2411-20.
94. Virgin HW, Presti RM, Li XY, Liu C, Speck SH. Three distinct regions of the murine gammaherpesvirus 68 genome are transcriptionally active in latently infected mice. J Virol. 1999 Mar;73(3):2321-32.
95. Polster BM, Pevsner J, Hardwick JM. Viral Bcl-2 homologs and their role in virus replication and associated diseases. Biochim Biophys Acta. 2004 Mar 1;1644(2-3):211-27.
96. Marshall WL, Yim C, Gustafson E, Graf T, Sage DR, Hanify K, et al. Epstein-Barr virus encodes a novel homolog of the bcl-2 oncogene that inhibits apoptosis and associates with Bax and Bak. J Virol. 1999 Jun;73(6):5181-5.
97. Henderson S, Huen D, Rowe M, Dawson C, Johnson G, Rickinson A. Epstein-Barr virus-coded BHRF1 protein, a viral homologue of Bcl-2, protects human B cells from programmed cell death. Proc Natl Acad Sci U S A. 1993 Sep 15;90(18):8479-83.
98. Altmann M, Hammerschmidt W. Epstein-Barr virus provides a new paradigm: a requirement for the immediate inhibition of apoptosis. PLoS Biol. 2005 Dec;3(12):e404.
99. Greenspan JS, Greenspan D, Lennette ET, Abrams DI, Conant MA, Petersen V, et al. Replication of Epstein-Barr virus within the epithelial cells of oral "hairy" leukoplakia, an AIDS-associated lesion. N Engl J Med. 1985 Dec 19;313(25):1564-71.
100. Becker J, Leser U, Marschall M, Langford A, Jilg W, Gelderblom H, et al. Expression of proteins encoded by Epstein-Barr virus trans-activator genes depends on the differentiation of epithelial cells in oral hairy leukoplakia. Proc Natl Acad Sci U S A. 1991 Oct 1;88(19):8332-6.
101. Kelly GL, Long HM, Stylianou J, Thomas WA, Leese A, Bell AI, et al. An Epstein-Barr virus anti-apoptotic protein constitutively expressed in transformed cells and implicated in burkitt lymphomagenesis: the Wp/BHRF1 link. PLoS Pathog. 2009 Mar;5(3):e1000341.
102. Watanabe A, Maruo S, Ito T, Ito M, Katsumura KR, Takada K. Epstein-Barr virus-encoded Bcl-2 homologue functions as a survival factor in Wp-restricted Burkitt lymphoma cell line P3HR-1. J Virol. 2010 Mar;84(6):2893-901.
103. Boya P, Pauleau AL, Poncet D, Gonzalez-Polo RA, Zamzami N, Kroemer G. Viral proteins targeting mitochondria: controlling cell death. Biochim Biophys Acta. 2004 Dec 6;1659(2-3):178-89.
104. Kvansakul M, Wei AH, Fletcher JI, Willis SN, Chen L, Roberts AW, et al. Structural basis for apoptosis inhibition by Epstein-Barr virus BHRF1. PLoS Pathog. 2010;6(12):e1001236.
105. Hardwick JM, Bellows DS. Viral versus cellular BCL-2 proteins. Cell Death Differ. 2003 Jan;10 Suppl 1:S68-76.
106. McCarthy NJ, Hazlewood SA, Huen DS, Rickinson AB, Williams GT. The Epstein-Barr virus gene BHRF1, a homologue of the cellular oncogene Bcl-2, inhibits apoptosis induced by gamma radiation and chemotherapeutic drugs. Adv Exp Med Biol. 1996;406:83-97.

107. Kawanishi M, Tada-Oikawa S, Kawanishi S. Epstein-Barr virus BHRF1 functions downstream of Bid cleavage and upstream of mitochondrial dysfunction to inhibit TRAIL-induced apoptosis in BJAB cells. Biochem Biophys Res Commun. 2002 Sep 27;297(3):682-7.
108. Kawanishi M. Epstein-Barr virus BHRF1 protein protects intestine 407 epithelial cells from apoptosis induced by tumor necrosis factor alpha and anti-Fas antibody. J Virol. 1997 Apr;71(4):3319-22.
109. Desbien AL, Kappler JW, Marrack P. The Epstein-Barr virus Bcl-2 homolog, BHRF1, blocks apoptosis by binding to a limited amount of Bim. Proc Natl Acad Sci U S A. 2009 Apr 7;106(14):5663-8.
110. Yee J, White RE, Anderton E, Allday MJ. Latent Epstein-Barr virus can inhibit apoptosis in B cells by blocking the induction of NOXA expression. PLoS One. 2011 2011;6(12):e28506.
111. Lee M. HS. BALF0/1- JUST ANOTHER BRHF? 2010.
112. Cabras G, Decaussin G, Zeng Y, Djennaoui D, Melouli H, Broully P, et al. Epstein-Barr virus encoded BALF1 gene is transcribed in Burkitt's lymphoma cell lines and in nasopharyngeal carcinoma's biopsies. J Clin Virol. 2005 Sep;34(1):26-34.
113. Davison AJ, Eberle R, Ehlers B, Hayward GS, McGeoch DJ, Minson AC, et al. The order Herpesvirales. Arch Virol. 2009;154(1):171-7.
114. Burkitt D. A sarcoma involving the jaws in African children. Br J Surg. 1958 Nov;46(197):218-23.
115. Burkitt D. A children's cancer dependent on climatic factors. Nature. 1962 Apr 21;194:232-4.
116. Burkitt D. Determining the climatic limitations of a children's cancer common in Africa. Br Med J. 1962 Oct 20;2(5311):1019-23.
117. Epstein MA, Achong BG, Barr YM. Virus Particles in Cultured Lymphoblasts from Burkitt's Lymphoma. Lancet. 1964 Mar 28;1(7335):702-3.
118. Epstein MA, Henle G, Achong BG, Barr YM. Morphological and Biological Studies on a Virus in Cultured Lymphoblasts from Burkitt's Lymphoma. J Exp Med. 1965 May 1;121:761-70.
119. Henle G, Henle W. Immunofluorescence in cells derived from Burkitt's lymphoma. J Bacteriol. 1966 Mar;91(3):1248-56.
120. Henle G, Henle W, Diehl V. Relation of Burkitt's tumor-associated herpes-ytpe virus to infectious mononucleosis. Proc Natl Acad Sci U S A. 1968 Jan;59(1):94-101.
121. Henle W, Diehl V, Kohn G, Zur Hausen H, Henle G. Herpes-type virus and chromosome marker in normal leukocytes after growth with irradiated Burkitt cells. Science. 1967 Sep 1;157(3792):1064-5.
122. Miller G. The oncogenicity of Epstein-Barr virus. J Infect Dis. 1974 Aug;130(2):187-205.
123. Dambaugh T, Raab-Traub N, Heller M, Beisel C, Hummel M, Cheung A, et al. Variations among isolates of Epstein-Barr virus. Ann N Y Acad Sci. 1980;354:309-25.
124. Baer R, Bankier AT, Biggin MD, Deininger PL, Farrell PJ, Gibson TJ, et al. DNA sequence and expression of the B95-8 Epstein-Barr virus genome. Nature. 1984 Jul 19-25;310(5974):207-11.
125. Kalla M, Hammerschmidt W. Human B cells on their route to latent infection - Early but transient expression of lytic genes of Epstein-Barr virus. Eur J Cell Biol. 2012 Mar 28.
126. Fingeroth JD, Weis JJ, Tedder TF, Strominger JL, Biro PA, Fearon DT. Epstein-Barr virus receptor of human B lymphocytes is the C3d receptor CR2. Proc Natl Acad Sci U S A. 1984 Jul;81(14):4510-4.
127. Nemerow GR, Wolfert R, McNaughton ME, Cooper NR. Identification and characterization of the Epstein-Barr virus receptor on human B lymphocytes and its relationship to the C3d complement receptor (CR2). J Virol. 1985 Aug;55(2):347-51.
128. Jondal M, Klein G, Oldstone MB, Bokish V, Yefenof E. Surface markers on human B and T lymphocytes. VIII. Association between complement and Epstein-Barr virus receptors on human lymphoid cells. Scand J Immunol. 1976;5(4):401-10.
129. Nemerow GR, Mullen JJ, 3rd, Dickson PW, Cooper NR. Soluble recombinant CR2 (CD21) inhibits Epstein-Barr virus infection. J Virol. 1990 Mar;64(3):1348-52.
130. Tanner J, Weis J, Fearon D, Whang Y, Kieff E. Epstein-Barr virus gp350/220 binding to the B lymphocyte C3d receptor mediates adsorption, capping, and endocytosis. Cell. 1987 Jul 17;50(2):203-13.

131. Henle G, Henle W. Epstein-Barr virus-specific IgA serum antibodies as an outstanding feature of nasopharyngeal carcinoma. Int J Cancer. 1976 Jan 15;17(1):1-7.
132. Tao Q, Ho FC, Loke SL, Srivastava G. Epstein-Barr virus is localized in the tumour cells of nasal lymphomas of NK, T or B cell type. Int J Cancer. 1995 Jan 27;60(3):315-20.
133. Harabuchi Y, Yamanaka N, Kataura A, Imai S, Kinoshita T, Mizuno F, et al. Epstein-Barr virus in nasal T-cell lymphomas in patients with lethal midline granuloma. Lancet. 1990 Jan 20;335(8682):128-30.
134. Anagnostopoulos I, Hummel M, Kreschel C, Stein H. Morphology, immunophenotype, and distribution of latently and/or productively Epstein-Barr virus-infected cells in acute infectious mononucleosis: implications for the interindividual infection route of Epstein-Barr virus. Blood. 1995 Feb 1;85(3):744-50.
135. Karajannis MA, Hummel M, Anagnostopoulos I, Stein H. Strict lymphotropism of Epstein-Barr virus during acute infectious mononucleosis in nonimmunocompromised individuals. Blood. 1997 Apr 15;89(8):2856-62.
136. Tao Q, Srivastava G, Chan AC, Chung LP, Loke SL, Ho FC. Evidence for lytic infection by Epstein-Barr virus in mucosal lymphocytes instead of nasopharyngeal epithelial cells in normal individuals. J Med Virol. 1995 Jan;45(1):71-7.
137. Laichalk LL, Thorley-Lawson DA. Terminal differentiation into plasma cells initiates the replicative cycle of Epstein-Barr virus in vivo. J Virol. 2005 Jan;79(2):1296-307.
138. Gerber P, Lucas S, Nonoyama M, Perlin E, Goldstein LI. Oral excretion of Epstein-Barr virus by healthy subjects and patients with infectious mononucleosis. Lancet. 1972 Nov 11;2(7785):988-9.
139. Countryman J, Miller G. Activation of expression of latent Epstein-Barr herpesvirus after gene transfer with a small cloned subfragment of heterogeneous viral DNA. Proc Natl Acad Sci U S A. 1985 Jun;82(12):4085-9.
140. Takada K, Shimizu N, Sakuma S, Ono Y. trans activation of the latent Epstein-Barr virus (EBV) genome after transfection of the EBV DNA fragment. J Virol. 1986 Mar;57(3):1016-22.
141. Cho MS, Tran VM. A concatenated form of Epstein-Barr viral DNA in lymphoblastoid cell lines induced by transfection with BZLF1. Virology. 1993 Jun;194(2):838-42.
142. Lu CC, Jeng YY, Tsai CH, Liu MY, Yeh SW, Hsu TY, et al. Genome-wide transcription program and expression of the Rta responsive gene of Epstein-Barr virus. Virology. 2006 Feb 20;345(2):358-72.
143. Yuan J, Cahir-McFarland E, Zhao B, Kieff E. Virus and cell RNAs expressed during Epstein-Barr virus replication. J Virol. 2006 Mar;80(5):2548-65.
144. Sample J, Hummel M, Braun D, Birkenbach M, Kieff E. Nucleotide sequences of mRNAs encoding Epstein-Barr virus nuclear proteins: a probable transcriptional initiation site. Proc Natl Acad Sci U S A. 1986 Jul;83(14):5096-100.
145. Speck SH, Pfitzner A, Strominger JL. An Epstein-Barr virus transcript from a latently infected, growth-transformed B-cell line encodes a highly repetitive polypeptide. Proc Natl Acad Sci U S A. 1986 Dec;83(24):9298-302.
146. Bodescot M, Perricaudet M. Epstein-Barr virus mRNAs produced by alternative splicing. Nucleic Acids Res. 1986 Sep 11;14(17):7103-14.
147. Woisetschlaeger M, Yandava CN, Furmanski LA, Strominger JL, Speck SH. Promoter switching in Epstein-Barr virus during the initial stages of infection of B lymphocytes. Proc Natl Acad Sci U S A. 1990 Mar;87(5):1725-9.
148. Rowe M, Lear AL, Croom-Carter D, Davies AH, Rickinson AB. Three pathways of Epstein-Barr virus gene activation from EBNA1-positive latency in B lymphocytes. J Virol. 1992 Jan;66(1):122-31.
149. Pfeffer S, Zavolan M, Grasser FA, Chien M, Russo JJ, Ju J, et al. Identification of virus-encoded microRNAs. Science. 2004 Apr 30;304(5671):734-6.
150. Gromminger S, Mautner J, Bornkamm GW. Burkitt lymphoma: the role of Epstein-Barr virus revisited. Br J Haematol. 2012 Mar;156(6):719-29.

151. Babcock GJ, Decker LL, Volk M, Thorley-Lawson DA. EBV persistence in memory B cells in vivo. Immunity. 1998 Sep;9(3):395-404.
152. Thorley-Lawson DA, Gross A. Persistence of the Epstein-Barr virus and the origins of associated lymphomas. N Engl J Med. 2004 Mar 25;350(13):1328-37.
153. Qiu J, Cosmopoulos K, Pegtel M, Hopmans E, Murray P, Middeldorp J, et al. A novel persistence associated EBV miRNA expression profile is disrupted in neoplasia. PLoS Pathog. 2011 Aug;7(8):e1002193.
154. Rickinson A. Feilds Virology. Philadelphia: Lippincott Williams and Wilkins; 2001.
155. Shannon-Lowe C, Adland E, Bell AI, Delecluse HJ, Rickinson AB, Rowe M. Features distinguishing Epstein-Barr virus infections of epithelial cells and B cells: viral genome expression, genome maintenance, and genome amplification. J Virol. 2009 Aug;83(15):7749-60.
156. Pope JH, Horne MK, Scott W. Transformation of foetal human keukocytes in vitro by filtrates of a human leukaemic cell line containing herpes-like virus. Int J Cancer. 1968 Nov 15;3(6):857-66.
157. Tierney RJ, Steven N, Young LS, Rickinson AB. Epstein-Barr virus latency in blood mononuclear cells: analysis of viral gene transcription during primary infection and in the carrier state. J Virol. 1994 Nov;68(11):7374-85.
158. Khanna R, Burrows SR. Role of cytotoxic T lymphocytes in Epstein-Barr virus-associated diseases. Annu Rev Microbiol. 2000;54:19-48.
159. Liebowitz D. Epstein-Barr virus and a cellular signaling pathway in lymphomas from immunosuppressed patients. N Engl J Med. 1998 May 14;338(20):1413-21.
160. Thomas JA, Hotchin NA, Allday MJ, Amlot P, Rose M, Yacoub M, et al. Immunohistology of Epstein-Barr virus-associated antigens in B cell disorders from immunocompromised individuals. Transplantation. 1990 May;49(5):944-53.
161. Young L, Alfieri C, Hennessy K, Evans H, O'Hara C, Anderson KC, et al. Expression of Epstein-Barr virus transformation-associated genes in tissues of patients with EBV lymphoproliferative disease. N Engl J Med. 1989 Oct 19;321(16):1080-5.
162. Gaidano G, Carbone A, Dalla-Favera R. Pathogenesis of AIDS-related lymphomas: molecular and histogenetic heterogeneity. Am J Pathol. 1998 Mar;152(3):623-30.
163. Delecluse HJ, Hummel M, Marafioti T, Anagnostopoulos I, Stein H. Common and HIV-related diffuse large B-cell lymphomas differ in their immunoglobulin gene mutation pattern. J Pathol. 1999 Jun;188(2):133-8.
164. Hamilton-Dutoit SJ, Rea D, Raphael M, Sandvej K, Delecluse HJ, Gisselbrecht C, et al. Epstein-Barr virus-latent gene expression and tumor cell phenotype in acquired immunodeficiency syndrome-related non-Hodgkin's lymphoma. Correlation of lymphoma phenotype with three distinct patterns of viral latency. Am J Pathol. 1993 Oct;143(4):1072-85.
165. Hamilton-Dutoit SJ, Pallesen G, Franzmann MB, Karkov J, Black F, Skinhoj P, et al. AIDS-related lymphoma. Histopathology, immunophenotype, and association with Epstein-Barr virus as demonstrated by in situ nucleic acid hybridization. Am J Pathol. 1991 Jan;138(1):149-63.
166. Kersten MJ, Klein MR, Holwerda AM, Miedema F, van Oers MH. Epstein-Barr virus-specific cytotoxic T cell responses in HIV-1 infection: different kinetics in patients progressing to opportunistic infection or non-Hodgkin's lymphoma. J Clin Invest. 1997 Apr 1;99(7):1525-33.
167. Schaefer BC, Strominger JL, Speck SH. Redefining the Epstein-Barr virus-encoded nuclear antigen EBNA-1 gene promoter and transcription initiation site in group I Burkitt lymphoma cell lines. Proc Natl Acad Sci U S A. 1995 Nov 7;92(23):10565-9.
168. Brooks L, Yao QY, Rickinson AB, Young LS. Epstein-Barr virus latent gene transcription in nasopharyngeal carcinoma cells: coexpression of EBNA1, LMP1, and LMP2 transcripts. J Virol. 1992 May;66(5):2689-97.
169. Brooks LA, Lear AL, Young LS, Rickinson AB. Transcripts from the Epstein-Barr virus BamHI A fragment are detectable in all three forms of virus latency. J Virol. 1993 Jun;67(6):3182-90.
170. Kerr BM, Lear AL, Rowe M, Croom-Carter D, Young LS, Rookes SM, et al. Three transcriptionally distinct forms of Epstein-Barr virus latency in somatic cell hybrids: cell phenotype dependence of virus promoter usage. Virology. 1992 Mar;187(1):189-201.

171. Deacon EM, Pallesen G, Niedobitek G, Crocker J, Brooks L, Rickinson AB, et al. Epstein-Barr virus and Hodgkin's disease: transcriptional analysis of virus latency in the malignant cells. J Exp Med. 1993 Feb 1;177(2):339-49.
172. Fahraeus R, Fu HL, Ernberg I, Finke J, Rowe M, Klein G, et al. Expression of Epstein-Barr virus-encoded proteins in nasopharyngeal carcinoma. Int J Cancer. 1988 Sep 15;42(3):329-38.
173. Young LS, Dawson CW, Clark D, Rupani H, Busson P, Tursz T, et al. Epstein-Barr virus gene expression in nasopharyngeal carcinoma. J Gen Virol. 1988 May;69 (Pt 5):1051-65.
174. Pallesen G, Hamilton-Dutoit SJ, Rowe M, Young LS. Expression of Epstein-Barr virus latent gene products in tumour cells of Hodgkin's disease. Lancet. 1991 Feb 9;337(8737):320-2.
175. Roughan JE, Thorley-Lawson DA. The intersection of Epstein-Barr virus with the germinal center. J Virol. 2009 Apr;83(8):3968-76.
176. Rowe M, Kelly GL, Bell AI, Rickinson AB. Burkitt's lymphoma: The Rosetta Stone deciphering Epstein-Barr virus biology. Semin Cancer Biol. 2009 Jul 18.
177. Hochberg D, Middeldorp JM, Catalina M, Sullivan JL, Luzuriaga K, Thorley-Lawson DA. Demonstration of the Burkitt's lymphoma Epstein-Barr virus phenotype in dividing latently infected memory cells in vivo. Proc Natl Acad Sci U S A. 2004 Jan 6;101(1):239-44.
178. Kelly G, Bell A, Rickinson A. Epstein-Barr virus-associated Burkitt lymphomagenesis selects for downregulation of the nuclear antigen EBNA2. Nat Med. 2002 Oct;8(10):1098-104.
179. Kelly GL, Milner AE, Tierney RJ, Croom-Carter DS, Altmann M, Hammerschmidt W, et al. Epstein-Barr virus nuclear antigen 2 (EBNA2) gene deletion is consistently linked with EBNA3A, -3B, and -3C expression in Burkitt's lymphoma cells and with increased resistance to apoptosis. J Virol. 2005 Aug;79(16):10709-17.
180. Joncas J, Boucher J, Granger-Julien M, Filion C. Epstein-Barr virus infection in the neonatal period and in childhood. Can Med Assoc J. 1974 Jan 5;110(1):33-7.
181. Niederman JC, McCollum RW, Henle G, Henle W. Infectious mononucleosis. Clinical manifestations in relation to EB virus antibodies. JAMA. 1968 Jan 15;203(3):205-9.
182. Hoagland RJ. The transmission of infectious mononucleosis. Am J Med Sci. 1955 Mar;229(3):262-72.
183. Shannon-Lowe C, Rowe M. Epstein-Barr virus infection of polarized epithelial cells via the basolateral surface by memory B cell-mediated transfer infection. PLoS Pathog. 2011 May;7(5):e1001338.
184. Pegtel DM, Middeldorp J, Thorley-Lawson DA. Epstein-Barr virus infection in ex vivo tonsil epithelial cell cultures of asymptomatic carriers. J Virol. 2004 Nov;78(22):12613-24.
185. Hadinoto V, Shapiro M, Sun CC, Thorley-Lawson DA. The dynamics of EBV shedding implicate a central role for epithelial cells in amplifying viral output. PLoS Pathog. 2009 Jul;5(7):e1000496.
186. Faulkner GC, Burrows SR, Khanna R, Moss DJ, Bird AG, Crawford DH. X-Linked agammaglobulinemia patients are not infected with Epstein-Barr virus: implications for the biology of the virus. J Virol. 1999 Feb;73(2):1555-64.
187. Frangou P, Buettner M, Niedobitek G. Epstein-Barr virus (EBV) infection in epithelial cells in vivo: rare detection of EBV replication in tongue mucosa but not in salivary glands. J Infect Dis. 2005 Jan 15;191(2):238-42.
188. Callan MF, Annels N, Steven N, Tan L, Wilson J, McMichael AJ, et al. T cell selection during the evolution of CD8+ T cell memory in vivo. Eur J Immunol. 1998 Dec;28(12):4382-90.
189. Sheldon PJ, Hemsted EH, Papamichail M, Holborow EJ. Thymic origin of atypical lymphoid cells in infectious mononucleosis. Lancet. 1973 May 26;1(7813):1153-5.
190. Tosato G, Steinberg AD, Yarchoan R, Heilman CA, Pike SE, De Seau V, et al. Abnormally elevated frequency of Epstein-Barr virus-infected B cells in the blood of patients with rheumatoid arthritis. J Clin Invest. 1984 Jun;73(6):1789-95.
191. Rocchi G, Felici A, Ragona G, Heinz A. Quantitative evaluation of Epstein-Barr-virus-infected mononuclear peripheral blood leukocytes in infectious mononucleosis. N Engl J Med. 1977 Jan 20;296(3):132-4.

192. Svedmyr E, Ernberg I, Seeley J, Weiland O, Masucci G, Tsukuda K, et al. Virologic, immunologic, and clinical observations on a patient during the incubation, acute, and convalescent phases of infectious mononucleosis. Clin Immunol Immunopathol. 1984 Mar;30(3):437-50.
193. Wagner HJ, Bein G, Bitsch A, Kirchner H. Detection and quantification of latently infected B lymphocytes in Epstein-Barr virus-seropositive, healthy individuals by polymerase chain reaction. J Clin Microbiol. 1992 Nov;30(11):2826-9.
194. Thorley-Lawson DA, Mann KP. Early events in Epstein-Barr virus infection provide a model for B cell activation. J Exp Med. 1985 Jul 1;162(1):45-59.
195. Niedobitek G, Kremmer E, Herbst H, Whitehead L, Dawson CW, Niedobitek E, et al. Immunohistochemical detection of the Epstein-Barr virus-encoded latent membrane protein 2A in Hodgkin's disease and infectious mononucleosis. Blood. 1997 Aug 15;90(4):1664-72.
196. Kurth J, Hansmann ML, Rajewsky K, Kuppers R. Epstein-Barr virus-infected B cells expanding in germinal centers of infectious mononucleosis patients do not participate in the germinal center reaction. Proc Natl Acad Sci U S A. 2003 Apr 15;100(8):4730-5.
197. Kurth J, Spieker T, Wustrow J, Strickler GJ, Hansmann LM, Rajewsky K, et al. EBV-infected B cells in infectious mononucleosis: viral strategies for spreading in the B cell compartment and establishing latency. Immunity. 2000 Oct;13(4):485-95.
198. Kempkes B, Spitkovsky D, Jansen-Durr P, Ellwart JW, Kremmer E, Delecluse HJ, et al. B-cell proliferation and induction of early G1-regulating proteins by Epstein-Barr virus mutants conditional for EBNA2. Embo J. 1995 Jan 3;14(1):88-96.
199. Casola S, Otipoby KL, Alimzhanov M, Humme S, Uyttersprot N, Kutok JL, et al. B cell receptor signal strength determines B cell fate. Nat Immunol. 2004 Mar;5(3):317-27.
200. Njie R, Bell AI, Jia H, Croom-Carter D, Chaganti S, Hislop AD, et al. The effects of acute malaria on Epstein-Barr virus (EBV) load and EBV-specific T cell immunity in Gambian children. J Infect Dis. 2009 Jan 1;199(1):31-8.
201. Scheeren FA, Nagasawa M, Weijer K, Cupedo T, Kirberg J, Legrand N, et al. T cell-independent development and induction of somatic hypermutation in human IgM+ IgD+ CD27+ B cells. J Exp Med. 2008 Sep 1;205(9):2033-42.
202. Chaganti S, Heath EM, Bergler W, Kuo M, Buettner M, Niedobitek G, et al. Epstein-Barr virus colonization of tonsillar and peripheral blood B-cell subsets in primary infection and persistence. Blood. 2009 Jun 18;113(25):6372-81.
203. Crawford DH, Ando I. EB virus induction is associated with B-cell maturation. Immunology. 1986 Nov;59(3):405-9.
204. Bhende PM, Seaman WT, Delecluse HJ, Kenney SC. The EBV lytic switch protein, Z, preferentially binds to and activates the methylated viral genome. Nat Genet. 2004 Oct;36(10):1099-104.
205. Kalla M, Schmeinck A, Bergbauer M, Pich D, Hammerschmidt W. AP-1 homolog BZLF1 of Epstein-Barr virus has two essential functions dependent on the epigenetic state of the viral genome. Proc Natl Acad Sci U S A. 2010 Jan 12;107(2):850-5.
206. Zuo J, Thomas WA, Haigh TA, Fitzsimmons L, Long HM, Hislop AD, et al. Epstein-Barr virus evades CD4+ T cell responses in lytic cycle through BZLF1-mediated downregulation of CD74 and the cooperation of vBcl-2. PLoS Pathog. 2011 Dec;7(12):e1002455.
207. Lantner F, Starlets D, Gore Y, Flaishon L, Yamit-Hezi A, Dikstein R, et al. CD74 induces TAp63 expression leading to B-cell survival. Blood. 2007 Dec;110(13):4303-11.
208. Strockbine LD, Cohen JI, Farrah T, Lyman SD, Wagener F, DuBose RF, et al. The Epstein-Barr virus BARF1 gene encodes a novel, soluble colony-stimulating factor-1 receptor. J Virol. 1998 May;72(5):4015-21.
209. Sall A, Caserta S, Jolicoeur P, Franqueville L, de Turenne-Tessier M, Ooka T. Mitogenic activity of Epstein-Barr virus-encoded BARF1 protein. Oncogene. 2004 Jun 17;23(28):4938-44.
210. Wang Q, Tsao SW, Ooka T, Nicholls JM, Cheung HW, Fu S, et al. Anti-apoptotic role of BARF1 in gastric cancer cells. Cancer Lett. 2006 Jul 8;238(1):90-103.

211. Sheng W, Decaussin G, Ligout A, Takada K, Ooka T. Malignant transformation of Epstein-Barr virus-negative Akata cells by introduction of the BARF1 gene carried by Epstein-Barr virus. J Virol. 2003 Mar;77(6):3859-65.
212. Fu Q, He C, Mao ZR. Epstein-Barr virus interactions with the Bcl-2 protein family and apoptosis in human tumor cells. J Zhejiang Univ Sci B. 2013 Jan;14(1):8-24.
213. McCann EM, Kelly GL, Rickinson AB, Bell AI. Genetic analysis of the Epstein-Barr virus-coded leader protein EBNA-LP as a co-activator of EBNA2 function. J Gen Virol. 2001 Dec;82(Pt 12):3067-79.
214. Alfieri C, Birkenbach M, Kieff E. Early events in Epstein-Barr virus infection of human B lymphocytes. Virology. 1991 Apr;181(2):595-608.
215. Allday MJ, Crawford DH, Griffin BE. Epstein-Barr virus latent gene expression during the initiation of B cell immortalization. J Gen Virol. 1989 Jul;70 (Pt 7):1755-64.
216. Young LS, Murray PG. Epstein-Barr virus and oncogenesis: from latent genes to tumours. Oncogene. 2003 Aug 11;22(33):5108-21.
217. Altmann M, Pich D, Ruiss R, Wang J, Sugden B, Hammerschmidt W. Transcriptional activation by EBV nuclear antigen 1 is essential for the expression of EBV's transforming genes. Proc Natl Acad Sci U S A. 2006 Sep 19;103(38):14188-93.
218. Elliott J, Goodhew EB, Krug LT, Shakhnovsky N, Yoo L, Speck SH. Variable methylation of the Epstein-Barr virus Wp EBNA gene promoter in B-lymphoblastoid cell lines. J Virol. 2004 Dec;78(24):14062-5.
219. Woisetschlaeger M, Jin XW, Yandava CN, Furmanski LA, Strominger JL, Speck SH. Role for the Epstein-Barr virus nuclear antigen 2 in viral promoter switching during initial stages of infection. Proc Natl Acad Sci U S A. 1991 May 1;88(9):3942-6.
220. Grossman SR, Johannsen E, Tong X, Yalamanchili R, Kieff E. The Epstein-Barr virus nuclear antigen 2 transactivator is directed to response elements by the J kappa recombination signal binding protein. Proc Natl Acad Sci U S A. 1994 Aug 2;91(16):7568-72.
221. Hsieh JJ, Henkel T, Salmon P, Robey E, Peterson MG, Hayward SD. Truncated mammalian Notch1 activates CBF1/RBPJk-repressed genes by a mechanism resembling that of Epstein-Barr virus EBNA2. Mol Cell Biol. 1996 Mar;16(3):952-9.
222. Pegman PM, Smith SM, D'Souza BN, Loughran ST, Maier S, Kempkes B, et al. Epstein-Barr virus nuclear antigen 2 trans-activates the cellular antiapoptotic bfl-1 gene by a CBF1/RBPJ kappa-dependent pathway. J Virol. 2006 Aug;80(16):8133-44.
223. Cordier M, Calender A, Billaud M, Zimber U, Rousselet G, Pavlish O, et al. Stable transfection of Epstein-Barr virus (EBV) nuclear antigen 2 in lymphoma cells containing the EBV P3HR1 genome induces expression of B-cell activation molecules CD21 and CD23. J Virol. 1990 Mar;64(3):1002-13.
224. Kaiser C, Laux G, Eick D, Jochner N, Bornkamm GW, Kempkes B. The proto-oncogene c-myc is a direct target gene of Epstein-Barr virus nuclear antigen 2. J Virol. 1999 May;73(5):4481-4.
225. Yenamandra SP, Sompallae R, Klein G, Kashuba E. Comparative analysis of the Epstein-Barr virus encoded nuclear proteins of EBNA-3 family. Comput Biol Med. 2009 Nov;39(11):1036-42.
226. Marshall D, Sample C. Epstein-Barr virus nuclear antigen 3C is a transcriptional regulator. J Virol. 1995 Jun;69(6):3624-30.
227. Zhao B, Marshall DR, Sample CE. A conserved domain of the Epstein-Barr virus nuclear antigens 3A and 3C binds to a discrete domain of Jkappa. J Virol. 1996 Jul;70(7):4228-36.
228. Cooper A, Johannsen E, Maruo S, Cahir-McFarland E, Illanes D, Davidson D, et al. EBNA3A association with RBP-Jkappa down-regulates c-myc and Epstein-Barr virus-transformed lymphoblast growth. J Virol. 2003 Jan;77(2):999-1010.
229. Krauer KG, Burgess A, Buck M, Flanagan J, Sculley TB, Gabrielli B. The EBNA-3 gene family proteins disrupt the G2/M checkpoint. Oncogene. 2004 Feb 19;23(7):1342-53.
230. Anderton E, Yee J, Smith P, Crook T, White RE, Allday MJ. Two Epstein-Barr virus (EBV) oncoproteins cooperate to repress expression of the proapoptotic tumour-suppressor Bim: clues to the pathogenesis of Burkitt's lymphoma. Oncogene. 2008 Jan;27(4):421-33.

231. Paschos K, Smith P, Anderton E, Middeldorp JM, White RE, Allday MJ. Epstein-barr virus latency in B cells leads to epigenetic repression and CpG methylation of the tumour suppressor gene Bim. PLoS Pathog. 2009 Jun;5(6):e1000492.
232. Silins SL, Sculley TB. Burkitt's lymphoma cells are resistant to programmed cell death in the presence of the Epstein-Barr virus latent antigen EBNA-4. Int J Cancer. 1995 Jan;60(1):65-72.
233. Wang F, Tsang SF, Kurilla MG, Cohen JI, Kieff E. Epstein-Barr virus nuclear antigen 2 transactivates latent membrane protein LMP1. J Virol. 1990 Jul;64(7):3407-16.
234. Sadler RH, Raab-Traub N. The Epstein-Barr virus 3.5-kilobase latent membrane protein 1 mRNA initiates from a TATA-Less promoter within the first terminal repeat. J Virol. 1995 Jul;69(7):4577-81.
235. Fennewald S, van Santen V, Kieff E. Nucleotide sequence of an mRNA transcribed in latent growth-transforming virus infection indicates that it may encode a membrane protein. J Virol. 1984 Aug;51(2):411-9.
236. Lee DY, Sugden B. The latent membrane protein 1 oncogene modifies B-cell physiology by regulating autophagy. Oncogene. 2008 May 1;27(20):2833-42.
237. Huen DS, Henderson SA, Croom-Carter D, Rowe M. The Epstein-Barr virus latent membrane protein-1 (LMP1) mediates activation of NF-kappa B and cell surface phenotype via two effector regions in its carboxy-terminal cytoplasmic domain. Oncogene. 1995 Feb 2;10(3):549-60.
238. Zheng H, Li LL, Hu DS, Deng XY, Cao Y. Role of Epstein-Barr virus encoded latent membrane protein 1 in the carcinogenesis of nasopharyngeal carcinoma. Cell Mol Immunol. 2007 Jun;4(3):185-96.
239. Morris MA, Dawson CW, Young LS. Role of the Epstein-Barr virus-encoded latent membrane protein-1, LMP1, in the pathogenesis of nasopharyngeal carcinoma. Future Oncol. 2009 Aug;5(6):811-25.
240. Wang S, Rowe M, Lundgren E. Expression of the Epstein Barr virus transforming protein LMP1 causes a rapid and transient stimulation of the Bcl-2 homologue Mcl-1 levels in B-cell lines. Cancer Res. 1996 Oct;56(20):4610-3.
241. Henderson S, Rowe M, Gregory C, Croom-Carter D, Wang F, Longnecker R, et al. Induction of bcl-2 expression by Epstein-Barr virus latent membrane protein 1 protects infected B cells from programmed cell death. Cell. 1991 Jun 28;65(7):1107-15.
242. Rowe M, Peng-Pilon M, Huen DS, Hardy R, Croom-Carter D, Lundgren E, et al. Upregulation of bcl-2 by the Epstein-Barr virus latent membrane protein LMP1: a B-cell-specific response that is delayed relative to NF-kappa B activation and to induction of cell surface markers. J Virol. 1994 Sep;68(9):5602-12.
243. Lee DY, Sugden B. The LMP1 oncogene of EBV activates PERK and the unfolded protein response to drive its own synthesis. Blood. 2008 Feb 15;111(4):2280-9.
244. Pratt ZL, Zhang J, Sugden B. The latent membrane protein 1 (LMP1) oncogene of Epstein-Barr virus can simultaneously induce and inhibit apoptosis in B cells. J Virol. 2012 Apr;86(8):4380-93.
245. D'Souza BN, Edelstein LC, Pegman PM, Smith SM, Loughran ST, Clarke A, et al. Nuclear factor kappa B-dependent activation of the antiapoptotic bfl-1 gene by the Epstein-Barr virus latent membrane protein 1 and activated CD40 receptor. J Virol. 2004 Feb;78(4):1800-16.
246. Miller CL, Burkhardt AL, Lee JH, Stealey B, Longnecker R, Bolen JB, et al. Integral membrane protein 2 of Epstein-Barr virus regulates reactivation from latency through dominant negative effects on protein-tyrosine kinases. Immunity. 1995 Feb;2(2):155-66.
247. Longnecker R. Epstein-Barr virus latency: LMP2, a regulator or means for Epstein-Barr virus persistence? Adv Cancer Res. 2000;79:175-200.
248. Portis T, Dyck P, Longnecker R. Epstein-Barr Virus (EBV) LMP2A induces alterations in gene transcription similar to those observed in Reed-Sternberg cells of Hodgkin lymphoma. Blood. 2003 Dec 1;102(12):4166-78.

249. Hino R, Uozaki H, Inoue Y, Shintani Y, Ushiku T, Sakatani T, et al. Survival advantage of EBV-associated gastric carcinoma: survivin up-regulation by viral latent membrane protein 2A. Cancer Res. 2008 Mar 1;68(5):1427-35.
250. Portis T, Longnecker R. Epstein-Barr virus (EBV) LMP2A mediates B-lymphocyte survival through constitutive activation of the Ras/PI3K/Akt pathway. Oncogene. 2004 Nov;23(53):8619-28.
251. Bultema R, Longnecker R, Swanson-Mungerson M. Epstein-Barr virus LMP2A accelerates MYC-induced lymphomagenesis. Oncogene. 2009 Mar 19;28(11):1471-6.
252. Rechsteiner MP, Berger C, Zauner L, Sigrist JA, Weber M, Longnecker R, et al. Latent membrane protein 2B regulates susceptibility to induction of lytic Epstein-Barr virus infection. J Virol. 2008 Feb;82(4):1739-47.
253. Schaadt E, Baier B, Mautner J, Bornkamm GW, Adler B. Epstein-Barr virus latent membrane protein 2A mimics B-cell receptor-dependent virus reactivation. J Gen Virol. 2005 Mar;86(Pt 3):551-9.
254. Rovedo M, Longnecker R. Epstein-barr virus latent membrane protein 2B (LMP2B) modulates LMP2A activity. J Virol. 2007 Jan;81(1):84-94.
255. Robertson HD, Mathews MB. The regulation of the protein kinase PKR by RNA. Biochimie. 1996;78(11-12):909-14.
256. Komano J, Sugiura M, Takada K. Epstein-Barr virus contributes to the malignant phenotype and to apoptosis resistance in Burkitt's lymphoma cell line Akata. J Virol. 1998 Nov;72(11):9150-6.
257. Wong HL, Wang X, Chang RC, Jin DY, Feng H, Wang Q, et al. Stable expression of EBERs in immortalized nasopharyngeal epithelial cells confers resistance to apoptotic stress. Mol Carcinog. 2005 Oct;44(2):92-101.
258. Yamamoto N, Takizawa T, Iwanaga Y, Shimizu N. Malignant transformation of B lymphoma cell line BJAB by Epstein-Barr virus-encoded small RNAs. FEBS Lett. 2000 Nov 3;484(2):153-8.
259. Swaminathan S, Huneycutt BS, Reiss CS, Kieff E. Epstein-Barr virus-encoded small RNAs (EBERs) do not modulate interferon effects in infected lymphocytes. J Virol. 1992 Aug;66(8):5133-6.
260. Barth S, Pfuhl T, Mamiani A, Ehses C, Roemer K, Kremmer E, et al. Epstein-Barr virus-encoded microRNA miR-BART2 down-regulates the viral DNA polymerase BALF5. Nucleic Acids Res. 2008 Feb;36(2):666-75.
261. Lo AK, To KF, Lo KW, Lung RW, Hui JW, Liao G, et al. Modulation of LMP1 protein expression by EBV-encoded microRNAs. Proc Natl Acad Sci U S A. 2007 Oct 9;104(41):16164-9.
262. Choy EY, Siu KL, Kok KH, Lung RW, Tsang CM, To KF, et al. An Epstein-Barr virus-encoded microRNA targets PUMA to promote host cell survival. J Exp Med. 2008 Oct;205(11):2551-60.
263. Swaminathan S. Noncoding RNAs produced by oncogenic human herpesviruses. J Cell Physiol. 2008 Aug;216(2):321-6.
264. Marquitz AR, Mathur A, Nam CS, Raab-Traub N. The Epstein-Barr Virus BART microRNAs target the pro-apoptotic protein Bim. Virology. 2011 Apr;412(2):392-400.
265. Hutchings IA, Tierney RJ, Kelly GL, Stylianou J, Rickinson AB, Bell AI. Methylation status of the Epstein-Barr virus (EBV) BamHI W latent cycle promoter and promoter activity: analysis with novel EBV-positive Burkitt and lymphoblastoid cell lines. J Virol. 2006 Nov;80(21):10700-11.
266. Levine PH, Kamaraju LS, Connelly RR, Berard CW, Dorfman RF, Magrath I, et al. The American Burkitt's Lymphoma Registry: eight years' experience. Cancer. 1982 Mar 1;49(5):1016-22.
267. Magrath I. The pathogenesis of Burkitt's lymphoma. Adv Cancer Res. 1990;55:133-270.
268. Goossens T, Klein U, Küppers R. Frequent occurrence of deletions and duplications during somatic hypermutation: implications for oncogene translocations and heavy chain disease. Proc Natl Acad Sci U S A. 1998 Mar;95(5):2463-8.
269. Coller HA, Grandori C, Tamayo P, Colbert T, Lander ES, Eisenman RN, et al. Expression analysis with oligonucleotide microarrays reveals that MYC regulates genes involved in growth, cell cycle, signaling, and adhesion. Proc Natl Acad Sci U S A. 2000 Mar 28;97(7):3260-5.
270. Erikson J, ar-Rushdi A, Drwinga HL, Nowell PC, Croce CM. Transcriptional activation of the translocated c-myc oncogene in burkitt lymphoma. Proc Natl Acad Sci U S A. 1983 Feb;80(3):820-4.

271. Evan GI, Wyllie AH, Gilbert CS, Littlewood TD, Land H, Brooks M, et al. Induction of apoptosis in fibroblasts by c-myc protein. Cell. 1992 Apr;69(1):119-28.
272. Askew DS, Ashmun RA, Simmons BC, Cleveland JL. Constitutive c-myc expression in an IL-3-dependent myeloid cell line suppresses cell cycle arrest and accelerates apoptosis. Oncogene. 1991 Oct;6(10):1915-22.
273. Nilsson JA, Cleveland JL. Myc pathways provoking cell suicide and cancer. Oncogene. 2003 Dec 8;22(56):9007-21.
274. Bhatia KG, Gutierrez MI, Huppi K, Siwarski D, Magrath IT. The pattern of p53 mutations in Burkitt's lymphoma differs from that of solid tumors. Cancer Res. 1992 Aug 1;52(15):4273-6.
275. Capoulade C, Bressac-de Paillerets B, Lefrere I, Ronsin M, Feunteun J, Tursz T, et al. Overexpression of MDM2, due to enhanced translation, results in inactivation of wild-type p53 in Burkitt's lymphoma cells. Oncogene. 1998 Mar 26;16(12):1603-10.
276. Lindström MS, Wiman KG. Role of genetic and epigenetic changes in Burkitt lymphoma. Semin Cancer Biol. 2002 Oct;12(5):381-7.
277. Kennedy G, Komano J, Sugden B. Epstein-Barr virus provides a survival factor to Burkitt's lymphomas. Proc Natl Acad Sci U S A. 2003 Nov;100(24):14269-74.
278. Saridakis V, Sheng Y, Sarkari F, Holowaty MN, Shire K, Nguyen T, et al. Structure of the p53 binding domain of HAUSP/USP7 bound to Epstein-Barr nuclear antigen 1 implications for EBV-mediated immortalization. Mol Cell. 2005 Apr;18(1):25-36.
279. Rowe M, Rowe DT, Gregory CD, Young LS, Farrell PJ, Rupani H, et al. Differences in B cell growth phenotype reflect novel patterns of Epstein-Barr virus latent gene expression in Burkitt's lymphoma cells. Embo J. 1987 Sep;6(9):2743-51.
280. Pajic A, Staege MS, Dudziak D, Schuhmacher M, Spitkovsky D, Eissner G, et al. Antagonistic effects of c-myc and Epstein-Barr virus latent genes on the phenotype of human B cells. Int J Cancer. 2001 Sep;93(6):810-6.
281. Polack A, Hortnagel K, Pajic A, Christoph B, Baier B, Falk M, et al. c-myc activation renders proliferation of Epstein-Barr virus (EBV)-transformed cells independent of EBV nuclear antigen 2 and latent membrane protein 1. Proc Natl Acad Sci U S A. 1996 Sep 17;93(19):10411-6.
282. Kelly GL, Milner AE, Baldwin GS, Bell AI, Rickinson AB. Three restricted forms of Epstein-Barr virus latency counteracting apoptosis in c-myc-expressing Burkitt lymphoma cells. Proc Natl Acad Sci U S A. 2006 Oct 3;103(40):14935-40.
283. Garibal J, Hollville E, Bell AI, Kelly GL, Renouf B, Kawaguchi Y, et al. Truncated form of the Epstein-Barr virus protein EBNA-LP protects against caspase-dependent apoptosis by inhibiting protein phosphatase 2A. J Virol. 2007 Jul;81(14):7598-607.
284. Blum KA, Lozanski G, Byrd JC. Adult Burkitt leukemia and lymphoma. Blood. 2004 Nov 15;104(10):3009-20.
285. Kvansakul M, van Delft MF, Lee EF, Gulbis JM, Fairlie WD, Huang DC, et al. A structural viral mimic of prosurvival Bcl-2: a pivotal role for sequestering proapoptotic Bax and Bak. Mol Cell. 2007 Mar;25(6):933-42.
286. Herold MJ, van den Brandt J, Seibler J, Reichardt HM. Inducible and reversible gene silencing by stable integration of an shRNA-encoding lentivirus in transgenic rats. Proc Natl Acad Sci U S A. 2008 Nov 25;105(47):18507-12.
287. Habeshaw G, Yao QY, Bell AI, Morton D, Rickinson AB. Epstein-barr virus nuclear antigen 1 sequences in endemic and sporadic Burkitt's lymphoma reflect virus strains prevalent in different geographic areas. J Virol. 1999 Feb;73(2):965-75.
288. Gregory CD, Rowe M, Rickinson AB. Different Epstein-Barr virus-B cell interactions in phenotypically distinct clones of a Burkitt's lymphoma cell line. J Gen Virol. 1990 Jul;71 (Pt 7):1481-95.
289. Ricksten A, Olsson A, Andersson T, Rymo L. The 5' flanking region of the gene for the Epstein-Barr virus-encoded nuclear antigen 2 contains a cell type specific cis-acting regulatory element that activates transcription in transfected B-cells. Nucleic Acids Res. 1988 Sep 12;16(17):8391-410.

290. Denepoux S, Razanajaona D, Blanchard D, Meffre G, Capra JD, Banchereau J, et al. Induction of somatic mutation in a human B cell line in vitro. Immunity. 1997 Jan;6(1):35-46.
291. Shlapatska LM, Berdova GG, Kovalevska LM, Kulyk GI, Klein G, Sidorenko SP, et al. Signal transduction pathways in Burkitt's lymphoma cell lines BL41 and DG75 with different sensitivity to doxorubicin. Exp Oncol. 2004 Sep;26(3):210-6.
292. Yandava CN, Speck SH. Characterization of the deletion and rearrangement in the BamHI C region of the X50-7 Epstein-Barr virus genome, a mutant viral strain which exhibits constitutive BamHI W promoter activity. J Virol. 1992 Sep;66(9):5646-50.
293. Bell AI, Groves K, Kelly GL, Croom-Carter D, Hui E, Chan AT, et al. Analysis of Epstein-Barr virus latent gene expression in endemic Burkitt's lymphoma and nasopharyngeal carcinoma tumour cells by using quantitative real-time PCR assays. J Gen Virol. 2006 Oct;87(Pt 10):2885-90.
294. Delecluse HJ, Hilsendegen T, Pich D, Zeidler R, Hammerschmidt W. Propagation and recovery of intact, infectious Epstein-Barr virus from prokaryotic to human cells. Proc Natl Acad Sci U S A. 1998 Jul 7;95(14):8245-50.
295. Tabata N, Aiba S, Ichinohazama R, Kikuchi K, Aoyama H, Watanabe M, et al. Hydroa vacciniforme-like lymphomatoid papulosis in a Japanese child: a new subset. J Am Acad Dermatol. 1995 Feb;32(2 Pt 2):378-81.
296. Nagata H, Konno A, Kimura N, Zhang Y, Kimura M, Demachi A, et al. Characterization of novel natural killer (NK)-cell and gammadelta T-cell lines established from primary lesions of nasal T/NK-cell lymphomas associated with the Epstein-Barr virus. Blood. 2001 Feb 1;97(3):708-13.
297. Zhang Y, Nagata H, Ikeuchi T, Mukai H, Oyoshi MK, Demachi A, et al. Common cytological and cytogenetic features of Epstein-Barr virus (EBV)-positive natural killer (NK) cells and cell lines derived from patients with nasal T/NK-cell lymphomas, chronic active EBV infection and hydroa vacciniforme-like eruptions. Br J Haematol. 2003 Jun;121(5):805-14.
298. Nagata H, Numata T, Konno A, Mikata I, Kurasawa K, Hara S, et al. Presence of natural killer-cell clones with variable proliferative capacity in chronic active Epstein-Barr virus infection. Pathol Int. 2001 Oct;51(10):778-85.
299. Cheung ST, Huang DP, Hui AB, Lo KW, Ko CW, Tsang YS, et al. Nasopharyngeal carcinoma cell line (C666-1) consistently harbouring Epstein-Barr virus. Int J Cancer. 1999 Sep 24;83(1):121-6.
300. Kassis J, Maeda A, Teramoto N, Takada K, Wu C, Klein G, et al. EBV-expressing AGS gastric carcinoma cell sublines present increased motility and invasiveness. Int J Cancer. 2002 Jun 10;99(5):644-51.
301. Diehl V, Pfreundschuh M, Fonatsch C, Stein H, Falk M, Burrichter H, et al. Phenotypic and genotypic analysis of Hodgkin's disease derived cell lines: histopathological and clinical implications. Cancer Surv. 1985;4(2):399-419.
302. Vockerodt M, Belge G, Kube D, Irsch J, Siebert R, Tesch H, et al. An unbalanced translocation involving chromosome 14 is the probable cause for loss of potentially functional rearranged immunoglobulin heavy chain genes in the Epstein-Barr virus-positive Hodgkin's lymphoma-derived cell line L591. Br J Haematol. 2002 Dec;119(3):640-6.
303. Manders EM, Hoebe R, Strackee J, Vossepoel AM, Aten JA. Largest contour segmentation: a tool for the localization of spots in confocal images. Cytometry. 1996 Jan 1;23(1):15-21.
304. Elbashir SM, Harborth J, Lendeckel W, Yalcin A, Weber K, Tuschl T. Duplexes of 21-nucleotide RNAs mediate RNA interference in cultured mammalian cells. Nature. 2001 May;411(6836):494-8.
305. Myer VE, Young RA. RNA polymerase II holoenzymes and subcomplexes. J Biol Chem. 1998 Oct 23;273(43):27757-60.
306. Lois C, Hong EJ, Pease S, Brown EJ, Baltimore D. Germline transmission and tissue-specific expression of transgenes delivered by lentiviral vectors. Science. 2002 Feb 1;295(5556):868-72.
307. Seibler J, Kleinridders A, Küter-Luks B, Niehaves S, Brüning JC, Schwenk F. Reversible gene knockdown in mice using a tight, inducible shRNA expression system. Nucleic Acids Res. 2007;35(7):e54.
308. Szymczak AL, Vignali DA. Development of 2A peptide-based strategies in the design of multicistronic vectors. Expert Opin Biol Ther. 2005 May;5(5):627-38.

309. Hager S, Frame FM, Collins AT, Burns JE, Maitland NJ. An internal polyadenylation signal substantially increases expression levels of lentivirus-delivered transgenes but has the potential to reduce viral titer in a promoter-dependent manner. Hum Gene Ther. 2008 Aug;19(8):840-50.
310. Khanim F, Dawson C, Meseda CA, Dawson J, Mackett M, Young LS. BHRF1, a viral homologue of the Bcl-2 oncogene, is conserved at both the sequence and functional level in different Epstein-Barr virus isolates. J Gen Virol. 1997 Nov;78 (Pt 11):2987-99.
311. Furth PA, St Onge L, Böger H, Gruss P, Gossen M, Kistner A, et al. Temporal control of gene expression in transgenic mice by a tetracycline-responsive promoter. Proc Natl Acad Sci U S A. 1994 Sep;91(20):9302-6.
312. Tolmachov O, Tolmachova T, Al-Allaf F. Viral Gene Therapy: InTech; 2011.
313. Guhaniyogi J, Brewer G. Regulation of mRNA stability in mammalian cells. Gene. 2001 Mar;265(1-2):11-23.
314. Jabbour AM, Puryer MA, Yu JY, Lithgow T, Riffkin CD, Ashley DM, et al. Human Bcl-2 cannot directly inhibit the Caenorhabditis elegans Apaf-1 homologue CED-4, but can interact with EGL-1. J Cell Sci. 2006 Jun;119(Pt 12):2572-82.
315. Tao W, Kurschner C, Morgan JI. Modulation of cell death in yeast by the Bcl-2 family of proteins. J Biol Chem. 1997 Jun;272(24):15547-52.
316. Frey T. Nucleic acid dyes for detection of apoptosis in live cells. Cytometry. 1995 Nov 1;21(3):265-74.
317. Wlodkowic D, Skommer J, Pelkonen J. Towards an understanding of apoptosis detection by SYTO dyes. Cytometry A. 2007 Feb;71(2):61-72.
318. Cohen GM, Sun XM, Snowden RT, Ormerod MG, Dinsdale D. Identification of a transitional preapoptotic population of thymocytes. Journal of immunology (Baltimore, Md : 1950). 1993 Jul 15;151(2):566-74.
319. Morgan AJ, Jacob R. Ionomycin enhances Ca2+ influx by stimulating store-regulated cation entry and not by a direct action at the plasma membrane. The Biochemical journal. 1994 Jun 15;300 (Pt 3):665-72.
320. McConkey DJ, Nicotera P, Hartzell P, Bellomo G, Wyllie AH, Orrenius S. Glucocorticoids activate a suicide process in thymocytes through an elevation of cytosolic Ca2+ concentration. Archives of biochemistry and biophysics. 1989 Feb 15;269(1):365-70.
321. McConkey DJ, Orrenius S. The role of calcium in the regulation of apoptosis. Biochem Biophys Res Commun. 1997 Oct 20;239(2):357-66.
322. Aagaard-Tillery KM, Jelinek DF. Differential activation of a calcium-dependent endonuclease in human B lymphocytes. Role in ionomycin-induced apoptosis. Journal of immunology (Baltimore, Md : 1950). 1995 Oct 1;155(7):3297-307.
323. Gold MR, DeFranco AL. Phorbol esters and dioctanoylglycerol block anti-IgM-stimulated phosphoinositide hydrolysis in the murine B cell lymphoma WEHI-231. Journal of immunology (Baltimore, Md : 1950). 1987 Feb 1;138(3):868-76.
324. Chen W, Wang HG, Srinivasula SM, Alnemri ES, Cooper NR. B cell apoptosis triggered by antigen receptor ligation proceeds via a novel caspase-dependent pathway. Journal of immunology (Baltimore, Md : 1950). 1999 Sep 1;163(5):2483-91.
325. Leao M, Anderton E, Wade M, Meekings K, Allday MJ. Epstein-barr virus-induced resistance to drugs that activate the mitotic spindle assembly checkpoint in Burkitt's lymphoma cells. J Virol. 2007 Jan;81(1):248-60.
326. Wade M, Allday MJ. Epstein-Barr virus suppresses a G(2)/M checkpoint activated by genotoxins. Mol Cell Biol. 2000 Feb;20(4):1344-60.
327. Hande KR. Etoposide: four decades of development of a topoisomerase II inhibitor. European journal of cancer. 1998 Sep;34(10):1514-21.
328. Alvi AJ, Austen B, Weston VJ, Fegan C, MacCallum D, Gianella-Borradori A, et al. A novel CDK inhibitor, CYC202 (R-roscovitine), overcomes the defect in p53-dependent apoptosis in B-CLL by down-regulation of genes involved in transcription regulation and survival. Blood. 2005 Jun 1;105(11):4484-91.

329. Meijer L, Borgne A, Mulner O, Chong JP, Blow JJ, Inagaki N, et al. Biochemical and cellular effects of roscovitine, a potent and selective inhibitor of the cyclin-dependent kinases cdc2, cdk2 and cdk5. European journal of biochemistry / FEBS. 1997 Jan 15;243(1-2):527-36.
330. Boyce A. Epstein-Barr Virus genome loss from Endemic Burkitt Lymphoma and its effect on cell phenotype. Birmingham: The University of Birmingham; 2009.
331. Ladbury JE. Calorimetry as a tool for understanding biomolecular interactions and an aid to drug design. Biochem Soc Trans. 2010 Aug;38(4):888-93.
332. Clybouw C, McHichi B, Mouhamad S, Auffredou MT, Bourgeade MF, Sharma S, et al. EBV infection of human B lymphocytes leads to down-regulation of Bim expression: relationship to resistance to apoptosis. Journal of immunology (Baltimore, Md : 1950). 2005 Sep;175(5):2968-73.
333. Puthalakath H, O'Reilly LA, Gunn P, Lee L, Kelly PN, Huntington ND, et al. ER stress triggers apoptosis by activating BH3-only protein Bim. Cell. 2007 Jun 29;129(7):1337-49.
334. Enders A, Bouillet P, Puthalakath H, Xu Y, Tarlinton DM, Strasser A. Loss of the pro-apoptotic BH3-only Bcl-2 family member Bim inhibits BCR stimulation-induced apoptosis and deletion of autoreactive B cells. J Exp Med. 2003 Oct 6;198(7):1119-26.
335. Chen AY, Liu LF. DNA topoisomerases: essential enzymes and lethal targets. Annu Rev Pharmacol Toxicol. 1994;34:191-218.
336. Lowe SW, Schmitt EM, Smith SW, Osborne BA, Jacks T. p53 is required for radiation-induced apoptosis in mouse thymocytes. Nature. 1993 Apr 29;362(6423):847-9.
337. Strasser A, Harris AW, Jacks T, Cory S. DNA damage can induce apoptosis in proliferating lymphoid cells via p53-independent mechanisms inhibitable by Bcl-2. Cell. 1994 Oct 21;79(2):329-39.
338. Oda E, Ohki R, Murasawa H, Nemoto J, Shibue T, Yamashita T, et al. Noxa, a BH3-only member of the Bcl-2 family and candidate mediator of p53-induced apoptosis. Science. 2000 May 12;288(5468):1053-8.
339. Nakano K, Vousden KH. PUMA, a novel proapoptotic gene, is induced by p53. Mol Cell. 2001 Mar;7(3):683-94.
340. Sax JK, Fei P, Murphy ME, Bernhard E, Korsmeyer SJ, El-Deiry WS. BID regulation by p53 contributes to chemosensitivity. Nat Cell Biol. 2002 Nov;4(11):842-9.
341. Miyashita T, Reed JC. Tumor suppressor p53 is a direct transcriptional activator of the human bax gene. Cell. 1995 Jan 27;80(2):293-9.
342. Chipuk JE, Green DR. Dissecting p53-dependent apoptosis. Cell Death Differ. 2006 Jun;13(6):994-1002.
343. Dey A, Wong ET, Cheok CF, Tergaonkar V, Lane DP. R-Roscovitine simultaneously targets both the p53 and NF-kappaB pathways and causes potentiation of apoptosis: implications in cancer therapy. Cell Death Differ. 2008 Feb;15(2):263-73.
344. Lu W, Chen L, Peng Y, Chen J. Activation of p53 by roscovitine-mediated suppression of MDM2 expression. Oncogene. 2001 May 31;20(25):3206-16.
345. Kvansakul M, Hinds MG. Structural biology of the Bcl-2 family and its mimicry by viral proteins. Cell Death Dis. 2013;4:e909.
346. Bouillet P, Metcalf D, Huang DC, Tarlinton DM, Kay TW, Kontgen F, et al. Proapoptotic Bcl-2 relative Bim required for certain apoptotic responses, leukocyte homeostasis, and to preclude autoimmunity. Science. 1999 Nov 26;286(5445):1735-8.
347. Putcha GV, Moulder KL, Golden JP, Bouillet P, Adams JA, Strasser A, et al. Induction of BIM, a proapoptotic BH3-only BCL-2 family member, is critical for neuronal apoptosis. Neuron. 2001 Mar;29(3):615-28.
348. Erlacher M, Labi V, Manzl C, Bock G, Tzankov A, Hacker G, et al. Puma cooperates with Bim, the rate-limiting BH3-only protein in cell death during lymphocyte development, in apoptosis induction. J Exp Med. 2006 Dec 25;203(13):2939-51.
349. Marchini A, Tomkinson B, Cohen JI, Kieff E. BHRF1, the Epstein-Barr virus gene with homology to Bc12, is dispensable for B-lymphocyte transformation and virus replication. J Virol. 1991 Nov;65(11):5991-6000.

350. Lee MA, Yates JL. BHRF1 of Epstein-Barr virus, which is homologous to human proto-oncogene bcl2, is not essential for transformation of B cells or for virus replication in vitro. J Virol. 1992 Apr;66(4):1899-906.
351. Liu X, Dai S, Zhu Y, Marrack P, Kappler JW. The structure of a Bcl-xL/Bim fragment complex: implications for Bim function. Immunity. 2003 Sep;19(3):341-52.
352. Gao C, Nakajima T, Taya Y, Tsuchida N. Activation of p53 in MDM2-overexpressing cells through phosphorylation. Biochem Biophys Res Commun. 1999 Nov 2;264(3):860-4.
353. Farrell PJ, Allan GJ, Shanahan F, Vousden KH, Crook T. p53 is frequently mutated in Burkitt's lymphoma cell lines. Embo J. 1991 Oct;10(10):2879-87.
354. Yu J, Zhang L, Hwang PM, Kinzler KW, Vogelstein B. PUMA induces the rapid apoptosis of colorectal cancer cells. Mol Cell. 2001 Mar;7(3):673-82.
355. Maas C, de Vries E, Tait SW, Borst J. Bid can mediate a pro-apoptotic response to etoposide and ionizing radiation without cleavage in its unstructured loop and in the absence of p53. Oncogene. 2011 Aug 18;30(33):3636-47.
356. Lama D, Sankararamakrishnan R. Anti-apoptotic Bcl-XL protein in complex with BH3 peptides of pro-apoptotic Bak, Bad, and Bim proteins: comparative molecular dynamics simulations. Proteins. 2008 Nov 1;73(2):492-514.
357. Hsu WL, Chung PJ, Tsai MH, Chang CL, Liang CL. A role for Epstein-Barr viral BALF1 in facilitating tumor formation and metastasis potential. Virus Res. 2012 Feb;163(2):617-27.
358. Nicholls J, Kremmer E, Meseda CA, Mackett M, Hahn P, Gulley ML, et al. Comparative analysis of the expression of the Epstein-Barr virus (EBV) anti-apoptotic gene BHRF1 in nasopharyngeal carcinoma and EBV-related lymphoid diseases. J Med Virol. 2001 Sep;65(1):105-13.
359. Hickish T, Robertson D, Clarke P, Hill M, di Stefano F, Clarke C, et al. Ultrastructural localization of BHRF1: an Epstein-Barr virus gene product which has homology with bcl-2. Cancer Res. 1994 May 15;54(10):2808-11.
360. Hsu YT, Youle RJ. Nonionic detergents induce dimerization among members of the Bcl-2 family. J Biol Chem. 1997 May 23;272(21):13829-34.
361. Zhai D, Jin C, Huang Z, Satterthwait AC, Reed JC. Differential regulation of Bax and Bak by anti-apoptotic Bcl-2 family proteins Bcl-B and Mcl-1. J Biol Chem. 2008 Apr 11;283(15):9580-6.
362. Gerecova G, Kopanicova J, Jaka P, Behalova L, Juhasova B, Bhatia-Kissova I, et al. BH3-only proteins Noxa, Bik, Bmf, and Bid activate Bax and Bak indirectly when studied in yeast model. FEMS Yeast Res. 2013 Dec;13(8):747-54.
363. Juhasova B, Mentel M, Bhatia-Kissova I, Zeman I, Kolarov J, Forte M, et al. BH3-only protein Bim inhibits activity of antiapoptotic members of Bcl-2 family when expressed in yeast. FEBS Lett. 2011 Sep 2;585(17):2709-13.
364. Dalla-Favera R, Bregni M, Erikson J, Patterson D, Gallo RC, Croce CM. Human c-myc onc gene is located on the region of chromosome 8 that is translocated in Burkitt lymphoma cells. Proc Natl Acad Sci U S A. 1982 Dec;79(24):7824-7.
365. Eischen CM, Weber JD, Roussel MF, Sherr CJ, Cleveland JL. Disruption of the ARF-Mdm2-p53 tumor suppressor pathway in Myc-induced lymphomagenesis. Genes Dev. 1999 Oct 15;13(20):2658-69.
366. Murphy SB, Bowman WP, Abromowitch M, Mirro J, Ochs J, Rivera G, et al. Results of treatment of advanced-stage Burkitt's lymphoma and B cell (SIg+) acute lymphoblastic leukemia with high-dose fractionated cyclophosphamide and coordinated high-dose methotrexate and cytarabine. J Clin Oncol. 1986 Dec;4(12):1732-9.
367. McMaster ML, Greer JP, Greco FA, Johnson DH, Wolff SN, Hainsworth JD. Effective treatment of small-noncleaved-cell lymphoma with high-intensity, brief-duration chemotherapy. J Clin Oncol. 1991 Jun;9(6):941-6.
368. Ladenstein R, Pearce R, Hartmann O, Patte C, Goldstone T, Philip T. High-dose chemotherapy with autologous bone marrow rescue in children with poor-risk Burkitt's lymphoma: a report from the European Lymphoma Bone Marrow Transplantation Registry. Blood. 1997 Oct 15;90(8):2921-30.

369. Allday MJ. How does Epstein-Barr virus (EBV) complement the activation of Myc in the pathogenesis of Burkitt's lymphoma? Semin Cancer Biol. 2009 Jul 25.
370. Macpherson N, Lesack D, Klasa R, Horsman D, Connors JM, Barnett M, et al. Small noncleaved, non-Burkitt's (Burkit-Like) lymphoma: cytogenetics predict outcome and reflect clinical presentation. J Clin Oncol. 1999 May;17(5):1558-67.
371. Ferry JA. Burkitt's lymphoma: clinicopathologic features and differential diagnosis. Oncologist. 2006 Apr;11(4):375-83.
372. Kelly GL, Strasser A. The essential role of evasion from cell death in cancer. Adv Cancer Res. 2011;111:39-96.
373. O'Brien S, Moore JO, Boyd TE, Larratt LM, Skotnicki A, Koziner B, et al. Randomized phase III trial of fludarabine plus cyclophosphamide with or without oblimersen sodium (Bcl-2 antisense) in patients with relapsed or refractory chronic lymphocytic leukemia. J Clin Oncol. 2007 Mar 20;25(9):1114-20.
374. O'Brien S, Moore JO, Boyd TE, Larratt LM, Skotnicki AB, Koziner B, et al. 5-year survival in patients with relapsed or refractory chronic lymphocytic leukemia in a randomized, phase III trial of fludarabine plus cyclophosphamide with or without oblimersen. J Clin Oncol. 2009 Nov 1;27(31):5208-12.
375. Jahrsdorfer B, Jox R, Muhlenhoff L, Tschoep K, Krug A, Rothenfusser S, et al. Modulation of malignant B cell activation and apoptosis by bcl-2 antisense ODN and immunostimulatory CpG ODN. J Leukoc Biol. 2002 Jul;72(1):83-92.
376. Ni Chonghaile T, Letai A. Mimicking the BH3 domain to kill cancer cells. Oncogene. 2008 Dec;27 Suppl 1:S149-57.
377. Tse C, Shoemaker AR, Adickes J, Anderson MG, Chen J, Jin S, et al. ABT-263: a potent and orally bioavailable Bcl-2 family inhibitor. Cancer Res. 2008 May 1;68(9):3421-8.
378. Oltersdorf T, Elmore SW, Shoemaker AR, Armstrong RC, Augeri DJ, Belli BA, et al. An inhibitor of Bcl-2 family proteins induces regression of solid tumours. Nature. 2005 Jun 2;435(7042):677-81.
379. van Delft MF, Wei AH, Mason KD, Vandenberg CJ, Chen L, Czabotar PE, et al. The BH3 mimetic ABT-737 targets selective Bcl-2 proteins and efficiently induces apoptosis via Bak/Bax if Mcl-1 is neutralized. Cancer Cell. 2006 Nov;10(5):389-99.
380. Cragg MS, Harris C, Strasser A, Scott CL. Unleashing the power of inhibitors of oncogenic kinases through BH3 mimetics. Nat Rev Cancer. 2009 May;9(5):321-6.
381. Mason KD, Carpinelli MR, Fletcher JI, Collinge JE, Hilton AA, Ellis S, et al. Programmed anuclear cell death delimits platelet life span. Cell. 2007 Mar 23;128(6):1173-86.
382. Zhang H, Nimmer PM, Tahir SK, Chen J, Fryer RM, Hahn KR, et al. Bcl-2 family proteins are essential for platelet survival. Cell Death Differ. 2007 May;14(5):943-51.
383. Souers AJ, Leverson JD, Boghaert ER, Ackler SL, Catron ND, Chen J, et al. ABT-199, a potent and selective BCL-2 inhibitor, achieves antitumor activity while sparing platelets. Nat Med. 2013;19(2):202-8.
384. Procko E, Berguig GY, Shen BW, Song Y, Frayo S, Convertine AJ, et al. A computationally designed inhibitor of an Epstein-Barr viral Bcl-2 protein induces apoptosis in infected cells. Cell. 2014 Jun 19;157(7):1644-56.
385. Ricca A, Biroccio A, Del Bufalo D, Mackay AR, Santoni A, Cippitelli M. bcl-2 over-expression enhances NF-kappaB activity and induces mmp-9 transcription in human MCF7(ADR) breast-cancer cells. Int J Cancer. 2000 Apr 15;86(2):188-96.